



Durham E-Theses

The development of thiophosphoryl 'click' chemistry

Trmcic, Milena

How to cite:

Trmcic, Milena (2009) *The development of thiophosphoryl 'click' chemistry*, Durham theses, Durham University. Available at Durham E-Theses Online: <http://etheses.dur.ac.uk/2035/>

Use policy

The full-text may be used and/or reproduced, and given to third parties in any format or medium, without prior permission or charge, for personal research or study, educational, or not-for-profit purposes provided that:

- a full bibliographic reference is made to the original source
- a [link](#) is made to the metadata record in Durham E-Theses
- the full-text is not changed in any way

The full-text must not be sold in any format or medium without the formal permission of the copyright holders.

Please consult the [full Durham E-Theses policy](#) for further details.

Durham University

A thesis entitled

**The Development of Thiophosphoryl
'Click' Chemistry**

The copyright of this thesis rests with the author or the university to which it was submitted. No quotation from it, or information derived from it may be published without the prior written consent of the author or university, and any information derived from it should be acknowledged.

Submitted by

Milena Trmcic

Department of Chemistry

A Candidate for the Degree of Doctor of Philosophy

2009

01 SEP 2009



ACKNOWLEDGMENTS

I would like to express my gratitude to my supervisor, Dr. David R W Hodgson, who enabled my PhD studies and has provided amazing support and supervision through entire project along with the great guidance in producing this thesis. In addition, I would also like to convey thanks to the Durham University Chemistry Department for providing the financial means and the laboratory facilities.

This research project was performed with great help of the departmental excellent technical stuff in the form of NMR spectroscopy analysis by Dr. Alan Kenwright, Mr Ian McKeag and Mrs Catherine Heffernan; mass spectroscopy analysis by Dr. Mile Jones, Dr. Jackie Mosely, and Miss Lara Turner; Mr Tony Baxter, Mrs Elizabeth Wood and Mr Philip Rochester in stores and glassblowing by Mr Peter Coyne and Mr Malcolm Richardson.

I would like to thank Prof. Robert Edwards and his group, especially to Dr. Ian Cummins, Dr. Mark Skipsey and Dr. David Dixon for generous and abundant help, advice in undertaking research, but also for fruitful chats and discussions. I would also like to thank the past and present members our group for all assistance and creation of pleasant laboratory atmosphere.

Very special thanks to my gorgeous nephew Luka Cvitas, my sister Jelena Trmcic Cvitas and brother-in-law Marko Cvitas for exceptional support in any means, great housting for my frequent visits and making my stay in Great Britain exceedingly enjoyable. Many thanks to my mum, father and, especially, brother Marko for all love and understanding. I would like to express big gratitude to my boyfriend, Igor Simovic, for endless love and patience through my stay abroad. Finally, I would like to thank to my friends back in Serbia and in Durham for all laughs, good food discussions, Sunday movie nights and support in studies, in particular to Anne Soleilhavoup whose friendship evaluation would lead to indefinite numbers.

MEMORANDUM

The work that is presented with in this thesis was carried out at Durham University between January 2006 and April 2009. The thesis is the work of the author, except where acknowledged by reference, and has not been submitted for any other degree. The copyright of these lies solely with the author and no quotation from it would be published from it should be published without written consent and information derived from it should be acknowledged.

This work has been presented at:

- RSC Nucleic Acids Group, The 2nd Nucleic Acids Forum, Bio-organic Chemistry and Biochemistry, July 2006, University of Manchester, Manchester, UK
- RSC Organic Reaction Mechanisms Meeting, Post-Graduate Symposium, September 2006 GlaxoSmithKline, Tonbridge, UK
- RSC Nucleic Acids Group, The 3rd Nucleic Acids Forum, Bio-organic Chemistry and Biochemistry, July 2007, University of Reading, Reading, UK
- RSC Organic Reaction Mechanisms Group, 'Younger' Physical Organic Chemists' Residential Meeting, July 2007, Castelton, UK
- RSC Organic Reaction Mechanisms Group, SymPoc 2008, Durham University, Durham, UK
- 19th IUPAC Conference on Physical Organic Chemistry July 2008, The Royal University of Santiago de Compostela, Santiago de Compostela, Spain
- RSC Organic Reaction Mechanisms Group, 'Younger' Physical Organic Chemists' residential Meeting, September 2008, Castelton, UK
- 2nd EuChMS Chemistry Congress, September 2008, Torino, Italy
- RSC Organic Reaction Mechanisms Group, Post-Graduate Symposium, November 2008, AstraZeneca, Loughborough, UK

STATEMENT OF COPYRIGHT

No part of this thesis may be reproduced by any means, nor translated, nor transmitted into any machine language without written permission of the author.

For Luka and Marko

ACKNOWLEDGMENTS	1
ABSTRACT	9
ABBREVIATIONS	10
1.0 INTRODUCTION	13
1.1. The ‘Click’ chemistry concept	14
1.1.1. Why water as the solvent?	16
1.1.2. Some of examples of ‘Click’ chemistry	17
1.1.3. Wide application in biological systems	22
1.2. Phosphates	26
1.3. Research targets in the form of glycosyltransferases	29
1.4. Nucleophilic reactions in water	31
1.4.1. The effect of the general base assisted hydrolysis on nucleophilic reactions in water	37
1.4.2. The phenomenon of high yields in the reactions of benzenesulfonyl chloride with amines at high pH⁵⁰	40
1.5. Project outline: Development of thiophosphoryl ‘Click’ chemistry	43
1.5.1. Thiophosphoroamidate system	43
1.5.2. Bromoacetyl system	44
2.0 The Thiophosphoroamidate system	46
2.1. The foundation of the thiophosphoramidate idea	48
2.2. Simplification of the diphosphate motif—development of mono S-alkylated thiophosphoramidates	51
2.3. Existing methods for generating thiophosphoramidates	53
2.4. Preliminary experiments: thiophosphorylation of amines	56
2.4.1. Thiophosphorylation of ethanolamine: optimisation	57
2.4.2. Thiophosphorylation of benzylamine	58
2.5. Hydrolysis stability studies on a thiophosphoramidate	61
2.5.1. Stability of oxy-phosphoroamidates	61
2.5.2. Stability of thiophosphoroamidates	64
2.5.3. NMR kinetic studies: ethanolamine thiophosphoramidate hydrolysis	68
2.6. Preliminary alkylation experiments: stepwise approach	76
2.6.1. The use of an excess of thiophosphoroamidate	77
2.6.2. Bis-(N-, S-) alkylation of thiophosphoramidates	81
2.6.3. The use of equal numbers of equivalents of thiophosphoramidate and alkylating agent	82
2.7. Design of a one-pot thiophosphoramidate system	84

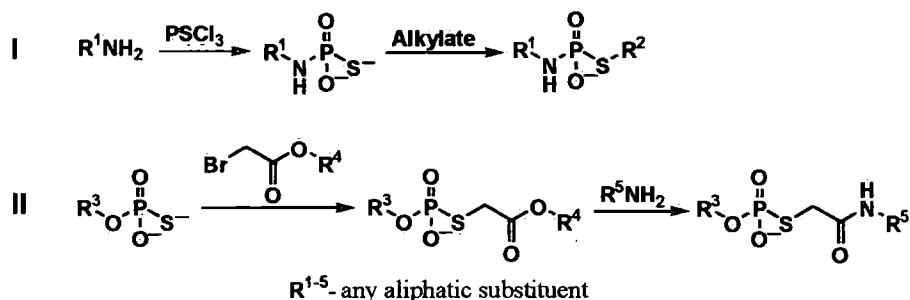
2.8. Model amines	86
2.9. Model alkylating agents	89
2.10. Continuous method with lipophilic amines and simple alkylating agents: benzylamine and allylamine	91
2.11. One-pot method with hydrophilic amines: the use of excess of thiophosphoryl chloride and methanol precipitation	95
2.12. Continuous method: the use of excess of morpholine	97
2.13. One-pot method: the use an equal number of equivalents of ethanolamine and thiophosphoryl chloride	99
2.14. Exploitation of the one-pot method: proof of concept generation of a library of amines	100
2.15. The stability of S-alkylated thiophosphoramidates	103
2.16. 'Challenging' amines: amino acids, aromatic amines and sugars	105
2.16.1. The aqueous thiophosphorylation of phenylalanine	105
2.16.2. Continuous Tripartite method: aniline	108
2.16.3. The aqueous thiophosphorylation of glucosamine	109
2.17. Expansion to a range of alkylating agents	112
2.18. Conclusions on and potential of the thiophosphoramidate system in future experiments	115
3.0 Nucleosides and their application in the thiophosphoramidate system	118
3.1. Research targets in the form of glycosyltransferases	120
3.1.1. Fucosyltransferase	120
3.1.2. Past and present inhibitors: mimics of the natural substrate	122
3.2. Synthesis of guanosine derivatives	126
3.2.1. Preparation of 5'-iodo-5'-deoxyguanosine	126
3.2.2. Preparation of 5'-azido-5'-deoxyguanosine	127
3.2.3. Novel aqueous procedure for the preparation of 5'-azido-5'-deoxyguanosine⁴⁶	127
3.2.4. Novel aqueous procedure for the preparation of 5'-amino-5'-deoxyguanosine⁴⁶	128
3.3. Continuous method involving nucleosides: 5'-amino-5'-deoxyguanosine	130
3.4. Continuous method involving nucleosides: 5'-amino-5'-deoxyadenosine	133
3.5. 5'-Iodo-5'-deoxyguanosine as an alkylating agent	134
3.6. Conclusions and future work on the involvement of nucleosides in the thiophosphoramidate system	137
4.0 Quinolines and their application in the thiophosphoramidate system	139
4.1. A simple opportunity for the application of the thiophosphoramidate system: quinoline-based thiophosphoramidates as antileishmanials	140
4.2. Leishmaniasis, past and present drugs	141
4.3. Library synthesis and analysis	142
4.4. Biological testing against <i>Leishmania mexicana</i>	144

4.4.1. Initial screening	144
4.4.2. Estimation of the IC ₅₀ s of the studied quinoline compounds	144
4.5. Hypothesis	148
4.6. Conclusions and future work on quinoline-based thiophosphoramidates	149
5.0 A bromoacetyl strategy	152
5.1. The strategy of the bromoacetyl system	152
5.2. Research targets in the form of glycosyltransferases	157
5.2.1. Chitin synthase	157
5.2.2. Past and present antifungal agents: natural substrate mimics	159
5.3. The preparation of uridine 5'-O-monothiophosphate (UMPS)	162
5.4. The synthesis of activated bromoacetyl esters	166
5.5. The bromoacetyl Tripartite reaction: HOBt as the leaving group	168
5.6. Tripartite reaction over a range of pH: HOBt as the leaving group	171
5.7. Tripartite reaction: NHS as the leaving group	174
5.8. Ester hydrolysis and aminolysis	176
5.9. Studies of the pH-rate dependence of amine formation: Dipartite 'Click' chemistry	176
5.9.1. ³¹ P NMR kinetic studies	178
5.9.2. UV kinetic studies	179
5.9.3. Preparation of samples for the UV-Vis kinetic studies	180
5.9.4. UV-Vis hydrolysis studies: p-nitrophenol as the leaving group	181
5.9.5. pH hydrolysis rate profile: p-nitrophenol as the leaving group	183
5.9.6. UV-Vis aminolysis studies: p-nitrophenol as the leaving group	185
5.9.7. Selectivity: p-nitrophenol as the leaving group	189
5.9.8. UV-Vis hydrolysis studies: m-nitrophenol as the leaving group	191
5.9.9. UV-Vis aminolysis studies: m-nitrophenol as the leaving group	192
5.9.10. Selectivity: p-nitrophenol vs m-nitrophenol as the leaving groups	192
5.10. Exploring the strategy of combining bromoacetyl and thiophosphoroamidates system	194
5.10.1. Bromoacetyl-thiophosphoroamidate system: allylamine	195
5.10.2. Bromoacetyl-thiophosphoroamidate system: 5'-amino-5'-guanosine	197
5.11. Conclusion and future work involving bromoacetyl strategy	199
6.0 Conclusions and future work after thesis	202
7.0 Experimental section	204
7.1. General Methods	204
7.2. The optimization of the ethanolamine thiophosphorylation	207
7.3. Thiophosphorylation of benzylamine	208

7.4. NMR kinetic studies of thiophosphoroamidate stability	209
7.5. Stepwise alkylation of thiophosphoroamidates	212
7.5.1. Use of an excess of the thiophosphoroamidate with the respect to alkylation agent	212
7.5.2. Bis-(N-, S-) alkylation of thiophosphoroamidates	214
7.5.3. Use of thiophosphoroamidate and alkylation agent in a 1:1 molar ratio	216
7.6. Continuous method for the preparation of alkylated thiophosphoroamidates	217
7.6.1. Lipophilic amines: benzylamine and allylamine	217
7.6.2. Hydrophilic amines: morpholine	221
7.6.3. Hydrophilic amines: the use of equal numbers of equivalents of ethanolamine and thiophosphoryl chloride	223
7.6.4. A library of amines	224
7.6.5. 'Challenging' amines: phenylalanine, aniline, D-glucosamine	230
7.7. Preparation of 5'-deoxy-5'-iodoguanosine ⁹⁹	231
7.8. Preparation of 5'-azido-5'-deoxyguanosine ⁵⁵	232
7.9. Aqueous method for preparation of 5'-azido-5'-deoxyguanosine	233
7.10. Aqueous method for preparation of 5'-amino-5'-deoxyguanosine	233
7.11. Nucleosides in the one-pot method for the preparation of alkylated thiophosphoroamidates:	234
7.11.1. Nucleoside amines: guanosine and adenosine	234
7.12. Iodo-guanosine as the alkylation agent	238
7.13. Synthesis of the quinoline derivative library	241
7.14. Initial screening	248
7.15. The estimation of the IC ₅₀ of the studied compounds	248
7.16. UMPS preparation ¹³³	249
7.17. Cation exchange using NaI/acetone system	250
7.18. Bromoacetyl-N-hydroxybenzotriazole	250
7.19. Tripartite reaction: N-hydroxybenzotriazole as the leaving group	251
7.20. pH range Tripartite reaction: N-hydroxybenzotriazole as the leaving group	253
7.21. Bromoacetyl-N-hydroxysuccinimide	255
7.22. Tripartate reaction: N-hydroxysuccinimide as the leaving group	255
7.23. Bromoacetyl p-nitrophenol	256
7.24. UV-Vis kinetic studies of Dipartate 'Click' chemistry: p-nitrophenol as leaving group	257
7.25. Hydrolysis assays: p-nitrophenol as the leaving group	257
7.26. Aminolysis: p-nitrophenol as the leaving group	260
7.27. Bromoacetyl m-nitrophenol	263
7.28. Bromoacetyl system and thiophosphoroamidates: allylamine and guanosine amine	264

ABSTRACT

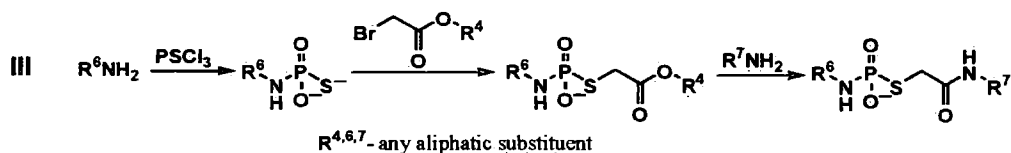
We have established novel, aqueous 'Click' chemistry that is based on the thiophosphoryl group. Two systems for the creation of thiophosphoryl derivatives were involved: Thiophosphoramidate I and Bromoacetyl II.



The first step in the Thiophosphoramidate system is our aqueous thiophosphorylation of amines using thiophosphoryl chloride. Through careful control of reaction conditions we have devised a method that allows us to prepare and alkylate the thiophosphoramidate group in aqueous media with high conversions, and thus provide a fast, clean and straightforward route to a number of products. The thiophosphoramidate system was, then, successfully applied towards the production of nucleoside monothiophosphoramidates. In addition, a number of quinoline-based thiophosphoramidates were generated as potential antileishmanials and *in vivo* assays were performed against *Leishmania mexicana*.

The bromoacetyl system uses thiophosphorylated alcohols that we alkylated with a range of activated bromoacetate esters. Hydrolysis and aminolysis kinetic studies were employed on this system for a better understanding of the conditions required for facile production of amides on these thiophosphoryl acetate esters in water.

Finally, we have combined the achievements from these two systems into the thiophosphoramidate-bromoacetyl strategy III, expanding the scope for generating thiophosphoryl derivatives.



ABBREVIATIONS

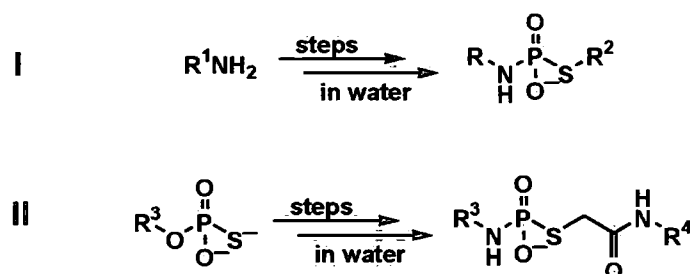
A-NH ₂	5'-amino-5' deoxyguanosine
br s	broad signal (or singlet)
BrAcBr	bromoacetyl bromide
CAPS	<i>N</i> -cyclohexyl-3-aminopropanesulfonic acid
Chs	chitin synthase
CMP	cytosine monophosphate
conc	concentration
d	doublet
<i>d</i> ₆ -DMSO	<i>d</i> ₆ -dimethylsulfoxide
DCM	dichloromethane
dd	doublet of doublets
DEAE	diethylamine ethylene
DP	nucleoside diphosphate
EPPS	3-[4-(2-hydroxyethyl)-1-piperazinyl]propanesulfonic acid
eq	equation
Eq	equivalent

f.b.	free base
FF	fast flow
GDP	guanosine diphosphate
G-I	5'-deoxy-5'iodoguanosine
GlcNAc	<i>N</i> -acetyl glycosamine
GlcNH ₂	D-glucosamine
G-N ₃	5'-azido-5' deoxyguanosine
G-NH ₂	5'-amino-5' deoxyguanosine
h	heptet
HEPES	4-(2-hydroxyethyl)-1-piperazinylethanesulfonic acid
HOBt	<i>N</i> -hydroxybenzotriazole
HPLC	high performance liquid chromatography
<i>i</i>	ipso-position
IR	infrared spectroscopy
<i>L. mexicana</i>	<i>Leishmania mexicana</i>
m	multipliset
<i>m</i> -	meta-position
MES	2-(<i>N</i> -morpholino)ethanesulfonic acid
mNP	<i>m</i> -nitrophenol
MPLC	medium pressure liquid chromatography
n.d.	no data
NDP	nucleoside diphosphate
NHS	<i>N</i> -hydroxysuccinimide
NMP	nucleoside monophosphate
<i>o</i>	orto-position
Phe	phenylalanine
Pi	inorganic phosphate
pNP	<i>p</i> -nitrophenol
q	quartet

qn	quintet
Qu	quinoline
RSC	Royal Society of Chemistry
s	singlet
SAX	strong Anion Exchange
sp	septet
SPi	inorganic thiophosphate
sx	sextet
t	triplet
TEAB	triethylammonium bicarbonate
THF	tetrahydrofuran
TLC	thin liquid chromatography
UDP	uridine diphosphate
UDP	uridine diphosphate
UDP-NAcGLC	5'- <i>O</i> -diphospho- <i>N</i> -acetyl D-glucosamine
UMPS	uridine 5'- <i>O</i> -monophosphorothioate
UMPSAc-pNP	<i>p</i> -nitrophenol acetyl uridine 5'- <i>O</i> -monophosphorothioate
UV-Vis	ultraviolet visible spectroscopy

1.0 INTRODUCTION

The strategic principles that we are hoping to establish fit into the criteria of the ‘Click’ chemistry reactions. We hope to launch a novel, aqueous thiophosphoryl-based chemistry that offers great potential for the introduction of thiophosphoryl groups as mimics of biologically important phosphate moieties. Phosphate esters have major functions in cells and have been the subject of a great number of investigations, both in terms of understanding of their functions and chemical synthesis, which will be presented in this chapter. We focus our attention on monophosphate systems, with a long-term aim towards nucleoside diphosphate features, as these are the natural substrates of the glycosyltransferases. The glycosyltransferases and their modes of action will be briefly introduced in this section. Our two synthetic strategies are outlined in the scheme 1.1.



Scheme 1. 1 Two proposed systems for the production of thiophosphoryl derivatives: I Thiophosphoramidate (Chapters 2.-4.), II Bromoacetyl (Chapter 5.). R¹⁻⁴- any aliphatic substituents

The nucleophiles that are employed in our systems are forced to compete with water and hydroxide ions as nucleophiles, therefore, we also review the findings of others in this context.

In addition, we tested some thiophosphoramidates containing a quinoline moiety generated using strategy I (scheme 1.1), against *Leishmania mexicana*, using *in vivo* assays. Chapter 4. is dedicated to a reviews of this protozoal parasite and the results that we gained in this study.

1.1. The 'Click' chemistry concept

'Click' reactions, named by K.B.Sharpless^{1, 2} are performed usually in water, under simple reaction conditions, and give crude products in high yields with inoffensive by-products. This approach presents the possibility of rapid generation of pools of new structures, by 'clicking' small repeating building blocks via heteroatom links (C-X-C). Nature's primary molecules: proteins, sugars, nucleic acids are also made from repeating amino acid units, monosaccharide and nucleotides, where connections are based on carbon-heteroatom bonds rather than carbon-carbon bonds. New compounds could then be used for '*in situ*' bioactivity tests without purification, which would allow for product screening approaches to proceed with greater ease.

Taking a cue from nature's approach, a set of powerful, highly reliable and selective reactions, in conjunction with the design of libraries of building blocks, has become a good strategy for the development and production of useful new compounds with desired property profiles.

'Click' chemistry uses only near-perfect chemical transformations, but there are only a few 'click' systems currently available, which limits the variety of products that may be accessed. However, it has been calculated, approximately, how many drug-like structures weighing less than 500 Da, consist of elements such as H, C, N, O, P, S, F, Cl, Br and are stable to water and oxygen could exist³. The number was around 10^{63} and an exceedingly small proportion has been touched so far. 'Click' chemistry enables the usage of a great variety of the building blocks which offers the potential for a greater repertoire of chemical entities being prepared in a facile manner.

The stringent criteria for a process to earn 'click' chemistry status are:

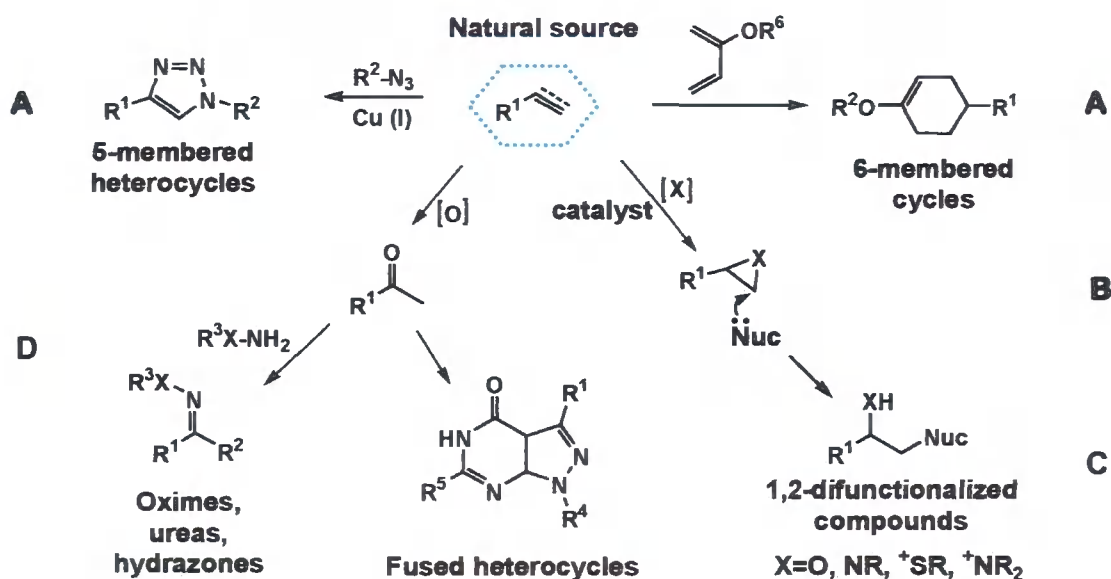
- application is modular and extensive in scope
- generates high chemical yield
- stereospecific
- generates innocuous side products, isolated *via* non-chromatographic procedures
- simple reaction conditions with systems insensitive to oxygen and water

- has readily available starting materials and reagents
- benign (preferably water) or easily removable or, even, no solvent
- easy product isolation by crystallization, distillation, extraction and not preparative chromatography
- products physiologically stable

The set of practical and reliable reactions for the synthesis of building blocks and compound libraries that fit into the click chemistry approach to date are (scheme 1.2):

- cycloaddition reactions with the premier example being the Huisgen 1,3 dipolar transformation, but also Diels-Alder reactions (A),
- addition to carbon-carbon multiple bonds, especially oxidation reactions such as epoxidation, aziridination and nitrosyl and sulfenyl halide additions (B)
- nucleophilic substitution chemistry in the form of ring opening reactions of strained heterocyclic electrophiles (C) such as epoxides, aziridines, cyclic sulfates, sulfamidates, aziridinium and episulfonium ions (B),
- carbonyl chemistry reactions of non-aldol type, such as formation of oxime ethers, hydrazones, ureas, thioureas, aromatic heterocycles and amides (D).

These transformations are illustrated below.



Scheme 1.2 A choice of reactions that meet the 'Click' criteria

1.1.1. Why water as the solvent?

Water is the basis and bearer of life. The human body consists of approximately 65% water; with lung and brain tissues containing nearly 80% water. All metabolic processes and transfers of crucial molecules affecting living systems occur in water. Together with carbon dioxide, water represents the beginning and the end of most of nature's reactions.

Organic chemistry, until recently was carried out almost exclusively in organic solvents. The success of Rideout and Breslow⁴ with Diels-Alder cyclisations performed in aqueous media, changed this traditional approach towards organic solvents application in organic transformations.

Water is surprisingly amenable to many processes for a range of reasons:

- readily recycled, decreases environmental concerns
- economical, the cheapest solvent
- very safe, not flammable, explosive, mutagenic or carcinogenic
- easy control of reaction temperature with water as the solvent, both endo- and exothermic reactions especially on large scale
- simple isolation of organic products in many cases

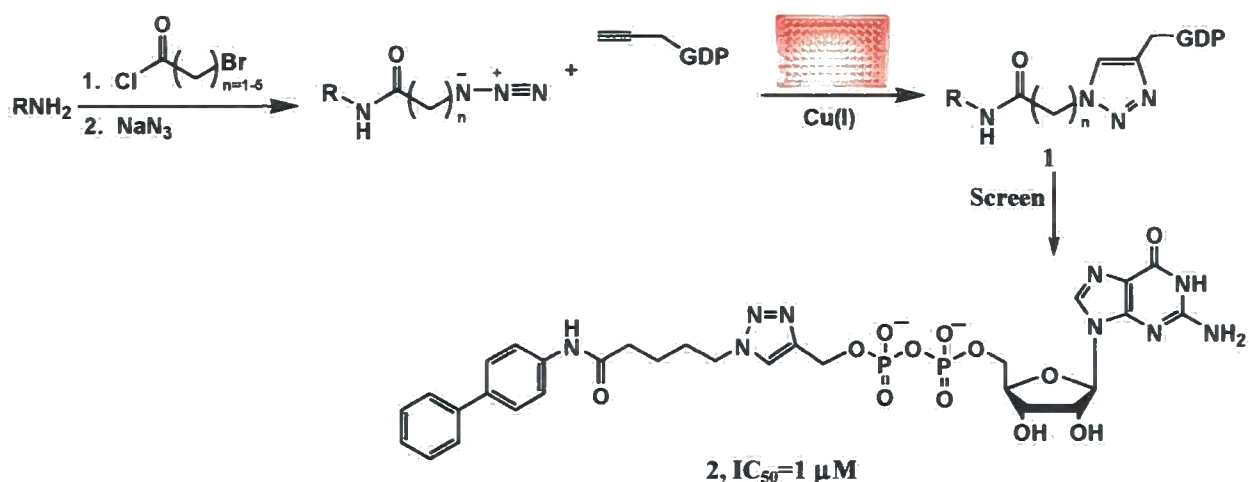
These are some of the reasons why water attracts much attention as a medium suitable for a range of reactions. Traditionally, organic reactions are performed in organic media, due to the opinion that solubility is essential for successful reaction. This approach has been suppressed by the practical realization of biphasic and water-solubilised reaction systems.

Whilst aqueous systems are not applicable in many cases of organic synthesis, we will present a few examples where water presented an ideal environment for highly efficient 'Click'-style reactions. The most popular and exploited triazole formation will be discussed in detail.

1.1.2. Some of examples of 'Click' chemistry

Of the reactions comprising the 'click' universe, one of the best examples is the Huisgen 1,3-dipolar fusion of alkynes and azides to form a broad spectrum of disubstituted triazoles.⁵ Until recently, concerns about the safety of work with organic azides have suppressed the employment of this group although it has great potential for use in synthetic transformations. Organic azides are potentially explosive substances that can decompose with input of energy from external sources (heat, light, pressure). Taking a number of precautions, however, azides can be prepared, purified and handled safely and this has renewed interest in their use in a number of organic routes. They are very effective at introducing nitrogen modifications into molecules with further reduction steps potentially leading to amines. This is a transformation that we have applied ourselves (section 3.2). As the structure is easily installed and very stable towards oxygen and water, azides present a crucial candidate for 'Click' chemistry reactions. Azide-structures are assumed to be the most energetic species, however, organic chemistry considers this functional group to be one of the least reactive groups. The spring-loaded nature of the azide group is not realised until it is exposed to a good dipolarophile. The slow nature and poor regioselectivity of the reactions performed with azides showed the need for a catalyst, which would help accelerate and control the cycloaddition reaction. Depending on the type of alkynes used in the reaction, there are two catalytic approaches to this cycloaddition process; copper -and ruthenium-catalysed.

The copper (I) catalyzed 'Click' union process of terminal alkynes and azides is a mild and very efficient process, requiring no protecting groups and easy product isolation procedures.⁵ It is a high yielding, regioselective and simple transformation that gives thermally and hydrolytically stable 1,4-disubstituted 1,2,3 triazoles (**1**). Sharpless and co-workers have exploited this approach in an investigation on novel, efficient fucosyltransferase inhibitors, which illustrated the enormous scope of this 'Click' system.⁶



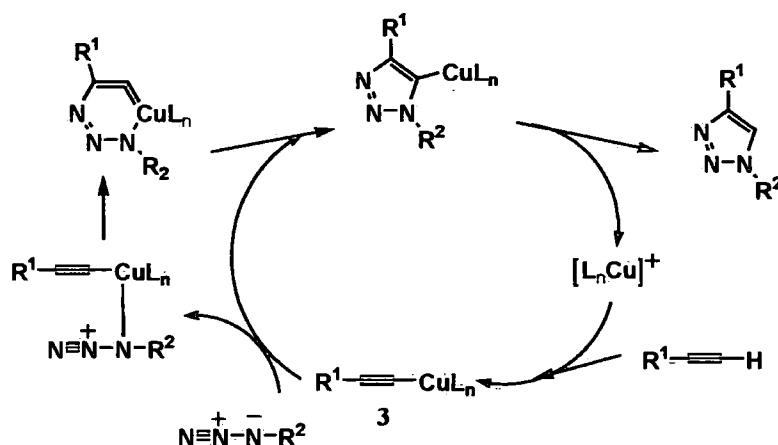
Scheme 1. 3 Alkyne-azide chemistry performed in microtitre plate with direct activity tests

The azide components in this screening process were prepared via formation of amides using an array of amines, followed by nucleophilic substitution of a terminal alkyl halide with sodium azide. Further cyclisation with a GDP-alkyne core generated a library of products. Yields as low as 39% were observed, however, the majority of the compounds were produced in the yields ranging from 70 to an amazing 100%, were pure enough to test directly against α -1,3-Fuc-T VI. This screen led to the finding of a highly potent, competitive inhibitor with structure **2** (scheme 1.3).

Copper catalysed 1,3-dipolar cycloaddition reactions are, in general, very tolerant to variations in the structures of substituted azides and alkynes and also pH-s (ranges from 4 to 12). No other special precautions were needed, however, the cyclisation process tends to take 18 h at room temperature to complete. Therefore, investigations into the acceleration of this process by applying microwave irradiation were carried out, enabling an impressive reduction of the reaction time from hours to minutes.⁷

The proposed mechanism for the cyclisation process involves formation of copper (I) acetylide **3** through a six-membered intermediate, retaining copper as a part of the ring (scheme 1.4).

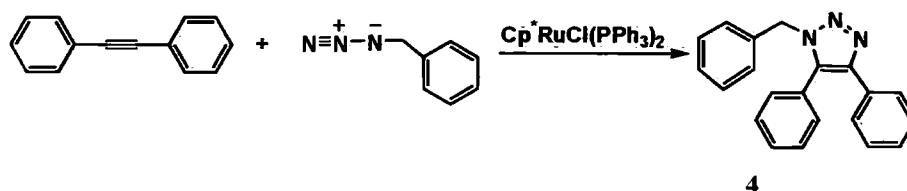
Further rearrangements in the cyclic structure release the catalyst, allowing the completion of this highly selective, reliable and productive connection process.



Scheme 1. 4 Proposed copper catalytic cycle for the formation of 1,4-disubstituted triazoles

With its dramatic rate acceleration and regioselectivity, this copper catalysed Huisgen 1,3-dipolar cycloaddition reaction with water as a solvent has fitted itself into the group of nearly perfect 'Click' chemistry transformations. This modular approach has been greatly exploited in a wide range of fields (described in the following sub-section).

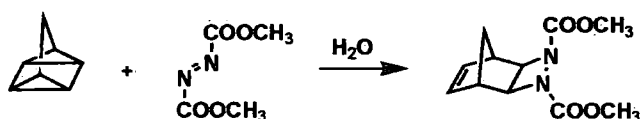
Recently, Sharpless and co-workers reported another possibility of catalytic cycloaddition of azides and alkynes to form the complementary 1,5-disubstituted triazoles (in satisfactory yields (>80%).⁸ Whereas Cu(I)-catalyzed fusion is limited to terminal alkynes, Ru(II) catalyzed cycloaddition is active with internal alkynes as well (scheme 1.5).



Scheme 1. 5 Ruthenium catalyzed synthesis of 1,5-disubstituted triazoles [Ru]=catalyst complex

However, the ruthenium supported cyclisation of two unsaturated molecules does not fulfil the standards for the nearly perfect 'Click' reactions, as it must be performed in pure organic solvents (benzene, toluene, THF).

One of many examples of the great rate acceleration that non-polar reactants may show ‘on water’ (a term coined by Sharpless) is the cycloaddition reaction of quadricyclane with azodicarboxylates (scheme 1.6).⁹ Originally, this reaction was carried out in toluene or benzene with heating and was completed after one day.¹⁰ When an aqueous suspension strategy was used at room temperature or even at 0 °C product was formed in 10 minutes and 1.5 hours, respectively, and high yields were observed.

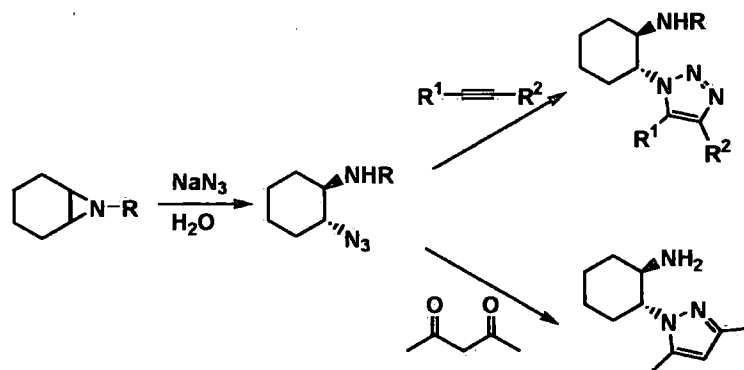


Scheme 1.6 Reaction of quadricyclane with dimethyl azodicarboxylate ‘on water’

In addition, a range of solvents and mixtures was tested in this system, in the search for effects of reaction heterogeneity/homogeneity on the rate of acceleration. In homogenous reactions (reactants dissolved in solvent), polar protic media such as methanol or methanol/water mixtures, acceleration of the reaction in comparison to organic solvents was observed. When water was used, forming a heterogenous reaction mixture, with or without methanol, rates were increased considerably. Similar water-effects on both rates and yields were recognized in the reaction of azodicarboxylates with alkenes as well.

Beside pericyclic reactions, nucleophilic ring openings of epoxides, aziridines, and cyclic sulfates, show ‘on water’ rate increases. It was suggested that in these cases, hydrogen bonding represents an important point for activation of these three-membered ring heterocyclic electrophiles.⁹ With epoxidation or aziridination of alkenes cyclic hetero-rings are formed. In the event of exposure of aziridine to a nucleophile e.g. sodium azide in water, a one-pot procedure towards 1,2-azido amines was possible. Aziridines are more elaborate as they offer the possibility of N-substitution and great variation of the products. However 1,2-azido alcohols are molecules important for synthetic processes in carbohydrate and nucleoside chemistry. Furthermore onward, cyclisation and condensation with alkynes and β -diketones makes these intermediates perfect for the rapid production of building blocks and library formation (scheme

1.7).¹ With pH and temperature control, very good yields, minimal side products and regioselectivity of epoxide and aziridine ring cleavage reactions can be achieved in water. Simple product isolation can be performed by phase separation or filtration.



Scheme 1. 7 Potential in application of nucleophilic ring opening. R=H, a substituent

The phenomenon of great rate acceleration of fusion of lipophilic compounds is currently poorly understood. However, some hypotheses have been made.^{1, 9} The free energies of organic molecules seem to be higher when solvation of components is reduced. Diels-Alder reactions are characterized by a negative volume of activation; the hydrophobic surface area of reactants in water is reduced on going from initial to transition state. Therefore, the Gibbs energy of the activation is lowered and the reaction is accelerated.^{11, 12} In additions to double bonds, differentiation of nonpolarizable and polarizable moieties is performed well in water. Partial and gradual slow solubilisation of compounds in water in some cases is possible, supported *via* intensive stirring that increases the surface area between non-polar reactant and water.¹³ The hydrogen bonding, charge stabilization and dipolar effects of water have been raised as potential factors. The large increases in rates could not be a simple dependence of polar effect, since some of polar solvents such as methanol, acetone and glycol do not present the same behavior of rate acceleration.¹⁴ When hydrogen bonding is not possible then it is obvious that hydrophobic interactions will play a crucial role in connection between non-polar reactants in water. Nature has largely exploited this phenomenon in the form of substrate-enzyme binding, membrane formation and the folding of proteins.

In conclusion, there are powerful precedents for efficient and simple reaction systems that avoid time-consuming chromatographic procedures that exemplify 'Click' chemistry. In particular, the copper catalysed 1,3-dipolar cycloaddition, has found great scope in applications in a number of fields.^{2, 15-19} Some of the enormous range of examples will be presented in the following section.

1.1.3. Wide application in biological systems

Azide and alkyne groups are largely inert towards biological molecules and the reaction conditions inside living systems, which allows the use of heterocycloaddition in target guided synthesis^{20, 21} and activity based protein profiling^{22,23}. 1,4-disubstituted 1,2,3-triazole linkages share useful topological and electronic features with Nature's ubiquitous amide connectors. In contrast to amides, triazoles are hydrolytically stable and are not susceptible to oxidizing or reducing systems. Nitrogen atoms are also possible electron donors in hydrogen bonding. Therefore, due to their favourable physicochemical characteristics and their biocompatibility, triazoles can be very useful in the process of biomedical research, such as drug discovery and tagging of biological systems.

Recognition of the highly potent inhibitor of α -1,3-fucosyltransferase with the help of the Cu(I) catalysed triazole formation was presented in the previous section. Another recent application of this triazole chemistry sought chitin synthase inhibitors in the form of novel 1,4-disubstituted-1,2,3-triazolyluridine derivatives with some compounds presenting high activity (section 5.2.2).²⁴

Structure guided synthesis of molecules with desired properties, has often not been as successful as hoped since the number of molecules that could be considered is often vast and sometimes the understanding of the systems involved has been poor to allow design. The idea of using an enzyme's binding site to fish out two small organic reactants and then force them to react with each other stereoselectively seemed like a very attractive new approach in the synthesis of a novel high-affinity inhibitors. 'Click' chemistry presents building blocks with

high built-in energy to stimulate spontaneous and irreversible connection with appropriate complementary portions in other blocks². Chemical and biological receptors can, thus, be used as templates to guide the formation of drug-like products. This 'in situ' approach is not a novel idea. A dramatic rate acceleration and increase in regioselectivity of a Diels-Alder cycloaddition in β -cyclodextrin was explored by Breslow some time ago⁴. The reaction between an azide and an alkyne in cucurbituril, which is a hosting cage compound, was first noticed by Mock^{25, 26}. However, using a biological target as the selector of building blocks has been relatively poorly explored.

Sharpless and co-workers have focused their search on acetylcholinesterase, responsible for neurotransmitter hydrolysis.^{27, 28} They used this enzyme as a reaction vessel for performing 1,3-dipolar cycloadditions between biocompatible azide and acetylene reagents²¹. Reacting structures were directed, by virtue of their structures, to the active and a peripheral site of the enzyme *via* binding groups and inoffensive spacers. When polar or hydrophobic structural groups of an azide containing and an acetylene-containing compound reside in adjacent binding sites, positioning reacting groups close to each other the click process is successfully performed in the absence of any other catalyst, yielding a product that is likely to be an inhibitor (figure 1.1).

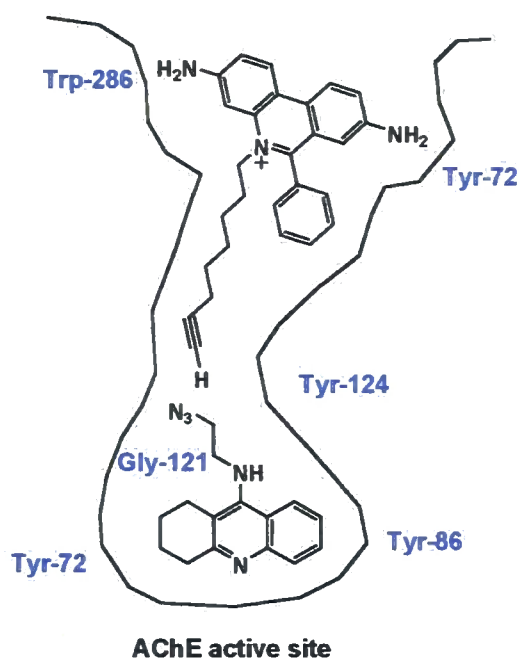


Figure 1. 1 Components brought together to 'click' in the acetylcholinesterase active site

This tactic resulted in the production of four extremely potent inhibitors (K_d in the femtomolar range) that are derivatives of tacrine and phenylpenethridinium azides and acetylenes. Combinations of building blocks that gave the *syn*- isomer showed more than 100 times greater potential in the inhibition process than *anti*-triazole isomers. With the application of an HPLC/MS selected ion monitoring technique, the selectivity and reliability of product identification was greatly enhanced enabling the testing of multicomponent mixtures and high throughput screening.

'Click' chemistry has also found its application *in vitro* and *in vivo* bioconjugation processes. Copper-catalyzed azide-acetylene union has been shown to be the best choice owing to its bio-orthogonal reactants, selectivity, reliability and tolerance to a wide range of solvents, most importantly, water. Tagging structures such as proteins, nucleic acids, oligosaccharides in live organisms for global analysis of their expression and functional levels is of great importance in the fields of proteomics, genetics and consequentially in medicine (cancer, HIV research).²²

Activity-based protein profiling employs triazole formation to analyze the functional state of and to track the location of enzymes in living cells and animals.²⁹ A 'perfect bioconjugation reaction' that does not affect living systems has been developed by Bertozzi *et al.*^{30, 31} Through the application of a cyclo-octyne activated by ring strain (figure 1.2) that lowers the activation energy of the alkyne-azide system, cycloaddition can occur without any catalyst and at lower temperatures.

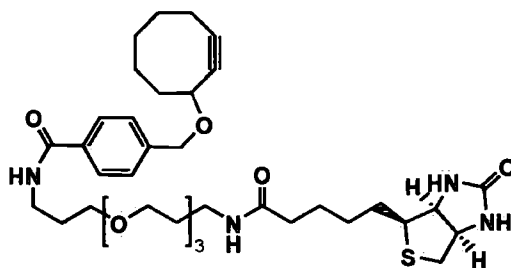
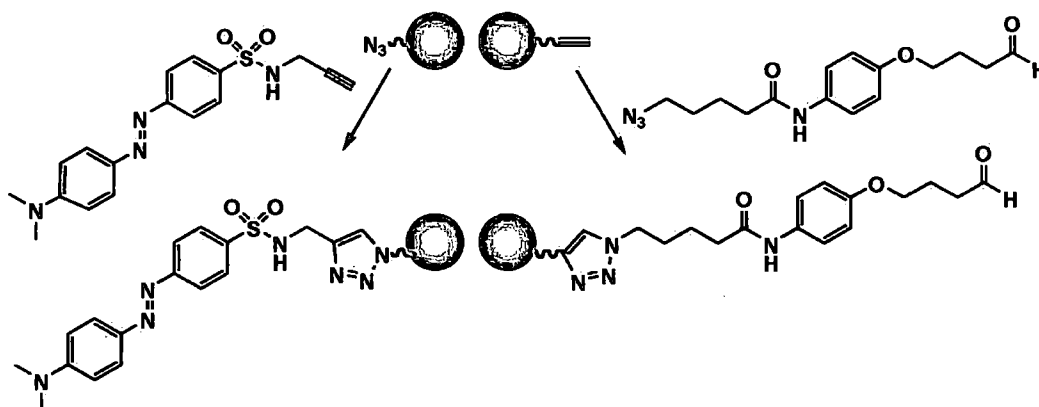


Figure 1. 2 Octoalkyne fragment utilised for strain promoted Huisgen cycloaddition

It is interesting that 'click' chemistry has found application in the area of separation chemistry as well, again using the azide-alkyne system. Finn³² has presented the possibility of using a 'click' strategy in affinity chromatography with agarose supports applied as the purification method for tagged biological molecules.



Scheme 1. 8 Agarose-based affinity chromatography agents

Great separation of monosaccharides and disaccharides has been performed on 'click' HPLC columns of different types³³ (figure 1.3). Applying the 'click' approach, different functional

substrates can be immobilized on the silica beads producing a few forms of functionalized HPLC packing. Some of these materials have shown great stability over a wide range of pH-s.

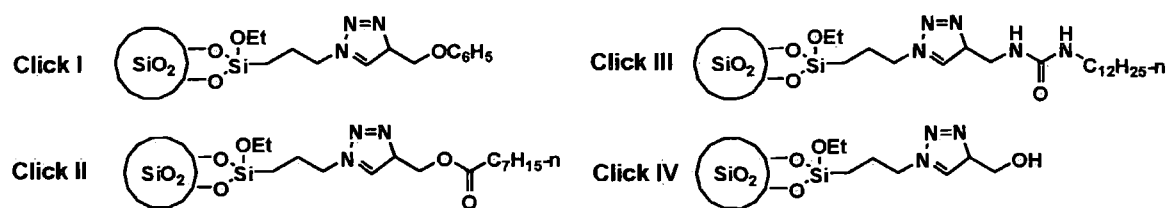


Figure 1. 3 'Click' HPLC resins

Great exploitation of this 'Click' Cu(I)-catalysed synthesis of triazoles was recognised in the formation of end-functional dendrimers, unsymmetric dendrimer structures and crosslinkers for nanoparticles and fine, defined thin-films³⁴. Also, *N*-glycosyl triazoles have been readily made using this method with potential for glycosyltransferase inhibition. *In vivo* imaging of fucosylated glycans is easily performed by incorporation of 5-azido-fucose into cell surface glycoproteins that are then exposed to an alkynylated fluorophore.³⁵ The list of the research subjects that have exploited this modular synthetic approach is extensive and is growing rapidly.

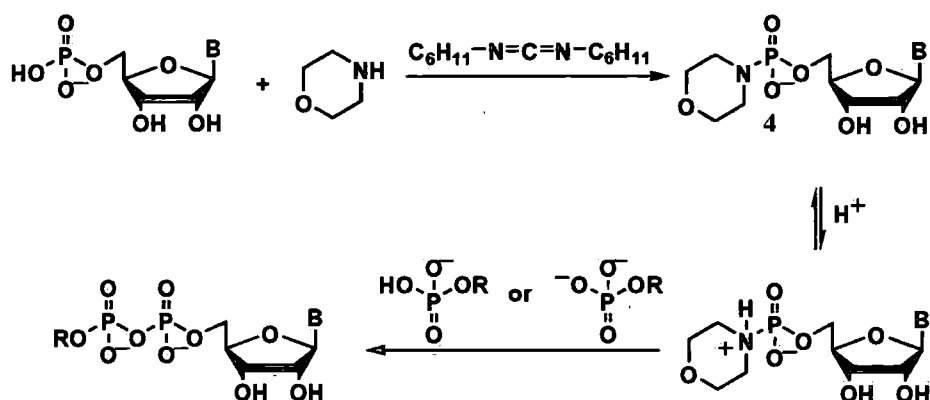
However, we have not used the Huisgen chemistry in our project, but the criteria and principles of the 'Click' approach, in the establishment and development of a simple and efficient reaction procedure based on thiophosphoryl group will be adopted.

1.2. Phosphates

Phosphate functional groups represent some of the most important and abundant features in biological systems, mainly in the form of mono-, di- and tri- esters. They play central roles in the physiology of cells and, therefore, are essential to every organism. Nucleic acids are built with the help of triphosphate linkages, which polymerise to give diesters with the expulsion of pyrophosphate. Phosphorylations and dephosphorylations of proteins are critical elements in the regulation of turning 'off' and 'on' the activities of many enzymes and receptors. Signalling networks are enabled via the phosphorylation of membrane components, i.e. proteins and lipids. Phospholipids, with their amphipathic behaviour, have the perfect characteristics for the

formation of cell walls. All processes in and between cells are feasible because of the facilitated release of energy *via* cleavage of pyrophosphate from ATP. The transport of sugar units, catalysed by glycosyltransferases, is performed with the help of nucleoside diphosphate moieties that we have an interest in mimicking.

In organisms, diphosphates of nucleosides are produced *via* the actions of the phosphorylating enzymes, nucleoside monophospho kinases.^{36, 37} In synthetic production, the most exploited method is Moffatt and Khorana's phosphorylation of nucleoside-5' monophosphoromorpholidates **4** from the 1960s.^{38, 39}

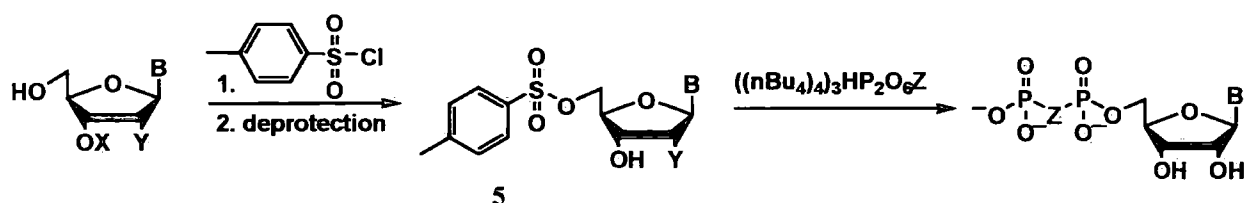


Scheme 1. 9 Morpholidate synthesis of diphosphates of nucleosides. R=monosaccharide

This method was based on the previously proposed synthesis of diphosphates using phosphoroamidates of nucleosides⁴⁰ and the assumption of efficient cleavage of the P-N bond in acidic media coupled with nucleophilic substitution by a phosphate moiety. In order to improve solubility and reactivity, a range of *N*-substituted phosphoroamidates were prepared (cyclohexylamine, piperidine, *p*-anisidine) and it was suggested that most of them afforded either lower yields or were very slow reacting when compared to morpholine (65-70%, over 3-5 days).⁴¹ This method was used to generate a range of nucleoside diphosphate derivatives (UDP-glucose, UDP-galactose, UDP-*N*-acetyl glucosamine, UDP-glucuronic acid, CDP-glycerol, GDP-mannose) and triphosphates⁴² and was employed during the total synthesis of Coenzyme A.^{38, 42} On the other side, the reaction time of this method was very long, three to five days at room temperature, and anion exchange chromatography was required, in some

cases re-chromatographing at a different pH was required in order to gain pure products. In addition, the nucleoside monophosphates used must also be prepared in some cases, and this is also a time-consuming task.

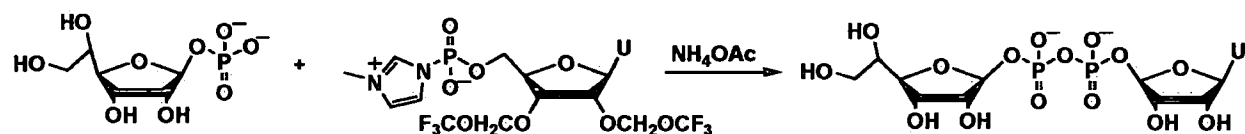
Another example of diphosphate synthesis involves direct displacement at the 5'-position of 5'-*O*-tosyl nucleosides **5** with organic-soluble salts of phosphoric acids.⁴³



Scheme 1.10 The synthesis of nucleoside 5'-diphosphate from 5'-*O*-tosyl nucleosides. X=protecting group, Y=H, OH and Z=O, CH₂

All NDP-s and a range of other nucleoside diphosphate derivatives (scheme 1.9) have been produced in varying yields from 43- to 93% by applying this method. Again, chromatographic purifications were required along with protection and deprotection steps for the preparation of tosylated nucleosides. Reaction times were, in some cases, as long as those described in the morpholidate approach (1-5 days) with the interesting exception of a dramatic rate acceleration in the example of 2',3'-*O*-isopropylidene-5'-*O*-tosyladenosine (12 fold) in comparison to the unprotected analogue, along with improved yields (from 72 to 93% for the protected nucleoside). It was believed that the effect of hydrogen bonding from the exposed hydroxyl groups decreased the nucleophilicity of phosphates towards the tosylate and a conformational change within the protected analogue also contributed to this observed result.

A procedure, similar to Moffat and Khorana's method, for the synthesis of UDP- α -D-galactofuranose employed a *N*-methylimidazole-activated nucleoside monophosphate⁴³, with the idea of increasing the activity of the electrophilic phosphoryl group.



In this example, the reaction time was shortened (2 h, 0 °C) with a slight excess of UMP-*N*-methylimidazolide **7** over α -D-galactofuranose 1-phosphate **6** being used. Acetonitrile was shown to be a better solvent for the uridine derivative than the anhydrous pyridine used in Moffatt and KhOrana's method. In addition, ammonium acetate buffer as the quenching solution decreased the appearance of side products and removed the trifluoroacetate protection of the nucleoside hydroxyl groups, which were added to improve the solubility of the UMP-derivative. ³¹P NMR spectroscopy suggested 83% of the desired product in the reaction mixture, which after ion-exchange HPLC, yielded only 35% of product.

All of the previously described methods suggest a demand for new and efficient procedures for preparation of nucleoside diphosphate derivatives that do not involve long reaction times and chromatographic purifications. The great number of synthetic methods for generating diphosphate linkers, described in this section, have also been used in the generation of mimics of natural substrates of glycosyltransferases.⁴³⁻⁴⁵ These enzymes and our interest in them will be briefly presented in the following section.

1.3. Research targets in the form of glycosyltransferases

Sugar transferases are enzymes that catalyse the transfer of monosaccharide units enabling the growth of oligo or polysaccharide chains. Also, glycosylation can occur on proteins, where both *O*-linked and *N*-linked glycoproteins can be formed. Depending on the sugar involved, there are fucosyl, glucosyl, galactosyl and many other transferases under the common name of glycosyltransferases (Gly-T). One type of glycosyltransferase, the non-Leloir type, utilizes lipid-linked glycosyl donors, with dolichol, polyprenol, sugar-1-phosphates or sugar-1-pyrophosphates, and they are present in a diverse range of organisms. The Leloir type, which are of interest to us, use glycosyl donors with nucleotide mono- or diphosphate (NMP and NDP) leaving groups for the biosynthesis of oligo- and polysaccharides.

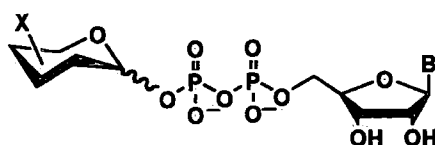
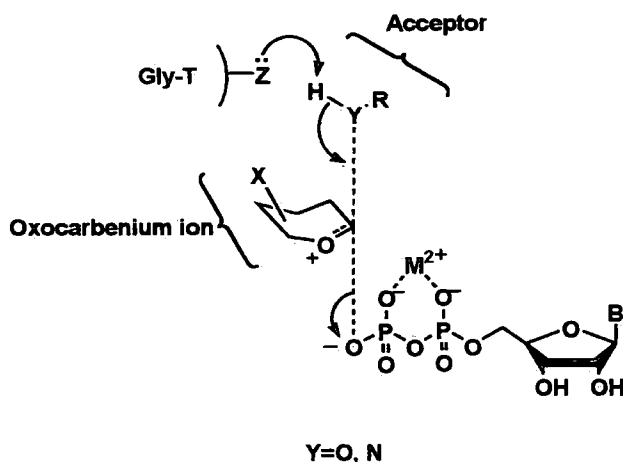


Figure 1. 4 General structure of the natural substrate of sugar transfer consists of a nucleoside connected to a sugar (-X) (with base B and -X being enzyme-dependent) over a diphosphate bridge

This is the way most glycoproteins, glycolipids and other glycoconjugates are produced in mammalian systems. It is interesting that mammals exploit just 9 sugar nucleotide donors: UDP-glucose, UDP-galactose, UDP-GlcNAc, UDP-GalNAc, UDP-xylose, UDP-glucuronic acid, GDP-mannose, GDP-fucose, and rather unusual CMP-sialic acid.

The general glycosyltransferase mode of action involves a four-partner transition state: sugar donor and acceptor, divalent metal ion and nucleotide (scheme 1.11). Therefore, natural substrate mimics or effective inhibitors require properties that enable recognition of the active centre of the glycosyltransferase as a natural substrate does.



Scheme 1. 12 General mechanism: transition state of the Gly-T-mediated sugar transfer to acceptor (RYH) where the base moiety (-Z) derives from the enzyme active site. In the case of NMP-sugar analogues the ionised phosphate group binds to the enzyme active site only, instead to metal ion (M)

In general, glycosyltransferases represent highly viable therapeutic targets as they are involved in the biosynthesis of glycoconjugates associated with immune response, metastasis and intracellular recognition and communication.

In the long term, our work is focused on fucosyltransferases and chitin synthases, which require guanosine and uridine diphosphate donors, respectively. We opted to investigate the synthetic procedures for the production of monothiophosphate derivatives of guanosine and uridine. Along the way, we have proposed and optimized new aqueous synthetic procedures for efficient preparation of substituted guanosines (section 3.2.4), in the form of the 5'-azide and 5'-amine⁴⁶, which enabled faster progress of our research. Once established, the methodology for the effective formation of monothiophosphate features can, in due course, be expanded to investigations on nucleoside diphosphate mimics that would, potentially, be active against glycosyltransferases. In addition, uridine monothiophosphate features coupled with an acetyl linker that structurally resembles the diphosphate group will also be developed. The understandings from these systems could be applied to almost all mammalian glycosyltransferases, as the majority of them require either guanosine or uridine nucleotide donors. This potentially opens up an array of fields where our achievements could be applied.

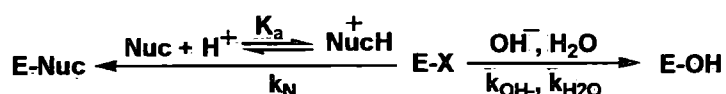
Reviews performed on fucosyltransferases and existing inhibitors along with our proposal towards strategies for novel agents are presented in the Chapter 3. Chitin synthase, its existing inhibitors and our progress towards uridine-like mimicking agents are described in the Chapter 5.

1.4. Nucleophilic reactions in water

As mentioned before (section 1.1), water is not a very common solvent in organic reactions. It was assumed that the solubility of the reactants was a crucial factor for the successful formation of desired products and that with the presence of water, the probability of side reactions occurring was increased. With the introduction of some examples of very efficient organic reactions,^{1, 4} where remarkable rate accelerations of reactions in water were observed, a new era of water-assisted chemistry was initiated (section 1.). The advantages of using water as the reaction medium are indispensable for investigations on biological systems, but also in terms of practical laboratory and industrial applications. In addition, the studies of King and co-workers¹³ have suggested great possibilities of directing reactions performed in water if a

thorough understanding of the reaction kinetics is available. The main tool that was used in these investigations was simple design and the appreciation of pH-rate profiles based on equations proposed by King and co-workers. This strategy is applicable to a variety of reaction systems. King has used C-alkylation of acidic ketones, sulfonylation and acylation of amines as representative electrophile-nucleophile systems, under pseudo first order conditions. In addition, the possibility of controlling nucleophile selectivity at either of the nucleophilic sites of 4-aminobenzylamine was investigated.

In the event of a reaction between a desired nucleophile, Nuc, and a hydrolysable electrophile, E-X, performed in water there is the possibility of competing hydrolysis processes occurring.



Scheme 1. 13 The potential pathways in the nucleophilic attack of a nucleophile Nuc onto an electrophile E-X in an aqueous environment. X= leaving group. The production of the desired substituted electrophile and decomposition via water and hydroxide ion

The overall pseudo first order rate constant k_T for the consumption of electrophile is the result of the sum of the hydrolysis and nucleophilic attack rate constants.

$$k_T = k_o + k_N \quad \text{eq.1}$$

where, $k_o = k_w + k_{\text{OH}^-} [\text{OH}^-] = k_w + k_{\text{OH}^-} K_w / [\text{H}^+]$ eq.2

represents the pseudo first order electrophile hydrolysis rate constant. This equation describes both un-catalysed (in this case, water assisted hydrolysis k_w) and hydroxide-supported events that have a far higher effect on the reaction outcome (k_{OH^-}), as hydroxide ion is stronger nucleophile than water, but its concentration can be varied as a function of pH.

$$k_N = k_{\text{Nuc}} [\text{Nuc}] = k_{\text{Nuc}} \text{Nuc}_T K_a / ([\text{H}^+] + K_a) \quad \text{eq.3}$$

The above equation represents the observed pseudo first order electrophile-nucleophilic attack rate constant. Both observed rate constants, k_o and k_{Nuc} can be used for the creation of pH-rate profiles and selectivity plots where the optimal pH conditions can easily be recognised (figure 1.5).

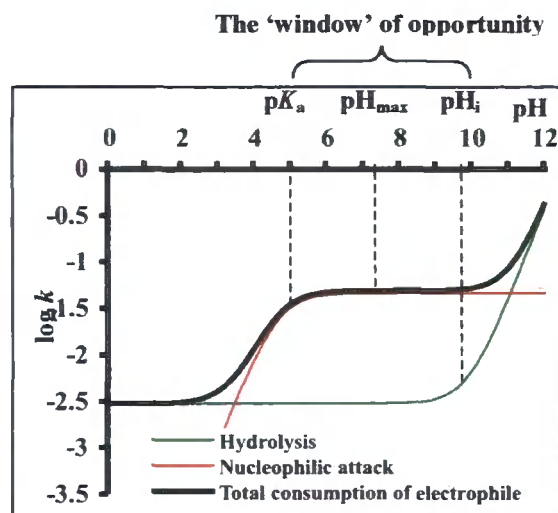


Figure 1. 5 pH profile for the nucleophilic attack of a nucleophile on a hydrolysable electrophile where the pH_{max} term can be recognised

It was suggested that the pH that provides maximal yield of desired product that arises from the nucleophilic attack of nucleophile on electrophile, rather than water and hydroxide ion, does not depend on the rate of the nucleophilic reaction or on the concentration of nucleophile [Nuc], as the following proposed equation shows:

$$pH_{max} = 1/2 [\log(k_w / k_{OH}) + pK_w + pK_a] \quad \text{eq.4}$$

The pH that provides the maximal reaction outcome in the electrophile-nucleophile system in water is defined by the rates of decomposition of electrophile (water and hydroxide assisted) and the pK_a of the conjugate acid of the nucleophile involved. The edges of the 'window' of opportunity, that define how far from the pH_{max} the variation can be while keeping the maximal yields of the reaction, are described by the pK_a value of the conjugated acid of the examined nucleophile at one end and pH_i ($\log(k_w / k_{OH}) + pK_w$) at the other end (the pH at which hydrolysis stops being pH-independent and is hydroxide ion dependent) and can be seen in the figure 1.5.

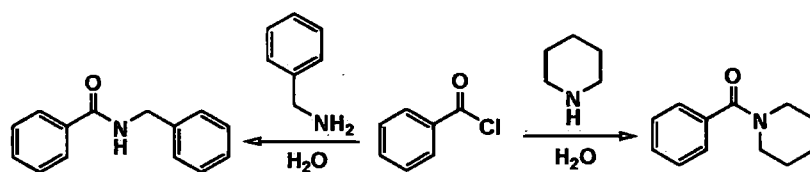
$$\text{Width of 'window' of opportunity} = pH_{max} \pm 1/2 [\log(k_w / k_{OH}) + pK_w - pK_a] \quad \text{eq.5}$$

The wider the 'window' is, the more flexibility there is in the pH conditions that can be used, while still gaining optimal yields. The 'window' of opportunity in the aminolysis of hydrolysable electrophiles can be also represented *via* a selectivity parameter that represents the theoretical yield (expressed as a fraction of total electrophile consumption) of the desired product as a function of pH:

$$f = \frac{k_N}{k_T} = \frac{k_{\text{Nuc}}[\text{Nuc}_T]K_a / ([\text{H}^+] + K_a)}{k_w + k_{\text{OH}}K_w / [\text{H}^+] + k_{\text{Nuc}}[\text{Nuc}_T]K_a / ([\text{H}^+] + K_a)} \quad \text{eq.6}$$

This term can conveniently be mapped onto the pH-independent section of the fraction-pH plot, where theoretical yield suffers no change with pH variation of the aqueous reaction solution (figures 1. and 1.7).

When the results gained both experimentally and *via* calculations, using the equations above under pseudo-first order conditions, were compared, deviations were minimal, confirming the validity of the proposed equations. If available in the literature; observed-rate constants for uncatalysed and hydroxide-promoted hydrolysis along with the pK_a s of the conjugate acid forms of nucleophiles can simply be applied in eq.5. In the case of constants that are not offered in the literature, simple kinetic experiments could give rise the required data. This was the case with the following example of reactions between benzoyl chloride and two amines, namely benzylamine and piperidine, to form the corresponding *N*-benzoyl amides (scheme 1.14).



Scheme 1. 14 Aminolysis of benzoyl chloride in water

Unlike the water catalysed observed rate constant k_w , the hydroxide ion rate constant k_{OH} was not found in the literature and, therefore, simple aminolysis experiments in water, with varying pH-s, were performed enabling, acquisition of pH_{max} from the pH rate profile. Through simple manipulation of equation 5, k_{OH} was obtained and used for the design of the calculated

selectivity (pH-yield) plot (eq.6, figure 1.6). Experimental points gained during aminolysis of benzoyl chloride with benzylamine and piperidine showed a good fit with the calculated curve.

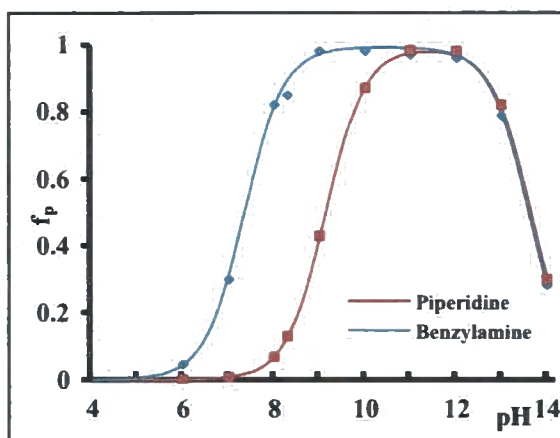
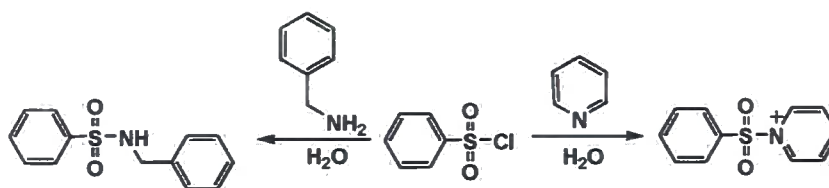


Figure 1. 6 pH-yield plot for the pseudo first order reactions of benzylamine and piperidine with benzoyl chloride. The selectivity of aminolysis over hydrolysis of the electrophile. ■, ♦ experimental points, — predicted curves

Another example of using this simple procedure for specifying, quite precisely, the most favourable pH conditions for nucleophilic substitution in water, with the potential of side reactions occurring, is the sulfonyl chloride system shown in the figure below.



Scheme 1. 15 Aminolysis of benzenesulfonyl chloride in water

The experimental points gained from this experiment were in the agreement with the estimations from equation 6. and can be seen from the figure 1. 7.

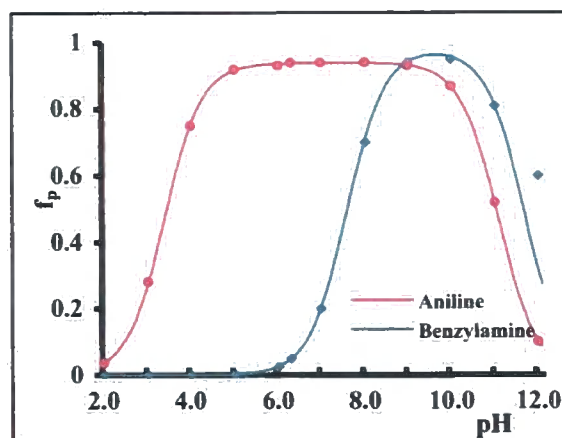


Figure 1. 7 pH-yield plot for the pseudo first order reactions of benzylamine and aniline with benzenesulfonyl chloride. The selectivity of aminolysis over hydrolysis of the electrophile.
 •, ■ experimental points, — predicted curves

It can be noticed from the above graph that the 'window' of opportunity in the case of aniline was much wider than for benzylamine, owing to the much lower pK_a of aniline, which is consistent with the amino function being less readily protonated as pH is decreased.

However, in both examples application of the optimal pH estimations assumed that nearly perfect reaction performance was applied. pH adjustment, control and mixing of the reaction system were believed to be faster than the desired reaction itself, otherwise the equations along with observed rate constants would deviate from the experimental outcomes. This would especially be the case if the electrophile were consumed *via* additional pathways rather than just by the attack of either water, hydroxide ion or the chosen nucleophile. With this in mind, general base promoted hydrolysis needs to be considered, through the nucleophile acting as general base, decreasing the formation of the desired product. However, the position of the pH_{max} is not dependent on the competing reactions in the system and the above-presented examples did not show any signs of general base catalysis.

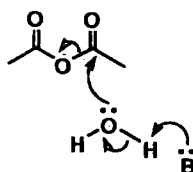
Constant pH conditions can be achieved using a pH stat meter that is not commonly available in every laboratory (certainly not in our laboratory). Efficient mixing of the reaction components in water and potential formation of the 'ideal solution conditions' can readily be achieved with

slow reactions in diluted mixtures. If a reaction is occurring in a separate organic layer, deviations in experimental vs estimated results can be expected. However, a co-solvent in a mixture does not effect the final outcome (as tested with the benzoyl chloride system), hence improvement in mixing and reagent distribution can be achieved by using a co-solvent in systems that present solubility problems, and the predictive equations can still be used.

In consideration of the above-mentioned factors, we have an approach of obtaining maximal yields of a desired product by a nucleophilic reaction, with competing hydrolysis reactions occurring, *via* prescription of the optimal pH using equation 4. This can be a particularly useful tool in the generation of libraries of products where a similar reaction method is applied across the library, and we hope to establish this type of technique in our work.

1.4.1. The effect of the general base assisted hydrolysis on nucleophilic reactions in water

In the event of the nucleophile being the additional factor in the hydrolysis of a studied electrophile *via* general base catalysis (scheme 1.16), the desired product cannot be gained in the predicted yields.



Scheme 1.16 General base catalysed hydrolysis of acetic anhydride

King and co-workers, noticing the existence of general base catalysis have investigated the easy routes to recognise and quantify this event.⁴⁷ In a system where e.g. acyl transfer onto an amine is performed, again, with known rate constants for water and hydroxide catalysed hydrolysis under a first order regime, using pH-yield profiles observed rate constants for aminolysis (k_{Nuc}) and amine assisted hydrolysis (k_{GB}) can be readily obtained. In order to adequately predict the yields, the potential effect of general base catalysis on the studied electrophile-nucleophile reaction must be considered. This can be performed using the following equation:

$$f = \frac{k_N}{k_T} = \frac{k_{\text{Nuc}}[\text{Nuc}_T]K_a / ([\text{H}^+] + K_a)}{k_w + k_{\text{OH}}K_w / [\text{H}^+] + (k_{\text{Nuc}} + k_{\text{GB}})[\text{Nuc}_T]K_a / ([\text{H}^+] + K_a)} \quad \text{eq.8}$$

A range of amines, including both primary and secondary, were acetylated with acetic anhydride under pseudo first order conditions, with the goal to test this equation and confirm the validity of its application. Aniline, was described in more details, using a pH-yield profile (figure 1.8)

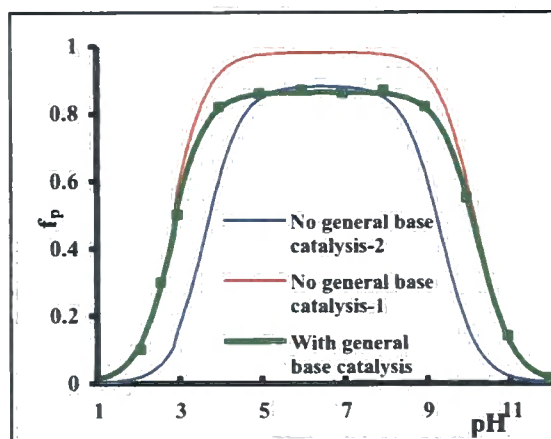


Figure 1. 8 pH-yield profiles for the reaction of acetic anhydride with aniline. 1 and 2 curves generated with two different reported values for the k_{Nuc} . ^{48, 49} ■ experimental points, — predicted curves

The lines 1 and 2 were created using equation 7 and previously reported observed rate constants. This gave a poor fit with either of the used k_{Nuc} values. When eq.8 was used, the fit of the experimentally collected data to the calculated pH-yield line was very much better.

In the examples with 3-methylbutylamine and piperidine, very little effect of general base catalysis was noticed as the application of the eq.7. that does not involve k_{GB} gave a passable fit (improved when a small k_{GB} value was included). In the case of *N,N*-diisopropylamine no amide product was formed, owing to the very slow acylation in comparison to hydrolysis. The rate of aminolysis was increasing, as the $\text{p}K_a$ of the corresponding conjugated acid of the amine was higher. However, 3-methylbutylamine, cyclohexylamine and *tert*-butylamine have presented rapidly decreasing rates (the ratio was 180:37:1) and a steric effect was blamed. On the other side, when rates for general base catalysis of hydrolysis by cyclohexylamine and *tert*-

butylamine were compared, the ratio was much lower (12:1) suggesting that, potentially, general base catalysis is not just a simple process of deprotonation of water by the nucleophile. The effect of the hydrogen bonding of the water's oxygen and the amine's hydrogens may be involved.

Another route to assist recognising general base assisted hydrolysis was proposed, using the product ratio-pH profile under pseudo first order conditions, that can be calculated *via* following the equation where no general base catalysis has occurred:

$$r = \frac{k_N}{k_o} = \frac{k_{Nuc} [Nuc_T] K_a / ([H^+] + K_a)}{k_w + k_{OH} K_w / [H^+]} \quad \text{eq.9}$$

and in the case of expected general base catalyses:

$$r = \frac{k_N}{k_o} = \frac{k_{Nuc} [Nuc_T] K_a / ([H^+] + K_a)}{k_w + k_{OH} K_w / [H^+] + k_{GB} [Nuc_T] K_a / ([H^+] + K_a)} \quad \text{eq.10}$$

Again, the practicality of using this approach enables quick detection of general base catalysis in the reaction system with the knowledge of the pK_a of the studied amine and pH_i ($\log(k_w / k_{OH}) + pK_w$) with no requirement for determination of rate constants for nucleophilic and general base catalysed consumption of the electrophile. Both of the methods (calculations using eq.8 and eq. 10) have direct application in synthetic chemistry for the examination of reaction mechanisms. The awareness of general base assisted hydrolysis is of a crucial importance, owing to the possible decrease in the expected yields should it be present. In addition, if the desired reaction is the full conversion of the nucleophile, this issue can be avoided *via* application of an excess of electrophile. This is applicable only when the excess of electrophile or side products can be readily removed from the desired product, which was not the case in some of our experiments (see experiments with thiophosphoryl chloride (Chapter 2.) and bromoacetyl phenol esters (Chapter 5.)).

1.4.2. The phenomenon of high yields in the reactions of benzenesulfonyl chloride with amines at high pH⁵⁰

King *et al.* performed studies on the aminolysis of benzenesulfonyl chloride under pseudo first order conditions, using both primary and secondary amines, and deviations from the results expected for general base catalysis alone were observed. At very high pH-s (1 M NaOH), much greater yields than the predicted were generated, leading to a sigmoid pH-yield curve (figure 1.9).

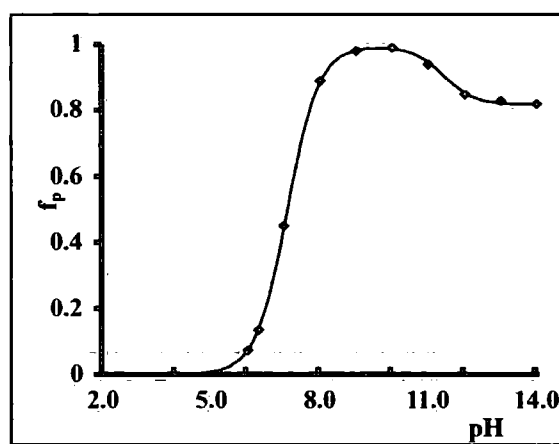


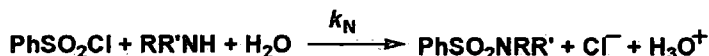
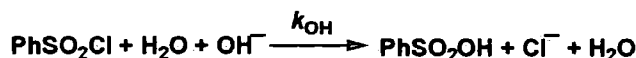
Figure 1.9 pH-yield profile for the reaction of benzenesulfonyl chloride with dibutylamine.
♦ experimental points, — predicted curves

This trend was observed for amines with larger numbers of carbons, suggesting the importance of hydrophobicity of amine substituents (benzyl, dimethyl, diethyl, dipropyl, dibutyl, hexamethylene). At high pH the concentration of free un-protonated amine is maximal and ionic strength is very high which can induce association of organic molecules and increase the productivity of the reaction. Therefore, King *et al.* proposed, and proved, the need for the introduction of new terms in the pH-yield profile equation, namely two third-order events (scheme 1.16).

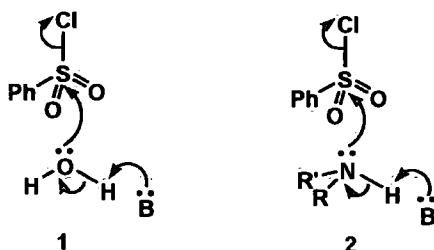
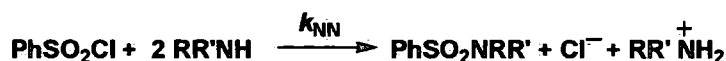
1st order reaction:



2nd order reaction:



3rd order reaction:



Scheme 1. 17 General base hydrolysis and aminolysis of sulfonyl chloride. **R, R'**= hydrophobic substituents

The third order aminolysis process 2 scheme 1.17 has clear analogy with general base catalysed hydrolysis and is involved in the pH-yield profile equation:

$$f = \frac{k_{\text{N}}}{k_{\text{T}}} = \frac{k_{\text{Nuc}}[\text{Nuc}] + k_{\text{NN}}[\text{Nuc}]^2 + k_{\text{NOH}}[\text{Nuc}][\text{OH}^-]}{k_{\text{w}} + k_{\text{OH}}[\text{OH}^-] + k_{\text{Nuc}}[\text{Nuc}] + k_{\text{GB}}[\text{Nuc}] + k_{\text{NN}}[\text{Nuc}]^2 + k_{\text{NOH}}[\text{Nuc}][\text{OH}^-]} \quad \text{eq.11}$$

With the previously measured observed rate constants for water, hydroxide and amine catalysed benzenesulfonyl chloride consumption and a few experiments with varying concentration of amine; the other rate constant (k_{GB} , k_{NN} and k_{NOH}) could be obtained.

In order to prove the assumption that greater yields gained at higher pH could be assigned to the hydrophobic effect, a few experiments that influenced the solubility of the compounds in water

were performed. An increase in the hydrophobic effect and, therefore, yield was noticed in a reaction performed at high ionic strength (addition of sodium chloride). This is a more polar medium than plain water, favouring greater development of charge separation in the transition state. When co-solvent was added to the reaction mixture improvement of yields at high pH was suppressed because the hydrophobic effect was reduced and the pK_a of the amine conjugate acid was lowered. In a comparison experiment between dibutylamine and bis(2-methoxyethyl)amine, which contains a polar ether oxygen, the hydrophobic effect was reduced and no sigmoid shape in the pH –yield profile of the latter was noticed.

To confirm that conclusions gained under pseudo-first order conditions were applicable to preparative experiments, a number of reactions were performed and yields recorded at pH_{max} (89-99% yield), pH below pH_{max} (45-96%) and in 1M NaOH (45-98%), at higher concentrations, and in the presence of a slight excess of benzenesulfonyl chloride, over a range of amines. Very high yields of octylamine, dipentylamine and hexamethylenamine benzenesulfonamides (>97%) were believed to have been attained, owing to the hydrophobic effect and the high k_{NOH} term.

In conclusion, pH-yield profiles are very useful and straightforward tools in elucidating the effects influencing the roles and interactions of water with organic molecules. Considerations of factors such as general base catalysis and the amine substituent hydrophobic effect, are needed in the design of organic reactions performed in water. Equations such as eq. 5, 6, 10, 11 can be applied in predictions of synthetic chemistry outcomes in electrophile-nucleophile systems in aqueous solutions, obviating the need for hard work on experiments that have a lower chance of a good performance. In addition, mechanistic studies on the interactions of organic structures in water can lead to very fruitful information that can help improve organic synthesis, especially in the cases of compound library production. These findings we hope to apply in our attempts to establish novel nucleophilic reactions in water, based on the thiophosphoryl moiety.

1.5. Project outline: Development of thiophosphoryl ‘Click’ chemistry

With the characteristics of the ‘Click’ approach in mind, we propose two novel Thiophosphoryl- based strategies for the development of (di)phosphate mimics.

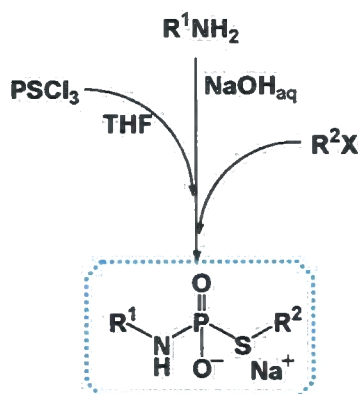
We opted to set up aqueous systems for the advantages they offer (section 1.), where a co-solvent would be applied, as needed. The experimental practice involves simple mixing of components, leaving them to stir followed by direct tests on the purity of the generated compounds, which would potentially also be used directly to test activity against chosen enzymes, as inhibitors or substrates. In order to enable direct efficacy assays, the chemistry could, be performed in 96-well microtitre plates, as described in section 1., and with, hopefully, high purity of the products, no chromatographic purification would be required. With the application of this approach, a great number of potential agents could be produced and screened. With the winning combination of components, hopefully, some potent agents could be identified.

We have adopted two approaches: the thiophosphoramidate system (Chapter 2.) and the bromoacetyl system (Chapter 5.). In both proposals, three components were mixed together, allowing the chemistry to happen (scheme 1.17 and 1.18). Given that three components were used in each of these strategies, we henceforth refer to them as the Thiophosphoramidate- and Bromoacetyl- Tripartite methods.

1.5.1. Thiophosphoramidate system

As a parallel to the previously established aqueous phosphorylation of 5'-amine-5'-deoxyguanosine in our group^{51, 52} (section 2.1), we hope to develop and optimize aqueous thiophosphorylation strategies for amines. The potential was recognised because of the high productivity of direct phosphorylation, using phosphoryl chloride of 5'-amine-5'-deoxyguanosine in aqueous sodium hydroxide. Therefore, we hoped that thiophosphoryl

chloride would perform with similar proficiency in the thiophosphorylation of amines. The resulting thiophosphoramidates can hopefully be readily alkylated through their sulfhydryl functionality, introducing great variation in product formation.

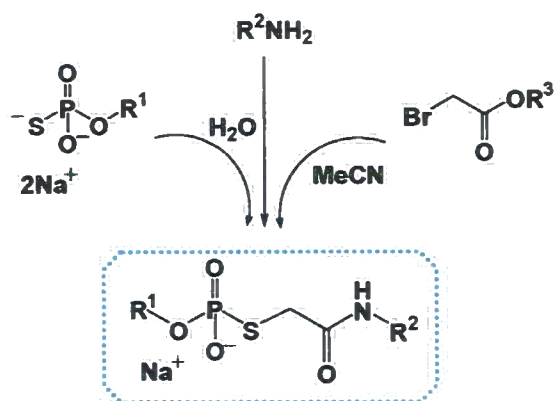


Scheme 1.18 Thiophosphoramidate Tripartite idea R^1, R^2 =any aliphatic substituents, including nucleosides

Our one-pot procedure would consist of an amino-thiophosphorylation step using thiophosphoryl chloride, in water/organic media, followed by alkylation. Optimisation experiments performed on this system using commercial amines and alkylation agents will be described in this thesis. Then, we moved to more challenging investigations involving nucleoside derivatives, amines and alkylating agents that, in due course, could lead towards production of mimics of glycosyltransferase natural substrates and our initial experiments in this area will be described in the Chapter 3.

1.5.2. Bromoacetyl system

In this example of Tripartite chemistry, the sulfhydryl moiety was alkylated using a bromoacetyl moiety offering product diversity *via* amide bond formation. In addition, thiophosphoramidates that have not been *S*-alkylated are hydrolytically labile, so we initially opted to investigate thiophosphorylated alcohols that would create less labile thiophosphate esters.

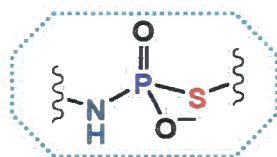


Scheme 1. 19 Bromoacetyl Tripartite reaction. R^1 = uridine used in our experiments, but it can be any aliphatic feature like R^2 , OR^3 -good leaving group

A set of experiments with a variety of leaving groups on the bromoacetyl system were performed and will be presented in this thesis. In addition, kinetic studies on the hydrolysis and aminolysis processes were investigated in an attempt to understand the reaction system.

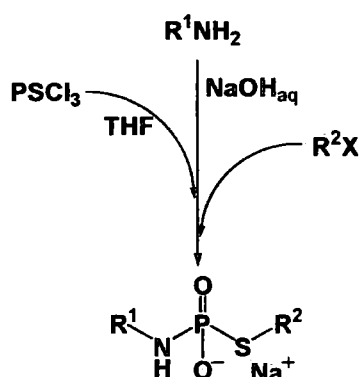
2.0 The Thiophosphoramidate system

P-N bond in the thiophosphoryl derivatives of amines, non-*S*-alkylated and *S*-alkylated, has shown reasonable stability in comparison to their parent oxy-phosphoryl analogues, both hydrolytically and biologically.^{53, 54} In addition, the softer sulfhydryl nucleophile opens up a wide range of possibilities in terms of reactivity towards electrophilic carbon centres. Amines are readily oxy- and thiophosphorylated as *N*-features are usually highly nucleophilic species. The P-N link is subject to faster degradation than its P-O originator, however, its hydrolysis is still slow on a laboratory timescale. This can be assumed as a disadvantage or an extreme benefit, depending on the chosen research target, compound or metabolite. As a combination of all these statements, we recognise thiophosphoramidates, as research targets that have been the subject of few investigations so far, even though they offer a diversity of possibilities and applications.



With the 'click' criteria in mind, we set out to, hopefully, establish efficient, simple and fast routes towards arrays of products with the thiophosphoramidate moiety as the foundation of one branch of our Tripartite strategies, previously introduced in the Chapter 1. The long-term aim of this approach is to enable, in due course, the production of library of compounds with a diphosphate element that would then, by mimicking natural substrates, potentially, be usable as glycosyltransferase inhibitors or substrates.

The Tripartite approach, in the context of thiophosphoramidate systems is illustrated by the scheme shown below.



Scheme 2. 1 The Thiophosphoramidate Tripartite idea

As introduced in section 1., the key features in this approach are the application of commercially available reagents (unfortunately, these are not accessible in the case of nucleoside derivatives), avoiding reagent preparation procedures, and to then simply mix the components and allow the chemistry to happen. In this particular example, thiophosphoryl chloride and a variety of amines and alkylation agents can be found in the chemical catalogues. Thus, our designed synthetic procedure involves thiophosphorylation of an amine dissolved in aqueous sodium hydroxide (in order to neutralise acidic species formed and ensure product stability), and direct use of thiophosphoryl chloride, dissolved in dry tetrahydrofuran (aqueous method established in our group, section 2.1). Then, in the same reaction vessel (in due course microtitre plate) simple alkylation will be performed, hopefully, achieving high conversions so that any chromatographic purification procedures are avoided. In this way, due to the benign solvents used and the high purity of the compounds, assays on the products towards target enzymes can be carried out directly in 96-well microtitre plates. With careful choice of reaction starting materials, hopefully, some active agents can be recognised, in the form of potential enzyme inhibitors or substrates.

As the first step of this method involves thiophosphorylation, which takes place in aqueous solution, this parallels previously established aqueous amine phosphorylation approaches in our group. Later in this chapter will be an introduction to how we noticed the prospect of this method in our thiophosphoramidate Tripartite idea. In order to further progress this

methodology, an understanding of the stability of thiophosphorylated amines is of a great importance and, therefore, hydrolytic studies have been performed. With recognition of optimal conditions for the highest stability of thiophosphoramidates in hand, we aimed to perform investigations on the alkylation of the thio-moiety and optimize this process. Our insight gained during these method development experiments, was then successfully applied through the involvement of nucleoside monothiophosphoramidate derivatives that, structurally, are the starting point for developing sugar transferase natural substrate mimics.

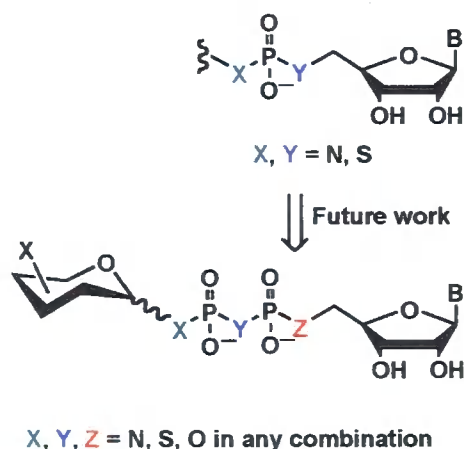
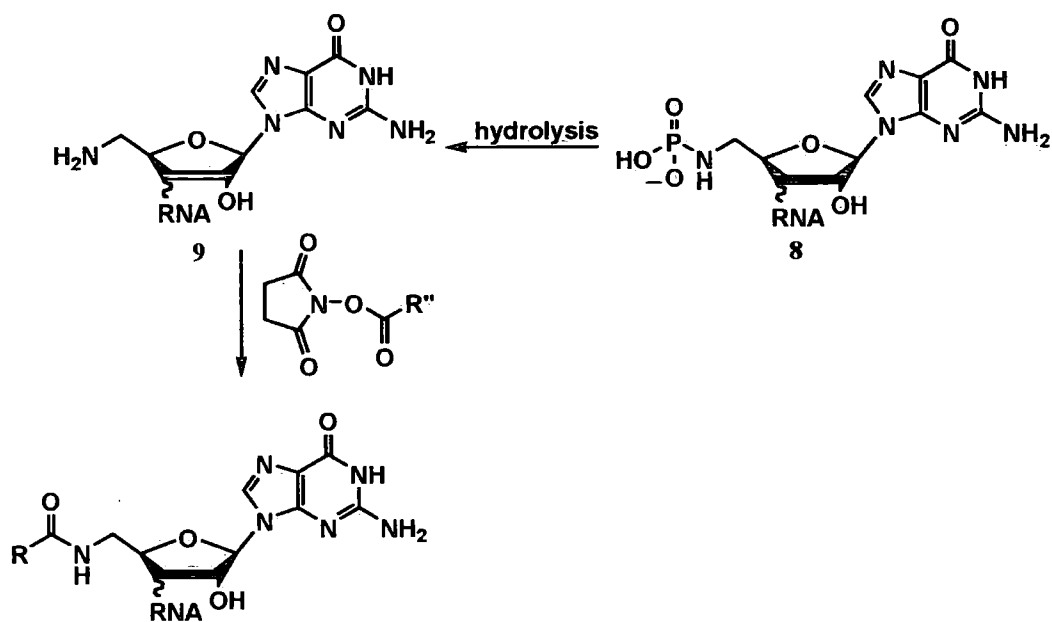


Figure 2. 1 The final goal of the research: generating diphosphate derivatives

2.1. The foundation of the thiophosphoramidate idea

During investigations towards enzymatic incorporation of 5'-aza guanosine features into RNA molecules, with the aim of improved initiation of T7 RNA polymerase-promoted transcriptions, David Williamson,^{51, 52} a former member of our group, developed and optimised a convenient method for the preparation of phosphorylated 5'-amino-5'-deoxyguanosine **8**. Once incorporated into the RNA, the possibility of bioconjugation with e.g. activated esters to afford amide-linked features, was enabled *via* spontaneous hydrolysis of the labile phosphoramidate and release of a free amine group.



Scheme 2. 2 Preparation and bioconjugation of modified RNA via methods established in our group

In this section we will briefly present how David Williamson went through the establishment and optimisation of an aqueous phosphorylation procedure. To start with, Dean's method⁵⁵ was employed to gain, 5'-azido-5'-deoxy guanosine that was effectively reduced to amine **9** (these methods are described in the section 3.2). After reviewing and attempting a range of methods, Williamson adopted Druckhammer's aqueous phosphorylation⁵⁶ approach. The key feature in this method was chemoselective amino-phosphorylation attained *via* slow exposure of highly nucleophilic amines to phosphoryl chloride, diluted in dry tetrahydrofuran. In this way competing hydrolysis of the phosphorylating agent was disfavoured. The presence of sodium hydroxide in the reaction solution was required for neutralising acidic species formed and maintaining the high pH needed for greater stability of the phosphoramidate that was being formed.

The first phosphorylation attempt was promising (monitored using coupled ³¹P NMR spectroscopy) affording low conversions of phosphorylated 5'-amino guanosine **10**. Therefore, after a reassessment of the key factors in the aqueous method and the assumption that hydroxide ion would be the most significant variable, a set of experiments was performed

where the number of equivalents of sodium hydroxide used was varied. For the optimisation studies, a simple procedure of dissolution of 5'-amino-5'-deoxyguanosine in aqueous sodium hydroxide and exposure to POCl₃ diluted in THF was applied.

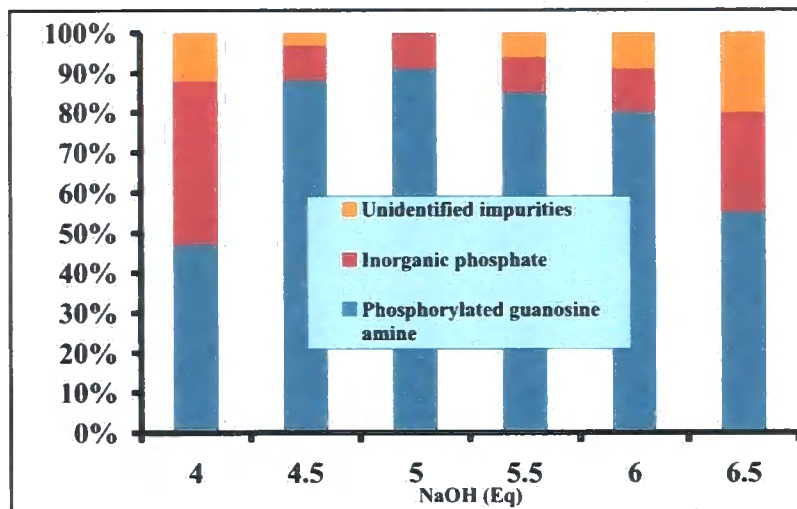
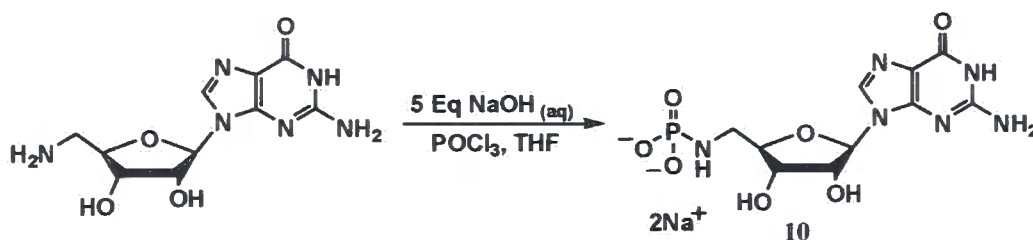


Figure 2. 2 Sodium hydroxide optimisation studies

The results of this study showed that excellent conversions of 5'-amino-5'-deoxyguanosine were achieved *via* this aqueous phosphorylation method if 5 equivalents of sodium hydroxide were applied.



Scheme 2. 3 Aqueous method for successful phosphorylation of guanosine amine

This showed that by using 5 equivalents of sodium hydroxide and dropwise addition of phosphoryl chloride in dry THF, the balance between solubilisation of guanosine through deprotonation of N-3 group (pK_a of 9.4) and competitive hydrolysis of the phosphorylation agent was achieved, and conversions as high as 91% according to ³¹P NMR spectroscopy were seen. Therefore, we hoped to use this approach in the analogous thiophosphorylation of amines,

both commercially available amines and biologically important amino nucleosides, and, hopefully, establish efficient thiophosphoramidate Tripartite chemistry.

2.2. Simplification of the diphosphate motif—development of mono *S*-alkylated thiophosphoramidates

As mentioned previously (section 1.3), the majority of the natural substrates of glycosyltransferases that we are interested in mimicking, which are of the Leloir type, employ nucleoside diphosphate carriers of monosaccharides. Some of the existing inhibitors contain mimics of the diphosphate bridge, while others modify the corresponding sugar features maintaining the metal binding abilities in the form of invariant diphosphate structures. The key to our strategy for the design of novel NDP-sugar analogues is the alteration of the diphosphate linker by the substitution of phosphate oxygens for sulfur or/and nitrogen with a number of different variations (figure 2.3). In addition, this offers a diversity of structures and methods of preparation.

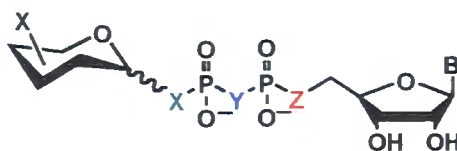


Figure 2. 3 Generic structure of an NDP-sugar mimic. **X, Y, Z** = O, S, NH

The combination of the heteroatoms in the diphosphate moiety depends on the practicalities of the synthetic methods towards them. Two philosophies can be put forward concerning stability. High stability would be preferred where direct activity tests and the synthesized compounds are to be performed against enzymes (most of the previously presented inhibitors). On the other hand, having the possibility of predictable and controlled degradation of synthesized molecule can be of particular potential in prodrug design (sections 3.6).

As direct investigations on the synthesis of modified diphosphates could be rather challenging, we simplified the strategy for our method development in order to understand the chemistry occurring and, ultimately, apply our insight to diphosphate methodology development in the future.

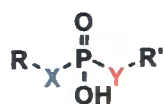
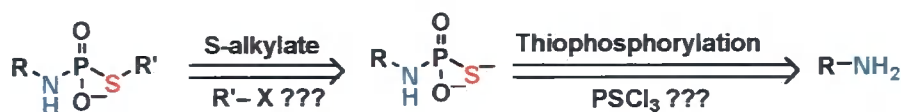


Figure 2. 4 A more approachable starting point. **X, Y** = S, NH and **R, R'** = any aliphatic moiety

In our thiophosphoroamidate chemistry we opted to create products that contain substituted phosphate features connected over nitrogen on one side and sulfur on the other. This change introduces hydrolytic instability compared to a normal phosphodiester, but, usually, resistance towards nucleolytic enzymes would be greatly improved^{54, 57}. In addition, P-N-R or P-S-R bonds are easier to make with a great number of possible synthetic routes open. A disconnection strategy that provides the inspiration for pathways towards the desired thiophosphoroamidate product is presented below (scheme 2.4).



Scheme 2. 4 Disconnection tactic towards creation of the synthetic strategy

Having the Tripartite idea and the ‘Click’ criteria in mind, we hoped to set up a very simple and quick reaction system that would, hopefully, be efficient. As we have already presented in the section 2.1, an aqueous method for phosphorylation of amines, established by David Williamson^{51, 52}, was very efficient for the introduction of a phosphate moiety onto a 5'-amino-5'-deoxyguanosine. We hoped to apply the same principles for the thiophosphorylation of amines. Establishment of the method was performed using commercially available amines of varying characteristics followed by application towards nucleoside derivatives. As for further elaboration of the thiophosphoramidate, simple alkylation of the soft S-nucleophile would hopefully proceed with high conversions and simple experimental practicality. Again, as for amines, many different types of alkylation agents could be used, increasing the possible diversity of alkylated thiophosphoroamidates that could be generated.

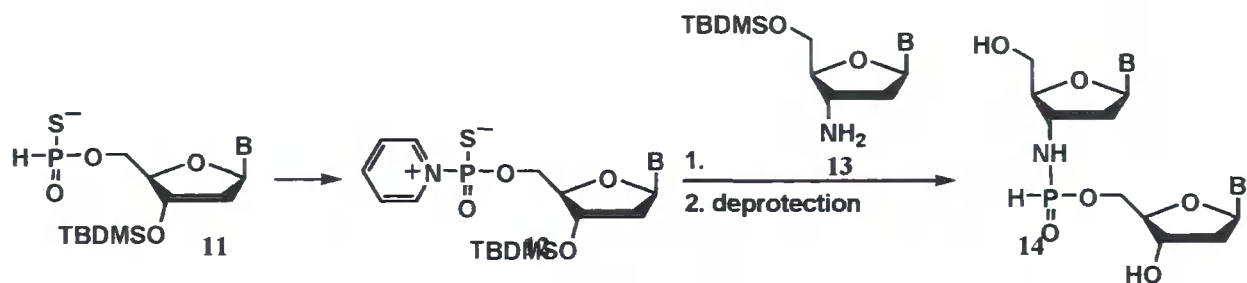
^{31}P NMR spectroscopy has proven to be essential as a very quick and easy indicator of the level of conversion in thiophosphoryl chemistry, as it allows us to monitor the outcome of reactions in the actual reaction media (water and tetrahydrofuran). This speeds up the investigation process significantly and enables rapid evaluation and optimisation of reaction conditions. In addition, when ^{31}P coupling to protons was applied, specific splitting patterns of phosphorus signals were generated depending on the number and position of protons neighbouring the thiophosphate group, and this was an extremely valuable tool for fast identification of the resulting reaction products. These principles of ^{31}P NMR spectra collection and analysis were applied throughout the whole research project.

Therefore, with a simple strategy of synthetic methods for effective thiophosphorylation and alkylation, and a quick and easy analytical technique for monitoring events in the reaction mixture, we started to investigate the preparation of thiophosphoramidate derivatives.

2.3. Existing methods for generating thiophosphoramidates

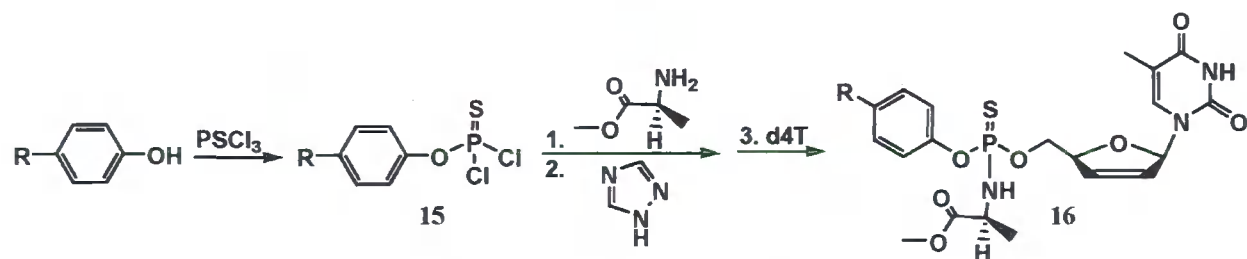
Methods for the preparation of nucleoside phosphoramidates are far more abundant in the literature than for the thiophosphoramidate analogues that we are interested in. Here, we briefly outline a few of the current methods used in the thiophosphoramidate area that have found applications in biologically useful compounds, along with their advantages and disadvantages.

Oligo thiophosphoramidates that were used in hydrolysis studies described in section 2., were prepared applying Stawinski's method⁵⁸ using *H*-phosphonothioate (11) methodology combined with the formation of a pyridine adduct of a nucleoside thiometaphosphate 12, which in a reaction with 3'-amino-3'-deoxynucleoside 13, gave rise to the desired dinucleoside thiophosphoroamidate 14 (scheme 2.5). This procedure required protection of starting materials and consequential deprotection steps, all performed in organic media.



Scheme 2. 5 Synthesis of dinucleoside thiophosphoramidates using H-phosphonothioate approach

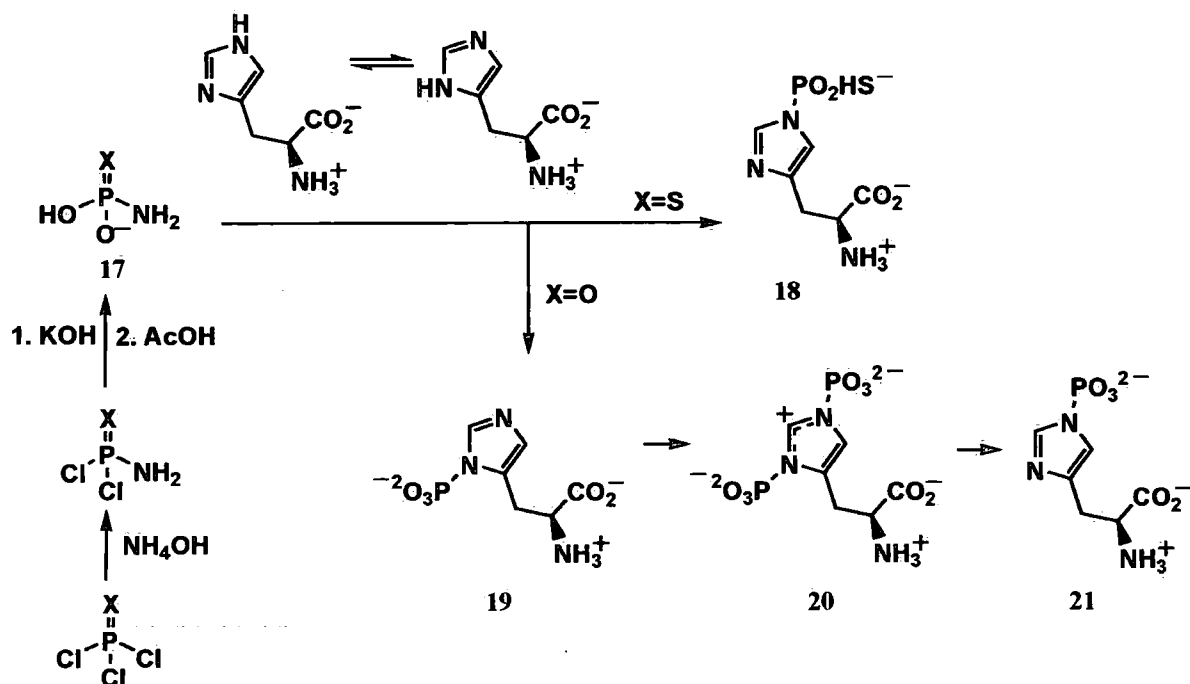
A typical route towards substituted aryl thiophosphoramidate derivatives of stavudine **16**, prodrugs investigated for application in the antiviral area involved preparation of a thiophosphorylating agent, *p*-substituted arylthiophosphoryl chloride **15**. After addition of the methyl ester of *L*-alanine, 1,2,4-triazole and stavudine (**d4T**), the crude mixture was separated *via* both column chromatography and preparative TLC to afford pure product in 12.3% yield.



Scheme 2. 6 Preparation of thiophosphoramidate derivatives of stavudine

The approach of the Turck⁵⁹ group is interesting, with direct thiophosphorylation of histidine by thiophosphoryl chloride in triethylamine and water, producing 3-thiophosphohistidine. Introduction of sulfur instead of oxygen increased the stability of the phosphohistidine derivative that was applied in an analysis of phosphohistidine-containing proteins, but the preparative method required HPLC purification and no yields were stated. Another histidine thiophosphorylation method⁶⁰ employed a previously prepared thiophosphoramidate **17** as the thiophosphorylation reagent to generate 3-thiophosphohistidine **18** that was isolated via simple precipitation in ethanol (in 45% yield). This was not the case with oxy-phosphorylation of the histidine, as the authors have stated that phosphorylation proceeded by N-1 (**19**) attack that was

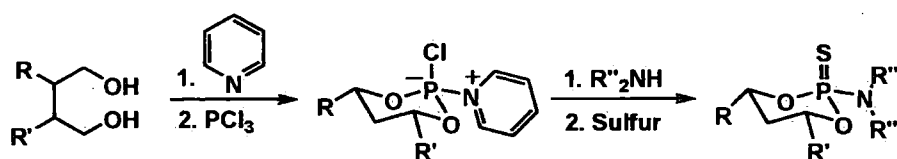
followed by N-3 phosphorylation, producing 1,3-diphosphohistidine **20** (scheme 2.7). After hydrolysis, 3-monophosphohistidine **11** was formed, which was confirmed by reaction monitoring *via* ^{31}P NMR spectroscopy.



Scheme 2.7 Oxy- and thiophosphorylation of histidine using oxy- or thiophosphoramidate salt

This event of selective thiophosphorylation was explained by greater instability of the N-1 product due to the steric interaction between the phosphate group and the neighbouring alkyl group, and this is more significant in the thio-analogue. Indeed, this directs the thiophosphorylation agent towards this nitrogen atom.

It was common to use phosphorus (III) chloride to phosphorylate nucleophiles e.g. alcohols and, then, after pyridine-mediated amine nucleophilic substitution, introduce a sulfhydryl moiety into the phosphorus amidate through exposure to elemental sulfur (scheme 2.8).⁶¹



Scheme 2.8 Application of elemental sulfur in the thiophosphoramidate synthesis

In this particular example, a cyclic intermediate was formed *via* an extensive and demanding procedure that afforded low yields of product after purification by flash chromatography.

Most of these procedures involve the application of protected starting materials, organic solvents and time-consuming purification steps. The method applying the thiophosphoramidate salt required preparation of the thiophosphoryl agent, but via a simple method. In addition, the purification of the desired product, via precipitation, was very simple, however, yields were moderate.

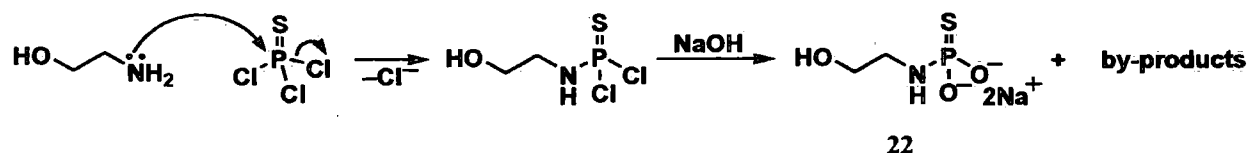
As previously mentioned, we opted to use an effective aqueous method, developed in our group. The following few sections will outline how efficient this method was when applied using thiophosphoryl chloride towards commercially available amines.

2.4. Preliminary experiments: thiophosphorylation of amines

Nucleoside amines can be challenging features to establish the methodology on. Some of them have solubility issues, like guanosine. On the other side, other nucleosides, such as uridine, adenosine and cytosine, are easier to deal with, but currently methods for the preparation of amine derivatives, as starting materials for the thiophosphoramidate chemistry, are not as efficient as in the guanosine example. Therefore, the application of commercially available amines offers the possibility of multiple trials and, therefore, the optimisation of the synthetic method. We performed our first experiments on the thiophosphorylation of amines using Williamson's aqueous method with 5 equivalents of sodium hydroxide, with two representative amines: water soluble ethanolamine and lipophilic benzylamine—both readily available in our laboratory (presented in the following section).

2.4.1. Thiophosphorylation of ethanolamine: optimisation

Ethanolamine was dissolved in 5 equivalents of aqueous sodium hydroxide and cooled on an ice bath. Thiophosphoryl chloride (1 Eq) was dissolved in dry tetrahydrofuran and added dropwise to the well-stirred aqueous solution of amine.



Scheme 2. 9 Thiophosphorylation of ethanolamine

The above reaction gave 96% conversion of the thiophosphoryl chloride by ^{31}P NMR spectroscopy to **22** as determined by the appearance of a triplet at 43 ppm. This was due to the three bond splitting of phosphorus signal with two neighbouring protons. This was a very satisfactory preliminary result, as only a small amount of the phosphorylating agent was converted into inorganic thiophosphate ((1.1%, singlet at 32 ppm). ^1H NMR spectroscopy confirmed effective conversion of ethanolamine (95%), with the only impurity being starting material, ethanolamine.

The experiment was assumed to work very well, but in order to explore the effect of increased thiophosphoryl chloride to amine molar ratio, a few additional experiments were performed. The obtained results are presented *via* stacked columns in figure 2.5.

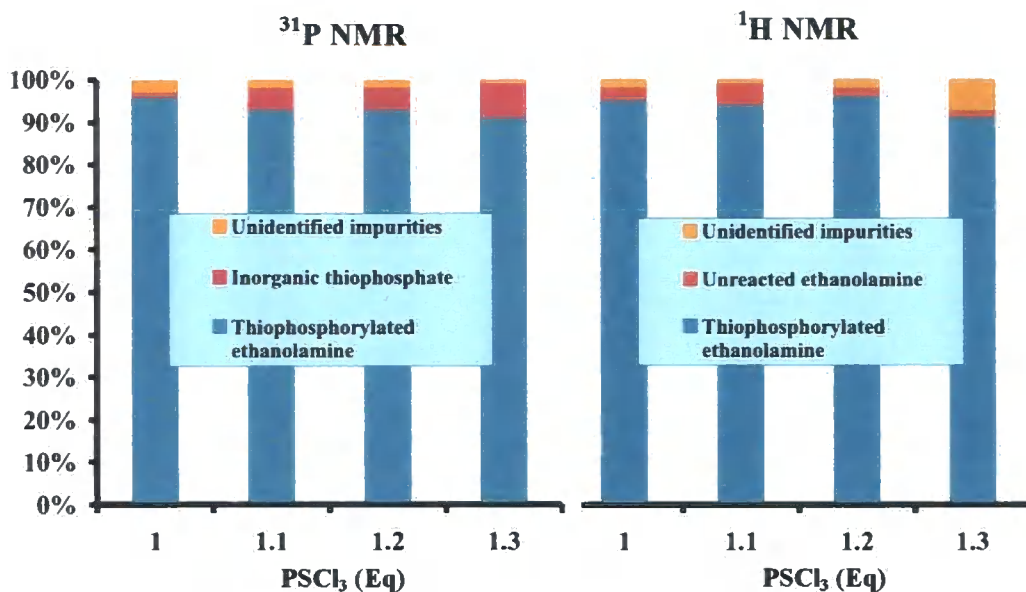
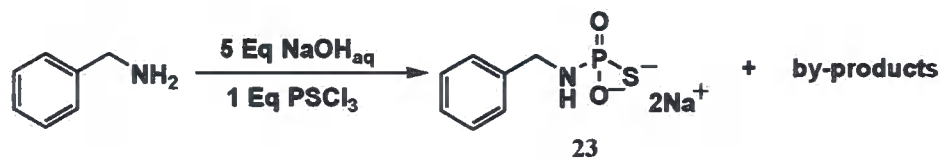


Figure 2. 5 Estimated purities of the range of ethanolamine thiophosphorylations

The additional available thiophosphoryl chloride improved the conversion of ethanolamine in some of the trials (1.3 Eq), however, only slightly and with scattered dependence on the quantity of PSCl₃ added. Most of the excess thiophosphoryl chloride was hydrolysed to inorganic thiophosphate. Therefore, an alternative where both amine and thiophosphoryl chloride were used in the same number of equivalents (1:1 Eq), was the method of choice as it gave the best results overall with minimal amounts of inorganic thiophosphate that, in further reactions, could be alkylated and introduce undesirable impurities into the product mixture.

2.4.2. Thiophosphorylation of benzylamine

The same thiophosphorylation principle as for ethanolamine was applied on benzylamine, using one equivalent of thiophosphorylating agent towards benzylamine and impressive, near complete, conversion was achieved (figures 2.6, 2.7 and 2.8).



Scheme 2. 10 Thiophosphorylation of benzylamine

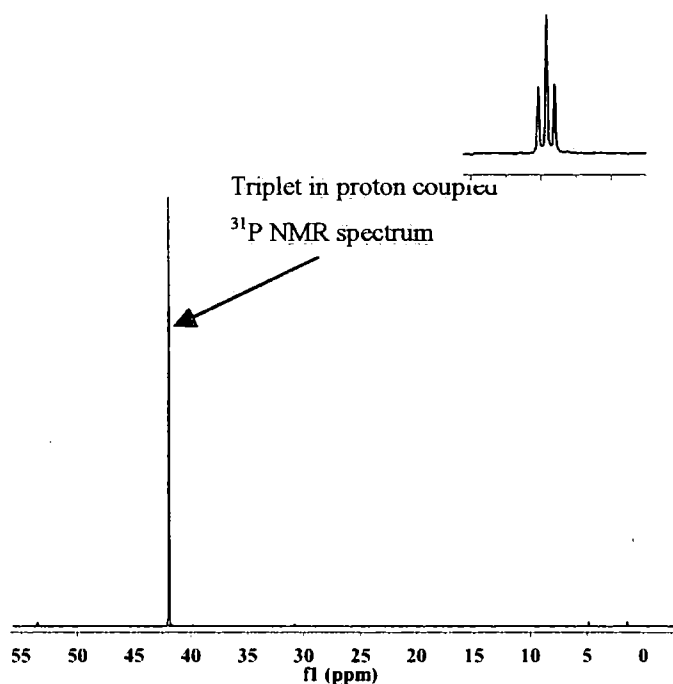


Figure 2. 6 ^{31}P proton coupled NMR spectrum of successfully thiophosphorylated benzylamine (in D_2O)

By-products created during reaction relate to two small peaks appearing at 2 and 5 ppm. Owing to their weak intensities (less than 0.5% each), they were disregarded in all future experiments. Furthermore, the peak appearing at 32 ppm indicated the presence of inorganic thiophosphate that, in this case, was present at less than 0.3%. The small multiplet at 54 ppm corresponds to the diamino thiophosphate form, shown below.

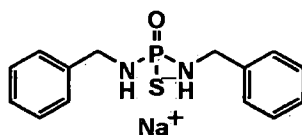


Figure 2. 7 Dibenzylamino thiophosphate

This product is not detected in the ^1H NMR spectrum owing to the low intensity and overlap of the peaks with the monoamino form (figure 2.8).

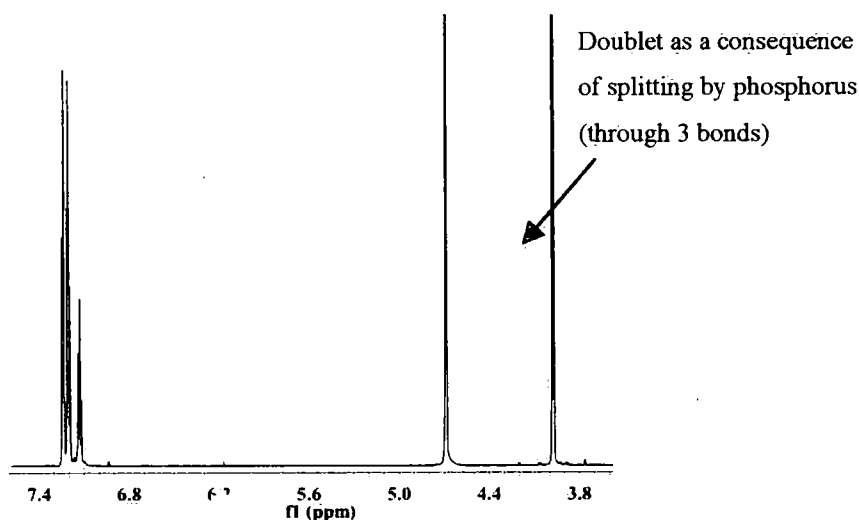


Figure 2. 8 ^1H NMR spectrum of the successful benzylamine thiophosphorylation (in D_2O)

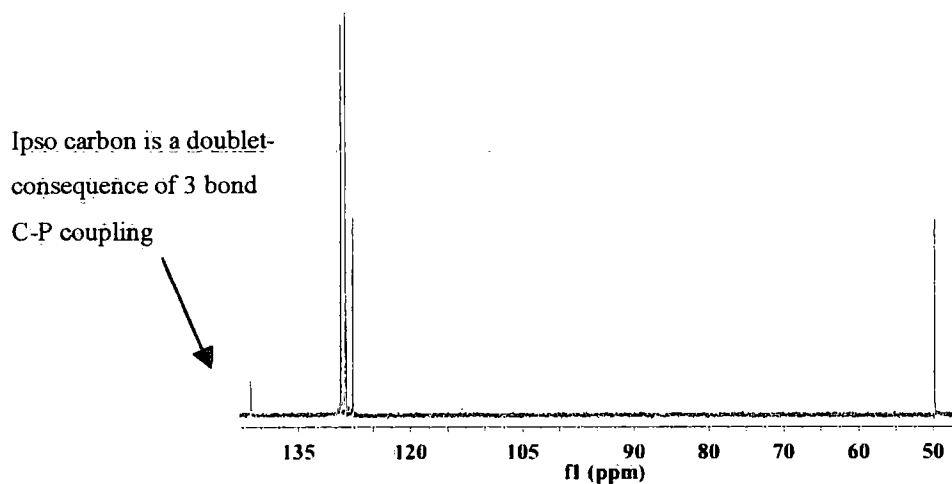


Figure 2. 9 ^{13}C NMR spectrum of the successful benzylamine thiophosphorylation (in D_2O)

Benzylamine showed remarkable conversions in the reaction with the thiophosphorylating agent, better than in the case of the less nucleophilic ethanolamine (discussed in the section 2.8). This result encouraged us to explore the application of this aqueous thiophosphorylating method to a range of amines (section 2.10-2.17) and further develop the method by investigations on the *S*-alkylation of the resulting thiophosphoramidates.

2.5. Hydrolysis stability studies on a thiophosphoramidate

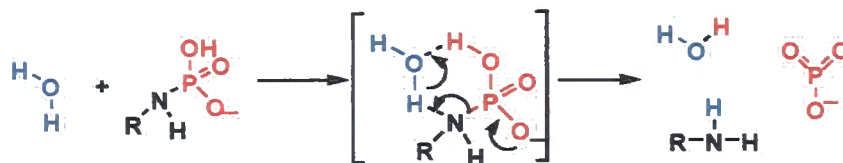
In the search for the reasons for poorer conversions in the ethanolamine example, the lower nucleophilicity of the amine came up as a reasonable explanation. On the other side, the assumption that the stability of thiophosphoramidates is relatively high at higher pH-s was made owing to a direct comparison with phosphoramidates studied previously within the Hodgson group. With our hydrolysis investigations, we hoped to get a better feeling of the stability of thiophosphoramidates over the pH range.

In the following few sections, we will outline some of the previous work performed on the stability of phosphoramidates that will be used to guide our investigations on thiophosphoroamidate systems. In addition, even though it was discussed more in the section 4.6, there will be a few examples describing how cleavage control of phosphoramidates can be a useful tool in the design of agents with prodrug-like abilities. Then, we will move to the results that we have collected during kinetic studies carried out on the ethanolamine thiophosphoramidate and how we hope to use these for the further development of our thiophosphoramidate Tripartite system.

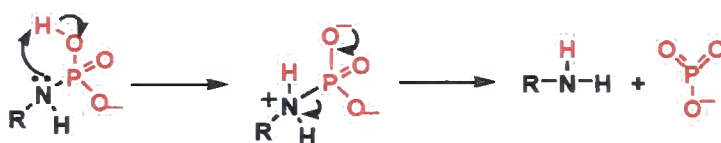
2.5.1. Stability of oxy-phosphoroamidates

In a detailed study, performed by Chanley and Feagerson⁶², on the hydrolysis of phosphoroamidates as a function of pH, a group of aryl phosphoroamidates was used as examples. It was noticed that phosphoramidates were very stable in alkali, with a pH-independent hydrolysis region at around neutral pH where hydrolysis occurred on the order of a few hours (measurements taken at 55 °C). The rates of the hydrolysis then increased as the pH of the phosphoramidate solution decreased, suggesting acid catalysed hydrolysis, with nitrogen protonation being required for release of the amine. However, the mechanism for the hydrolysis in the plateau region was challenging to explain. Therefore, Chanley and Feageson⁶² concentrated their research on the monoionic species X that they believed to be the major component of the reaction mixture in the neutral pH region. One proposed, 'Shift' mechanism, was distinguished by a bimolecular cyclic transition state (scheme 2.11), where proton transfer

to the amine group was assisted by a water molecule from the solvent. The other reaction pathway suggested the formation of the zwitterion species, shown below, that was possible by an internally provided proton in a O-N transfer and subsequent N-P cleavage. Both mechanisms could result in production of the parent amine and a metaphosphate species.



The 'Shift' mechanism

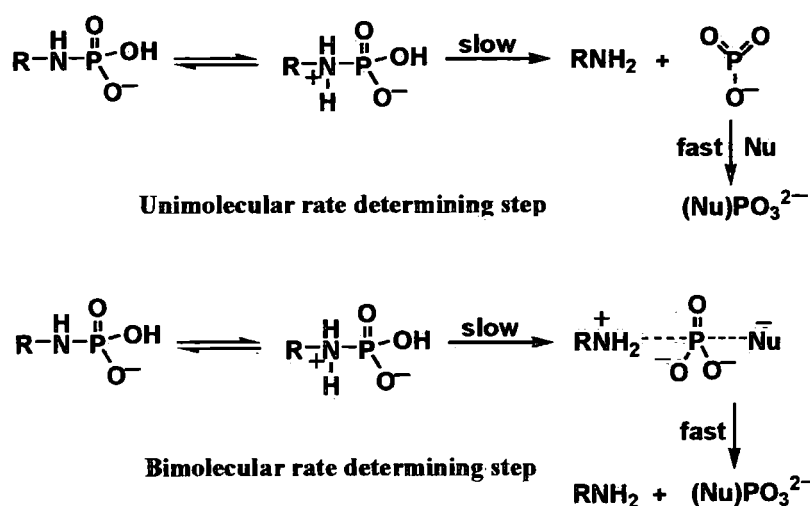


Zwitterionic species

Scheme 2. 11 Chanley and Feagerson's proposed mechanisms of phosphoramidate monoanion hydrolysis

Even with thorough investigations involving solvolysis experiments in order to prove the release of the metaphosphate species, neither of the mechanisms was clearly proven to be the degradation pathway.

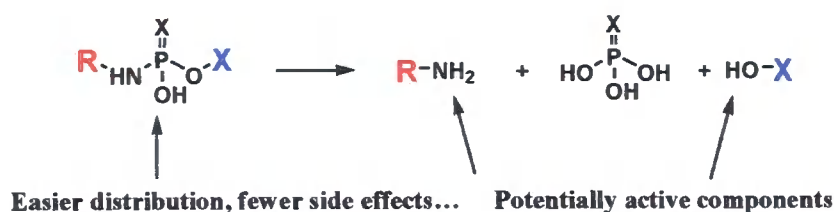
Some time later, Benkovic and Sampson⁶³ proposed the theory of direct dependence of phosphoroamidate solvolysis rate on the pK_{aH} of the liberated amine (amine conjugate acid). By analogy to phosphate monoesters hydrolysis, they put forward the suggestion of both the non-zwitterionic and the zwitterionic form, which are in the equilibrium, being involved in the mechanism of phosphoramidate hydrolysis (scheme 2.12). Though, the reactive zwitterionic form is directly responsible for the degradation process, its formation is directly proportional to the ΔpK_a between the amine and the orthophosphate groups (pK_a 7.2). Again, two propositions were put forward, unimolecular dissociation and bimolecular with the help of a nucleophilic species.



Scheme 2. 12 The proposed phosphoramidate zwitterionic hydrolysis mechanisms

The preponderance for the hypothesized bimolecular mechanism of monoanion hydrolysis, was supported by mixed solvent experiments that provided evidence for the preference of phosphoramidates towards reaction with an added alcohol nucleophile over water, that would not be the case if the reactive, and unselective, metaphosphate species were formed (unimolecular mechanism).

McGuigan *et al.*⁶⁴⁻⁶⁶ have done a vast amount of work on phosphoramidate derivatives *via* manipulation of their hydrolysis properties with the aim of generating desirable tools for drug delivery and increased selectivity of prospective antiviral agents (more in section 4.6). Ora and co-workers from the Turku group^{53, 67} have studied hydrolytic reactions of oligonucleosides that are bridged *via* thio- and also oxy-phosphoramidates (more in the following section). In addition, they have used their insight into these systems to create mononucleoside phosphoramidate derivatives as promising antiviral prodrugs.⁶⁸ The research of both of these groups will be discussed more in the section 4.



Scheme 4. 1 The release of the active agents via phosphoramidate cleavage. **R**, **X** structures of the active compounds, **X**=O, S

As the great interest in our group is the use of phosphoryl/thiophosphoryl derivatives of nucleosides, the behaviours of these species over ranges of pH are of high importance. As previously introduced in the section 2.1, David Williamson⁵² performed stability studies on the phosphorylated 5'-amino-5'-deoxyguanosine. The pH-log k_0 profile for hydrolysis, collected at 37 °C, had a very similar shape to that proposed by the group of Benkovic, for alkyl phosphoramidates. The stability of the 5'-amino-5'-deoxyguanosine phosphoramidate was great at higher pH regions, with the half-life at neutral pH, on the plateau, of approximately 2 hours. This enabled successful incorporation of the guanosine derivatives into RNA molecules.

Similarly, we are interested in the stability of thiophosphoroamidates to allow us to successfully alkylate the thiophosphate moiety, providing a method for the introduction of a wide range of substituents including the formation of the nucleoside thiophosphoramidates, potential glycosyltransferase inhibitors or substrates.

2.5.2. Stability of thiophosphoroamidates

Far fewer kinetic studies have been performed on the thiophosphoramidate system than for their oxy-analogues. Hence, the Turku group^{53, 67} explored the hydrolytic properties of 3'-5'-phosphoramidate oligonucleosides, containing both oxy- and thio-features in order to create a comparative study (figure 2.10 and scheme 2.13).

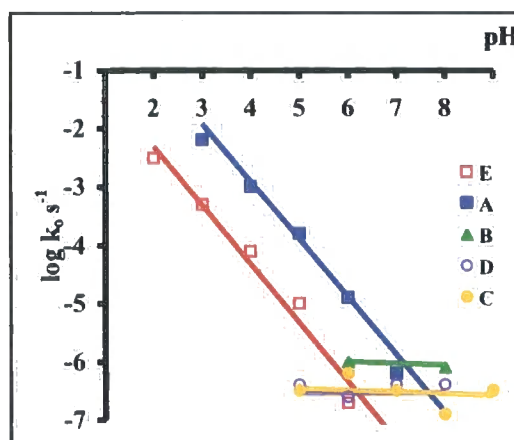
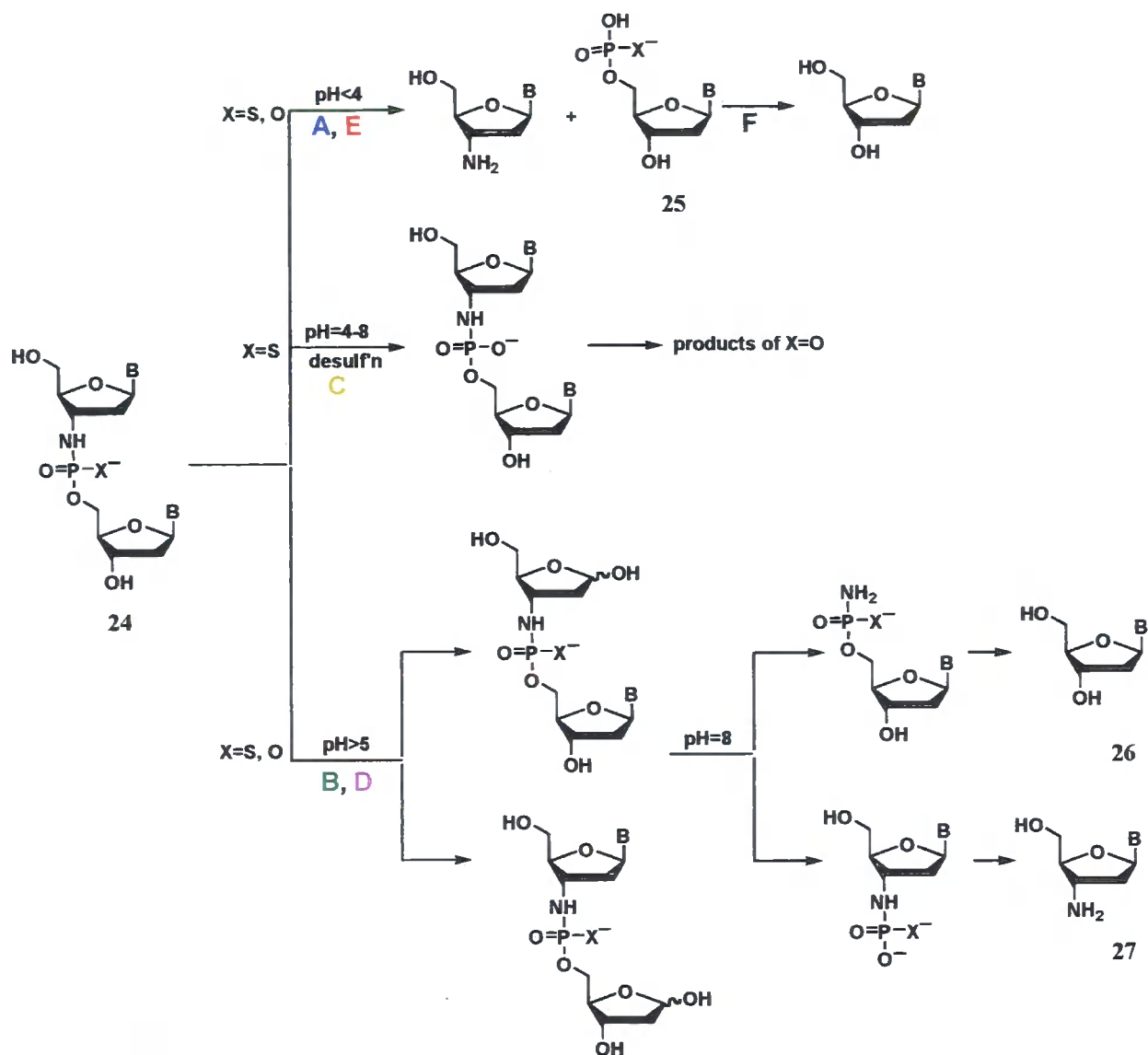


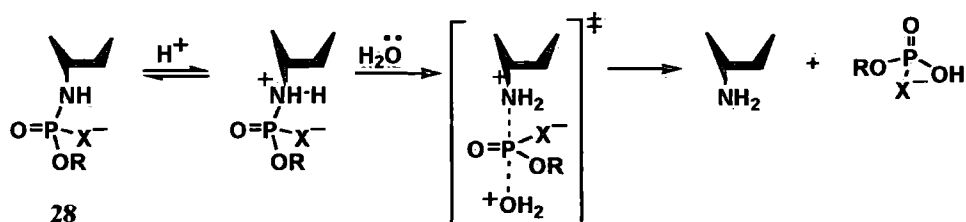
Figure 2. 10 pH- $\log k_0$ rate profiles for the hydrolysis reactions of oligonucleoside thio- and oxythiophosphoramidates. Routes E, A, B, F, G presented in the scheme 2.13



Scheme 2.13 Hydrolysis pathways of thio and oxy-phosphoramidates, in pH ranges from 1 to 8

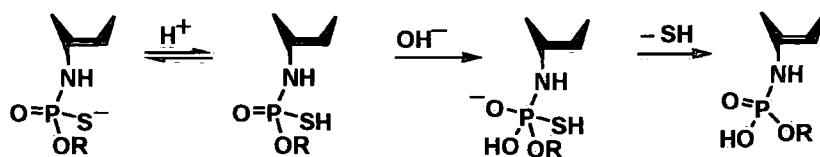
It was noticed that at pH < 6 prevailing acid-catalyzed P-N bond cleavage was occurring with a 12-fold greater hydrolysis rates in the case of the oxy-phosphoramidate feature in contrast to the thio-analogue (24, routes A, E.). The resulting thiophosphate, 25, was shown to be 2 orders of magnitude more labile than the corresponding nucleoside phosphate (route F). At pH 4-5, along with the phosphoramidate breakage, desulfurization of the thio-form (route C) and removal of the nucleo-base (routes B, D) in both species were competing processes (half lives

around 4 days in both cases). Above pH 5, the rate of P-N cleavage decreased rapidly and a complicated mixture of products of base-sugar cleavage and desulfurization processes was detected. At basic pH both C-N and C-O bonds showed instability and the final products were starting nucleoside **26** and 3'-amino-3'-deoxynucleoside **27**. In addition, the influence of choice of nucleoside base has been reflected in the P-N bond rate hydrolysis, as thymidine presented almost twice the reactivity of the uridine analogue. Again, it was presumed that under slightly acidic conditions (pH 2-6) the most abundant species in the solution were the monoionic forms of both thio- and oxy-analogues **28** (scheme 2.14). The mechanism of hydrolysis follows the proposal of protonation of nitrogen, which would then behave as the leaving group, in both oxo and thio-moiety with the assistance of a water molecule in the transition state.



Scheme 2. 14 The proposed P-N acid catalyzed cleavage mechanisms⁵³. X=O, S

The assumption that was the thiophosphoramidate offers greater stability than the oxy-analogue was due to the lower pK_a of the nitrogen feature of the thiophosphoramidate group (with no exact values up to date) that would then show a lower propensity towards protonation on the amine, decreasing the possibility of zwitterion formation and consequential degradation. In addition, desulfurization has been shown to be a more rapid process than P-O cleavage as thiolate is a better leaving group than alkoxide (pK_a of conjugate acids of ~10 and ~16 respectively).



Scheme 2. 15 The proposed desulfurization mechanism

Similarly, by the replacement of the phosphate oxygen with a sulfur in a substituted aryl phosphoroamidate derivatives of stavudine (triester analogues), alkaline hydrolysis has been shown to slow down by two-fold. This controlled degradation has been applied in the development of biologically more potent anti-retroviral agents.⁶⁹

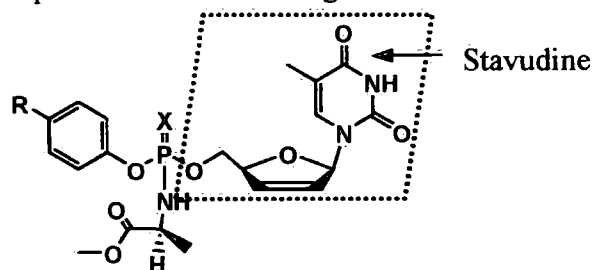


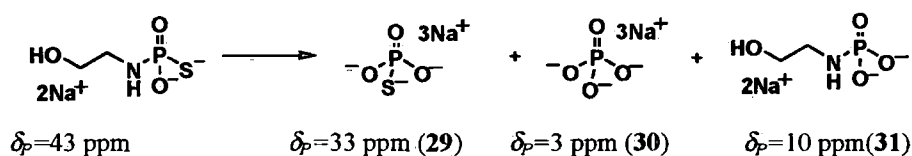
Figure 2. 11 Stavudine prodrug. X=O, S

We hope to use this advantage of higher stability of thiophosphoramidates through the pH range along with the potential of possible elongation and diversity of the thiophosphoramidate features via *S*-alkylation. The following section will present our experience on the stability of thiophosphoramidate systems using the simple example of *N*-thiophosphorylated-ethanolamine.

2.5.3. NMR kinetic studies: ethanolamine thiophosphoramidate hydrolysis

To ensure the maximal availability of thiophosphoramidate for the alkylation step of the Tripartite method, any potential degradation must be minimised. This could possibly be performed by pH adjustment and control of the examined reaction media. Using knowledge from the previously outlined kinetic studies on the solvolysis of ranges of phosphoramidates along with the conclusions from the studies of 5'-amino-5'-deoxyguanosine phosphoroamidate hydrolysis, performed in our group, we hope to open a picture of reactivity of our thiophosphoramidates system through the range of pH-s.

Preliminary studies on the hydrolysis of ethanol thiophosphoroamidate suggested the formation of inorganic thiophosphate **29**, phosphate **30** and small amounts of phosphoroamidate **31**.



Scheme 2. 16 Features detected during hydrolysis of ethanolamine thiophosphoramidate hydrolysis, according to ^{31}P NMR spectroscopy

Owing to the very distinct signals in the spectra, ^{31}P NMR spectroscopy seemed to offer a very simple and fast way to determine the kinetics of this system and, therefore, was employed as the analytical technique for data collection.

The crude ethanolamine thiophosphoramidate, prepared as previously described in section 2.4.1, was dissolved in buffer and lyophilised. Buffers were prepared by the dissolution of buffer components in water and appropriate adjustment of pH with the addition of base or acid. The residual lyophilised solid was then dissolved in D_2O prior to recording of the starting pD of the solution. In order to gain good quality spectra, that would be competent in presenting small changes in the product distribution, because the sensitivity the phosphorus NMR spectroscopy is somewhat lower than of the proton, close to 30 mg of sample was used in each experiment. Proportionally, 10-fold higher buffer concentrations were applied to preserve constant pH through both short and long data collection times. The resulting solution was of very high concentrations in both components, containing 0.4 M of analysed ethanolamine thiophosphoramidates and 4 M of appropriate buffer. The sample was then subjected for to collection of ^{31}P NMR spectra at 50 °C every 30 (CAPS, CHES, EPPS, HEPES), 15 (MES), 10 (acetate buffer) and 8 (citric buffer) minutes. An example of the resulting NMR data is shown below.

Disappearance of the thiophosphoramidate

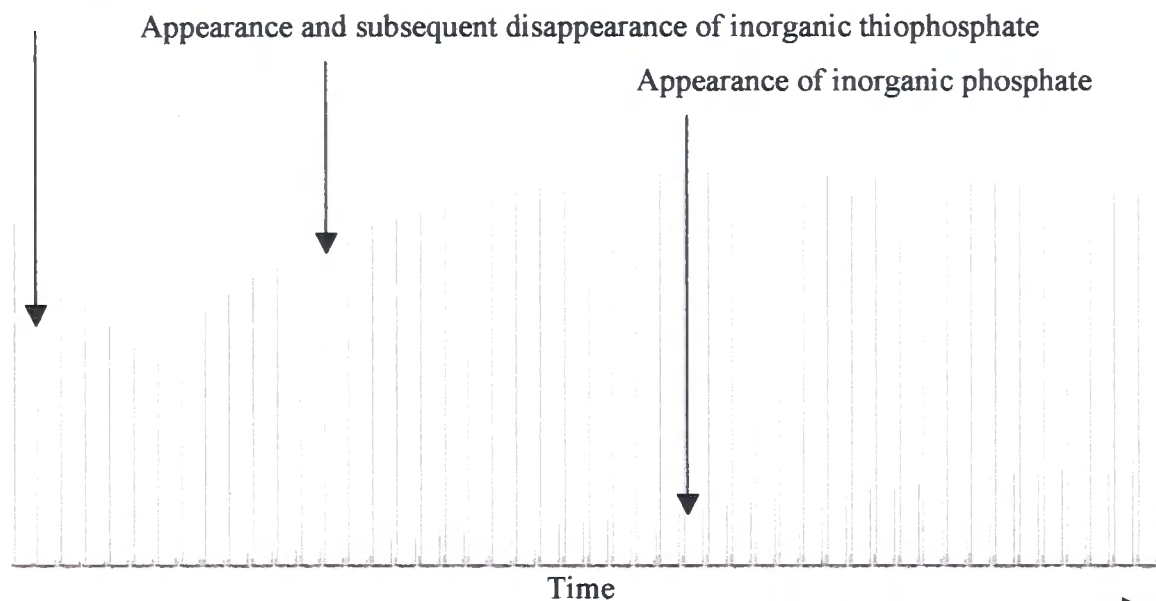
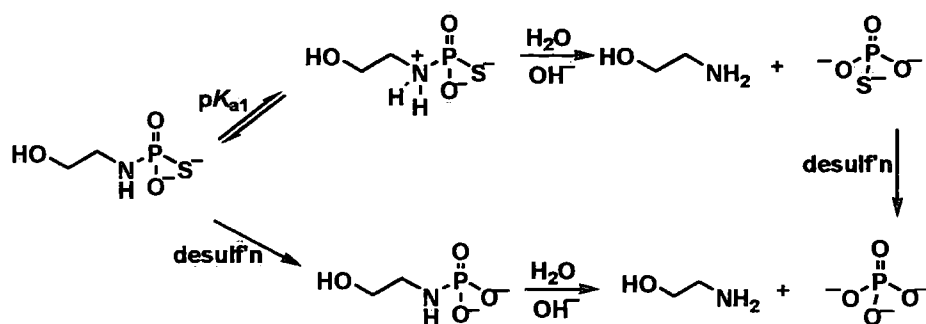


Figure 2. 12 A typical spectrum collected over the time of thiophosphoramidate hydrolysis in chosen buffer at 50 °C

This is an example of the experiment performed in citrate buffer, pH 2.6, where the decrease in the intensity of the corresponding thiophosphoramidate peak was linked to the formation of inorganic thiophosphate that then suffers desulfurization. In addition, the possible desulfurization of the thiophosphoramidate has been noticed in some of the basic media, with a very long half-life (7-20 days) so the assumption of phosphate formation as the consequence of the hydrolysis of the oxy-phosphoramidate was disregarded. The proposed pathways for the disappearance of the ethanolamine thiophosphoramidate, formed with the help of previously explored mechanisms for the oxy-phosphoramidates (presented in the section 2.5.1) are shown below.



Scheme 2. 17 The proposed mechanism of the thiophosphoramidate disappearance

The analysis of each of the possible degradation steps would require a great deal of investigation. In order to determine the most suitable pH for performing alkylations we will focus our attention on the rates of disappearance of the thiophosphoramidate signal only.

The normalised peak areas were plotted as a function of time and analysed as pseudo first order processes, owing to the big excess in which water and buffer components were present. Therefore, with the assumption that, in this case, the rate of the reaction is dependent on the concentration of analysed product only, the observed rate constant can be extracted from the exponential decay curve shown below:

$$I_t = I \times e^{-k_o \times t}$$

where, I_t is the normalised peak area at the examined time, t

I is the starting normalised peak area, and

k_o is the pseudo first order rate constant for thiophosphoramidate degradation at a specified pH.

To avoid presenting a large number of plots, an example kinetic trace and the least squares fitting method are presented here.

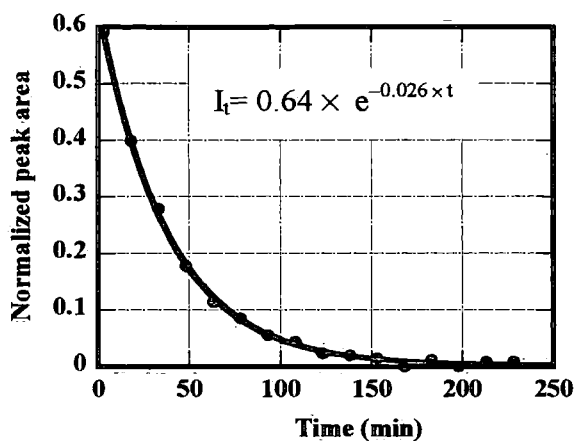


Figure 2. 13 A representative normalised peak area–time plot for the thiophosphoramidate degradation followed by ^{31}P NMR

With a series of plots, like the one shown above, we derived the observed rate constants for each studied pD level. k_o data were fitted as functions of pD using least square fitting method and the fitted data are presented graphically in figure 2.14 with pH corrected for pD using equation $\text{pH} = \text{pD} - 0.4^{70}$. As the deuterium exchange was not rigorously performed, variation of $\pm 10\%$ must be considered.

Table 2. 1 The parameters used for the creation of the pH-log k_o profile for the degradation of the thiophosphoramidate of ethanolamine

pH	4 M buffer used		
	k_o (min^{-1})	$\log k_o$	$t_{1/2}$ (min)
10.2	0.00021	-3.68	3300
9.2	0.0012	-2.93	597
8.7	0.0023	-2.64	301
7.9	0.0046	-2.33	150
7.4	0.0075	-1.12	91
7.1	0.014	-1.86	50
6.8	0.027	-1.57	26
5.8	0.03	-1.52	23
5.3	0.027	-1.57	26
5	0.023	-1.64	30
3.6	0.028	-1.55	25
2.9	0.015	-1.83	47
2.2	0.023	-1.64	30

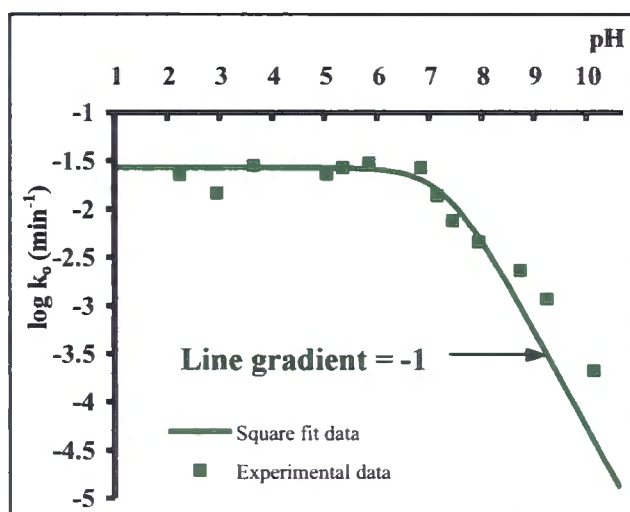
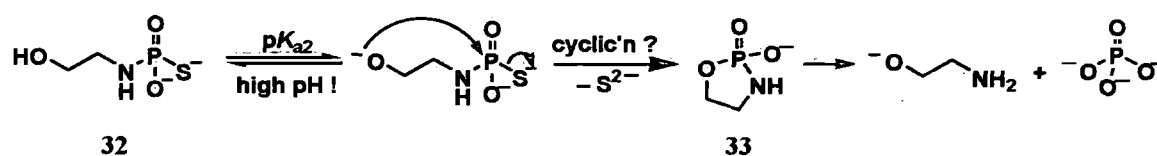


Figure 2. 14 pH log k_o profile of ethanolamine thiophosphoroamidate hydrolysis. $k_o = 0.026 / (1 + 10^{\text{pH} - \text{p}K_a})$, $\text{p}K_a = 7.26$

At the plateau, hydrolysis was happening with a half life of half an hour at 50 °C, compared to 1.8 hours in the case of 5'-amino-5'-deoxyguanosine phosphoramidate hydrolysis occurring at 37 °C⁵². This was unexpected, as previous studies (section 2.5.2) have shown much greater stability of thiophosphoramidates compared to their oxy-analogues. Therefore, in the search for the potential cause, the question of the effect of the terminal hydroxyl group was considered. In addition, deviation of the experimental data and the generated trend-line in this high pH region was significant. Ethanolamine contains a potentially nucleophilic hydroxyl group and the possibility of intramolecular cyclisation was considered (scheme 2.18). Unlike in the case of an RNA transcription process where the stability/lability at pH 8 was the crucial factor, we were more interested in the part of the rate profile at higher pH where compound stability is greater, with half-lives longer than 10 hours at 50 °C.



Scheme 2. 18 The proposed mechanism for the hydrolysis of thiophosphoramidate by intramolecular nucleophilic attack

The cyclic form **33** has not been detected with the analytical techniques that we have applied, with the assumption that even if it formed its half-life would be short. On the other side the approaching nucleophile would have to be very strong, as the presence of two anionic features in the phosphoryl group acts to repel the incoming nucleophile. In addition, deprotonation of the hydroxyl group was likely to happen when study was only at high pH (as noticed in the later experiments with ethanolamine and bromoethanol, sections 2.6.1 and 2.13). Firstly, the search for the explanation of the poor fit in the high pH range was continued by re-analysing the procedure that experiments were performed under.

Very high concentrations of thiophosphoramidate **32** (scheme 2.18) and, therefore, buffer were applied in order to gain as high quality spectra as possible while maintaining the constant pH during data collection. With the goal to test if this was having any effect on the slope of the pH

curve, the experiments were performed the same way as previously explained with a final buffer concentration of 0.5 M. The resulting pH hydrolysis rate profile have been added to the profile for the 4 M buffer data and the combined data are presented in the figure below.

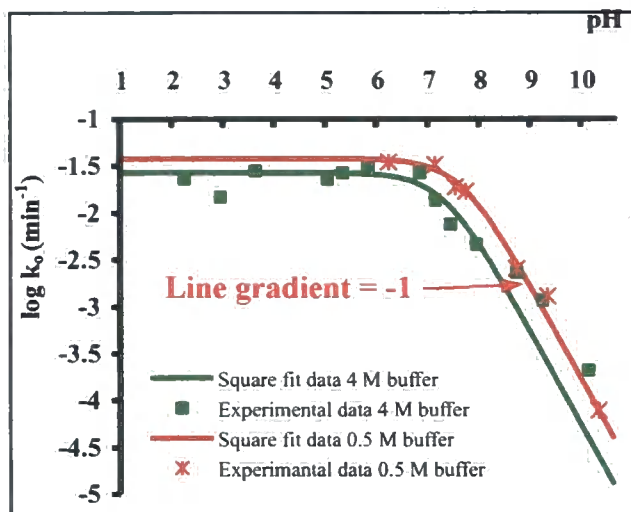


Figure 7. 1 pH rate profile for ethanolamine thiophosphoroamidate hydrolysis: 4 M used vs 0.5 M buffer used

$$k_o = 0.026 / (1 + K_a / [H^+]), \text{ p}K_a = 7.26 \quad (4 \text{ M buffer})$$

$$k_o = 0.038 / (1 + K_a / [H^+]), \text{ p}K_a = 7.61 \quad (0.5 \text{ M buffer})$$

With the new results, much better fitting was achieved. The plateaus of both pH profiles were at the approximately same level, with an increased $\text{p}K_a$ of the ethanolamine thiophosphoroamidate being observed using the 0.5 M buffer. On the other hand, the important fact that needs to be considered when the lower buffer concentration was applied, is the variation in pH of the studied solutions. At the beginning and end of the run a significant pH change was noticed ($\Delta\text{pH}=0.2\text{-}0.5$).

The inherent limitations that the approach of using ^{31}P NMR spectroscopy presents, are probably the cause of the deviation of the experimental data from the expected trend-line in both cases. Large amounts of the analysed sample were required (~ 30 mg), introducing the possibility of high ionic strength being an issue, as the performance of NMR spectroscopy

would be reduced. The collection of good quality ^{31}P NMR spectra required 128 scans which took approximately 6.5 minutes, which, on the time scale of kinetic events, is in some cases of the same magnitude as the half life. Therefore, decreasing the time of the NMR run offered more scope for the shorter experiments, but at the same time decreased the reliability of the NMR data and led to less accurate peak integration.

While this technique may not be the most robust kinetic method, it had the advantage of being relatively simple and quick way to the conclusions needed for the continuation of the thiophosphoramidate Tripartite method development. With the main goal of these studies in mind, we deduced that the highest stability of the thiophosphoramidate occurs in highly basic media, with more than 10 hours half life at 50 °C. In addition, NMR spectroscopy gave direct evidence of the appearance of inorganic phosphate and thiophosphate that other techniques such UV-Vis spectroscopy would not provide (no chromophore present) and also the formation of phosphoramidate as the product of desulfurization process. Therefore, the design of the thiophosphoramidate alkylation procedure should probably involve pH adjustment of the reaction mixture to pH 9 or 10, which would, hopefully, prevent any undesired thiophosphoramidate degradation allowing maximal productivity in the generation of desired *S*-alkylated derivatives.

2.6. Preliminary alkylation experiments: stepwise approach

We have seen that amines can be readily thiophosphorylated with very high conversions. On the other hand, the stability of the products is pH-dependant, as phosphoamide P-N bonds break under neutral and acidic conditions. In order to perform successful alkylation of the thiophosphate group, reaction mixtures need to be adjusted to high pH where phosphoramidate hydrolysis is slower. After thiophosphorylation, the sample mixture already contains some excess hydroxide so trial alkylations were performed directly in the NMR tube using lyophilised thiophosphoroamidate.

Commercially available bromoethanol and the more challenging 5'-iodo'5'-guanosine (preparation is shown in section 3.2.1) were chosen to start with. Thiophosphorylated benzylamine and ethanolamine were used from previous experiments (section 2.4) dissolved in D₂O and added into NMR tubes with either bromoethanol or 5'-iodo'5'-guanosine as alkylating agents. In order to follow the approximate rates of the alkylation processes in these systems, screening was performed *via* ³¹P NMR spectroscopy at 50 °C and, in one case, with bromoethanol at 70° C. In addition, different approaches were applied, concerning the excess of one of the components to examine the effects on the reaction outcomes.

2.6.1. The use of an excess of thiophosphoramidate

To ensure that all alkylating agent was used up, around 4 equivalents of the thiophosphoramidate were applied. The exact excess of the thiophosphorylation component was not determined as a crude reaction sample of thiophosphoramidate was used. In any case, reaction was performed using high reaction concentrations (~0.4 M of thiophosphoramidate and ~0.1 M of alkylating agent) to support rapid alkylation.

The examined samples were prepared directly in NMR tubes, as described in the previous section, and subjected to ³¹P NMR spectroscopy at 50 °C over 12 hours with spectra collection every 30 minutes. When the sulfur functionality was alkylated, a corresponding phosphorus signal in the ³¹P NMR spectra at 25 ppm appeared.

The increase in the intensity in the normalised peak area of the new peak at 25 ppm (apparent quintet in coupled spectra), corresponding to the alkylated product was then plotted against time (graphs shown below) and the data were fitted using the least squares fitting method for the exponential equation:

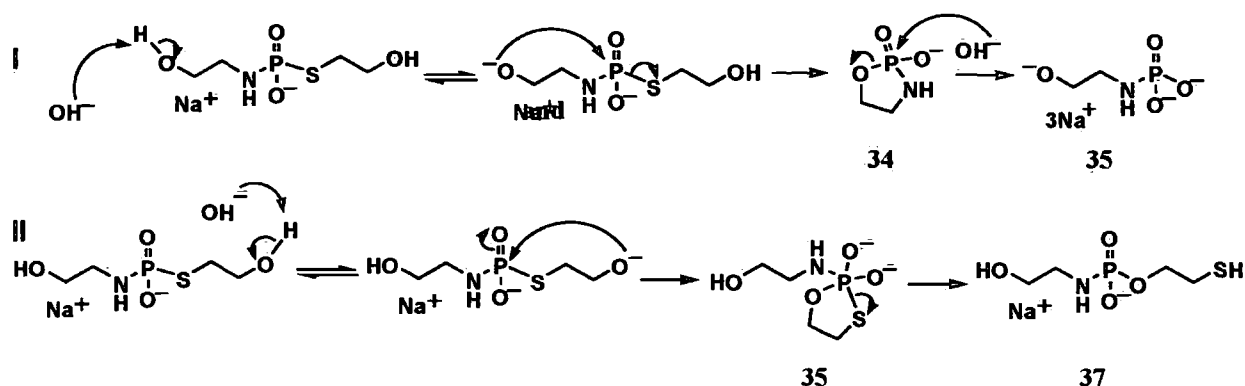
$$I_t = I_{\infty} \times (1 - e^{-k_A \times t})$$

where, I_t is the value of normalised peak area at the time point, t

I_{∞} is the maximal value for the normalised peak area, $t = \infty$

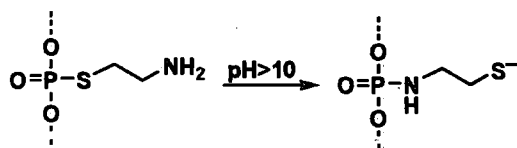
k_A is the observed rate constant for the alkylation process.

seemed likely that there was an issue with the stability of the alkylated thiophosphoramidate, as its signal decreased through time. Formation of the two ethanolamine phosphoramidate species **35** and **37** were detected, therefore, we propose the following the degradation pathway:



Scheme 2. 19 The proposed mechanisms for the intracyclisation occurring at high pH.

A small multiplet at around 30 ppm suggested the presence of a putative cyclic intermediate **34** potentially formed in path I. However, the chemical shifts for 1,2-amidocyclophosphates of sugars observed by Eschenmoser⁷¹ (section 2.16.3), were at slightly higher field, around 26 ppm. Therefore, without further investigation on our system, we cannot confirm the proposed formation of cyclic phosphoramidate **1**. On the other side, the ³¹P signal of the sulfur-containing cyclic intermediate **36** (path II) would be positioned at much lower field (~70 ppm) and it was not detected. A similar rearrangement to the proposed path II, where the terminal group was an amine instead of a hydroxyl, has been used as a strategy for the formation of phosphoramidates.^{72, 73}

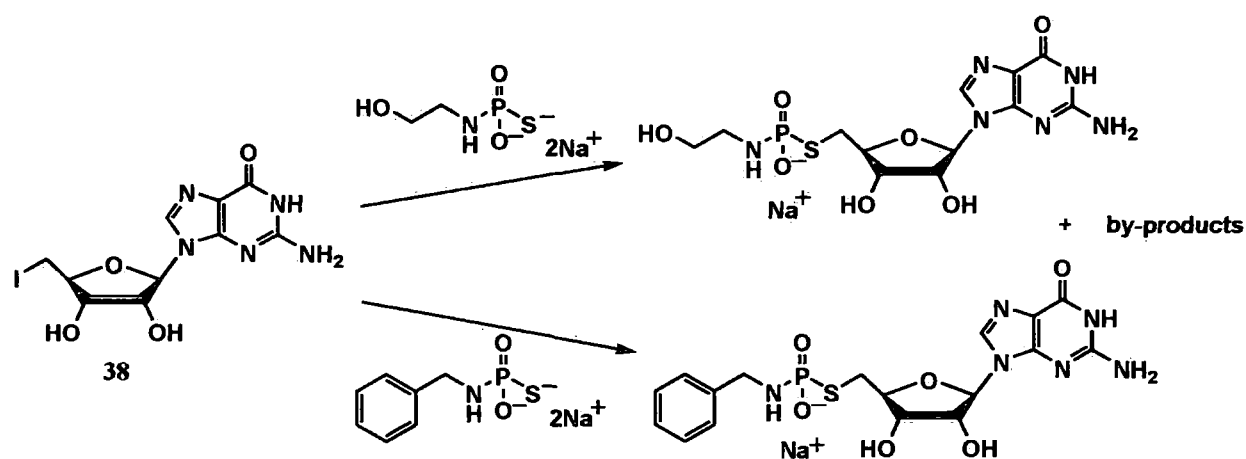


Scheme 2. 20 *S*-(2-aminoethyl) thiophosphates to *N*-(2-mercaptoethyl) phosphoramidates used for DNA labeling²⁴

However, we believe that pathways shown in scheme 2.20 induced instability of this alkylated thiophosphoramidate, affecting the outcome of the alkylation reaction. In contrast, benzyl

thiophosphoramidate showed greater conversion and stability at 50 °C during 15 hours of ^{31}P NMR data collection.

Preliminary experiments on 5'-iodo-5'-deoxyguanosine as the alkylating agent were performed using the same procedure as described above.



Scheme 2. 21 Stepwise alkylation of ethanalamine and benzylamine thiophosphoramidates with 5'-iodo-5'-deoxyguanosine

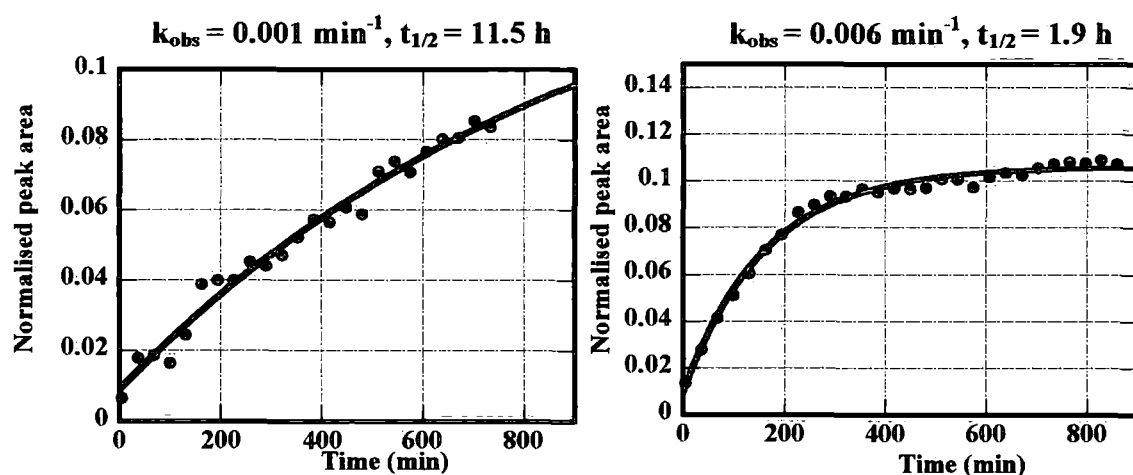


Figure 2. 17 Graphs showing thiophosphoramidates (ethanalamine-left and benzylamine-right) alkylation with 5'-iodo-5'-deoxyguanosine. Bimolecular rate constants for ethanalamine and benzylamine 0.0025 and 0.015 M/min, respectively

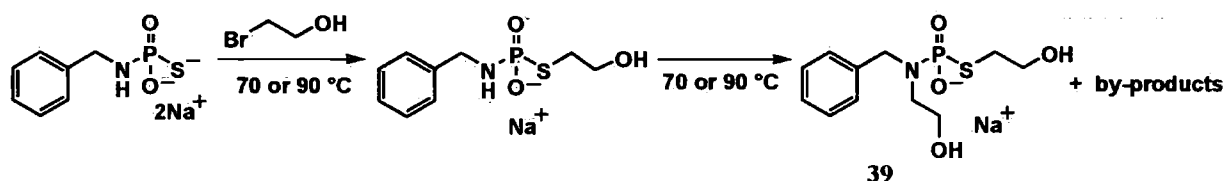
The poor solubility of iodoguanosine might have caused lower conversion (less than 10%) than in the case of bromoethanol, which, in addition, is a much better alkylating agent. There was

10-fold difference in the rates of alkylation benzylamine and ethanolamine thiophosphoramidate, with the faster being the former.

Both in the bromoethanol and 5'-iodo-5'-deoxyguanosine examples, by-products formed as consequences of thiophosphoramidate hydrolysis and desulfurization, which, due to the high pH of the reaction mixture were both slow processes, thus allowing electrophile to react with the sulfur nucleophile. Beside hydrolysis products in the form of inorganic thiophosphate and phosphate, some phosphoramidate and alkylated inorganic thiophosphate were also formed.

2.6.2. Bis-(*N*-, *S*-) alkylation of thiophosphoramidates

When the stepwise experiment involving bromoethanol alkylation of benzyl thiophosphoroamidate, described in the previous section, was repeated, but at 70 °C, in order to test possible acceleration of the alkylation, a new feature was detected in the ³¹P NMR spectrum (scheme 2.22).



Scheme 2. 22 Prolonged alkylation at 70 °C enabled *N*-alkylation

After alkylation of the thiophosphoryl group was complete (peak at 25 ppm in the phosphorus NMR spectra), the appearance of a peak at lower field at around 45 ppm, with multiple splitting, attracted our attention. In order to check if some degradation in the form of the reverse reaction (releasing thiophosphoroamidate) had occurred, mass spectrometry was performed. Rather than de-alkylation, the mass spectrum confirmed the additional *N*-alkylation of the thiophosphoroamidate, occurred with a half-life of around 9 hours, the kinetics of thereaction are shown in the graph below.

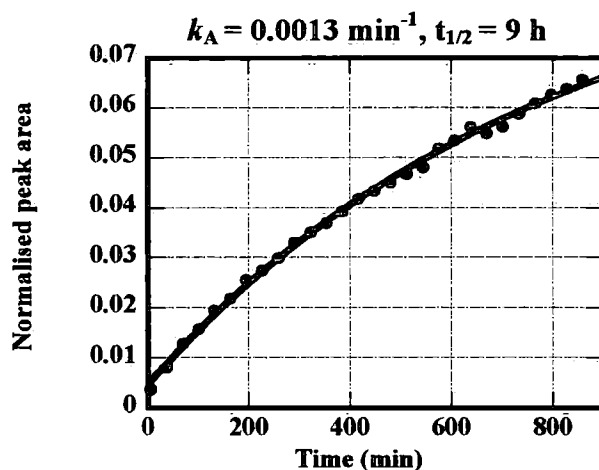


Figure 2. 18 Kinetics of the *N*-alkylation of *S*-alkylated benzyl thiophosphoramidate. Bimolecular rate constant is $0.003 \text{ M}^{-1}\text{min}^{-1}$

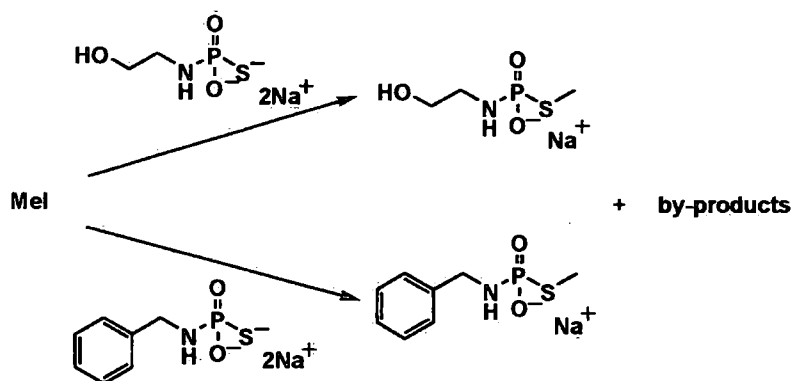
As a harder nucleophile, the amine group was less susceptible to alkylation than the thiol group of the thiophosphyl feature. Only when *S*-alkylation was completed, did *N*-alkylation, forced by the prolonged heating, occur. This could be a useful tool for making a wider range of products, with bis-(*N*-, *S*-) derivatisation. However, in the rest of this thesis, we will concentrate on development of an efficient method for performing mono-*S*-alkylations.

All these products together with starting thiophosphoramidates are readily soluble in water, so in order to gain pure products, chromatography methods would be required, which we were trying to avoid. Having concluded from our first experiments that alkylation of thiophosphoramidate is feasible, and having gained insight into the kinetics of alkylations we moved to the more practical approach of using no excess of the thiophosphoramidate over alkylating agent.

2.6.3. The use of equal numbers of equivalents of thiophosphoramidate and alkylating agent

Methyl iodide is a very effective alkylating agent and the advantage of its application is that it can be easily removed from the reaction mixture with ammonium hydroxide, transforming it into the non-electrophilic methyl amine that is safer to handle and volatile.

When one equivalent of methyl iodide was added to the solution of thiophosphorylated ethanolamine or benzylamine in D₂O, again, directly in the NMR tube, alkylation products were formed in less than 20 minutes (scheme 2.23).



Scheme 2. 23 Stepwise alkylation of thiophosphoramidates: 1 Eq of methyl iodide

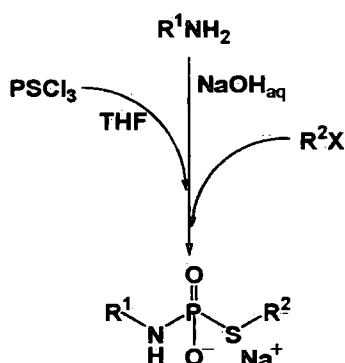
When using 2.3 equivalents of methyl iodide, the conversions of both ethanolamine and benzylamine thiophosphoramidates was not complete (65% and 25%, respectively) and there was still unreacted starting thiophosphoramidates. Methyl iodide, with its low boiling point, is quite volatile and probably some of it evaporated before being able to react. So additional alkylating agent was needed. Another two equivalents in the case of ethanolamine thiophosphoramidate gave full conversion into the desired methylated thiophosphoramidate of ethanolamine, with an estimated purity of 95% *via* ³¹P NMR spectroscopy and 82% by ¹H NMR spectra. Known impurities were in the form of inorganic phosphate and alkylated inorganic thiophosphate (at less than 1% each). A number of unidentified impurities were also present at less than 0.5% each in the phosphorus NMR spectrum. The ¹H NMR spectrum gave lower estimates of purity due to the presence of un-thiophosphorylated ethanolamine and ammonium salt of triple alkylated benzylamine. In contrast, ¹H NMR spectroscopy on the methylated benzyl thiophosphoramidate showed 93% purity with the only side products being trimethyl benzylammonium salt, benzylamine thiophosphorylation was complete. In addition, ³¹P NMR spectrum indicated 97% conversion with inorganic phosphate present as the only impurity.

These preliminary experiments were considered a great success and indicated the possibility of expansion of the reaction system towards many examples of amines and alkylating agents. As a two-step approach, with thiophosphorylation of amine followed by appropriate alkylation, we have proved the idea, but not in the practical sense, therefore, the method needed some adaptation. With the avoidance of the lyophilisation step and direct alkylation of crude thiophosphoramidate in the water-THF mixture, the reaction procedure could be accelerated greatly, enabling the possibility of performing reactions in microtitre plates and direct screening of the products. This was the next goal that we hoped to accomplish. Therefore, we revised our method from a stepwise to a one-pot reaction system involving thiophosphorylation of amines, followed by alkylation of thiophosphoramidates. The development of this approach will be presented in the following sections.

2.7. Design of a one-pot thiophosphoramidate system

Based on the Tripartite idea, presented in the Chapter 1, that promotes simple, quick, uncomplicated preparation procedures avoiding long chromatographic techniques, we now present a one-pot method for the preparation of alkylated thiophosphoramidates.

The principles of the one-pot method follow the stepwise approach with the difference of being performed in 'one-pot', removing the additional step of thiophosphoramidate lyophilisation. An amine is thiophosphorylated in basic media containing 5 equivalents of aqueous sodium hydroxide. Thiophosphoryl chloride was used, as the thiophosphorylating agent and was dissolved in dry THF, to prevent any unwanted early hydrolysis. This was added dropwise into the rigorously mixed amine solution that was cooled in an ice bath. As the thiophosphorylation was assumed to be finished within a very short time frame, alkylating agent was added directly into the reaction mixture, where tetrahydrofuran likely helps with dissolution and mixing of the reagent (scheme 2.24).



Scheme 2. 24 General Tripartite idea applied to the thiophosphoramidate system. R^1, R^2 = any aliphatic feature

The key of the ‘one-pot’ tactic is based on the solubility differences of the desired product, amines and alkylation agents. The target product is mono-ionised in water solution and, therefore, most probably readily soluble in water (the exceptions are some examples with large R^2 aromatic substituents that decrease the solubility of the molecule, Chapter 4.). In contrast, most of the alkylating agents are promptly soluble in organic solvents, such as chloroform or diethyl ether, and could easily be removed from the mixture *via* solvent extraction. Lipophilic and amphiphilic amines, as well, are soluble in organic solvents and could be easily extracted, leaving pure product in the aqueous solution. Water-soluble amines, hopefully, would react with maximal conversion with thiophosphoryl chloride, otherwise, the amine would have to be accepted as an impurity in the sample and additionally tested for its own effects on any subsequent bioassay.

With these factors in mind, our initial experiments on the one-pot approach involved the application of the amine and alkylating agent in excess over thiophosphorylating agent followed by extraction of unreacted amine and alkylating agent. In this way the reaction could give maximal conversions with an easy purification method to remove excess starting materials. The remaining aqueous solutions after extraction were lyophilised to give rise to solid products that were subjected to analysis. An even simpler purification method could use diethyl ether, which, being less dense than water would stay on the surface during extraction and could be readily eliminated from wells, in the case of reactions being performed in microtitre plates. Owing to the lack of availability of diethyl ether (at some periods during this project, diethyl

ether was not available for several months), on some occasions in the method establishment chloroform was used as the extraction solvent. In these cases, the aqueous solutions containing the product were isolated from the top layers of the extraction mixture.

To establish the one-pot method, commercial starting materials were used. The strategy concerning the example amines and alkylating agents is presented in the following sections. In addition, before acting upon any biological tests, the methodology needs to be established on a larger scale; therefore, the microtitre plates as the reaction vessels were substituted with normal laboratory glassware. In order to avoid repetition, all experiments performed *via* this one-pot method, applied the procedure presented in this section, and will be recalled. The exception was ethanolamine, with the differences described in the section 2.13.

2.8. Model amines

In this section we will outline a few examples of amines that we used as representative systems in the foundation of the thiophosphoramidate system. In order to create the method and set up the reaction conditions, we tried to use different types of amines and apply what we observed to a wide array of amines.

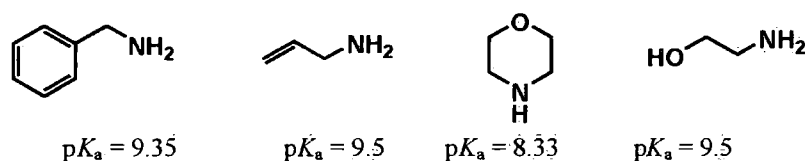


Figure 2. 19 Model amines use in the creating of the thiophosphoramidate system

Benzylamine and allylamine are lipophilic amines, and can be easily extracted from basic aqueous solution, while morpholine is soluble in both water and organic solvents. Therefore, with careful adjustment of the pH of the reaction media, morpholine can be used in the excess to assist the successful thiophosphorylation step and later be removed from the sample. Ethanolamine, as a water-soluble amine, does not offer the possibility of an easy isolation from the aqueous solution so conversion of amine into the thiophosphoramidate product could not be improved more than, a still very satisfying, 95% conversion level.

The pK_a of ethanolamine (9.5) is slightly higher than that of benzylamine (9.35), therefore according to this parameter, the nucleophilicity should be very similar and very much the same as allylamine. With morpholine, which is less basic, it can be expected that the thiophosphorylation rates would be much lower. However, in many cases, relative nucleophilicity and basicity of amines have shown poor correlation according to Mayr.⁷⁴⁻⁷⁶ Mayr's studies involved investigation on nucleophilicities of a range of amines in water in reactions with benzhydrylium ions to define a nucleophilicity parameter, N and nucleophile specific slope parameter, s as tools for prediction of nucleophilic reactivity. The best example is aniline with nucleophilicity comparable to ethanolamine but a pK_a value that is five units lower. In addition, secondary alkyl amines with almost the same basicity as typical primary amines, had nucleophilicities 100-1000 fold greater. These are not comparable systems to ours, as with benzhydrylium ions water attack can be discounted as it is much slower than amine attack, however, these systems can still be used as a general guide of nucleophilicities in water. Water in our system, readily reacts with thiophosphoryl chloride but with the greater nucleophilicities of the amines used and pH control, we managed to gain desirable conversions to thiophosphoramidates. Benzylamine, according to the Mayr nucleophilicity scale has higher reactivity towards electrophiles than ethanolamine ($N=13.44$ and 12.61 , respectively), which was seen in the case of our initial thiophosphoramidate experiments as well.

5'-Amino-5'-deoxynucleosides are not commercially available, but their broad utility urged us to investigate the synthesis of these systems. In our work, we concentrated on the 5'-amino-5'-deoxyguanosine, as the continuation of previous experience in our group has resolved issues of insolubility of guanosine and its derivatives. In analogy with the established aqueous method for the phosphorylation,^{51, 52} we examined the possibilities of thiophosphorylation of 5'-amino-5'-deoxyguanosine and 5'-amino-5'-deoxyadenosine (figure 2.21).

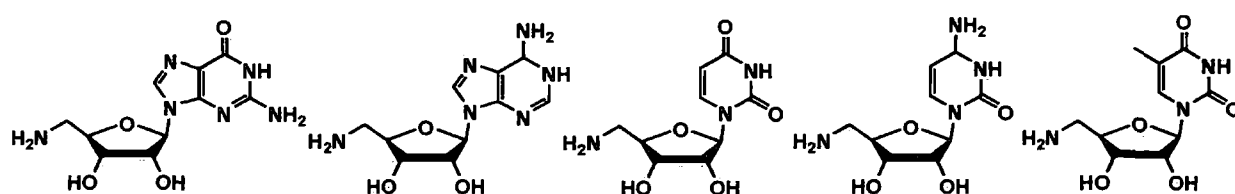


Figure 2. 20 5'-Amino-5'-deoxynucleosides that could be used in our Tripartite thiophosphoryl system

Furthermore, *S*-alkylation of thiophosphoramidates stabilises them towards hydrolysis at relevant pH and offers the possibility of structural variation with the final goal of method development towards the design of more involved, diphosphates (introduced more in the Chapter 3.). As a side project, we also worked on the aqueous preparation of 5'-amino-5'-deoxyguanosine and its precursor, 5'-azido-5'-deoxynucleosides (section 3.2.3. and 3.2.4), to permit easier access to this starting material. Hopefully, this synthetic approach should be applicable to other nucleosides escalating the usefulness of our investigations.

Thiophosphorylation of amino acids and amino sugars have high potential in biological studies (section 2.16) We chose phenylalanine, in order to avoid any side reaction occurring with hydroxyl or amine groups present in side chains of some other amino acids. In addition, it was suggested that phenylalanine has one of the highest nucleophilicities amongst the amino acids, though much lower than that of proline⁷⁷ and other amines discussed previously. As an example of an aromatic amine, aniline seemed like the least complicated option. With its relatively high nucleophilicity, aniline offered the highest probability of successful thiophosphorylation. On the other hand, the amine group is strongly activating group, so the possibility of electrophilic aromatic substitution by thiophosphoryl chloride must also be borne in mind.

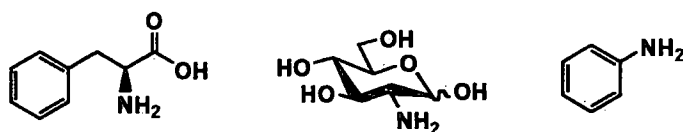


Figure 2. 21 Some more 'challenging' amines that can open some new areas of application

Monosaccharides that contain the amine functionality could also be considered for thiophosphorylation, however, this could be challenging as their lower nucleophilicities caused by the additional steric effect of neighbouring hydroxide groups.

The proposed order of nucleophilicities of amines that we have been using in our studies is presented in the figure 2.23.

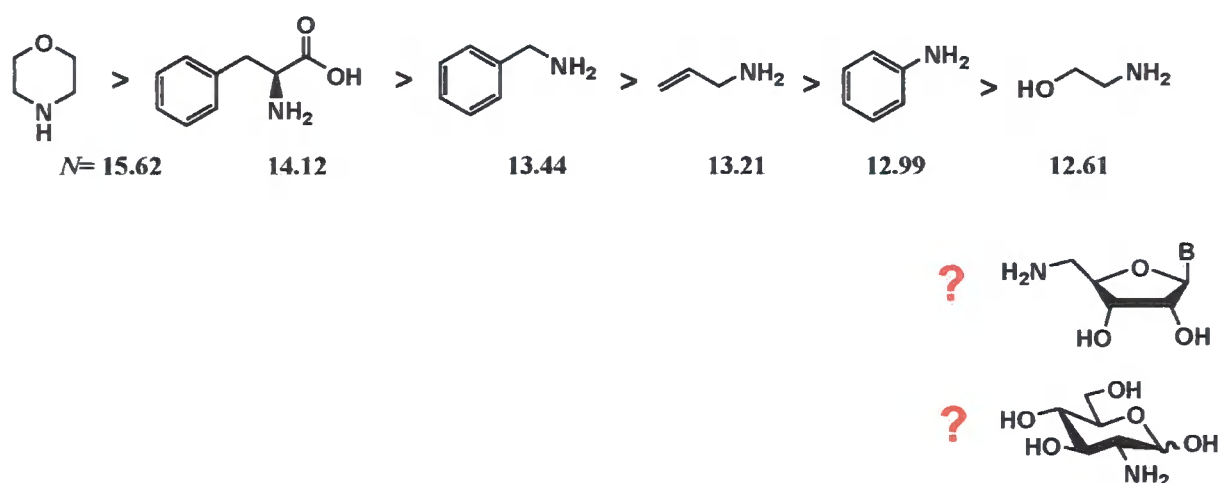


Figure 2.22 Nucleophilicities of amines compared according to Mayr's scale^{74, 75, 77}

The involvement of aromatic amines, in addition to primary and secondary alkyl amines, along with amino acids and amino sugars would expand the potential of our aqueous thiophosphorylation method. Later in the study, a library of amines was tested (section 2.14), involving both primary and secondary amines.

2.9. Model alkylating agents

In terms of the range of alkylating agents, we chose to test our thiophosphoramidate system on representative primary and secondary alkyl halides, and then move to more complex examples (section 2.17) in order to challenge the limits of the Tripartite reaction. Most of these alkylating agents are potentially carcinogenic, therefore, handling and disposal of these in the reactions was performed according to the safety instructions (quenching with ammonium hydroxide solution).

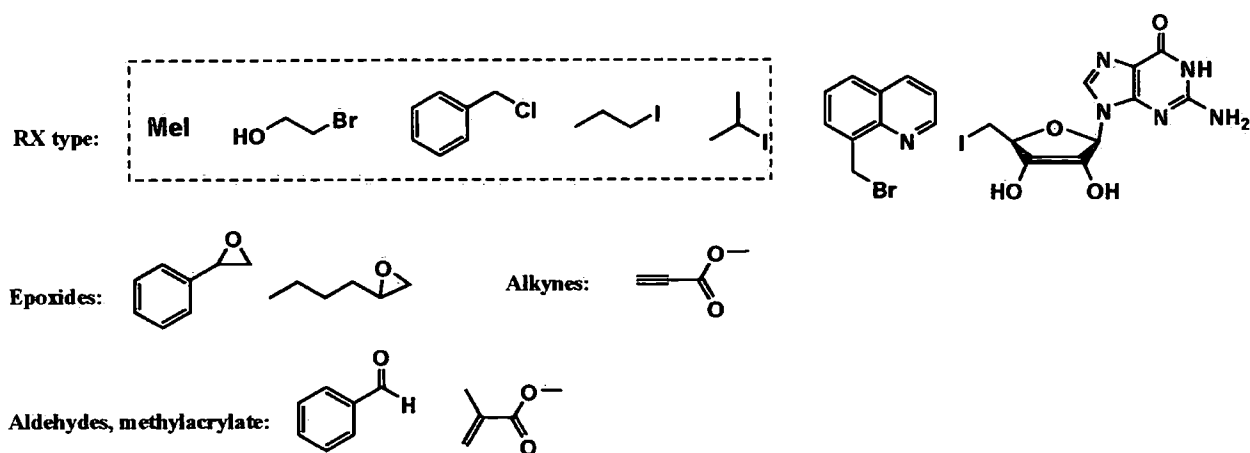


Figure 2. 23 Model alkylating agents used in the study. Method establishment was performed with simple **RX** types, highlighted dotted black.

In order to create a procedure that would work for a range of different alkylating agents and, on the other side, enable clear analysis of results, structurally simple electrophiles (**RX** highlighted in the figure 2.24) were used for methodology development studies. The strategy of using an excess of alkylation agent would be applied, followed by the removal of the unreacted alkylation agent *via* extraction. In this way, the danger of the unreacted alkylating agent can be removed from the samples without contaminating the sample with ammonium hydroxide, as used earlier.

Methyl iodide is a very effective electrophile, with a very good leaving group, that is promptly displaced by 'soft' nucleophiles, such as the thiolate feature of the thiophosphoramidate group. In addition, the methyl group allows sterically easy access to the nucleophile. With its high volatility, methyl iodide requires cooling of the reaction mixture to limit its evaporation from the reaction mixture, which, obviously, decreased reaction rates. Bromoethanol, like ethanolamine, contains a hydroxyl group that, as a nucleophilic feature, could possibly attack the phosphoryl group of thiophosphoramidate and cause P-N or P-S bond cleavage. However, a cyclic intermediate was not detected in either case. The slowest electrophile 2-propyl iodide, with its secondary structural configuration comparing to linear propyl iodide, had very low reactivity and needed an additional 'push' in the form of heating in order to carry out successful alkylation.

2.10. Continuous method with lipophilic amines and simple alkylating agents: benzylamine and allylamine

Applying the one-pot Tripartite method, previously presented in section 2.7, on the lipophilic amines, benzylamine and allylamine, a number of products were prepared (figure 2.25).

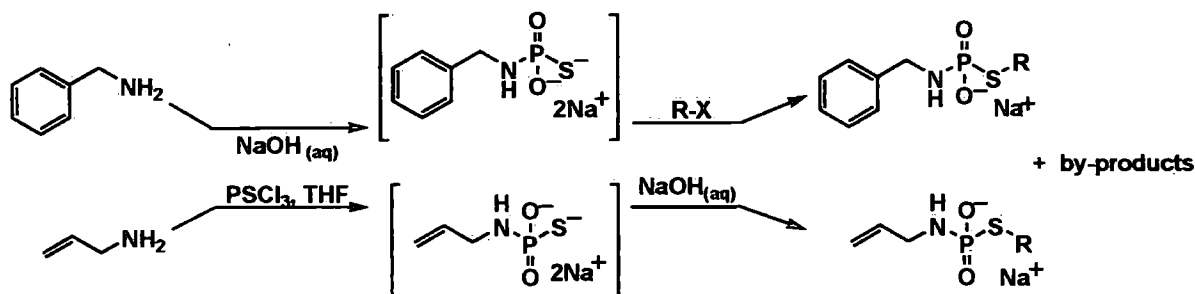


Figure 2. 24 One-pot preparation of S-alkylated benzylamine and allylamine thiophosphoramidates

Vigorous stirring of amine (benzylamine or allylamine) in 5 equivalents of aqueous sodium hydroxide was continued after the addition of thiophosphyryl chloride in THF. Depending on the alkylating agent used, additional aqueous sodium hydroxide was applied to maintain the high of pH the reaction media (experimental section 7.6.1). However, a general procedure for each alkylation agent with a range of amines was not established, as pH seemed to vary more in some experiments than the others. Reaction pH control could, probably, be easily performed using a pH stat, however, like in many laboratories, we do not have access to such equipment, thus a simpler approach of adding sodium hydroxide solution portion-wise was adopted. The purities of the products were very pleasing (figure 7.28) with identified impurities mainly being inorganic phosphate or/and alkylated inorganic thiophosphate.

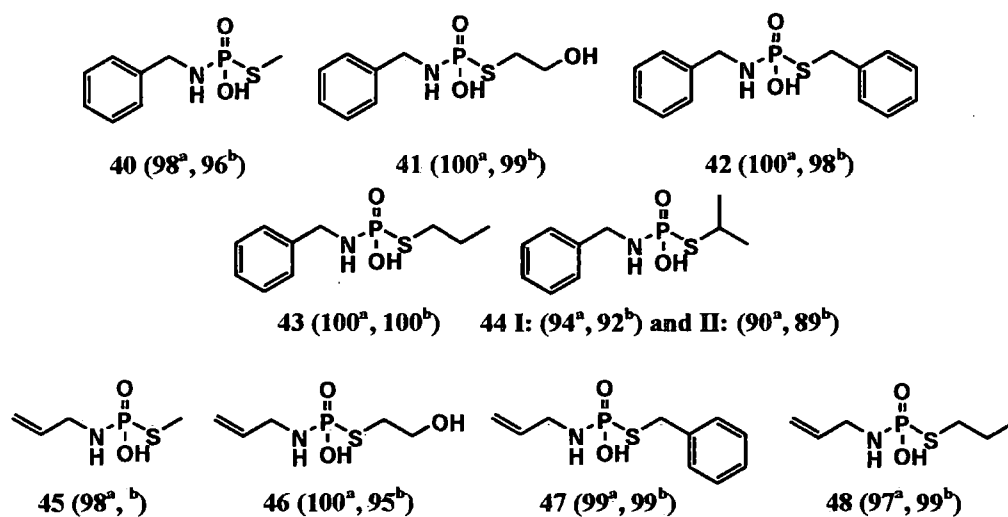


Figure 2. 25 Products gained *via* one-pot Tripartite thiophosphoramidate method using benzylamine and allylamine. ^aPurity (%) estimated by ³¹P NMR spectroscopy, ^bPurity (%) estimated by ¹H NMR spectroscopy

A representative spectra of the highly pure compound 43 are shown below.

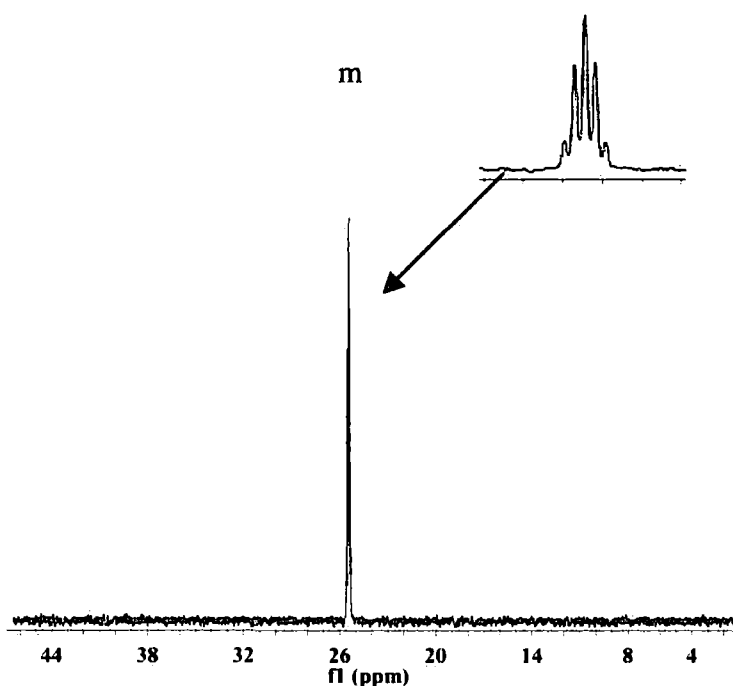


Figure 2. 26 Proton coupled ³¹P NMR spectrum of the compound 43 (multiplet) (in D₂O)

Successful alkylation can be easily detected *via* the fact that the ^{31}P NMR signal had transformed from a triplet at 43 ppm for the thiophosphoramidate (section 2.4.2) to a multiplet at 26 ppm (figure 2.27), owing to two additional protons derived from the alkylation agent (3 bond H-P coupling). These two protons will not have exactly the same coupling effects as the ones from the amine methylene, therefore, a multiplet was observed rather than a pure quintet. This behaviour applied to the alkylation examples that will be described in the following sections.

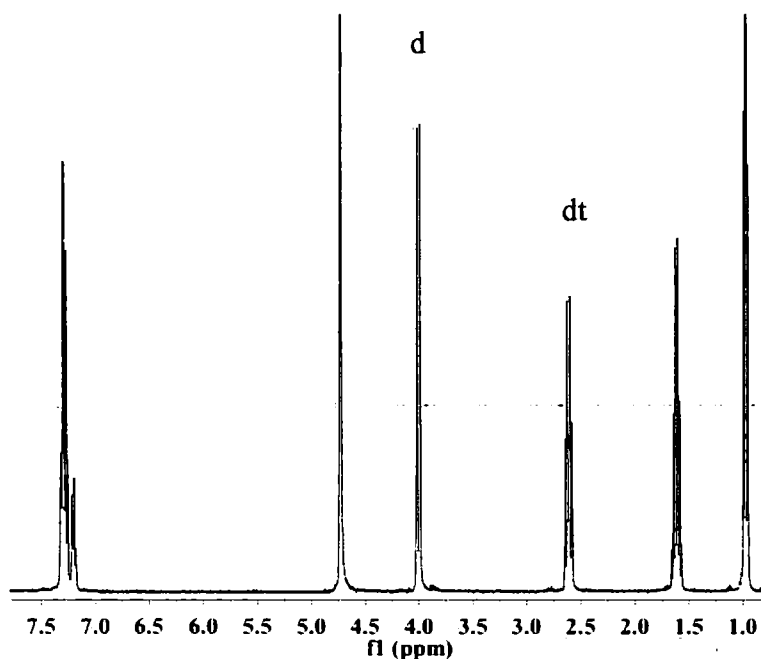


Figure 2. 27 ^1H NMR spectrum of the compound 43 (in D_2O)

Beside the methylene doublet of benzylamine thiophosphoramidate ($-\text{CH}_2\text{NH}-$) (section 2.4.2), ^1H NMR spectroscopy showed another 3-bond coupling of protons to phosphorus. The triplet signals for the methylene protons ($-\text{SCH}_2-$) of propyl iodide were split by phosphorus, forming a doublet of triplets in the ^1H NMR spectrum. In, addition ^{13}C NMR spectroscopy was also a good indicator of product formation, as 3 bond C-P coupling causes the formation of doublet signals on both the ipso carbon of the benzylamine and the central methylene ($-\text{CH}_2\text{CH}_2\text{CH}_3$) carbon of the propyl group.

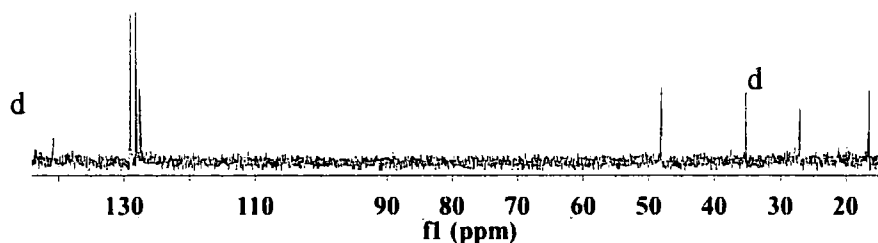


Figure 2. 28 ^{13}C NMR spectrum of the compound 43 (in D_2O)

Methylated products were also of high purity estimated *via* ^{31}P NMR spectrum integration, but ^1H NMR spectroscopy revealed the formation of the quaternary ammonium salt owing to the triple alkylation of benzylamine. This salt was not extracted with organic solvent, and, therefore, remained as the impurity in all methylations. Even though cooling of the reaction mixture was required, methylation occurred with relatively high rates and was completed within 20 minutes.

Bromoethanol, benzyl chloride and propyl iodide needed somewhat longer thiophosphoramidate alkylation times, proportional to their electrophilicities. Estimated reaction times at room temperature were less than 2 h, 22 h and 25 h, respectively. In the example of propyl iodide and allylamine thiophosphoroamidate, alkylation took 120 h! This was unexpected, owing to the much shorter times seen for benzylamine thiophosphoramidate and other amine thiophosphoramidates with this alkylating agent.

In order to optimise the rather slow alkylation using 2-propyl iodide, two experiments were performed. The first attempt involved heating of the vigorously stirred reaction mixture of freshly thiophosphorylated benzylamine and 10 equivalents of 2-propyl iodide at $50\text{ }^\circ\text{C}$. To maintain pH 10, 5 equivalents of sodium hydroxide were re-added along with the alkylating agent. After 96 h of reaction time 94% and 92% conversion was achieved (**44 I**), estimated *via* ^{31}P and ^1H NMR spectroscopies, respectively. When the reaction was performed at $80\text{ }^\circ\text{C}$, in order to test the possible decrease of the alkylating agent excess, 2-propyl iodide was added in three separate portions of 5+5+1 Eq. After 2 h, 18.5 h and 0.5 h of stirring, conversions,

according to ^{31}P NMR spectroscopy of crude reaction mixture, were approximately 48%, 95% and 97%, respectively. After the first two additions of the alkylation agent, aqueous sodium hydroxide 5+5 Eq was added as well. Comparing these two approaches, only a small difference in final conversions was noticed (90% by ^{31}P spectroscopy and 92% by ^1H NMR spectroscopy, 44 II). In the second experiment, more sodium hydroxide was used, however, the reaction time was shortened more than 4-fold. Therefore, the balance depending on the demands has to be made.

Overall, alkylations of both benzylamine and allylamine thiophosphoramidates, using simple RX agents, were fairly comparable, owing to similar nucleophilic properties, and gave marvellous conversions demonstrating the versatility of the Tripartite approach, with the only purification step in the form of trouble-free ether extraction. These results encouraged us to carry out investigations on other types of amines, water-soluble ethanolamine and the amphiphilic secondary, morpholine.

2.11. One-pot method with hydrophilic amines: the use of excess of thiophosphoryl chloride and methanol precipitation

Initial experiments with water-soluble ethanolamine, when used in a 1:1 molar ratio with thiophosphoryl produced satisfactory conversions of 96%, estimated by ^{31}P NMR spectroscopy, and 95%, estimated by ^1H NMR spectroscopy. Furthermore, stepwise alkylation gave promising results of almost complete conversions of thiophosphoramidate to the desired *S*-alkylated product, using commercially available methyl iodide. However, a portion of amine was not converted into the desired thiophosphoramidate (~5% according to ^1H NMR spectroscopy), and therefore was present as an impurity in the alkylated thiophosphoramidate sample. In order to try to improve the thiophosphorylation step, an excess of thiophosphorylating agent was applied. The key of this tactic lays in the actual ability to precipitate inorganic phosphate and thiophosphate. This method originates from Hampton⁷⁸ and was optimised by Paul Brear, a former 4th year student in our laboratory when purifying guanosine 5'-monophosphothioate using methanol precipitation method (62% of methanol in

water). This precipitation step would require removal of the THF from the solution of thiophosphorylated amine and would be performed prior to the alkylation.

On the other hand, preliminary investigations on another hydrophilic amine, morpholine, reinforced the high nucleophilicity characteristics of this amine. In an experiment with one equivalent of thiophosphorylating agent, all of the amine was used up; leaving some thiophosphoryl chloride unreacted (2% of inorganic thiophosphate in the ^{31}P NMR spectrum). In addition, formation of a new feature was noticed. The appearance of a signal at 62 ppm in the ^{31}P NMR spectrum (5%) along with ^1H NMR spectroscopy suggested the formation of the thiophosphorodiamidate form of morpholine **49**.

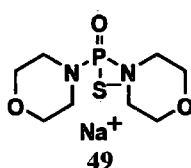


Figure 2. 29 Morpholine thiophosphorodiamidate

Morpholine, as a secondary amine, is a very good nucleophile even though its basicity is lower than of ethanolamine (discussed more in the section 2.). In the light of this remark, we will try to adapt the reactivity of morpholine using an excess of thiophosphoryl chloride, which we hope, should inhibit the formation of the undesirable diamino form of morpholine thiophosphoramidate. Again methanol precipitation would be applied, to afford, hopefully, pure thiophosphoramidate that could be further alkylated. Unfortunately, in both experiments, methanol precipitation was unsuccessful.

Morpholine, with its reasonable solubility in organic solvents, offered another possibility for dealing with the formation of by-products. When morpholine was used in excess over the thiophosphorylation agent, some formation of both diamino **49** and triamino **51** features occurred.

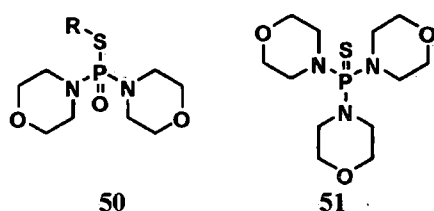
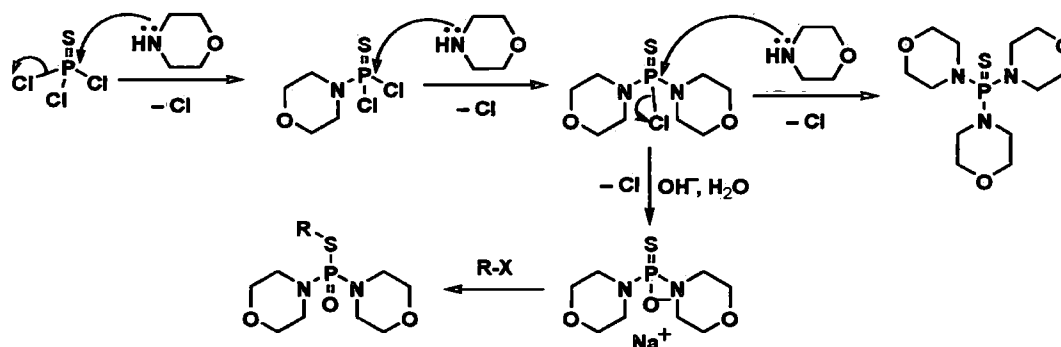


Figure 2. 30 Liposoluble morpholine thiophosphortriamidate and alkylated morpholine thiophosphordiamidate. R- aliphatic moiety derived from alkylating agent

The rationale behind this strategy was the assumption that the triamidate product should simply be removable *via* extraction. The issue of the diamino feature formation would, hopefully, be resolved *via* alkylation of the sulfhydryl group, which would produce a non-ionic structure **50** that would also be easily extracted as well. The desired product *S*-alkylated monomorpholine thiophosphoramidate would, on the other hand, remain in the aqueous layer as a water-soluble molecule. Therefore, an ‘excess then extraction’ approach, as presented in the previous section for benzylamine and allylamine, was attempted and will be presented in the following section.

2.12. Continuous method: the use of excess of morpholine

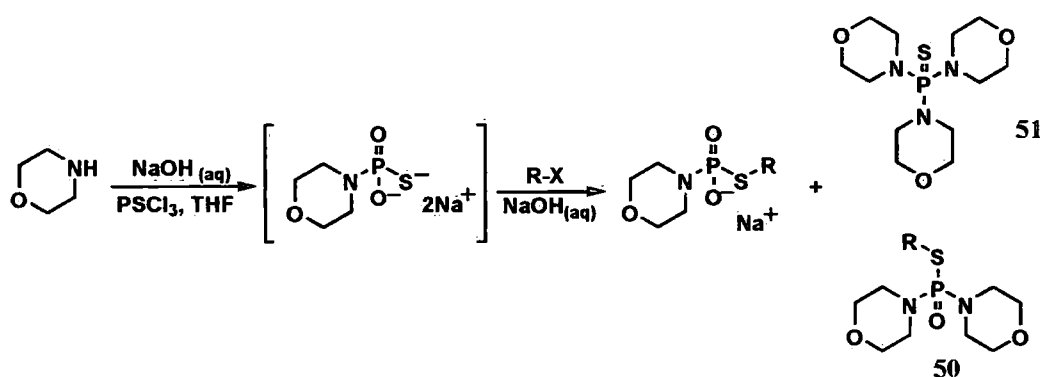
As outlined in the previous section, preliminary experiments suggested multiple amine nucleophilic substitutions on the thiophosphoryl centre (scheme 2.25).



Scheme 2. 25 Amidation of thiophosphoryl chloride producing diamidates **49**, **50** and triamidates **51**

We hoped to use the high reactivity of morpholine towards thiophosphoryl chloride and multiple additions, as a strategy for the generation of highly pure morpholine thiophosphoramidate derivatives. As expected, the increase in the generation of both di- **49** and

thiamidates **50** was in line with applied excess of amine. After a few optimisation experiments, it was concluded that, in aqueous thiophosphorylation, excess of morpholine higher than 20% was unnecessary, as all of the thiophosphoryl chloride was, already, used up and the formation of undesired diamino and triamino products increased. Therefore, using the one-pot procedure (described in the section 2.7) with aqueous thiophosphorylation and 1.2 equivalents of morpholine, followed by addition of 2 equivalents of alkylation agent and extraction, a range of alkylated thiophosphoramidates of morpholine was generated (scheme 2. 26 and figure 2.32).



Scheme 2. 26 One-pot method for the production of alkylated thiophosphoramidates using morpholine excess

In order to accelerate alkylations using benzyl chloride, 1-propyl iodide and 2-propyl iodide, vigorous stirring at 80 °C was applied. After completion of the reaction, monitored *via* ^{31}P NMR spectroscopy, triamidate derivative **51** and *S*-alkylated di-amidate products **50** along with the excess of alkylating agent were removed from the mixture, using chloroform, which showed the highest extraction ability of the solvents tested. Products and conversions gained are presented in the figure below.

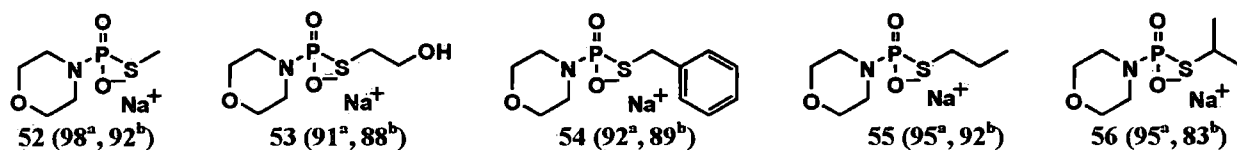


Figure 2. 31 Products gained *via* the one-pot Tripartite thiophosphoramidate method using morpholine.
 % ^a purity estimated *via* ^{31}P NMR spectroscopy, ^b purity estimated *via* ^1H NMR spectroscopy

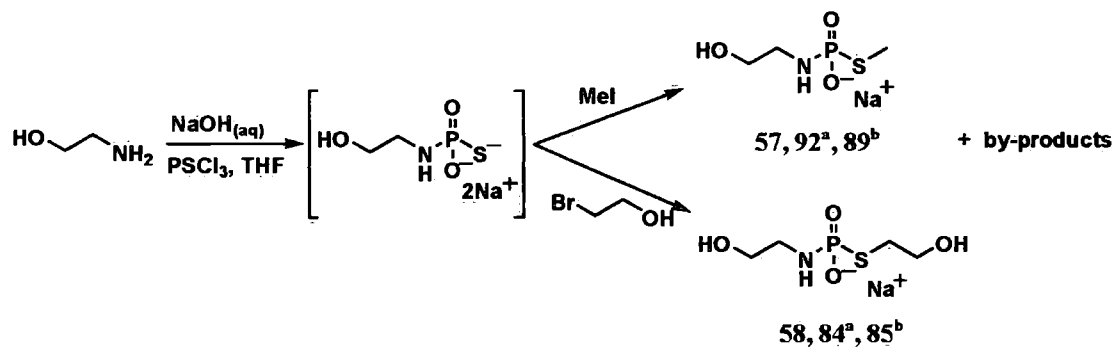
Even though, some of the predicted by-products (**50** and **51**) were removed from the reaction mixtures, compounds the samples still contained impurities in the form of phosphoramidates, alkylated inorganic phosphate and thiophosphate. In some cases, where the diamidate product

49 had not been fully alkylated, desulfurization occurred and a few percentage of the phosphordiamidate of morpholine were detected. However, the results gained on these investigations on morpholine as a representative amphiphilic molecule were very satisfactory and confirmed the wide applicability of the one-pot Tripartite method.

2.13. One-pot method: the use an equal number of equivalents of ethanolamine and thiophosphoryl chloride

Owing to the undesired number of impurities in 'the excess of thiophosphoryl chloride-methanol precipitation' approach and having excluded the possibility of using 'the excess of amine-extraction' strategy because of the poor partitioning of ethanolamine towards organic solvents, we were forced to accept the limitations in performance that ethanolamine presented under in our one-pot Tripartite thiophosphoramidate methodology.

Therefore, the simple approach of using of 1 equivalent of ethanolamines in the aqueous thiophosphorylation step was applied.



Scheme 2.27 One-pot method of formation of the alkylated thiophosphoramidate of ethanolamine.
 %^a purity estimated via ³¹P NMR spectroscopy, %^b purity estimated via ¹H NMR spectroscopy

In both experiments, the by-products that were formed were small amounts of alkylated thiophosphate, ethanolamine phosphoramidate and inorganic thiophosphate (< 6% by ³¹P NMR spectroscopy and <12% by ¹H NMR spectroscopy). A minor broad signal at around 23 ppm, suggested the formation of an unidentified feature (<2% ³¹P NMR spectroscopy) that can be connected to some unassigned signals in the ¹H NMR spectra. ¹H NMR spectroscopy also

revealed the presence of some unreacted ethanolamine (<5%) and around 6% of quaternary ammonium salt, trimethylate of ethanolamine.

The effect of the amount of additional aqueous sodium hydroxide used for preserving high pH of the reaction mixture on the outcome of the bromoethanol alkylation was investigated.

Table 2. 2 Variation of the additional sodium hydroxide on the conversions: 2-bromoethanol

1M NaOH (Eq)	0	0.5	0.9	1.5	1.7
Purity (%)^a	98	87	90	80	66

^aDetermined by ³¹P NMR spectroscopy performed on crude reaction mixture (H₂O and THF)

A reduction in the signal of the alkylated phosphoramidate of ethanolamine in ³¹P NMR spectra with the increased addition of sodium hydroxide was observed. This was probably due to the deprotonation of hydroxyl group and an increase in the likelihood of intramolecular cyclisation resulting in hydrolysis at the thiophosphate. A similar phenomenon was noticed in the stepwise alkylation experiment and was described in section 2.6.1, where the mechanism is illustrated,

In the light of our work with ethanolamine, we would also expect to meet similar issues other water-soluble amines. However, an additional complication connected to ethanolamine, is the nucleophilic hydroxyl group that potentially could have performed intramolecular cyclisation. Even though conversion were not as high as we hoped for, the outcome of this quick and simple strategy for making alkylated thiophosphoramidates of water-soluble amines was still very satisfying, in the case of methyl iodide conversions as high as 92% were attained, according to ³¹P NMR spectroscopy.

2.14. Exploitation of the one-pot method: proof of concept generation of a library of amines

Sharpless used a library of amines for the Huisgen 1,3-dipolar cycloaddition, the most popular ‘Click’ reaction, to generate an array of triazole products, which were further tested as potential fucosyltransferase inhibitors (section 3.1.2).⁶ The yields in these experiments were in the range from very poor 39% to 100%. In order to test the scope of our one-pot Tripartite

thiophosphoramidate method, a library of amines that contained some of the large lipophilic amines that Sharpless used for his fucosyltransferase library, were employed and a range of products were generated (scheme 2.32).

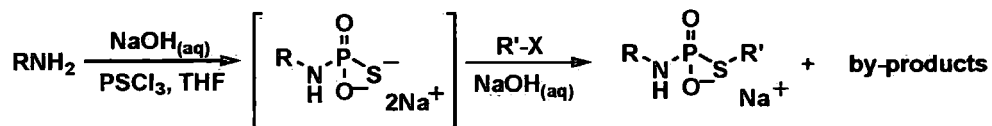


Figure 2. 32 Exploitation of the one-pot method; generation of the library of compounds

Some of the alkylated thiophosphoramidates (71, 72, 74 and 75) showed signs of precipitation during extraction, suggesting poor solubility of the products in both water and diethyl ether, owing to the large lipophilic aromatic substituents and the ionised thiophosphate feature. In these examples, the aqueous layer was centrifuged and the precipitate was dried prior to NMR spectroscopic analysis, which was then performed in methanol, which did actually dissolve these products. The purity of each member of the library of alkylated thiophosphoramidates was estimated using ^{31}P and ^1H NMR spectroscopies.



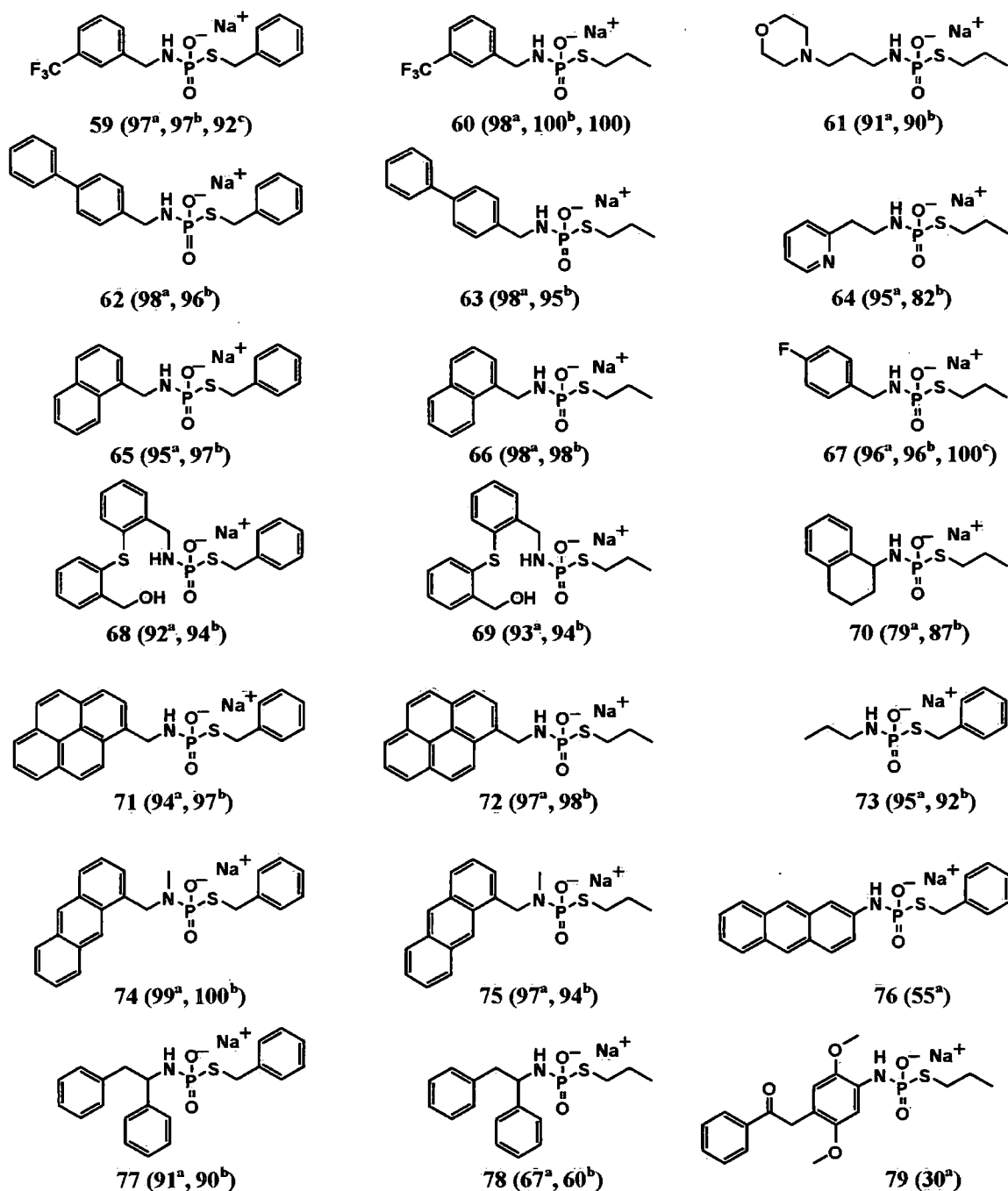


Figure 2.33 A library of alkylated thiophosphoramidates. Estimated purity (%) ^adetermined by ³¹P NMR spectroscopy, ^bdetermined by ¹H NMR spectroscopy and ^cdetermined by ¹⁹F NMR spectroscopy.

The range of amines involved primary and secondary lipophilic amines containing large and small aromatic blocks and heterocyclic features. Some aromatic amines were employed as well

but the resulting product mixtures were difficult to analyse owing to the large number of impurities in these examples. However, conversions to products were, in any case, less than 30-50% and did not give signal in the mass spectrometry (76 and 79, figure 2.38).

The estimated conversions ranged from 70% to an impressive 100%, according to ^{31}P NMR spectroscopy. The impurities, if any, were mainly phosphoramidate and *S*-alkylated inorganic thiophosphate (seen in the ^{31}P NMR spectra). The library of alkylated thiophosphoramidates was produced quickly using our simple and efficient one-pot Tripartite thiophosphoramidate chemistry, suggesting its applicability to a wide range of reaction systems. In order to apply the understandings we have gained from these and all previously performed experiments, a tentative study, involving nucleoside monophosphate derivatives as the first steps towards the generation of diphosphate mimics, for applications in biologically interesting systems, was carried out and the results are presented in Chapter 3.

2.15. The stability of *S*-alkylated thiophosphoramidates

Depending on the research targets, the stability issue of *S*-alkylated thiophosphoramidates can be approached in two ways, as either a desirable or an unwanted characteristic of the produced compound. If the mode of biological action requires the complete structure then obviously high stability is of a great importance. A number of drugs, because of their mechanisms of delivery, require high lipophilicity or polarity, but gain their activity only after being subjected to a metabolic process in the live organism (some examples are outlined in the section 4.6). To our knowledge, there is no direct detailed study in the literature about the hydrolytic stability of *S*-alkylated thiophosphoramidates. Therefore, we have decided to check on the hydrolysis characteristics of our thiophosphoramidate systems. Simple stability experiments at two pH-s with a representative compound were performed.

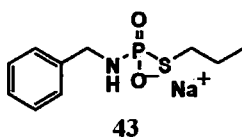


Figure 2. 34 *S*-propylated benzylamine thiophosphoramidate was used as the stability test compound

This compound was chosen as it contains no other functionalities (such as hydroxyl, an carboxyl, sections 2.17 and 5.10), so the only possible degradation pathways of this thiophosphoramidate would be via cleavage of P-N or P-S bond as a consequence of the pH conditions.

The stability experiments were performed using ^{31}P NMR spectroscopy as the kinetic approach. The hydrolysis studies on ethanolamine thiophosphoramidate (section 2.5.3) suggested that ^{31}P NMR spectroscopy was not a suitable kinetic method, where the issue of balance between high concentrations of sample, pH control and quality of spectra collected, was not easily met. However, owing to the shortage of time available and the desire to gain a rough feeling of the stability of these compounds, ^{31}P NMR spectroscopy was applied again. In addition, only two pH points were tested pH~7.5, as close to physiological conditions and pH 5.2 where the possibility of degradation is more probable (this pH was chosen to parallel *in vivo* tests performed with quinoline systems Chapter 4.).

Samples were prepared as described in section 2. 5.3 by dissolution of 25 mg of sample **43** in HEPES buffer pH 7.5 or acetate buffer pH 5.2, recording the pH of the resulting solution (7.45 and 5.26, respectively) and the sample was lyophilised. The sample to buffer ratio used this time was only 1:3, in order to decrease the effect of ionic strength on NMR performance. The dry solid was dissolved in D_2O to a give final concentration of 0.32 M of the sample **43** and was subjected to ^{31}P NMR spectroscopy through time at 37 °C. After the analysis of the resulting spectra, no change in the intensities of the peak corresponding to the *S*-alkylated thiophosphoroamidate over the time scale of 16 h occurred and it was concluded that the sample **43** was stable at both pH 7.5 and 5.2.

In addition, at the end of data collection the pD was measured, and after conversion to pH ($\text{pH}=\text{pD}-0.4$), a small change of pH 7.5 sample was noticed ($\Delta\text{pH}=0.08$). However, not all of the deuterium was exchanged, therefore the ± 10 variation would be expected. At pH=5.2,

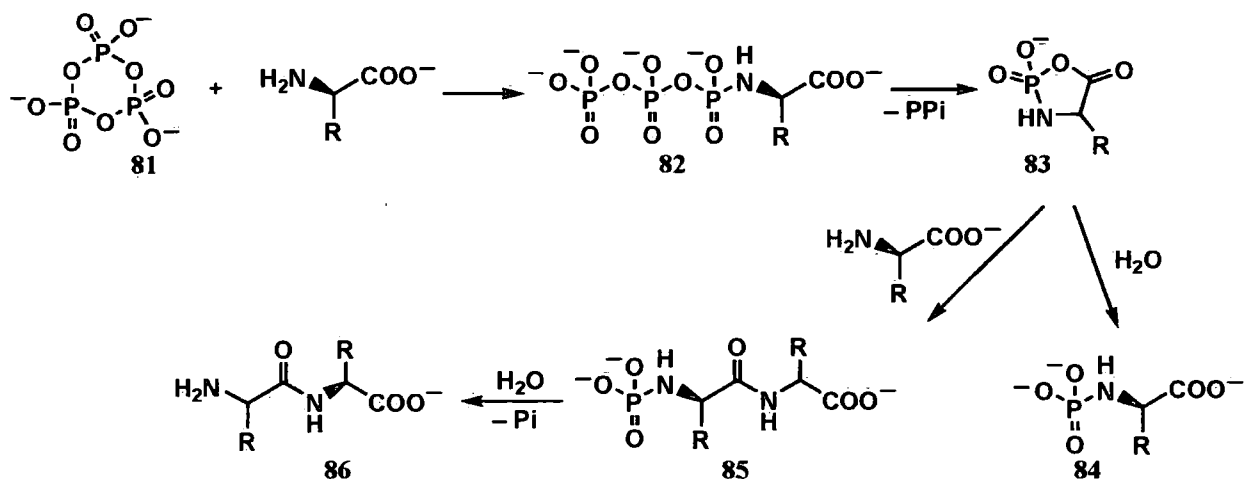
$\Delta\text{pH}=0.5$, which was of higher significance, however, the experiments have provided us with confirmation of high stability of *S*-alkylated thiophosphoramidates at both physiological and slightly acidic pH-s over 16 h at 37 °C. P-N cleavage is prompted by protonation of nitrogen, which makes the amine-substituent a better leaving group. Therefore, with some exceptions, corresponding to intramolecular reactions, we can conclude that, as expected, the stability of thiophosphoramidate when *S*-alkylated has greatly improved.

2.16. ‘Challenging’ amines: amino acids, aromatic amines and sugars

In order to explore the possibilities with respect to more complex amines in the thiophosphoramidate Tripartite chemistry, a few preliminary experiments on phenylalanine, aniline and glucosamine were carried out.

2.16.1. The aqueous thiophosphorylation of phenylalanine

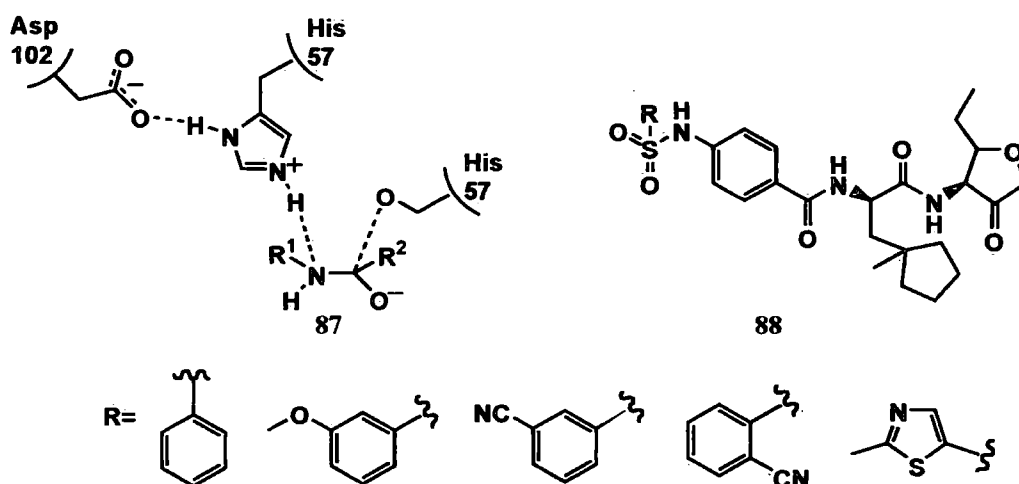
As previously introduced in section 1., posttranslational phosphorylation of proteins and peptides is an important modification in many cellular processes, that functions by switching cellular activities from one stage to another and regulates the events of signal transduction, cell differentiation and proliferation, gene expression.⁷⁹ The majority of current studies have been dedicated to the phosphorylation of serine, threonine and tyrosine as *O*-phosphorylations. *N*-phosphorylations of amino acids are important factors in biosynthesis and function of proteins as well.^{80, 81} An example of the formation of dipeptides **85** that uses phosphorylation of amino acids as the starting point is illustrated below.⁸²



Scheme 2. 28 The formation of the dipeptide with the mono- and tri-phosphoramidate as the mediators

Cyclic triphosphate **81** was used as the source of for the introduction of phosphate moiety. The carboxylate group of the triphosphoramidate **82** induced cyclisation that, with the expulsion of the pyrophosphate, gave rise to cyclic product **83**. In the nucleophilic attack by water monophosphate **84** was generated, while, with the excess of amino acid, monophosphordipeptide **85** was generated. Finally, after hydrolysis of the intermediate **85**, dipeptide **86** was released.

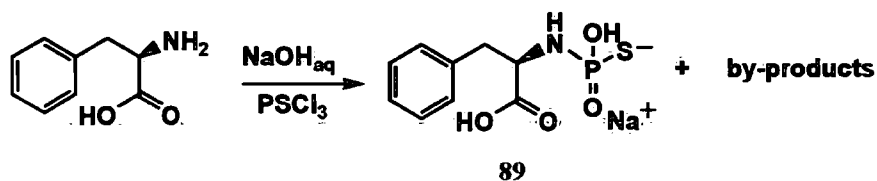
A recent paper introduces sulphonamide derivatives **88** as mimics of the serine protease transition state **87** that inhibit peptide cleavage at sub-nanomolar concentrations.⁸³



Scheme 2. 29 Serine protease inhibitors

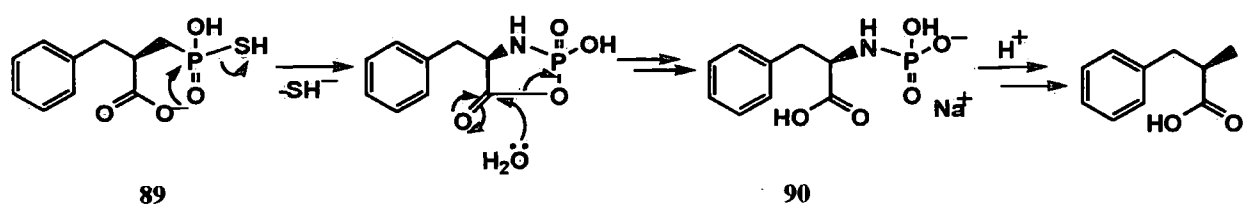
The high potency of these inhibitors was believed to lie in the hydrogen bonding that the sulfonamide offers. The resemblance with our thiophosphoramidate system could potentially be used to mimic similar systems.

Some of the existing methods for thiophosphorylation of histidine were described in section 2. We hope to generate alkylated thiophosphoramidates of amino acids applying our one-pot Tripartite method. Therefore, we chose phenylalanine (Phe), as a simple representative with no hydroxyl or amino groups on the side chain to interfere in the thiophosphorylation step. A preliminary experiment was performed applying aqueous thiophosphorylation using a 20% excess of thiophosphoryl chloride (the attempt using 1 Eq resulted in incomplete Phe thiophosphorylation=55% according to ^{31}P NMR).



Scheme 2. 30 Aqueous thiophosphorylation of phenylalanine

The expected doublet for Phe-thiophosphoramidate at 42 ppm in the ^{31}P NMR spectrum was detected in 70% conversion. A number of unidentified phosphorus impurities were noticed, all present at less than 2% each (8% in total). Inorganic thiophosphate was present at 19% and phosphoramidate in 3%, which was also detected *via* ^1H NMR spectrometry as the only impurity (5%) suggesting 95% conversion of Phe into the desired thiophosphoramidate. However, HPLC coupled with mass spectrometry suggested the presence of mainly Phe, phosphoramidate (desulfurised form off 89), dipeptide Phe-Phe and small amounts of the desired thiophosphoramidate. The possibility of intramolecular cyclisation resulting in P-N cleavage and desulfurization during HPLC/MS was highly probable, as HPLC was performed at low pH (~3).



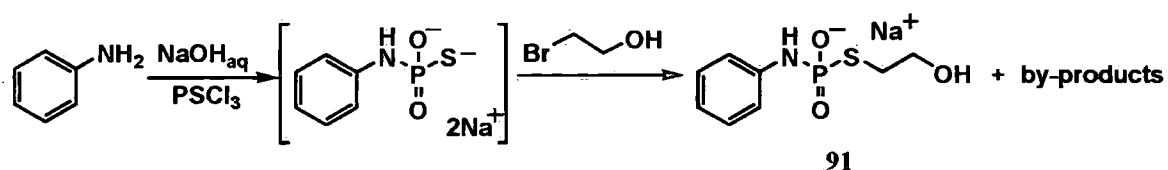
Scheme 2.31 Desulfurization and hydrolysis of thiophosphoramidate of Phe

An attempt towards alkylation of Phe-thiophosphoramidate was performed stepwise directly in an NMR tube using dry Phe-thiophosphoramidate dissolved in D_2O . On the addition of methyl iodide, it was noticed that alkylation occurred with only 24% conversion (according to ^{31}P NMR spectroscopy). A number of impurities were detected with the most significant being Phe phosphoramidate **90** and inorganic phosphate as the products of desulfurization of Phe thiophosphoramidate and inorganic thiophosphate at the high pH.

In any case, an encouraging thiophosphorylation of Phe was performed that with appropriate optimisation studies might be improved, however, owing to the project time limitation no further experiments were carried out.

2.16.2. Continuous Tripartite method: aniline

In the thiophosphoramidate system so far aliphatic, primary and secondary amines were used. An introduction of aromatic amines into our aqueous thiophosphorylation method coupled with continued alkylation of the resulting aryl thiophosphoramidates would greatly expand the application of our thiophosphoryl Tripartite method. As mentioned previously, we have used aniline as the simplest example of an aromatic amine, which has much higher nucleophilicity⁷⁴ than it would be expected if the corresponding pK_a of the conjugate acid of aniline (4.6) was considered. In order to test this aromatic amine in our one-pot method bromoethanol was used as alkylating agent.



Scheme 2.32 One-pot method for preparation of bromoalkylated aniline thiophosphoramidate

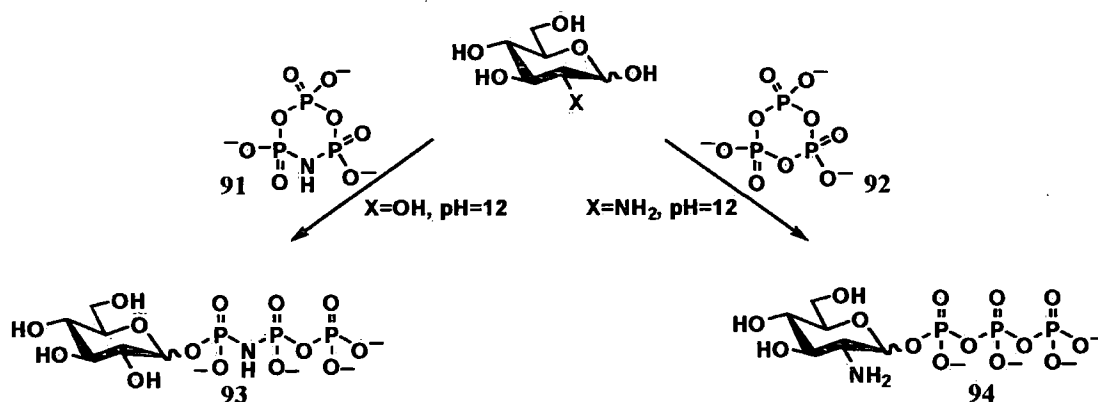
^{31}P NMR spectroscopy revealed two triplets at 17 and 18 ppm that had different coupling constants (11.4 and 13.4 Hz, respectively) and at conversion levels of 32% and 47%, respectively. Owing to our experiences from previous experiments, it was concluded that the signal at 17 ppm matched the alkylated inorganic thiophosphate impurity. With the help of ^1H NMR spectroscopy and HPLC/MS, it was confirmed that two triplets seen in ^{31}P NMR correspond to desired product **91** and alkylated inorganic phosphate. However, estimation of the purity via HPLC was not possible as the desired product and alkylated inorganic phosphate eluted with the same retention time. As for other impurities, some unreacted aniline (19%) was detected *via* ^1H NMR spectroscopy and around a 10% total of unidentified products. Another signal in ^{31}P NMR spectrum a slightly lower field (22 ppm) occurred in around 11%, which closely relates in term of integral to the unidentified impurity seen in the ^1H NMR spectrum.

In conclusion, the performance of aniline in our one-pot method was moderate with conversion of 47% according to ^{31}P NMR spectroscopy and 41% according to ^1H NMR spectroscopy. Owing to the limited time available no optimisation was performed, however, these preliminary results suggested that this area should be explored in the future.

2.16.3. The aqueous thiophosphorylation of glucosamine

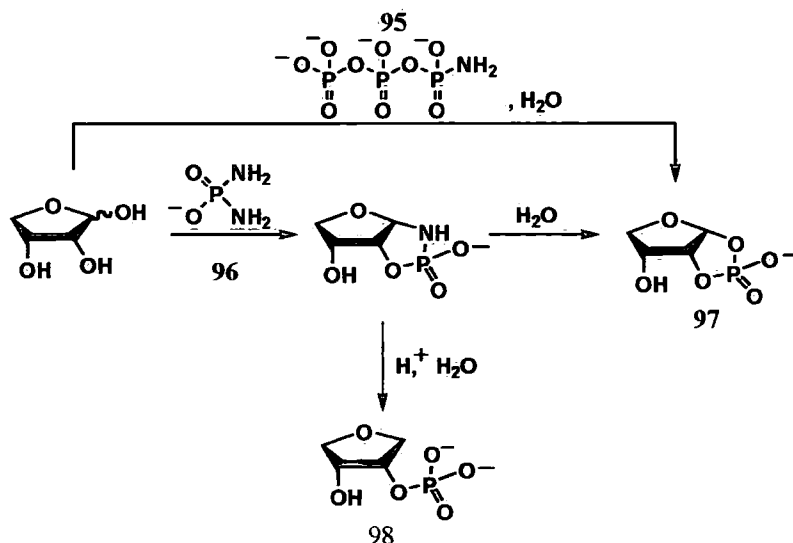
Phosphorylation of sugars is a trigger for many processes in organisms. An important event is sugar metabolism and energy exploitation starts with the 6-phosphorylated derivatives of glucose.⁸⁴ On the other side, phosphorylation of hexoses causes sugar induced cell death in yeast.⁸⁵ In organisms sugar phosphorylation occurs with the help of sugar kinases. An aqueous method found to phosphorylate sugars, similar to the one described for amino acids (section 2.16.1), used inorganic sodium cyclotriphosphoramidate **91** or cyclotriphosphate **92** as phosphorylating agents. The yields of the reactions were poor, 32% in the case of formation 1-*O*-diphosphoramidophosphono-D-glucose **93** and 14% 1-triphosphoamidate product **94**, respectively (scheme 2.33).^{86, 87} In these examples *N*-phosphorylation of D-glucosamine was

reported to have occurred in very small proportions (5%) with the assumption that the anomeric OH group was readily phosphorylated compared to the amine group.



Scheme 2.33 Formation of 1-glucose triphosphates

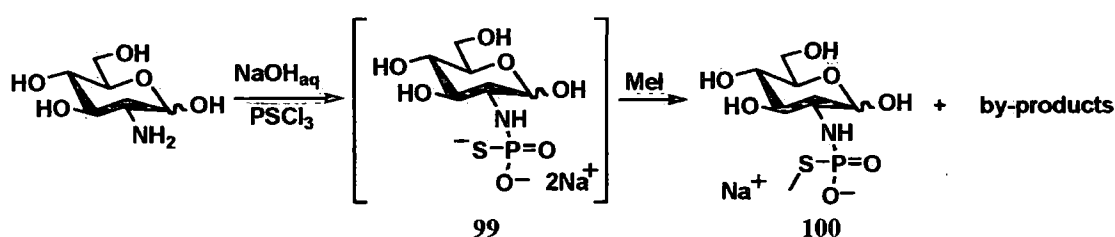
In the following examples of phosphorylation of aldoses in aqueous solution, amidotriphosphate **95** and diamidophosphate **96** were used in aqueous systems and the formation of the cyclic intermediate **7** was achieved regioselectively (scheme 2.34).⁷¹



Scheme 2.34 Regioselective phosphorylation of aldoses

In a one-pot transformation with appropriate pH control, the phosphoamide bond is cleaved and the 2-phosphate derivative **98**, in yields as high as 79%, is formed.

We set off to try to monothiophosphorylate and alkylate glucosamine (Glc-NH₂) using our one-pot method. As the initial ³¹P NMR spectrum of the crude mixture after the thiophosphorylation step presented great conversions of 97% (2% of inorganic phosphate and 1% of an unidentified phosphorus impurity), we were encouraged to carry out the experiment with the addition of methyl iodide.



Scheme 2. 35 An attempt towards generating *S*-alkylated thiophosphoramidate of GlcNH₂ using the one-pot method

However, on addition of methyl iodide hydrolysis of **99** occurred and beside the major signal being for inorganic phosphate, there were two other phosphorus⁸⁷ signals at 25 and 22 ppm in around 12% conversion each, which might be the desired product **100** (both anomers) and alkylated inorganic thiophosphate (17%). In another attempt to generate the thiophosphorylated glucosamine **99** only, two doublets at 42 and 44 ppm in the ³¹P NMR spectrum (33% conversion each) were detected, presumably, for the α- and β-anomers of GlcNH₂, along with a broad signal in the inorganic thiophosphate area (35 ppm). ¹H NMR spectroscopy was in agreement with the ³¹P NMR spectrum with 63% conversion to thiophosphorylated amine, where 37% of glucosamine was left unreacted. However, mass spectrometry did not detect either the desired product **99** or the desulphurisation product that is commonly found in these systems. The possibility of intramolecular nucleophilic substitution at the anomeric centre by the sulfhydryl group (scheme 2.) was considered, however, it was not confirmed owing to the complicated ¹H NMR spectrum and no signal being detected for **101** via mass spectrometry.

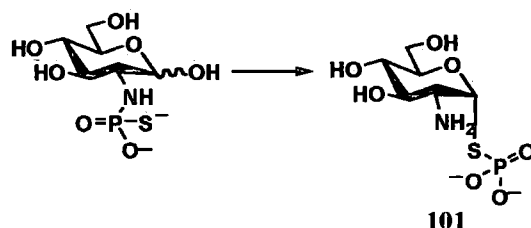


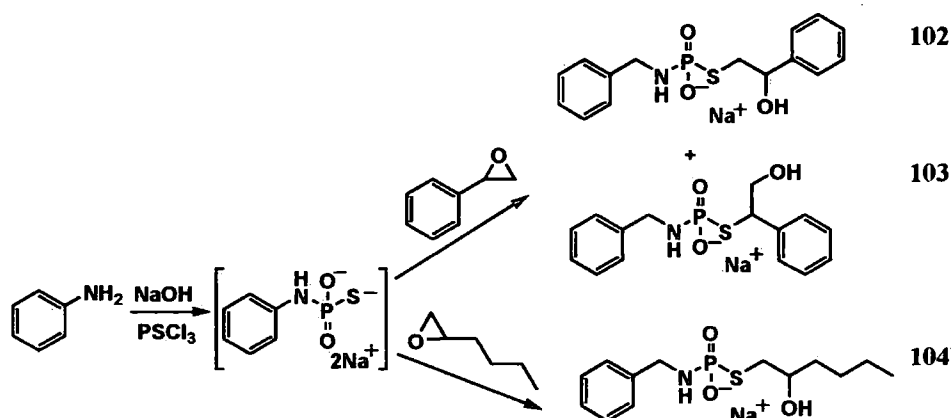
Figure 2. 35 Possible intramolecular nucleophilic substitution in thiophosphorylated D-glucosamine

No further optimisation studies were performed, but because of the promising results that ^{31}P NMR spectra presented for the thiophosphorylation step, future studies in this are likely to be fruitful.

2.17. Expansion to a range of alkylating agents

The alkylating agents used in the establishment of the one-pot thiophosphoramidate Tripartite chemistry were simple alkyl halides. As mentioned in the introductory chapter (section 1.1.2), nucleophilic ring opening of the epoxides readily happens in aqueous environments. Therefore, we opted to see what level of success we would achieve if our thiophosphoramidate were to be exposed to an epoxide functional group. In addition, another few examples were studied. Unsaturated carbon-carbon systems, including both electrophilic alkene and alkyne examples along with a trial experiment with benzaldehyde were performed. Alkyl acrylates are known to act as electrophiles in conjugate additions. They are, as RX alkylation agents, potentially toxic and carcinogenic as they readily react with thiol and amine groups of enzymes. This reactivity of methyl methacrylate we hoped to use to our advantage. sp -carbon is even more susceptible to nucleophilic attack than the alkene systems and we used a terminal alkyne in the form of methyl propiolate. Our one-pot Tripartite method for lipophilic amine (section 2.7) was applied using an excess of benzylamine in all experiments.

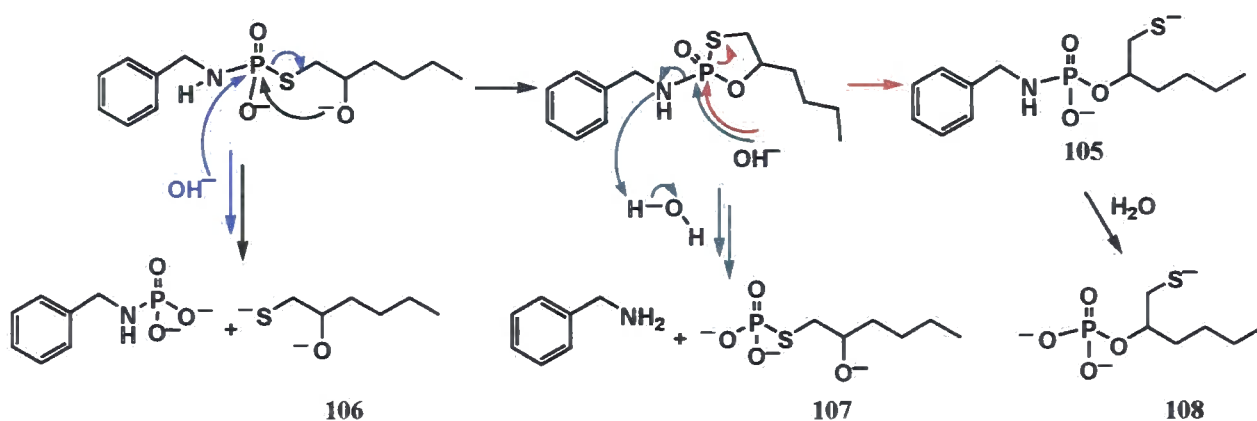
In the epoxide experiments, styrene oxide and 1,2-epoxyhexene were used.



Scheme 2.36 Epoxides in the one-pot method

Styrene oxide suffered nucleophilic attack on both sides of the epoxide ring, yielding a mixture of products **102** and **103** in conversions of 63% and 26%, respectively, according to integration of the ^{31}P NMR spectrum. The impurities present were, phosphoramidate (1%) and alkylated inorganic thiophosphates where epoxide ring opening occurred in both positions. ^1H NMR spectroscopy has presented a quite complicated mixture of all previously mentioned products. A similar result occurred in an attempt to increase selectivity by cooling the reaction mixture to $0\text{ }^\circ\text{C}$. With the possibility of benzyl resonance stabilisation, styrene oxide in water can exhibit electrophilicity on both carbon atoms. Thus, in this case water probably reduces regioselectivity in epoxide attack, as it stabilises the positive charge of more substituted carbon.

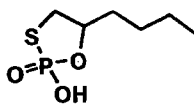
In the case of 1,2-epoxyhexane, nucleophilic addition occurred selectively only at the non-substituted end of the epoxide ring, owing to steric hindrance the more substituted epoxide carbon. However, a significant degree of degradation of product **104** was noticed, which happened during the lyophilisation of the aqueous solution of sample. The assumption was made that, owing to the high pH of the aqueous solution (~ 10), The hydroxyl group of the alkyl chain was deprotonated and initiated an intramolecular cyclisation, which resulted in P-N cleavage and formation of alkylated inorganic thiophosphate **107** (scheme 2.36).



Scheme 2. 37 Possible intramolecular cyclisation caused by high pH of the media

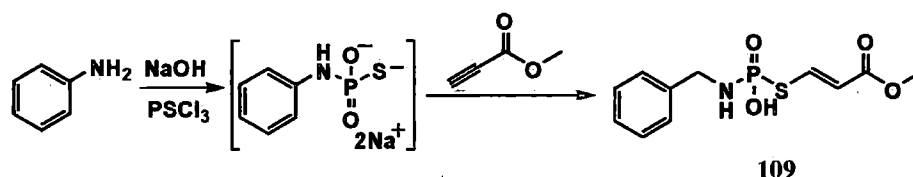
The proposed formation of derivatives **106** and **108** was backed up by the appearance of triplets at 10 ppm and doublet at 4 ppm in the ^{31}P NMR spectrum.

For this reason, following the extraction step and prior to lyophilisation, the aqueous solution was adjusted to pH 8 using diluted hydrochloric acid (50 mM). This prevented the hydrolysis of the desired product **104** during lyophilisation, which was, then, generated with 96% conversion estimated by ^{31}P NMR spectroscopy and 95% according to ^1H NMR spectroscopy. During optimisation of the reaction condition, it was noticed that 2 M hydrochloric acid caused cleavage of P-N bond and formation of a cyclic alkylated inorganic phosphate formed (figure 2.37).



Scheme 2. 38 Product of acid catalysed hydrolysis of 1,2-epoxidehexane alkylated benzylamine thiophosphoramidate

In the reaction between methyl propiolate and benzylamine thiophosphoramidate at room temperature, using the one-pot tripartite thiophosphoramidate method, product **109** was formed with 92%, 94% conversion according to ^{31}P , ^1H NMR spectra. Some of hydrolysis occurred and a signal 2 ppm higher than desired product was detected (7%) in the ^{31}P NMR spectrum, which was in the agreement with proton and carbon NMR spectra.



Scheme 2. 39 Methyl propiolate as a successful agent for the alkylation of thiophosphoramidates

Experiments performed using benzaldehyde and methyl methacrylate were unsuccessful, as no shift of signal from ~ 45 ppm in the ^{31}P NMR spectra for the thiophosphoramidate of benzylamine was observed.

The deprotonated sulfhydryl group is a soft nucleophile and thus it is not surprising that nucleophilic attack on the hard carbonyl electrophile of benzaldehyde did not occur. In addition, the adduct formation may have been reversible. As for methyl methacrylate, it was

surprising that no reaction has occurred. However, great successes using 1,2-epoxyhexane and methyl propiolate, and moderate success with less selective styrene oxide were demonstrated, which greatly expands the scope of our one-pot Tripartite thiophosphoramidate method.

2.18. Conclusions on and potential of the thiophosphoramidate system in future experiments

We have successfully applied the principles of the aqueous amine phosphorylation method established in our group to the thiophosphorylation of amines using thiophosphoryl chloride. ^{31}P NMR hydrolysis studies on ethanolamine thiophosphoramidate were carried out to create a pH profile was used to determine the most proficient conditions for alkylation. In the high pH region ($\text{pH} > 9$), which thiophosphoramidate hydrolysed with the half-life of more than 6 h. Therefore, the alkylation reaction was performed in highly basic media. Two synthetic strategies were explored, stepwise and Tripartite continuous. In the stepwise approach, thiophosphoramidates were lyophilised prior to alkylation. The success of the stepwise method encouraged us to move to the more practical, one-pot approach. We have established the aqueous Tripartite strategy in a one-pot manner that, in easy steps, allowed for the thiophosphorylation of amines followed by alkylation of the resulting thiophosphoramidates. In this way a number of products were generated quickly and efficiently in conversions that ranged from 70% to 100%, according to ^{31}P and ^1H NMR spectroscopy. A range of commercially available amines of different natures, such as primary and secondary, lipophilic and hydrophilic, and commercially available alkyl halides were employed to design the most suitable thiophosphoramidate procedure that was then successfully applied to a library of amines to prove the concept.

With the goals of challenging the limits and expanding the applicability of the one-pot Tripartite thiophosphoramidate method, we performed preliminary experiments on phenylalanine, glucosamine and aniline. The success with aniline was moderate, but still promising. Straightforward conclusions on the phenylalanine and glucosamine examples were not possible. The NMR spectroscopy, on one hand, strongly suggested positive outcomes,

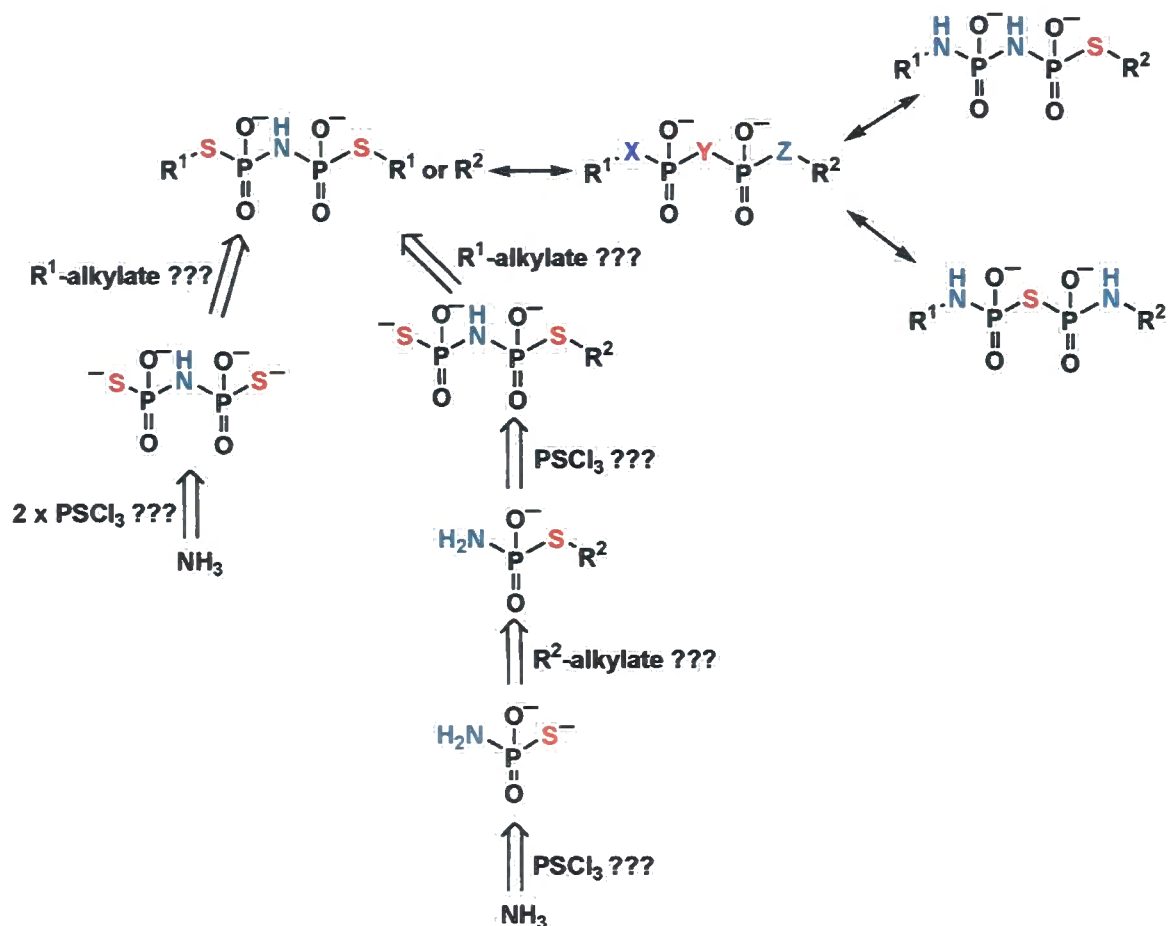
however, mass spectrometry did not confirm these results. In any case, we believe that these systems have potential and are worthy of further examination and optimisation. In the context of expanding the range of alkylating agents, we explored the involvement of epoxides, of which the monosubstituted alkyl epoxide showed great potential, unlike, the less selective styrene epoxide that generated a mixture of products. Terminal alkynes gave good conversions, while a methacrylate alkynes and an aldehydes presented no alkylation activity towards a thiophosphoramidates.

The issues that we encountered, and that have been studied by others as well, during the development of the thiophosphoramidate systems can be related mainly to the instability of the P-N or P-S bond of thiophosphoramidates. In the case of non-alkylated thiophosphoramidates the P-N bond is cleaved readily in acidic media. Desulfurization occurred more readily with the non-alkylated forms of the thiophosphoramidate than the *S*-alkylated. However, with long exposure to high pH and the possibility of the intramolecular reactions with free hydroxyl groups (e.g. with ethanolamine, 1,2-epoxyhexane), both P-N and P-S bonds were cleaved leading to the formation of undesired products. This issue we dealt with by pH adjustment to lower pH where deprotonation of the hydroxyl groups was disabled.

The one-pot Tripartite thiophosphoramidate method was successfully employed for the synthesis of alkylated thiophosphoramidates of nucleoside amines as a first step on the way to investigations on the synthesis of nucleoside diphosphate mimics (described in the following Chapter). In addition, the generation of a library of quinoline-based thiophosphoramidates that are potential antileishmanials showed the simple application of the Thiophosphoramidate system.

The insights gained from the development of the one-pot method for the production of *S*-alkylated monothiophosphoramidates could be extended to diphosphates and, in due course, triphosphate analogues. The aim is, again, to establish simple, effective and preferably one-pot procedures that avoid time-consuming chromatographic procedures. The method for production

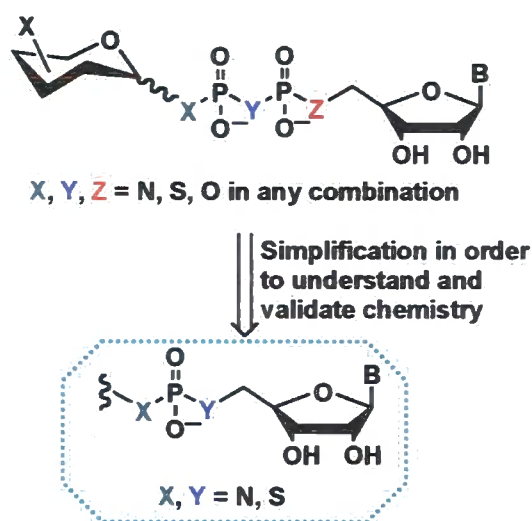
of diphosphate analogues would potentially enable the generation of the nucleoside diphosphate mimics that could be potential glycosyltransferase inhibitors. The proposed generic structures are shown below.



Scheme 2. 40 Potential future work on thiophosphoramidate systems

3.0 Nucleosides and their application in the thiophosphoramidate system

If we look back at the start of the thiophosphoramidate story and remember what the final, biologically important target was, one major aspect of the thiophosphoryl chemistry that we were trying to establish involved nucleoside features. In particular, in the thiophosphoramidate system, attention was focused on fucosyltransferase that requires a guanosine diphosphate moiety as the transporter of monosaccharide units (presented in the following section). In order to mimic this species, we have designed a system based on thiophosphoramidate-like features that offer great possibilities in terms of variation in structure. Diphosphate mimics are more challenging to work with, so as a starting point we shall study nucleoside monothiophosphoramidates, as presented in the figure below (introduced in the section 2.2), in order to validate our methodology



Scheme 3. 1 Simplification strategy as the first step in generating nucleoside-based thiophosphoramidate systems

The rationale behind examining fucosyltransferase enzymes reflects our previous experience and knowledge gained from dealing with guanosine and its derivatives in our group (section 2.1). In addition, as mentioned before, guanosine and uridine moieties are present in the majority of the sugar transferases natural substrate structures. Therefore, with our understanding of one system, such as guanosine, in future it should be possible to quickly expand the guanosine

thiophosphoramidate method to other nucleosides. With investigations on uridine, given that the uridine diphosphate-requiring enzyme systems, such as chitin synthase are ubiquitous, many glycosyltransferases could be open to inhibition studies.

The guanosine feature could be introduced at either side of the thiophosphoramidate bridge (figure 3.1).

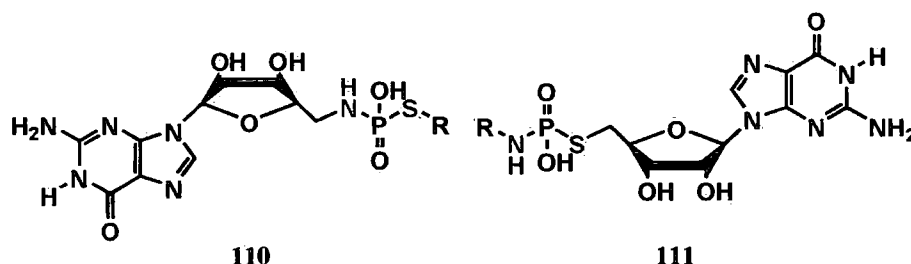


Figure 3. 1 Guanosine at either end of the thiophosphoramidate moiety. **R** = any aliphatic feature

If 5'-amino-5'-guanosine were used for thiophosphorylation, the structural variation in the molecule **110** can be brought *via* a range of alkylating agents. 5'-Amino-5'-guanosine can be generated using a three-stage method described in the following sections. On the synthetic pathway the first intermediate was 5'-iodo-5'-guanosine. This was also used for another approach towards nucleoside thiophosphoramidates, as iodoguanosine acts as an alkylating agent towards thiophosphoryl groups allowing connection to ranges of amines to generate structures of the same form as molecule **111** (figure 3.1).

A general introduction to the importance of glycosyltransferases was given in the first chapter. Here follows a short outline of the fucosyltransferase enzyme systems and some existing inhibitors, which are mimics of the natural substrate. Literature methods that we have used to prepare 5'-azido-5'-guanosine and 5'-amino-5'-guanosine will be compared and contrasted to novel aqueous approaches, established by us. Finally, achievements on nucleoside derivatives in the context of the thiophosphoramidate Tripartite system will be presented and used to design future experiments for the expansion of our newly established methods.

3.1. Research targets in the form of glycosyltransferases

Previously in the section 1.3, we introduced a group enzymes that function as sugar transferases that catalyse monosaccharide transfer onto accepting units and which are currently the main target application area for our thiophosphoryl research. We hope to establish methods that, in due course, would lead to the generation of potential glycosyltransferase inhibitors or substrates. Chitin synthase-related investigations will be presented in the Chapter 5, whereas here we will concentrate on the opportunities that investigations on fucosyltransferase may offer. First we will review the mode of enzyme action and then present a few examples of existing inhibitors.

3.1.1. Fucosyltransferase

Fucosyltransferases (Fuc-T) are a group of enzymes that belong to the class of Leloir type sugar transferases, as they require a guanosine-diphosphate carrier of a monosaccharide unit. During transfer the sugar suffers an anomeric configurational inversion ($\beta \rightarrow \alpha$). As a result of sugar transport catalysed by Fuc-T, the final step of biosynthesis of cell surface glycoproteins and glycolipids is enabled. This triggers many biological processes that are critical to either maintain health or the establishment of disease, and in all forms of cancer metastasis, lymphocyte trafficking, fertilisation and immune response.⁸⁸ One of the most important classes of fucosylated saccharides are sialyl Lewis x and sialyl Lewis a, which play vital roles in cell-cell recognition processes, such as leucocyte adhesion in the process of inflammation.

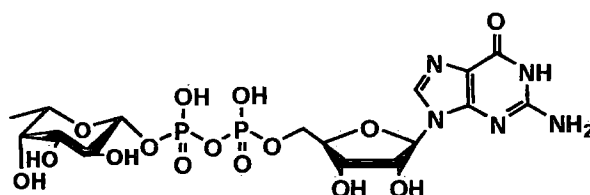
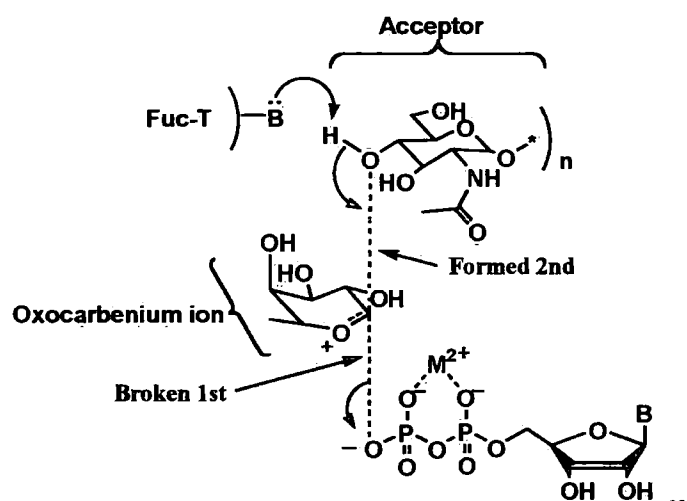


Figure 3. 2 GDP-fucose, the natural substrate of fucosyltransferases

As any glycosyltransferase, Fuc-T can either *O*-glycosylate, on a protein acceptor, or *N*-glycosylate. There are nine types of fucosyltransferases in humans, grouped depending on the connection that they form being α -1,2, α -1,3/4 and α -1,6, where 2, 3/4 and 6 correspond to the

fucosyl acceptors hydroxyl groups. The key features that vary amongst these isozymes are their requirements for cation cofactors and their selectivity towards certain substrates. This leads to different interactions with different inhibitors. Most of the Fuc-T are located in the Golgi apparatus, however, it was found that some of the *N*-glycosylating Fuc-T perform their function in the endoplasmatic reticulum.

The mode of action is common for all Leloir glycosyltransferases (section 1.3), including Fuc-T and chitin synthase, described in the section 5.2. In the transition state fucosyl transfer is mediated by several events. A metal ion is coordinated to the diphosphate bridge while fucose adopts a half-chair conformation with formation of an anomeric oxocarbenium cation closely followed by nucleophilic attack of the acceptor's hydroxide or amine group (scheme 3.2). For example, it has been proposed that in Fuc-T V assisted cleavage of the glycoside-diphosphate bond occurs prior to the nucleophilic attack of acceptor on carbon-1 of the GDP-donor.



Scheme 3. 2 Transition state of Fuc-T V mediated sugar transfer⁸⁹

An approach towards inhibition of this process involves fulfilling requirements for all four-partner events in the transition state, which makes the design of suitable agents quite challenging. Some of the past and present attempts rely on transition state mimicry. A vast variety of acceptor analogues and fucose analogues have been prepared, but as our approach is based on mimicking of the Fuc-T donor, it would be more useful to review natural substrate analogues, to which the following section is, therefore, dedicated.

3.1.2. Past and present inhibitors: mimics of the natural substrate

Two types of the natural substrate mimics that share an intact guanosine feature will be discussed in this section. One retains the diphosphate bridge with a modified fucose end. The other involves substitution of the diphosphate bridge for a C=O or S=O based linker, with an unmodified sugar end.

One of the quite famous precedents in the preparation of human fucosyltransferase inhibitors was set by Wong and Sharpless⁶ and it attracted attention by virtue of the preparation method and the extent of inhibitory activity. The famous 'Click' chemistry approach and 1,3-dipolar cycloaddition were employed (discussed more in section 1.1). With an array of products generated, one of the most effective and highly selective agent **112** for α -1,3-fucosyltransferase, was identified using inhibition assays performed directly in a 96-well microtitre plate that was used for the synthesis of the inhibitors.

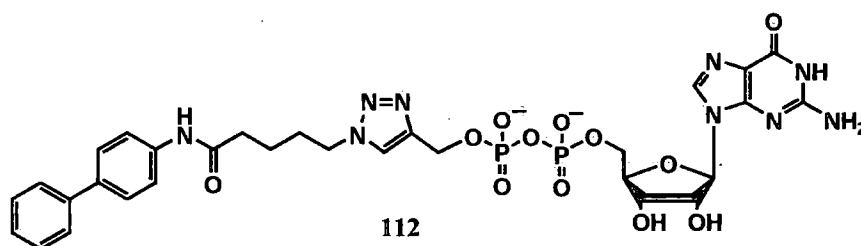


Figure 3. 3 Active fucosyltransferase inhibitor with $IC_{50}=1 \mu M$

The authors recognised that retaining the guanosine diphosphate moiety was important in binding to the enzyme active site. The significance of a hydrophobic pocket adjacent to the enzyme active site directed the compound design strategy towards lipophilic amines and their diversity was introduced by varying the length of the amide-triazole connector.

A more recent paper⁹⁰ shows the development of an enzyme activity screen using a method based on fluorescence energy resonance transfer (FRET). This study also led to the discovery of potent inhibitor compound **113** (figure 3.4), which was synthesised by applying Cu-catalysed Huisgen cycloaddition, but directed against synthesis of sialyl LewisX.

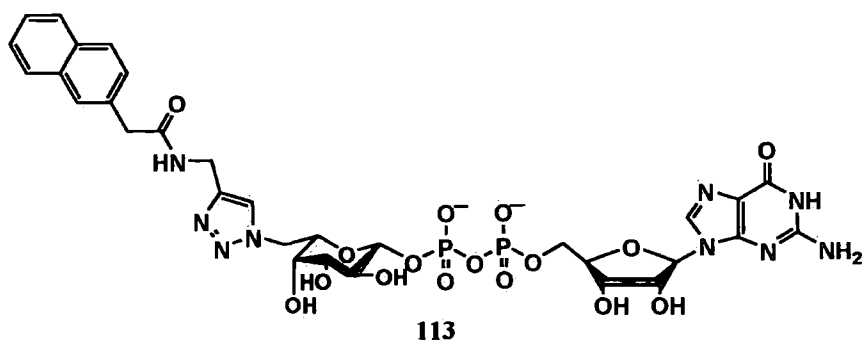


Figure 3. 4 Another efficient ($IC_{50}=5.4 \mu M$) Fuc-T inhibitor produced using the 1,3-dipolar cycloaddition method adopted by Sharpless

This compound resembled the active product generated by Wong, containing an unchanged GDP moiety and lipophilic structure to bind with the hydrophobic pocket in the active centre of the fucosyltransferase. Since the sugar feature, derived from D-galactose, was also present in this molecule, a great similarity towards the natural substrate was achieved, which was believed to be an important factor. The lipophilic group had fluorogenic properties and, therefore, was ideal for testing a FRET-based method.

Fluorinated sugar nucleotides were used as probes in mechanistic studies of enzyme activity and were found to be competitive inhibitors.^{89,91} The position of the fluoro-substituent varied but the most potent ($K_i=1-22 \mu M$) against four of the mammalian fucosyltransferases (III, V, VI and VII) was the C-6 fluoro C-6-deoxy-L-galactose analogue shown below.

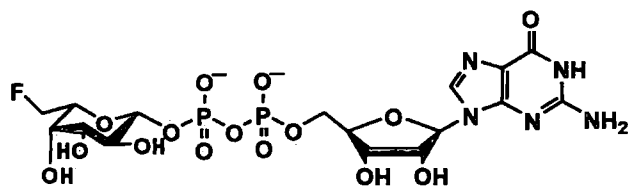
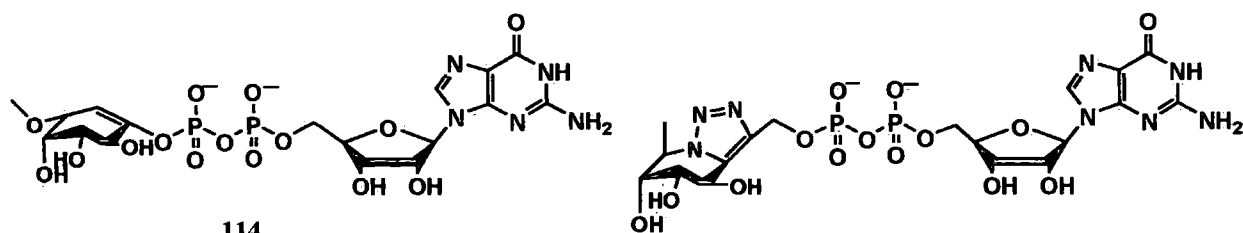


Figure 3. 5 Fluoro-analogue of GDP-fucose

Unlike in the examples of the 'Click' chemistry approach, these fluoro-compounds were prepared *via* several synthetic steps, including purification using column chromatography.

With the idea of mimicking the flattened half-chair conformation of the fucose moiety, a few considerably active anti-Fuc-T V and VI agents were generated (figure 3.6).⁹² These isosteric analogues were suggested to increase their stability towards enzymatic cleavage.



114

Figure 3. 6 Inhibitors of Fuc-T V and VI, $K_i=6-13 \mu\text{M}$

The preparation procedure for these relatively potent inhibitors required a number of steps involving protection of the hydroxyl groups of the fucose-mimics.

Structurally very similar to previous example 114, is the unsaturated pseudo sugar analogue 115 (figure 3.7), which with a K_i value of $25 \mu\text{M}$, suggested a preference of Fuc-T towards half-chair mimicking analogues.⁹³ On the other side, the same research group reported carba-fucose analogues that were supposed to mimic the fucosyltransferase transition state did not exhibit high efficacy. Carba-Fuc compounds 116a and 116b (figure 3.7) presented moderate and weak inhibition activity, $K_i=67 \mu\text{M}$ and $890 \mu\text{M}$, respectively. However, these studies showed that the ring oxygen was not so significant for enzyme recognition, but, as for the fucosyl transfer, ring oxygen assisted charge distribution was critical.

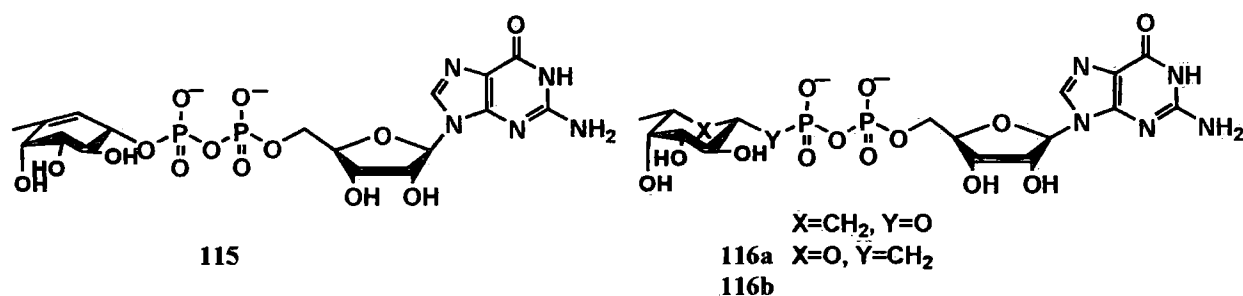


Figure 3. 7 Carba and C-Fuc analogues (left) and unsaturated carba-Fuc analogue (right)

Another approach can be taken in the design of enzyme inhibitors, where both donor and acceptor are mimicked and the mimics are covalently connected to each other. These

bisubstrate analogues enable high affinity to be achieved and selectivity for the acceptor-binding site.^{94, 95} A representative example is shown below.

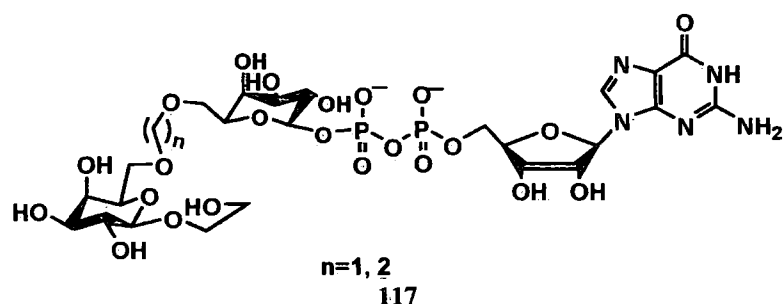


Figure 3. 8 Bisubstrate analogue targeting α -1,3-fucosyltransferase

These compounds, differing in the length of their methylene linkers, have poor inhibitory activity ($n=1$, (117a), $IC_{50}=0.26$ mM and $n=2$, (117b), $IC_{50}=0.27$ mM). However, their binding towards the acceptor pocket of the fucosyltransferase active centre did not follow the compound binding for the substrate position. Therefore, the authors concluded that these bisubstrate analogues were substrates rather than inhibiting.

All previous examples of fucosyltransferases inhibitors have included sugar modifications and an unmodified GDP structure. Here are some examples where the diphosphate bridge has been replaced by a mimic and the fucose portion has been retained.

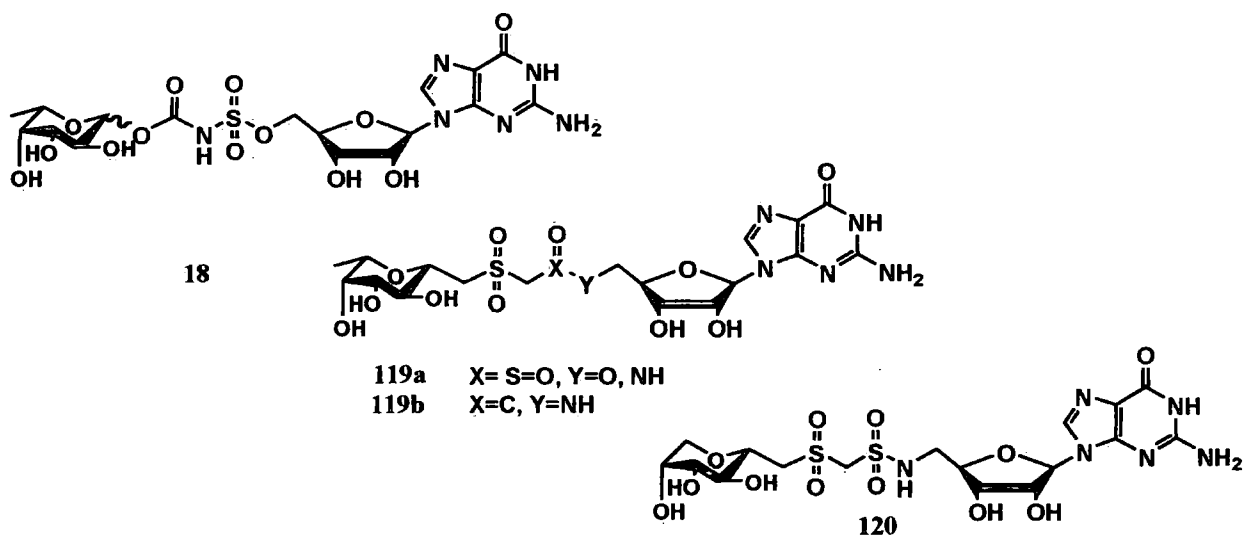


Figure 3. 9 Diphosphate mimics of Fuc-T

In these examples the connection between the guanosine and sugar groups was in the form of oxycarbonylaminosulfonyl⁹⁶ (**118**), sulphono-amide (**119a**), or methylene disulfone (**119b**, **120**) groups^{97, 98}. Uncharged systems were chosen based on their potential for better membrane transport. However, none of these mimics presented significant activity against fucosyltransferases, reiterating the importance of the diphosphate moiety.

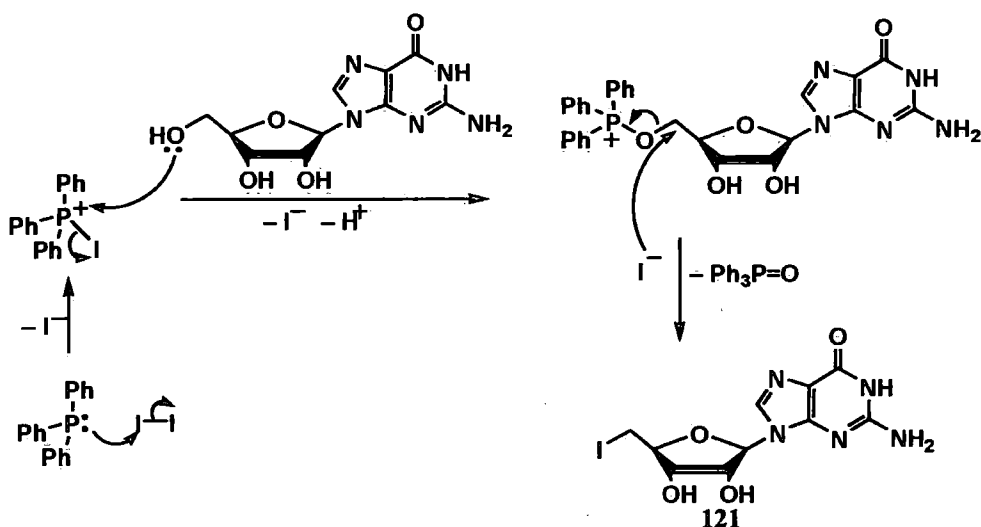
It can be concluded that, in mimicking natural substrates of fucosyltransferases, an intact guanosine diphosphate feature was of high importance. With modification of the diphosphate bridge, binding of an agent to the active site was not as successful. Most of the potent inhibitors also contained lipophilic structures. With our design of the target molecule (presented in the section 3.1), we hope to replace P-O bonds with P-N and P-S linkers that change the ionic diphosphate moiety only partially. These changes will, hopefully, not affect recognition of the modified phosphoryl centres by Fuc-T, but will significantly simplify the synthetic procedures. In the long term, with guanosine derivatives connected to a number of substituents over a -X-P-Y-P-Z- bridge where X, Y and Z are one or more of O, N, S we hope to generate potential inhibitors of fucosyltransferase. We will test first our one-pot thiophosphoramidate Tripartite chemistry on simpler guanosine monophosphate derivatives.

3.2. Synthesis of guanosine derivatives

3.2.1. Preparation of 5'-iodo-5'-deoxyguanosine

On the way to the desired 5'-amino-5'-guanosine, the precursor azide is required. Inorganic azides have the power to perform simple nucleophilic displacements, when a leaving group is present, which is not the case of guanosine. Therefore, 5'-iodo-5'-deoxyguanosine **121**, with its very good iodide-leaving group, was prepared.

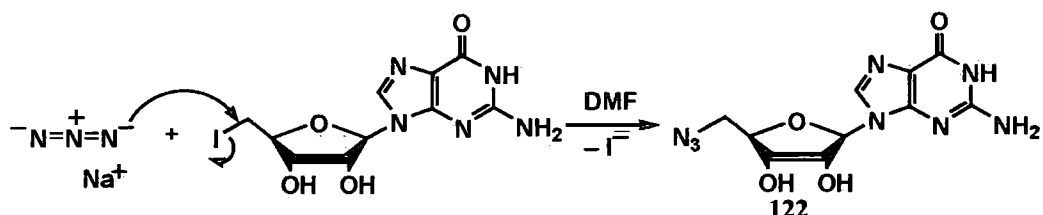
Applying the procedure of McGee⁹⁹ 5'-iodo-5'-deoxyguanosine was prepared in a yield of 55%. The procedure involved slow iodine addition to a vigorously stirred, light and moisture sensitive, mixture of guanosine, imidazole and triphenyl phosphine in *N*-methyl pyrrolidinone. The transformation likely occurs via the following pathway.



Scheme 3. 3 Proposed mechanism for the synthesis of 5'-iodo-5'-deoxyguanosine from guanosine and with the help of triphenylphosphine in *N*-methyl pyrrolidinone

3.2.2. Preparation of 5'-azido-5'-deoxyguanosine

Dean⁵⁵ established an effective method for the generation of 5'-azido-5'-deoxyguanosine **122** using sodium azide in DMF. Sodium azide was heated under a nitrogen atmosphere with the suspension of 5'-deoxy-5'-iodoguanosine in dry *N,N*-dimethylformamide to give the desired azide product via simple nucleophilic substitution (scheme 3.4).

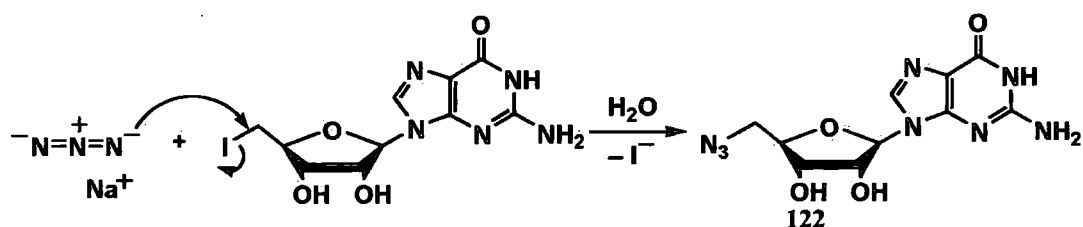


Scheme 3. 4 Reaction mechanism for the iodine-azide nucleophilic substitution

3.2.3. Novel aqueous procedure for the preparation of 5'-azido-5'-deoxyguanosine⁴⁶

We propose a simple procedure for the preparation of 5'-azido-5'-deoxyguanosine **122** using 5'-deoxy-5'-iodoguanosine refluxed in water with an excess of sodium azide and high concentration of substrate and reagent to increase the rate of the substitution process. This we hoped, to some extent, would overcome the retardation in rate that would occur through solvation of azide ions in water. This work was initiated by Gemma R. Freeman, a former

member of our group. The thesis author optimised this procedure and new procedures for 5'-amino-5'-deoxyguanosine.



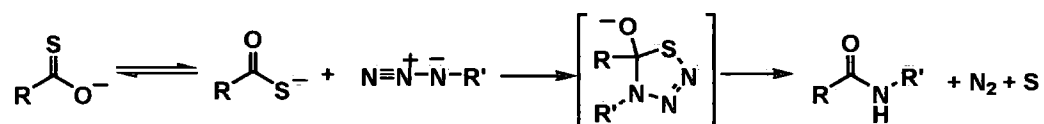
Scheme 3.5 Aqueous method for the preparation 5'-azido-5'-deoxyguanosine

As a poorly water insoluble molecule, the 5'-azido-5'-deoxyguanosine precipitated on cooling of the reaction mixture. After washing, pure 5'-azido-5'-deoxyguanosine was formed in 42% yield. The yields of this reaction were moderate, but given that dry solvents are avoided, this aqueous procedure represents an easy and quick new way towards 5'-azido-5'-deoxyguanosine.

3.2.4. Novel aqueous procedure for the preparation of 5'-amino-5'-deoxyguanosine⁴⁶

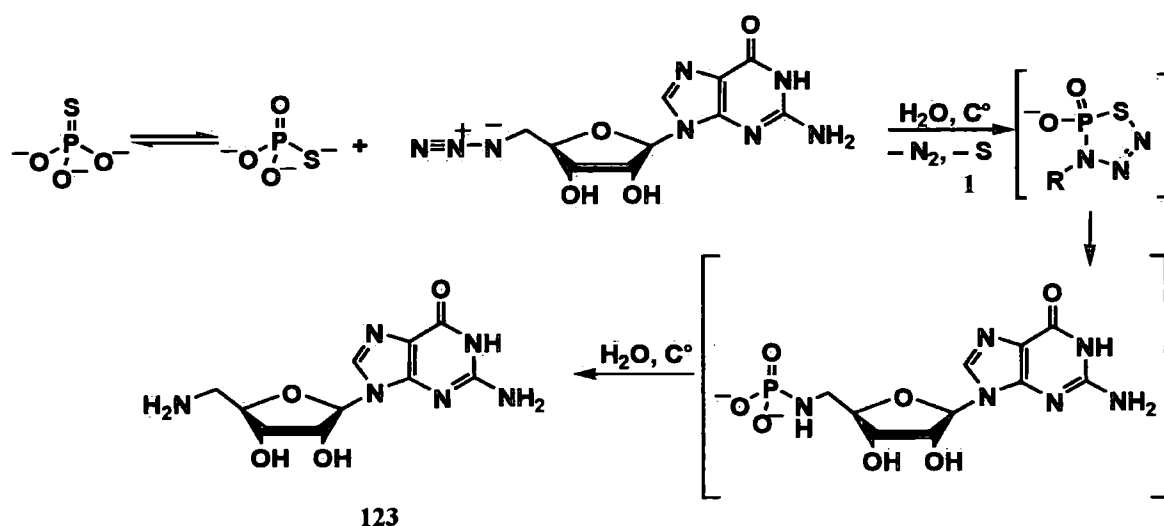
One of the conventional methods for the reduction of azides involves Staudinger reduction with triphenyl phosphine, assisted with water hydrolysis to give rise to the amine.¹⁰⁰ We began to study and optimise a simpler aqueous method for the synthesis of 5'-amino-5'-deoxyguanosine, avoiding application of organic solvents and any long purification procedures.

Williams¹⁰¹ established an alternative method for formation of amides and sulfonamides using thio acid/azide amidation.



Scheme 3.6 Generation of amides via thiazotriazoline formation

As a parallel, we recognised the similarity between the sulphydryl groups of thiophosphates and thiocarboxylates in acting as nucleophiles and that this had the potential to produce nitrogen gas, releasing elementary sulfur and the cyclic phosphoramidate 1 that, under controlled conditions, readily hydrolyses into the desired amine (schemes 3.6 and 3.7).



Scheme 3. 7 Aqueous method for the preparation of 5'-amino-5'-deoxyguanosine. **R** = guanosine

Simple reflux of an excess of sodium thiophosphate with 5'-azido-5'-deoxyguanosine in high concentrations in water gave rise to a light orange solution that, when cooled down on ice, precipitated out a beige product. To remove inorganic phosphate and excess thiophosphate, the precipitate was then washed with cold water, until the filtrate was colourless. The product was dried in a vacuum desiccator overnight yielding 70 % of a light beige powder of 5'-amino-5'-deoxyguanosine, estimated to be 99% pure by ^1H NMR spectroscopy. Depending on the time of reaction reflux, the purity and yield of sample changed as degradation of the product appeared to occur at extended reaction times (table 3.1).

Table 3. 1 Optimisation of the aqueous method for 5'-amino-5'-deoxyguanosine preparation

Reflux time (hours)	20	9.5	3	1
Purity (%)	95 ^a	98.4 ^a	98.9 ^a	99.2 ^a
Yield (%)	50	54	74	70

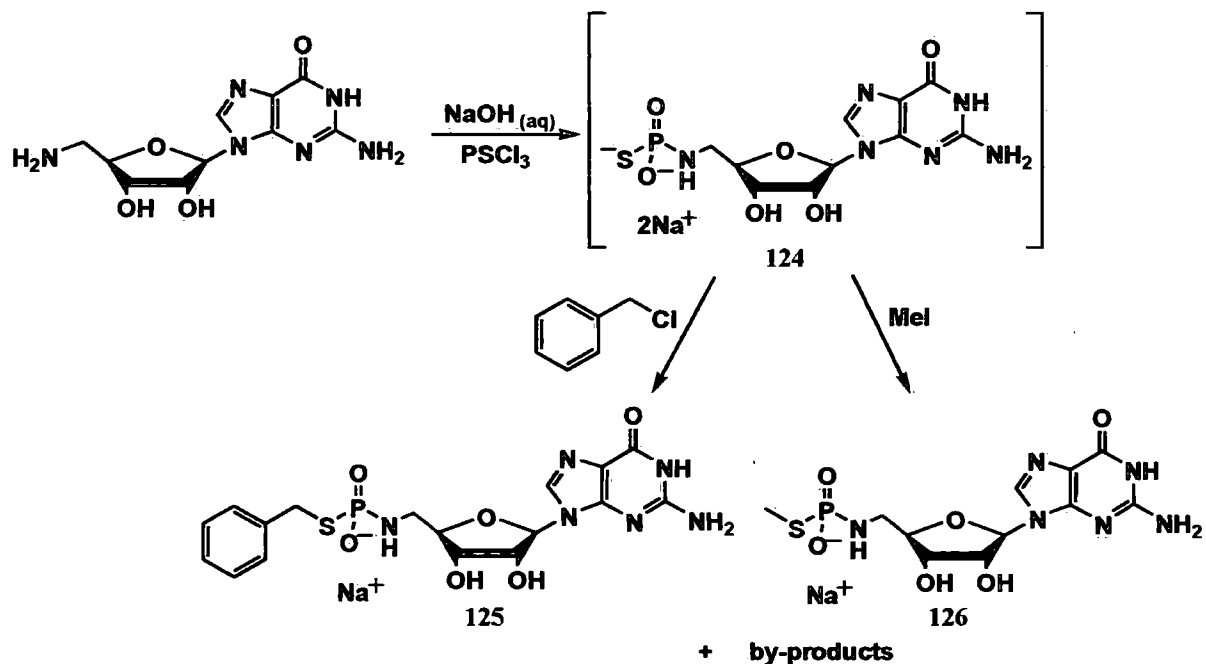
^aDetermined via ^1H NMR spectroscopy

In the case of the experiment producing the highest sample purity, the water volume was decreased by 25% in order to increase the kinetics of the bimolecular process. With overall yields of 70-74% this quick and simple aqueous method can compete with the existing literature methodology (78%⁵⁵).

With 5'-amino-5'-deoxyguanosine in our hands we were ready for attempts to thiophosphorylate 5'-amino-5'-deoxyguanosine using our aqueous approach, followed by alkylation of the resulting thiophosphoramidate, in the same pot.

3.3. Continuous method involving nucleosides: 5'-amino-5'-deoxyguanosine

5'-Amino-5'-deoxyguanosine is a sparingly soluble molecule but in alkali it becomes soluble (section 2.1), therefore, the aqueous method for thiophosphorylation that we propose, seems to be an effective method for the introduction of the thiophosphoryl group. In this case the strategy of using an excess of amine, owing to the insolubility of 5'-amino-5'-deoxyguanosine in organic solvents, was not suitable, as the excess could not be extracted post-reaction. Therefore, one equivalent of 5'-amino-5'-deoxyguanosine was used in the aqueous thiophosphorylation procedure, towards thiophosphoramidate derivative **124**. Then we applied an excess of methyl iodide or benzyl chloride as thiophosphoramidate *S*-alkylating agents. The unreacted alkylating agent was removed from the aqueous solution of products **125** and **126** via extraction.



Scheme 3.8 5'-Amino-5'-deoxyguanosine in the one-pot thiophosphate chemistry

For the product **125**, the conversion was estimated to be 78% via ^{31}P NMR spectroscopy and 76% according to ^1H NMR spectroscopy. By-products after benzylation were inorganic phosphate (5%), some un-alkylated 5'-amino-5'-deoxyguanosine thiophosphoramidate (7%) and other phosphate-containing moieties that were not further identified. A number of impurities were detected by ^1H NMR spectroscopy, with the assumption that some of them corresponded to thiophosphoramidate that was left un-alkylated and some 5'-amino-5'-deoxyguanosine. The desired product **126** was formed with conversion of 74% according to ^{31}P NMR spectroscopy and 69% estimated by ^1H NMR spectroscopy, which showed a number of guanosine-like impurities. The impurities in methylated derivative **126** identified by ^{31}P NMR spectroscopy were assigned to be *S*-alkylated inorganic thiophosphate (5%), inorganic phosphate (5%), 5'-amino-5'-deoxyguanosine phosphoramidate (3%), which is a desulfurization product, and some unidentified phosphorus containing features (13%).

In order to estimate the purity of the sample chromatographically as well and fully isolate and characterise the products, anion exchange chromatography was performed on the methylated guanosine thiophosphoramidate **126** (scheme 3.8). We used anion exchange chromatography with DEAE Sepharose[®] fast flow resin and a gradient (50-250 mM) of triethylammonium bicarbonate buffer set to have pH 7.6. The resulting chromatogram, shown below, was collected with the absorbance being monitored at 280 nm.

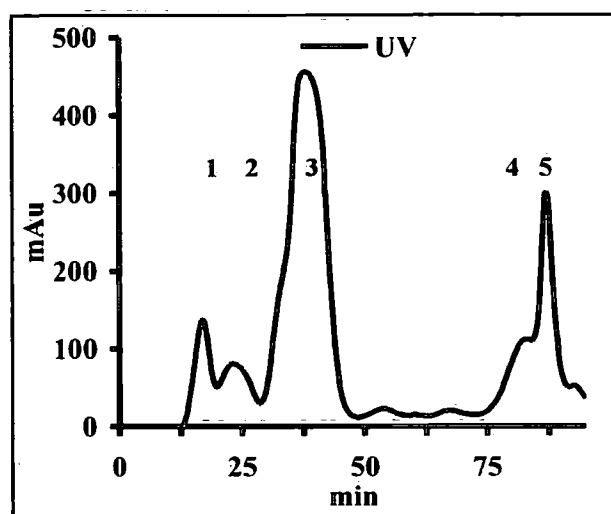


Figure 3. 10 Anion exchange chromatography of crude product 126

The trace suggests that the desired product, *S*-methylated guanosine thiophosphoramidate (peak 3) formed the majority of the detected compounds in the product mixture (61% by peak integration). The ^{31}P NMR spectrum of material from peak 3 showed contamination with around 5% of inorganic phosphate. Therefore, the purified material was then 95% pure according to the ^{31}P NMR spectroscopy, however, ^1H NMR spectroscopy presented product 126 in 100% purity. As for the other peaks present in the chromatogram, the first two contained undistinguishable guanosine-like structures, but owing to the low peak intensity in the ^1H NMR spectra and no signal in the ^{31}P NMR spectroscopy, these were not further identified. The shoulder on the fourth peak surprisingly showed the presence of the desired product by ^{31}P NMR spectroscopy along with a weak signal at 26 ppm and undefined guanosine-like moieties in the ^1H NMR spectrum. The final two peaks contained very weak mixtures composed primarily of the *S*-alkylated inorganic thiophosphate and inorganic phosphate.

S-Methylated guanosine thiophosphoramidate was isolated as the triethylammonium salt. Therefore, we subjected the product to cation exchange chromatography to obtain the simple sodium salt that would be more appropriate for the full spectroscopic characterisation of the product. For this, Dowex[®] 50W×2, 200–400 Na^+ resin was employed with water as the mobile phase.

We concluded that *S*-alkylated thiophosphoramidates of guanosine can be produced via a simple and quick one-pot Tripartite method, with moderate, but still satisfactory, conversions and isolated with the assistance of ion exchange chromatographies as highly pure materials (5% of Pi as the contaminant). The approach concerning biological assays would involve the decision to test these compounds as the part of a reaction mixture, additionally investigating the effect of the impurities formed during reaction. Other options involve undesirable purification steps that can isolate products with great purity. As presented in Chapter 3, which describes a quinoline-thiophosphoramidate system, our preference lies clearly towards direct screening, which offers quick conclusions on the effectiveness of compounds.

3.4. Continuous method involving nucleosides: 5'-amino-5'-deoxyadenosine

5'-Amino-5'-deoxyguanosine showed moderate conversions when transformed into an *S*-alkylated thiophosphoroamidate. Since 5'-amino-5'-deoxyadenosine was available in the laboratory (work of 4th year student Gemma R. Freeman), we compared the effect of using a different nucleoside amine. As with the 5'-amino-5'-deoxyguanosine example, one equivalent of 5'-amino-5'-deoxyadenosine was used, with a 20% excess of methyl iodide, to support successful transformation into the desired product **127** and the excess was extracted with diethyl ether.

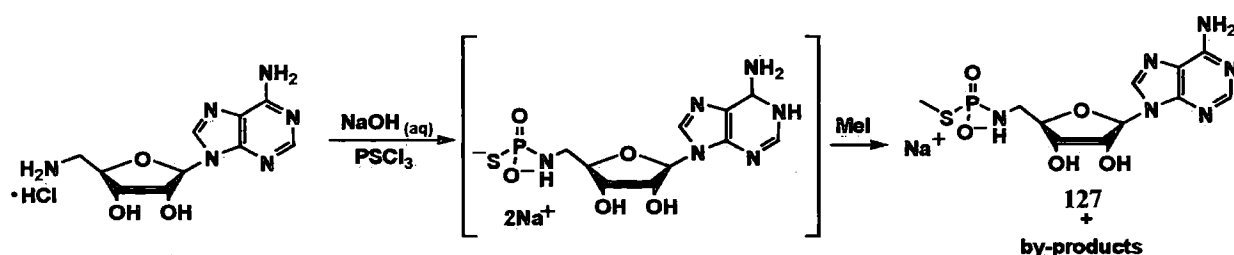


Figure 2. 36 Adenosine amine the one-pot thiophosphate chemistry

³¹P and ¹H NMR spectroscopies reported on the purity of the resulting product, with estimates of 71% and 74% conversion, respectively. The major impurities, as in the previous examples were *S*-alkylated thiophosphate (8%) and inorganic phosphate (7%). Standard anion exchange

chromatography, was used to confirm conversion levels and purify material for detailed analysis.

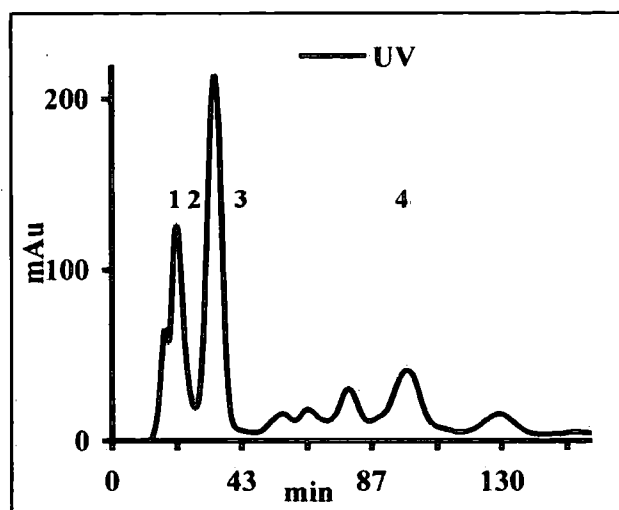


Figure 3. 11 Anion exchange chromatography of the compound MT378. Absorbance performed at 280 nm

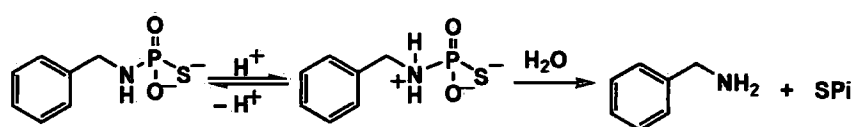
Integration of the chromatogram showed the desired product to be present at ~40%. This was unexpectedly low, as NMR spectroscopies had suggested much higher conversion. However, this does not take account the presence of coloured impurities from e.g. methyl iodide. After cation exchange chromatography, the sodium salt of the *S*-methylated adenosine thiophosphoramidate was isolated in 100% purity, as determined from both ^{31}P and ^1H NMR spectra. As for the by-products in the adenosine system, some non-phosphorus containing adenosine species along with un-reacted starting material were detected (peak 2 with the shoulder 1). *S*-Alkylated inorganic thiophosphate was not detected in the analysed fractions, as its elution did not coincide with UV-active species. The group of peaks following the elution of the desired product contained small amounts inorganic phosphate, but other species were not identified.

3.5. 5'-Iodo-5'-deoxyguanosine as an alkylating agent

5'-Iodo-5'-deoxyguanosine, as a primary alkyl halide, could attract nucleophilic attack by the thiolate group of the thiophosphoramidate feature. The reactivity of the nucleoside iodide is

somewhat lower than the simple alkylating agents that we have used so far. But, with an appropriate strategy we hoped to overcome this lower reactivity and access thiophosphoramidates based on this nucleoside-alkylating agent.

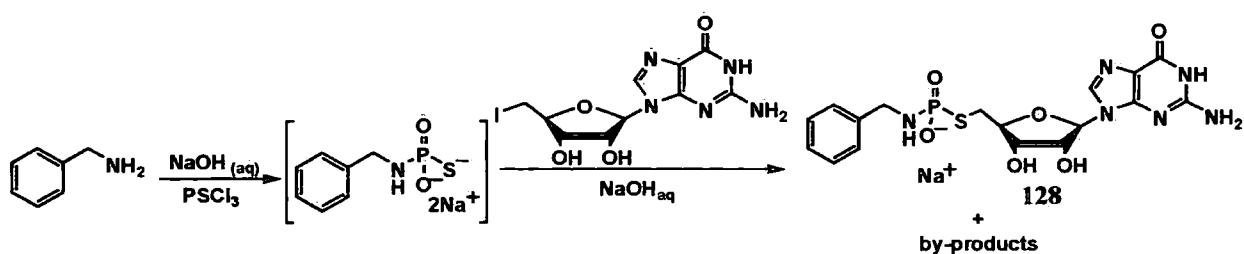
Some preliminary experiments, where an excess of the thiophosphoramidate over 5'-iodo-5'-deoxyguanosine (section 2.6) was used, suggested that the reaction is feasible. With an excess of thiophosphoramidate we hoped to promote more efficient alkylation and increase the rates of the bimolecular reaction. In order to remove the un-reacted thiophosphoramidate we attempted selective acid hydrolysis of the excess material and extraction of the resulting amine with organic solvent (scheme 3.9).



Scheme 3.9 Acid catalysed hydrolysis of thiophosphoroamidate

As the result of hydrolysis, both thio and oxo phosphates should form, which could potentially be isolated via methanol precipitation. Unfortunately, the method did not give rise to clean desired product, as the phosphates did not precipitate completely.

Therefore, we moved to the approach of an excess of both benzylamine and 5'-iodo-5'-deoxyguanosine, which was added in portions. Thiophosphorylation of the excess of amine was done via the aqueous method. *S*-Alkylation was started with one equivalent of 5'-iodo-5'-deoxyguanosine and additional aqueous sodium hydroxide to ensure the maintenance of the high pH of the media (pH 9). As no reaction was detected (monitoring of crude mixture *via* ^{31}P NMR spectroscopy), acceleration was attempted by heating at 50 °C. After two days, the reaction had reached 32% conversion. At this point no further conversion was observed. Therefore, another batch of 5'-iodo-5'-deoxyguanosine (1 Eq) was applied and after another 32 hours 73% conversion had been achieved.



Scheme 3.10 Application of iodo guanosine in the one-pot thiophosphate method

Standard anion exchange chromatography was used for purity estimation and purification of the desired product for characterisation purposes. This led to reasonable separation of products from the reaction mixture as illustrated in the chromatogram below.

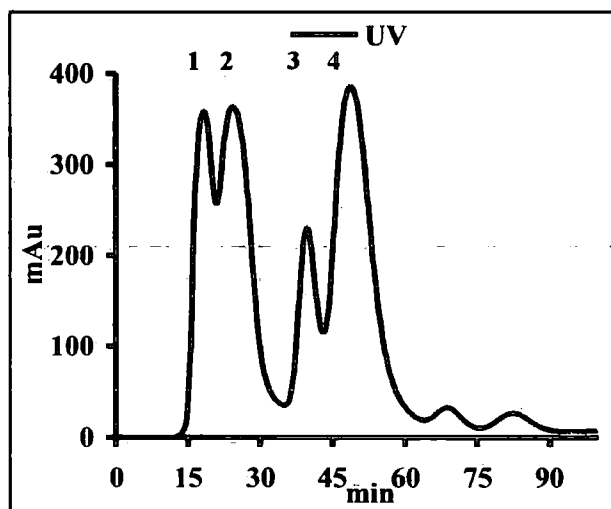


Figure 3.12 Anion exchange chromatography of the crude product MT501. Absorbance trace monitored at 280 nm

The excess of 5'-iodo-5'-deoxyguanosine and some other guanosine-containing species eluted at the beginning, in two close-running (1 and 2) peaks. The second peak contained some inorganic phosphate and some undefined guanosine-like structures. The third eluting peak, consisted of some guanosine-containing molecules that were seen in the ^1H NMR spectra, however, it was dominated by inorganic phosphate. Finally, the desired product, *S*-guanosinylated benzylamine thiophosphoramidate **128**, eluted with 3% of Pi as a contaminant, and was estimated *via* chromatogram integration to be 38% of the total crude mixture. In order to simplify characterisation sodium ion exchange was performed. The sodium salt of guanosine

alkylated benzyl thiophosphoramidate was isolated as a 95% pure product estimated *via* ^{31}P NMR spectroscopy and 100% according to ^1H NMR spectroscopy. The residual 5% in the phosphorus spectrum belonged to inorganic phosphate.

3.6. Conclusions and future work on the involvement of nucleosides in the thiophosphoramidate system

The thiophosphorylation of 5'-amino-5'-deoxyguanosine and, similarly, 5'-amino-5'-deoxyadenosine, followed by *S*-alkylation with commercially available agents gave rise to reasonable conversions that could be desirable starting points for the generation of biologically important products containing a diphosphate mimicking moiety (as introduced in the section 3.1). *S*-Alkylation with 5'-iodo-5'-deoxyguanosine was possible and satisfactory conversion was observed, however, the rates were slow. Acceleration *via* heating and the use of a large excess of alkylating agent enforced the need for chromatographic purification. On the other hand the nucleoside alkylating approach was demonstrated and this new thiophosphoramidate Tripartite thiophosphate branch was explored.

The expansion of the application of thiophosphoramidate system would involve other nucleosides, such as cytidine, uridine and thymidine. Simple synthetic procedures for these nucleosides are not available, which was one of the reasons why 5'-guanosine- and 5'-adenosine derivatives were the most suitable choices. However, future investigations will involve other nucleosides as they offer great potential. In one of the examples of Leloir-type glycosyltransferases that we are interested in, sialyltransferase (ST) inhibitors with the ability to mimic the natural substrate were made using a cytidine monophosphate moiety, in contrast to other mimicking inhibitors of mammalian sugar transferases, which require a nucleoside diphosphate features in their structure.

Some of the existing inhibitors that are the mimics of the natural substrate of STs presented high activity (figure 3.13).⁹¹

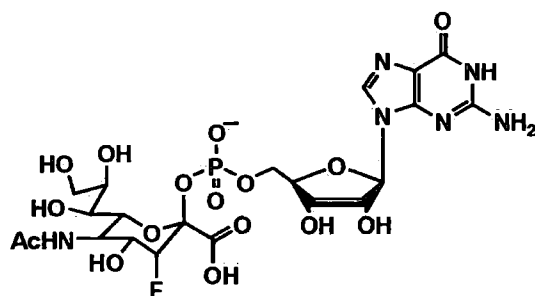
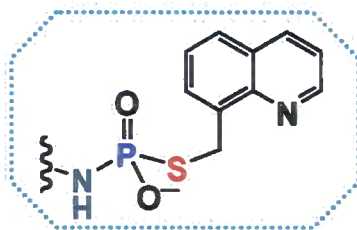


Figure 3. 13 A fluoroneuramic acid analogue that is a potent competitive inhibitor of 2,6-ST with $K_i=5.7 \mu\text{M}$ where the natural substrate CMP-Neu5Ac' has $K_m=15 \mu\text{M}$

The preparation of monophosphate compounds with potential inhibitory functions is, therefore, simplified in this case because it would involve the introduction of just one thiophosphate or thiophosphoramidate feature, which makes STs very attractive target sfors for future exploration. In addition, the great advantage of this strategy is that α --2,3-sialyltransferase (2,6-ST) is commercially available, which allows simple inhibition assays of the generated monothiophosphoryl derivatives of cytidine to be performed.

4.0 Quinolines and their application in the thiophosphoramidate system

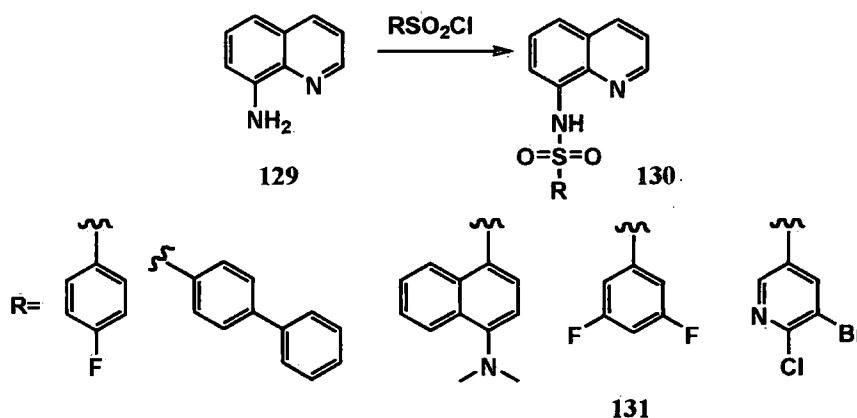
We showed that simple primary and secondary amines could be readily thiophosphorylated using our aqueous thiophosphorylation method and that the resulting thiophosphoramidates could be alkylated in a ‘one pot’ manner, using different alkylation agents, with good conversion levels (70% to 100% estimated by ^{31}P and ^1H NMR spectrometry, Chapter 2.). This one-pot thiophosphoramidate Tripartite method was then applied successfully to a library of amines where a range of alkylated thiophosphoramidates were produced in conversions mostly greater than 90% according to ^{31}P and ^1H NMR spectroscopy (Chapter 2.). This encouraged us to employ our one-pot method in alkylating the same library of amine thiophosphoramidates with another alkylation agent, 8-(bromomethyl)quinoline with a potential application in the development of novel antileishmanials.



A series of compounds was produced and tested *in vivo* for possible activity against *Leishmania mexicana* (*L. mexicana*) in a collaboration with Dr Paul Denny, The School for Health, Durham University. Even though some of the compounds showed promising results, unfortunately, it was not possible to make clear conclusions, owing to the large variations observed in the results. Therefore, this chapter will be a chronological presentation of the use of quinoline-like features in the one-pot thiophosphoramidate Tripartite system and the *in vivo* assays. To start with, we will introduce how we saw the potential in the quinoline-thiophosphoramidate strategy along with some of the currently used medicines against *Leishmania* spp.

4.1. A simple opportunity for the application of the thiophosphoramidate system: quinoline-based thiophosphoramidates as antileishmanials

A recent literature paper¹⁰² that presented work on the synthesis and biological testing of the leishmanicidal and trypanocidal activities of *N*-quinolin-8-yl-arylsulfonamides, attracted our attention due to the structural resemblance of these systems to our thiophosphoramidate system.



Scheme 4. 2 Sulfonamide derivatives as antiprotozoal agents

The authors used commercially available 8-aminoquinoline **129** that was then exposed to an array of substituted arylsulfonylchlorides **130** in organic solvent at low temperatures (scheme 4.1). The yields were 65-97%, gained after precipitation and crystallisation. The synthetic method used was available in the literature¹⁰³ and the *in vivo* assay was performed against *L. amazonensis*, *L. chagasi* and *Trypanosima cruzi*. A number of compounds showed some effect on the growth of the studied species, however, one of them was recognised as highly selective for *Leishmania* spp (**131**, $\text{IC}_{50}=2 \mu\text{M}$ for *L. amazonensis* and $0.45 \mu\text{M}$ for *L. chagasi*).

We propose an aqueous system that generates thiophosphorylated amines that can be further alkylated with a quinoline derivative. Since we found that the alkylating agent 8-(bromomethyl)quinoline is commercially available, our investigation focused on the system shown in the figure below, where aqueous thiophosphorylation of a range of amines was performed as a first step.

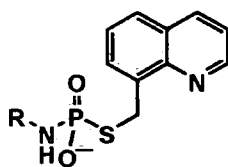


Figure 4. 1 Our quinoline-thiophosphoramidate strategy. R=alkyl, aryl substituent

4.2. Leishmaniasis, past and present drugs

More than 15 protozoan species induce a spectrum of diseases with characteristic clinical manifestations that belong to the genus *Leishmania*.^{104, 105} Leishmaniasis is caused in mammals by transfer of these parasites from their promastigote form in blood-feeding sand flies. In mammals, these non-infective promastigotes transform into the amastigote form and a number of clinical forms of Leishmaniasis can then develop. The type of disease depends on the geographical region with the most common being visceral and cutaneous forms.

The resistance of these parasites to existing drugs, which is believed to be the consequence of varied selectivity towards different species or pharmacokinetic properties of the drugs, have emphasised the need for the expansion of the limited number of antileishmanial agents.¹⁰⁴ The first antiprotozoal agent used almost a century ago was pentostam (disodium stibogluconat, figure 4.2), but over years of application, it has become ineffective against *Leishmania* spp. Miltefosine was one of the latest phospholipid analogues introduced into the armoury of oral antileishmanial drugs.¹⁰⁶ *L. donovani* seemed to be the most sensitive species to this alkylphosphocholine, both in its amastigote and promastigote forms ($IC_{50} = 0.12-4.6 \mu M$). This drug will be used as a positive control in our assays.

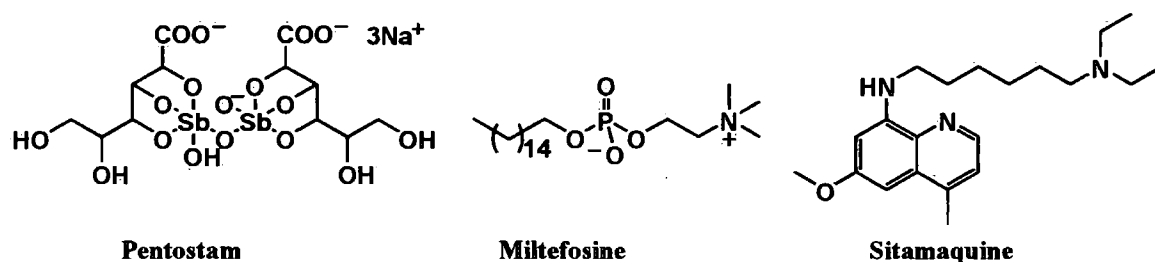
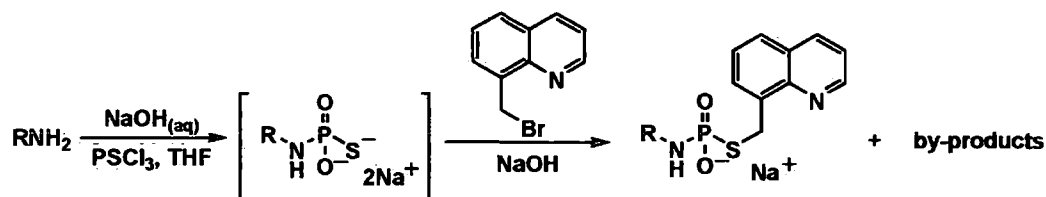


Figure 4. 2 Some of the past and the present antileishmanial drugs

The quinoline derivatives are well used as antiprotozoal agents and research on novel structures is constantly on-going.^{107, 108} A representative is sitamaquine (figure 4.2) that has a broad-spectrum antiprotozoal activity. It was believed that sitamaquine is metabolised by hydroxylation and *N*-alkylation, however, there is no report about the activity of the metabolites or indeed about the mode of action of quinolines in general in antiprotozoal therapy. Thus a rational approach to the design and identification of new amidate antiprotozoal drugs is not possible and a screening approach is justified. This philosophy fits well with our development of novel aqueous strategies for the rapid preparation of thiophosphoramidates. In the following sections, we will outline our synthetic approach and the outcome of *in vivo* assays on mammalian *L. mexicana* in our attempts towards novel antileishmanials.

4.3. Library synthesis and analysis

A library of quinoline derivatives with a range of thiophosphorylated amines was generated using our one-pot thiophosphoramidate Tripartite method (section 2.7).



Scheme 4. 3 The quinoline library production using one-pot method

Conversions to the desired thiophosphoramidates varied from approximately 60% to 96% estimated *via* ³¹P NMR spectroscopy. Details are presented in the figure below.

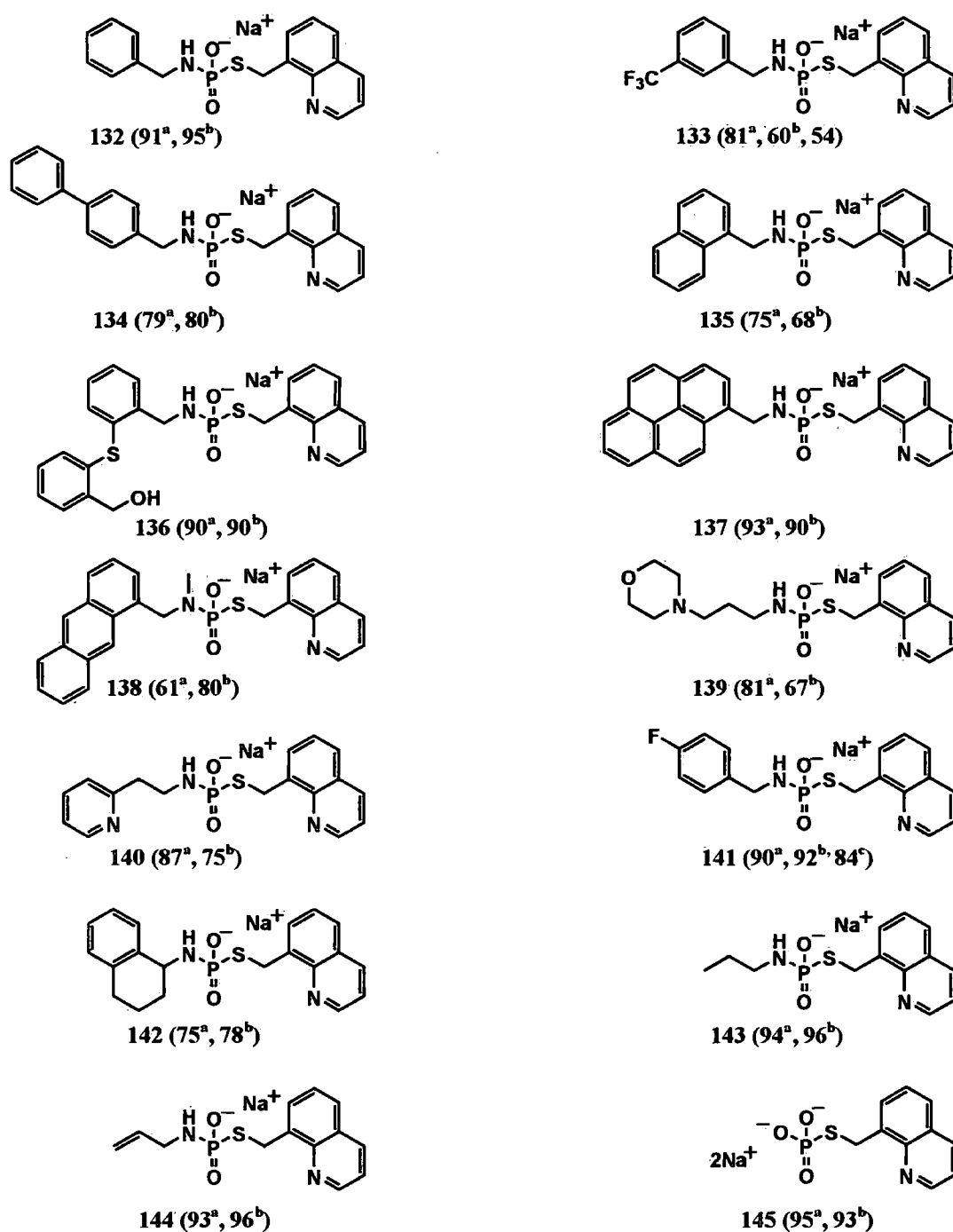


Figure 4. 3 The quinoline library and conversions achieved. Estimated purity (%) ^adetermined by ³¹P NMR spectroscopy, ^bdetermined by ¹H NMR spectroscopy and ^cdetermined by ¹⁹F NMR spectroscopy.

In some of the examples, such as compounds 137 and 138, precipitation of the products occurred, which were then isolated after centrifuging. All crude compounds were then

dissolved in DMSO to give rise to stock solutions (10 mM) that were then used for *in vivo* bioassays.

4.4. Biological testing against *Leishmania mexicana*

The promastigote form of *L. mexicana* is carried by insects. Whilst humans initially get infected with this form, it then develops into the amastigote that we chose to test our compounds against. An initial screen of all compounds was performed, followed by experiments for the determination of IC₅₀ values of a selected few potential 'hits'.

4.4.1. Initial screening

L. mexicana amastigotes, suspended in the Schneider's Gibco® media, pH 5.5, were used in the exponential growth phase in a concentration of 2×10^6 parasites/mL. The crude compounds (figure 4.3), dissolved in DMSO, were applied to the parasite suspension in 24-well microtitre plates in duplicate to give final compound concentrations of 100 µM (1/100 dilution). The negative and positive controls were DMSO and miltefosine (15 µM), respectively. After incubation for 72 h at 31 °C, the numbers of the live cells were recorded using a Neubauer haemocytometer and these were compared with positive and negative controls. Crude compounds 133, 137, 138, 143 and 144 (figure 4.3) attracted attention as potential hits, owing to the apparent inhibitory effect on parasite growth at similar levels to miltefosine. These five hits were then subjected to IC₅₀ estimation.

4.4.2. Estimation of the IC₅₀s of the studied quinoline compounds

The experiments for the estimation of IC₅₀ values were performed using a range of compound solutions to give final assay concentrations of 0.8 µM, 4 µM, 20 µM and 100 µM, applied in triplicate. The starting concentration of the parasites was again 2×10^6 parasites/mL. Miltefosine with final concentrations of 0.24 µM, 1.2 µM, 6 µM and 30 µM was also applied in triplicate and DMSO as negative control. The assays were performed as for the initial screening (section 4.4.1). Plots of the number of live parasites (presented as the percentage of the number of the cells in the negative control) as functions of concentrations are presented

below. The data on the plots are represented with average values of the cell viability with error bars expressed as \pm SEM (the standard error of means).

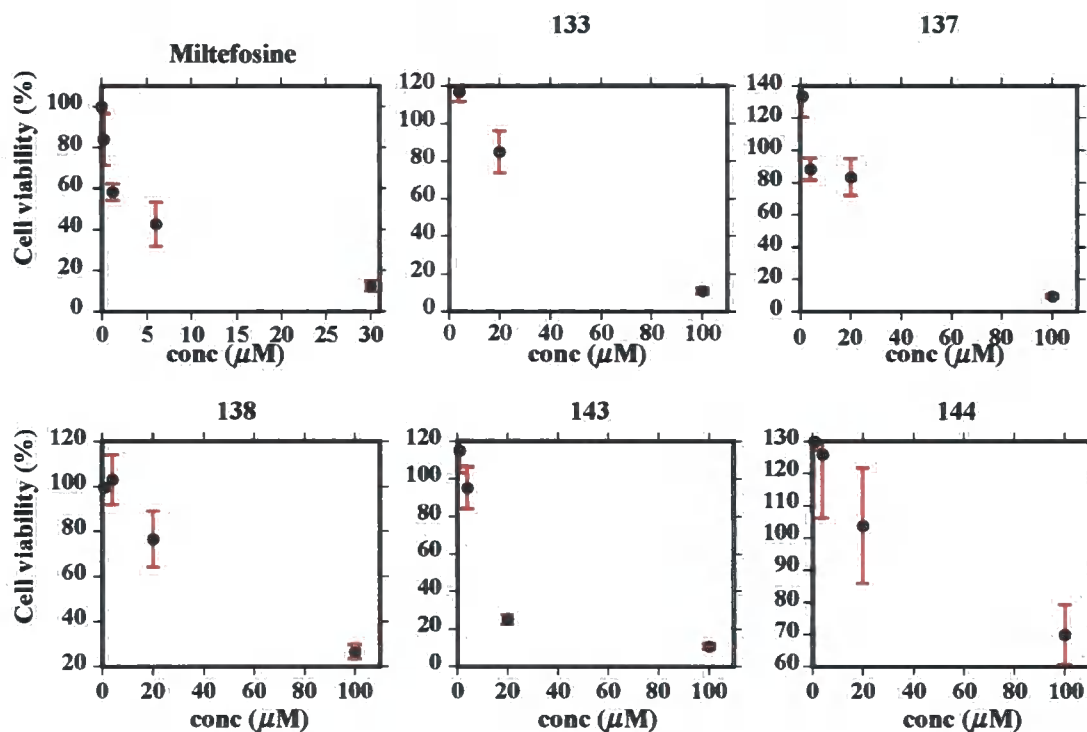


Figure 4. 4 The IC_{50} estimation experiments: 133, 137, 138, 143 and 144

No fitting was performed on the above plots, as we do not have a fitting model, because the mode of action is not known. Therefore, the estimations of the IC_{50} were performed by simply reading from the plots, using interpolation if necessary. These results were encouraging, with the IC_{50} of miltefosine being in the literature range¹⁰⁶ (2.3-12.7 μM) confirming the reliability of our experiment. The IC_{50} s of the compounds 133, 137 and 138 were in the range of 50-60 μM , while compound 143 seemed to have higher activity against *L. mexicana* with IC_{50} around 10 μM . As compound 143 presented large variations in the triplicate with estimated $\text{IC}_{50} > 100 \mu\text{M}$, we decided to repeat the assay. In addition, sample 144 used in this particular experiment had purity of only 65% estimated by ^{31}P NMR spectroscopy, with alkylated inorganic thiophosphate 145 as the impurity. Therefore, we re-synthesised a new batch of 144 that had conversion of 94% according to ^{31}P NMR spectroscopy (figure 4.3). In order to explore

the possible effect of 8-(methyl)quinolinyl thiophosphate **145** we also generated this product via alkylation of inorganic thiophosphate and included it in the assay.

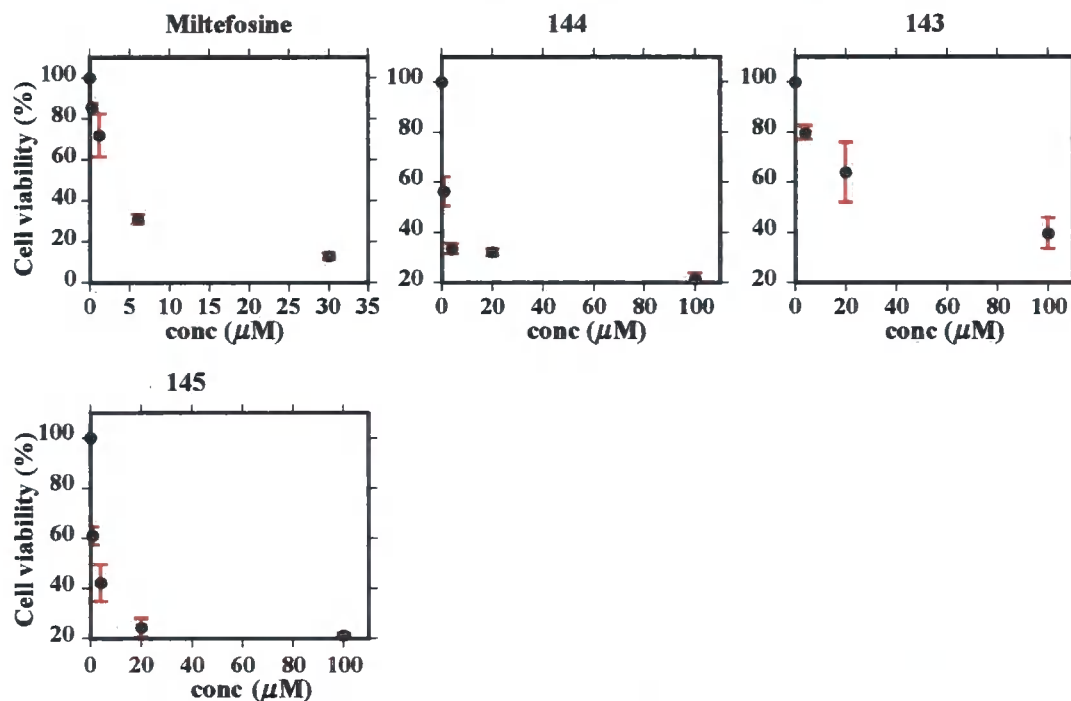


Figure 4. 5 The IC₅₀ estimation experiments: 144, 143 and 145

The positive control was again in the agreement with the literature values and the purer compound **144**, presented an impressive IC₅₀ of around 1 μM. The compound **144**, with large error bars again, this time showed higher activity with IC₅₀ in the range of 50-60 μM. However, alkylated inorganic thiophosphate **145** also showed high potency in the inhibition of the growth of *L. mexicana* (IC₅₀ <5 μM). To confirm this event, we repeated the assays involving compounds **144** and **145**.

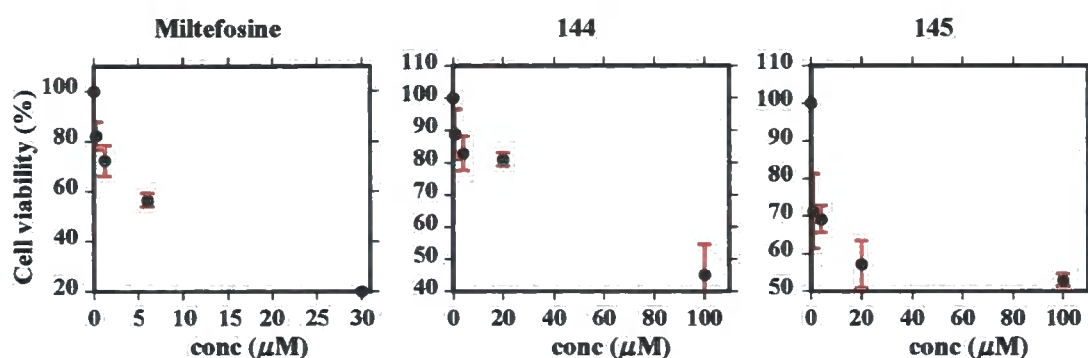


Figure 4. 6 The IC₅₀ estimation experiments: 144 and 145

Miltefosine showed an increase in its value for IC₅₀, which was still in the range presented in the literature. The compound **144** also suggested larger IC₅₀, however, the point at 20 μM was ‘off-trend’ leading to a change in the estimated IC₅₀. The compound **145** showed a much higher IC₅₀ than earlier, this time greater than 100 μM.

The variations in triplicates and between all the experiments were very high. Therefore, in order to discount the subjectivity of the manual counting we opted to employ another approach, using fluorescence-based assays.¹⁰⁹ The experiment was performed as the previous examples with the addition of a dye, alamar blue, after the 72 h incubation. The number of the viable cells was proportional to the intensity of fluorescence detected, as the alamar blue was metabolised into a fluorescent component *in vivo*. The results for compounds 144 and 143 are presented in the figure below.

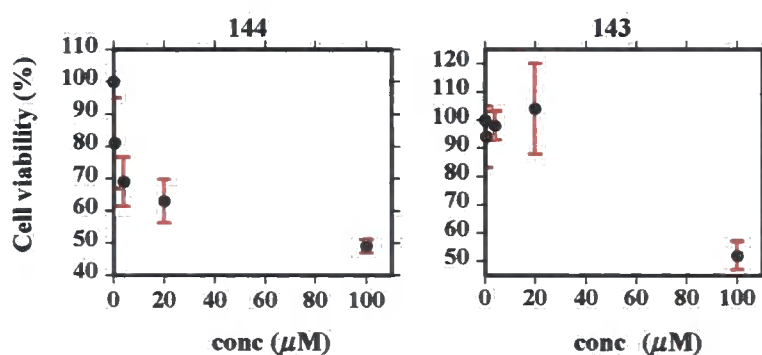
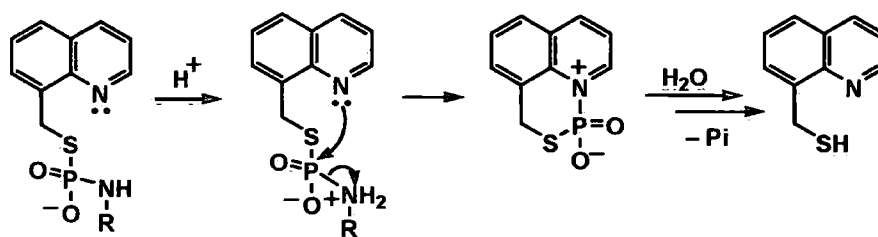


Figure 4. 7 The IC₅₀ estimation experiments: 144 and 143

In this experiment, compound **144** showed an IC_{50} of $\sim 100 \mu\text{M}$. The plot for compound **144** presented scattered data, therefore, an estimation of the value for IC_{50} was not possible. In addition, the positive control presented a value of $97\% \pm 15$ viability of the cells at of $3 \mu\text{M}$ of miltefosine, which was its previously determined IC_{50} value. The results of fluorescence assays suggested the possible degradation of miltefosine or the poor reliability of this experiment. At this stage, no further experiments were performed as the design of the new approaches to biological assays needed to be considered. In the following section we will reflect on the options of what has potentially occurred during these *in vivo* assays, notwithstanding uncertainties associated with the *in vivo* assays.

4.5. Hypothesis

Even though the results from the *in vivo* inhibition assays of our compounds suggested some high activities against *L. mexicana* we were not able to make clear conclusions. The activity of compound **145** suggested that degradation fragments of all compounds studied had affected the growth of the parasites. The pH of the media was low at 5.5, which could have affected the stability of the compounds. Alkylated thiophosphoramidates showed great stability at pH 7.5 and 5.5 (section 2.). However, the quinoline system contains an aromatic nitrogen with a lone pair that could have induced a rapid intramolecular degradation mechanism (scheme 4.3).



Scheme 4. 4 The proposed pathway for the degradation of alkylated thiophosphoramidates supported by expulsion of amine by quinoline. The degradation product inorganic phosphate (Pi) has been detected in the ^{31}P NMR spectra

Therefore, hydrolytic stability experiments on compound **144** were performed in the same manner as described in section 2. The stability of the compound **144** was monitored over 16 h at $31 \text{ }^\circ\text{C}$ using a starting of pH 5.3. At the end of run, an increase in pH was noticed, pH 6.4, but the data were still used to estimate the half-life to be around 4 hours ($k_0=0.003 \text{ min}^{-1}$),

which on the time scale of the biological assay of 3 days suggests that the compound 144 would have fully degraded in the parasite suspension. However, at pH 7.5 and 31 °C, the half-life of compound 262 was around 3 days ($k_0=0.00017 \text{ min}^{-1}$, for measured 16 h). The media that the assay was performed in was at pH 5.5, but the intracellular media would have pH~7.5. Thus, there is the possibility that our studied compounds entered the parasites rapidly and avoided degradation. However, we have not done any studies in this context. On the other hand, the high inhibition effect seen in the assays might have been induced by the degradation products. Owing to the inconsistent results, we could not confirm this theory either. If this second hypothesis were the case, this principle of ‘hydrolysis management’ could be used as a product delivery strategy (discussed in the following section). These investigations could potentially be fruitful and will be considered in future experiments.

4.6. Conclusions and future work on quinoline-based thiophosphoramidates

The employment of the thiophosphoramidate system for the production of an array of 8-(bromomethyl)quinoline-alkylated thiophosphoramidates was successful. The majority of the compounds were generated in high conversions (figure 4.3). With no purification performed, the crude compounds were subjected to *in vivo* inhibition activity assays against the amastigote form of the *L. mexicana* parasite that is infective to humans. Two approaches were taken in the estimation of the effect that our quinoline-based thiophosphoramidate library had on the growth of this parasite. Some of our compounds attracted attention with high, but inconsistent, activity levels that were comparable to the presently used drug miltefosine. Potentially subjective manual microscopic counting of the live parasites was substituted with dye-based fluorescence method in the assays. However, large variations in the results indicated that either the reliability of the performed assays or the detection methods applied were not sufficiently appropriate. In addition, we considered another explanation that involves the degradation of our compounds under the conditions of the mildly acidic media. The potential uptake of our compounds or the degradation products might have varied and could have contributed to the inconsistent results in the assay. The degradation products of the acid catalysed hydrolyses of our compounds were amines, inorganic phosphate and 8-(mercaptomethyl)quinoline. As the mode of quinoline

derivatives action towards *Leishmania* spp. is not known, the possibility of 8-(mercaptomethyl)quinoline being an efficient growth inhibitor can not be excluded. With this in mind, the potential of these thiophosphoramidate derivatives as delivery tools for quinolines could suggest that these systems are worthy of further investigation.

Prodrug strategies are employed actively in modern medicine and they are the research targets of many groups. A vast amount of work was done on antiviral agents with nucleoside phosphoramidate triesters as potential active compound carriers that, via hydrolysis in the organism, release the bioactive free nucleotide. Parent nucleosides fail as antivirals as they undergo poor 5' phosphorylation in cells to give the triphosphates that are the potent antiviral agents. The delivery of free nucleoside monophosphates into cells is limited by membrane permeability and susceptibility of monophosphates to enzymatic dephosphorylation. Therefore, the successful intracellular transport of free nucleotides was proposed to be facilitated by the application of masked triester prodrugs. Some of the representatives of the ProTide approach for anti-Hepatitis C virus and anti-herpes simplex virus agents, 146 and 147 respectively, with low micromolar EC_{50} values established by McGuigan^{64, 65} are shown in the figure below.

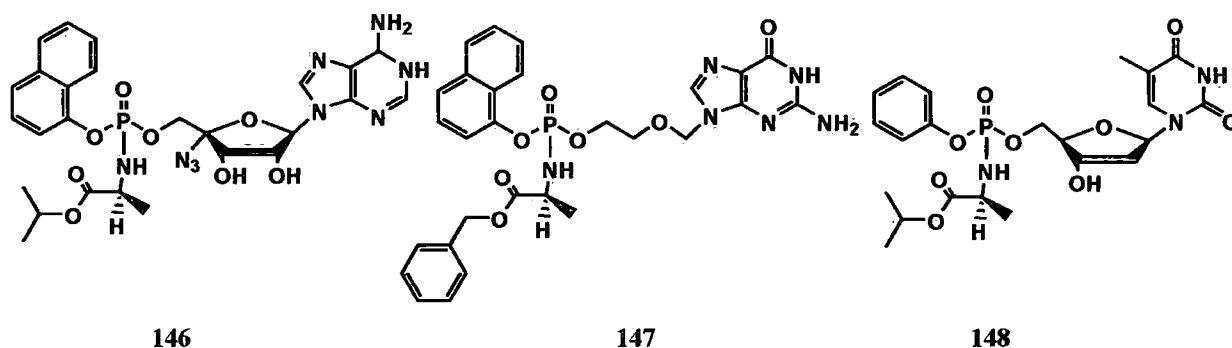


Figure 4. 8 The ProTide antiviral agents

Naphthalene esters were chosen owing to the positive effect they had on potency and an increase in lipophilicity, which certainly affected the delivery of the monophosphate feature. Bypassing the dependence on nucleoside kinases benefits the activity of the prodrugs. Representatives of stavudine analogues, studied as the potential anti-HIV agents, that employ both thio- and oxy-phosphoramidates were presented in section 2. Lonnberg *et al.* explored the

hydrolytic pathways throughout the pH range suggesting different routes of the degradation of the thymidine 5-monophosphoramidate prodrug **148**.⁶⁸

The work on phosphoramidate analogues as prodrugs presents great potential in discovery of novel, potent agents, which could be the case of our quinoline-based thiophosphoramidate system. In addition, we propose another approach for the quinoline-thiophosphoramidate strategy with 8-(aminomethyl)quinoline where the positions in the NPS linker would be inverted and could rapidly expand our library of structures.

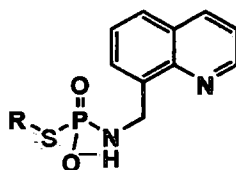
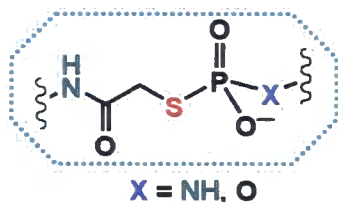


Figure 4. 9 Quinoline amine in the thiophosphoramidate chemistry

8-(aminomethyl)quinoline is available commercially, but rather expensive, however, it can be readily produced from 8-(bromomethyl)quinoline in a two step procedure mediated by the 8-(azodomethyl)quinoline.¹¹⁰ This system could be employed in future investigations, following a more-detailed exploration of the bromo-analogue when an appropriate in vivo assay has been developed.

5.0 A bromoacetyl strategy

The bromoacetyl system is another novel Tripartite method (introduced in the Chapter 1), that potentially has 'Click'-properties that would allow for cross-linking of amines to thiophosphoryl groups in the synthesis of ranges of amide products.



It involves organic synthesis to start with and requires investigations on optimisation of the reaction conditions, with the help of kinetic experiments that will explore the occurrence of desired competing process. The novelty of this method, compared to the thiophosphoramidate system, is based on the ability to prepare different alkylation agents. The bromoacetyl moiety allows formation of an amide bond at one end while the other end may alkylate sulfhydryl groups on the other. The sulfhydryl group could be either a segment of a thiophosphoramidate structure or an oxo-thiophosphorylated component. Along with the achievements on thiophosphoramidate 'Click' chemistry (Chapter 2.), the bromoacetyl strategy adds another perspective to the approach of the synthesis of thiophosphoryl analogues of NDP-sugars.

The first few section of this chapter will outline the differences and similarities in the strategies of the thiophosphoramidate and the bromoacetyl chemistries and introduce a potential new biological target for the products from this bromoacetyl Tripartite strategy.

5.1. The strategy of the bromoacetyl system

A typical model thiophosphoramidate structure (presented in the Chapter 2.) consists of an amino group ($\text{R}^1\text{-NH-}$) bridged over *via* a thiophosphoryl group to an alkyl moiety ($-\text{R}^2$).

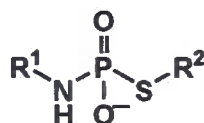


Figure 5. 1 General structure of alkylated thiophosphoramidate

where, R^1 and R^2 groups can be a variety of aliphatic moieties, including more challenging nucleoside moieties shown below (more about in the Chapter 3.):

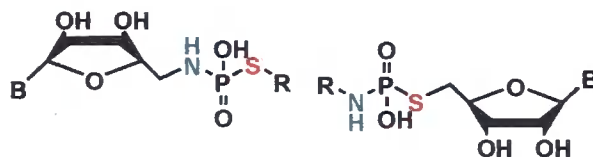
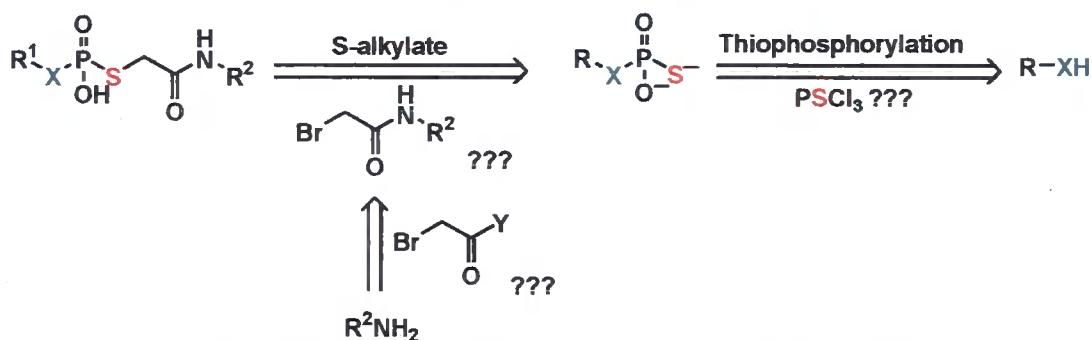


Figure 5. 2 Nucleoside-like thiophosphoramidate derivatives. **B** = adenosyl, uracyl, guanosyl...

The R^1 feature was introduced through the exposure of a thiophosphorylated amine to a range of alkylation agents: alkyl halides, epoxides, alkynes (see figure 2.24). The success varied, but conversions ranging from 70% up to 100% were attained (Chapter 2.).

Here, we hope to expand the number of alkylation agents that we may use, through the exploitation of the bromoacetyl system, which turns, offer the product diversity *via* formation of an amide bond.



Scheme 5. 1 The strategy of the bromoacetyl system, where $X = O, NH$; $Y =$ a leaving group

Using a disconnection strategy, we arrived at starting materials for the bromoacetyl system. The bromoacetyl element could be brought into the molecule with the help of acid halides, which could then bridge amides over to the thiophosphate *via* its electrophilic alkyl end. For instance, bromoacetyl moieties are easily introduced to amino groups of proteins and react well with peptides containing cysteine residues, with further application for peptide research and therapeutics. This could potentially be performed using highly reactive bromoacetyl bromide.

Unfortunately, BrAcBr, decomposes violently by heating or on exposure to moist air or water, so the formation of bromoacetic acid is likely to occur if not performed under dry conditions.

However, as introduced in the sections 1., in aqueous Tripartite chemistry a key aim is to be able to simply mix reagents and let reaction take place, which, in the case of bromoacetyl bromide, is not feasible as water is involved as the solvent and uncontrolled hydrolysis is highly probable. In addition, preparation of the acetyl amide linker would be required for each compound designed, which is absolutely incompatible with the fast and easy Tripartite method that we have in mind. Therefore, we needed to design a common intermediate that would accomplish bromoacetylation of amines in water.

In order to prepare a bromoacetyl mediator, BrAcBr could be exposed to alcohols, which would, then, give rise to esters. Depending on the alcohol used, esters are more or less reactive, but, generally are much more stable towards reaction with water than acid halides. In the range of notable structures shown below, different pK_a s, either increase or decrease the performance value of a leaving group, reactivity of the ester and hopefully selectivity towards aminolysis over hydrolysis.

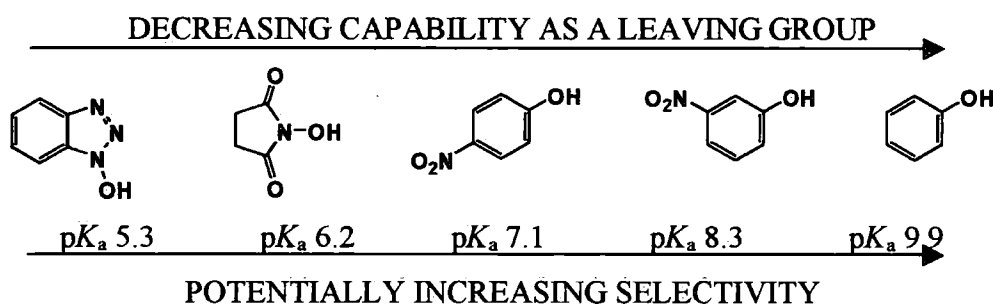
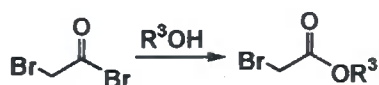


Figure 5. 3 Leaving groups and their characteristics: HOBt, NHS, *p*NP, *m*NP and phenol (left to right)

Activated esters can be formed under dry conditions to avoid unwanted hydrolysis of the starting bromoacetyl bromide.



Scheme 5. 2 Moderation of the bromoacetyl bromide reactivity *via* ester formation

Furthermore, the intermediate ester should still react readily with a range of amines in water, hopefully, generating whole libraries of compounds. If the leaving, $\mathbf{R^3O-}$, group is very good (e.g. as HOBt and NHS), the aminolysis will probably proceed with high rates but the selectivity might be poorer. On the other hand, less reactive esters (poorer leaving groups such as phenols) would maybe show more selectivity towards aminolysis, allowing less scope for competing hydrolysis to occur but the reaction would be much slower. This is the balance that we plan to examine and, hopefully, find.

In the bromoacetyl system, we opted to use a different approach of introduction of thiophosphoryl group, which involved oxo-thiophosphorylation. So far, we have been applying the principles of aqueous thiophosphorylation of amines, as a way to bring the thiophosphate feature into a molecule that can, then, be alkylated (Chapter 2.). It has been shown to be very convenient method for quick, easy and effective generation of array of thiophosphorylated amines, including nucleoside analogues as starting points for generating potential inhibitors. Thiophosphoramidates, presented a degree of instability in the form of P-N bond hydrolysis thus for method development directed our research efforts towards thiophosphates that provide better stability over a wider range of pH conditions.¹¹¹

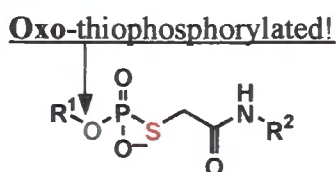
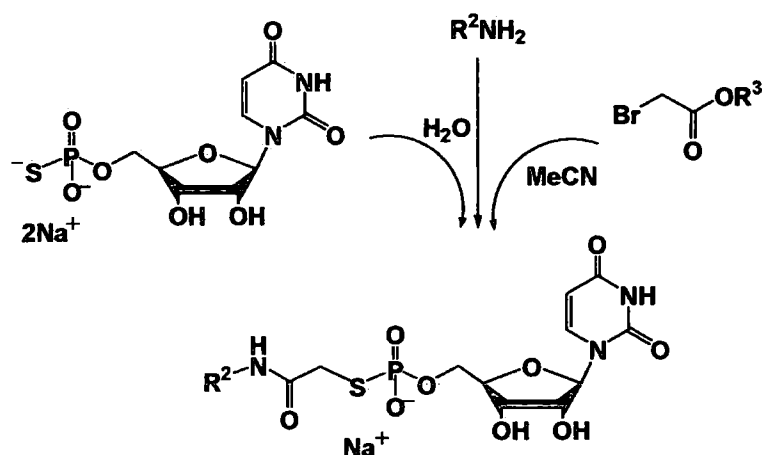


Figure 5. 4 Model for bromoacetyl system with thiophosphorylated alcohols

Thiophosphorylation of amines was performed with high conversion levels (70% to 100%, Chapter 2.). An inherent limitation of the oxo-approach is that alcohols are in general poorer nucleophiles than amines, and can therefore, be expected to be less effective. However, literature methods for the successful thiophosphorylation of nucleosides are available (section

5.3). In particular, we are interested in the thiophosphorylation of the 5'-hydroxyl group of uridine given that the form of the natural substrate of chitin synthase contains this nucleoside (section 5.2.1). In addition, a facile method for the detection of the chitin derived from fungi has been developed in our group using ^{15}N labelling of glucosamine units that that enabled determination of a degree of acetylation in chitin.¹¹² This could potentially be used in the inhibition assays against chitin synthase in fungi with our thiophosphoryl compounds.

With the thiophosphate substrate in place we will be in a position to explore an array of bromoacetylating agents and amines, which could then be used effectively to approach thiophosphoryl systems (scheme 5.3.).



Scheme 5. 3 Bromoacetyl Tripartite chemistry on formation of uridine derivatives. R^2 =any aliphatic substituent, R^3 = good leaving group

If products are generated in sufficiently high purity long purification procedures can be avoided. The material could then be used for direct inhibition screening assays on purified enzymes because synthetic reactions would have been performed in aqueous solution and the by-products would be benign. The development studies will be carried out in laboratory glassware, however, in due course bromoacetyl chemistry could, hopefully, be performed directly in 96-well microtitre plates. An amine conveniently used in this branch of thiophosphoryl Tripartite chemistry was D-glucosamine, as it is water-soluble, commercially available and resembles the structure of the natural substrate of chitin synthase (section 5.). Therefore, with simple and efficient synthetic bromoacetyl tripartite method that would provide

a range of compounds that mimics of pyrophosphate group and sugar end, we hope to recognise potential chitin synthase inhibitors, which would be the ultimate measurement of success.

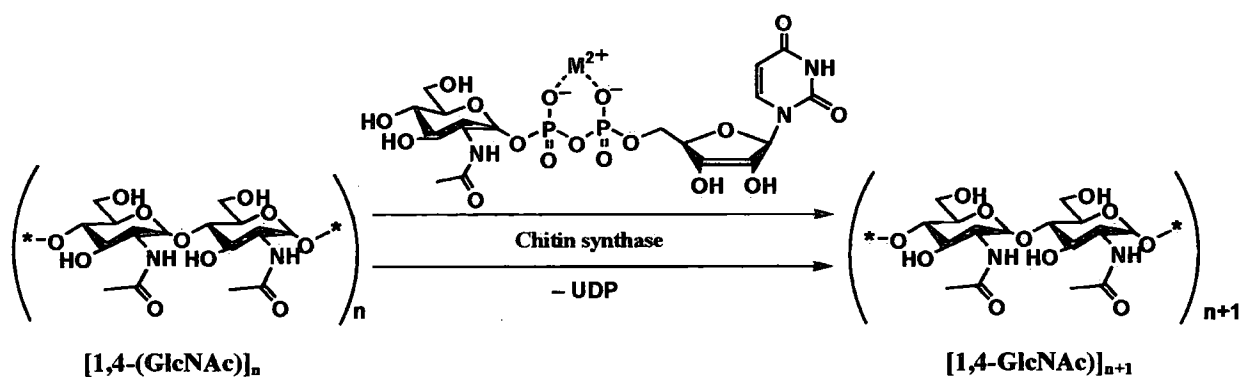
Initially in this chapter, we will introduce chitin synthase as the target enzyme of the bromoacetyl system and some existing inhibitors of chitin synthase. Then, the work performed on uridine 5'-O-monophosphorothioate (in future referred to as UMPS) will be described where we tried to alkylate efficiently with bromoacetyl esters. Furthermore, due to the occurrence of competing hydrolysis of bromoacetyl esters, attempts towards optimisation of amide formation will be performed via kinetic studies that employed NMR spectroscopy and UV-Vis spectrometry. Finally, preliminary experiments on the combined experiences from thiophosphoroamidate and bromoacetyl systems will be described.

5.2. Research targets in the form of glycosyltransferases

Next few sections will be dedicated to the function and importance of chitin synthase along with present inhibitors used in antifungal therapy and the ones that are newly designed, which have the common goal to mimicking enzyme natural substrate.

5.2.1. Chitin synthase

Chitin synthase (Chs) is an enzyme that catalyzes production of chitin by transfer of *N*-acetyl D-glucosamine (GlcNAc) units from the donor, uridine 5'-*O*-diphospho-*N*-acetyl D-glucosamine (UDP-GlcNAc), to a growing β -(1-4)-polysaccharide chain¹¹³ (scheme 5.).



Scheme 5. 4 The growing chitin chain. $M^{2+} = \text{Mn}^{2+}, \text{Mg}^{2+}, \text{Co}^{2+}$

There are three isoforms of chitin synthase that have been characterized and their functions defined by means of gene disruption. Although none of the Chs genes have been reported, so far, to be essential for the vegetative growth of yeast cells, simultaneous disruption of Chs2 and Chs3 was lethal.^{114,115} All three chitin synthases have the same polymerizing activity, but they deposit chitin at different times and at different locations during the cell cycle. Chs 1 is responsible for the repair of damaged chitin while Chs2 forms the primary septum. Chs3 performs lateral wall formation, and is needed for function of all other isozymes. Chs3 is employed in the synthesis of 90 % of cell wall chitin¹¹³. Cation dependence is not the same among the three chitin synthases¹¹⁶. Chs1 and Chs3 have a preference for Mg^{2+} , whereas Chs 2 showed the highest activity when assayed in vitro with Co^{2+} .

Chitin is the most widespread amino polysaccharide in nature. The annual global production of chitin in the biosphere is believed to be just one order of magnitude less than that of cellulose. Chitin synthase is present in the cuticles of Artropodes and Nemathodes¹¹⁷ and in yeasts that belong to the kingdom of Fungi. Chitin mainly serves as a structural component supporting cell and body surfaces, increasing mechanical strength of fungal cell walls and the exoskeletons of Artropodes. Insect growth and morphogenesis are strictly dependent on the ability to replace old cuticles during molting.

Fungal chitin synthase from *Saccharomyces cerevisiae*^{113,114,115} has been studied most widely as a biological model for the determination of structure, function and behaviour of Chs wider

different conditions. In addition, Chs from other organisms such as *Candida albicans*^{118, 119}. *S. cerevisiae* is used widely in industry for bread production and the fermentation of wine and beer. On the other side *C. albicans* is a big issue in medicine, since it causes very persistent fungal infections in humans. The reason for unsuccessful chemotherapy could be due to the increasing resistance of fungi against drugs and also the toxicity¹²⁰ of antifungal agents. The structure and biosynthesis of fungal cell walls is unique to fungi, no mammalian cell contains chitin. Therefore, chitin synthases are considered excellent targets for the development of antifungal drugs. Several examples of work in this field are reviewed below.

5.2.2. Past and present antifungal agents: natural substrate mimics

There is a number of series of antifungal drugs with big variation in their structures and modes of action. For a long time, the only drugs used for persistent and serious fungal infections were amphotericin B and flucytosine, which have polyene and heterocyclic structures, respectively. These agents have different modes of fungal growth inhibition. Amphotericin B was believed to interact with the cholesterol in the cell membrane forming channels that induce the electrolyte leakage and cell death. However, some investigations suggested that the phenomenon of cell death and ion imbalance were not connected.¹²¹ Flucytosine converts into 5-fluorouracil and then to 5-fluorouridinetriphosphate, which interferes with DNA and RNA synthesis.¹²² Often they are applied in the combined therapy.

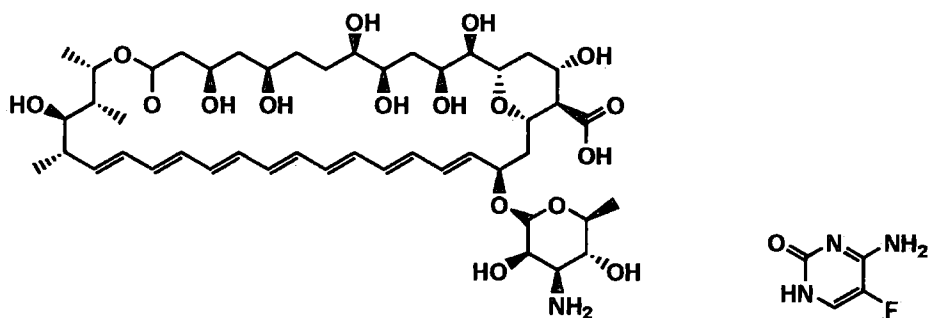


Figure 5. 5 Antimycotics amphotericin B (left) and flucytosine (right)

However, we are interested in inhibitors of chitin synthase that are characterised by nucleoside-like motifs therefore, literature investigations on some of the wide array of existing nucleoside drug molecules will be presented in this section.

Through the 1960s, Isono and co-workers¹²³ introduced a group of peptidyl nucleoside substances, the polyoxins and, later, the neopolyoxins, which were isolated from fermentation of *Streptomyces cacaoi*. The compounds were active against phytopathogenic fungi, with the possibility of agricultural application. Naturally occurring nikkomycins, isolated from *Streptomyces tendae*, which are harmless to non-fungal species, were a promising category of antibiotics in the therapy of opportunistic fungal infections. The best known examples of these two classes of molecules are Nikkomycin Z and Polyoxin D, which act as competitive inhibitors of Chs, presumably due to their structural resemblance to the natural substrate UDP-GlcNAc (figure 5.6).

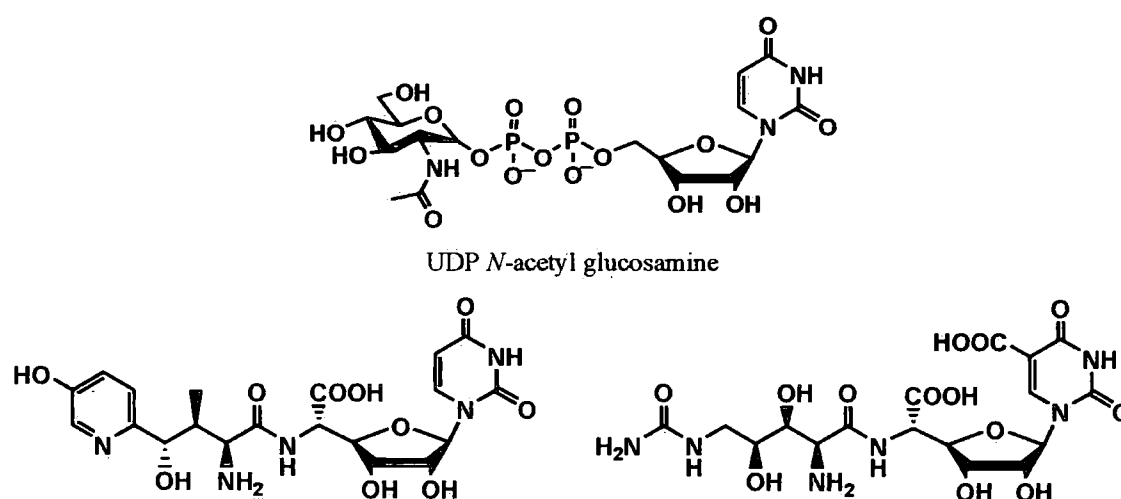


Figure 5. 6 Well known antifungal agents: Nikkomycin Z (left) and Polyoxin D (right)

Nikkamycin Z is very effective against Chs 3 *in vitro* and *in vivo* ($K_i=1 \mu\text{M}$), but poor activity for Chs 2 ($K_i=890 \mu\text{M}$) presents a major obstacle *in vivo*¹²⁴. In the case of Polyoxin D, the inhibition properties *in vivo* were determined only for Chs3, which showed $K_i=8 \mu\text{M}$ and is lower than for nikkomycin. This poorer activity probably arises due to the metabolism of these compounds or their low permeability to cells, as the possibility for competitive uptake by peptide permease transport systems exists.¹²⁴

A vast amount of work was done on the design and synthesis of novel nikkomycin analogues and most of them had uridine in their basic structures^{125,126,127}. Most substituents included aromatic, aliphatic, heterocyclic and amino acid motifs (figure 5.7). Some of them showed activity, but low binding affinity was an issue.

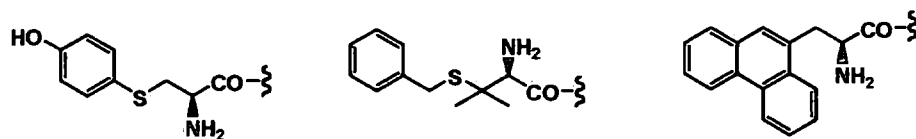


Figure 5.7 Variety of substituents at the terminal amino acid moiety of novel nikkomycins

There have been some other proposals for making new chitin synthase inhibitors, which contain heterocyclic features **149** and **150** (Figure 5.8), which aimed to mimic the half chair conformation of the forming glycosyl cation in the postulated transition state during sugar transfer (see section 1.3). Inhibitor **149**, shown in the figure 5.8, include a mimics of the diphosphate linker with protecting groups on the sugar mimic to increase the *in vivo* stability of the molecule. however, it showed only moderate activity against chitin synthase ($K_i=30 \mu\text{M}$). A range of compounds, represented by the structure **150**, were proposed as potential Chs inhibitors as they should have increased cellular uptake owing to the lipophilic isoxazole moiety that masks a pyrophosphate mimics. After the cleavage of heterocycle, dicarbonyl feature would be ready to bind to metal ion. In summary, none of these molecules showed significant *in vivo* pesticidal activity.¹²⁸

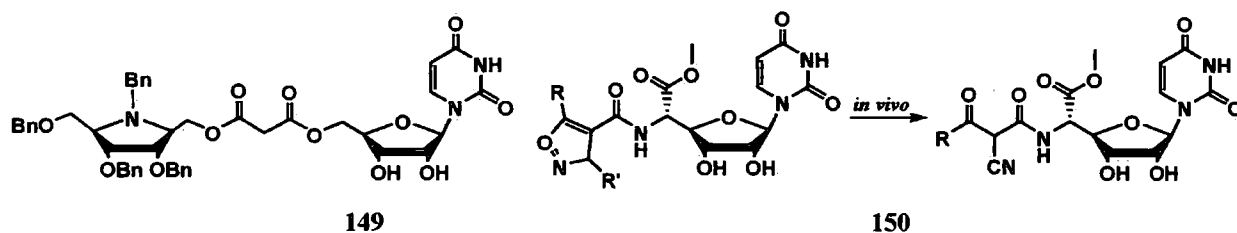


Figure 5.8 Heterocyclic potential inhibitors of chitin synthase

One of the most recent attempts towards the production of novel chitin synthase inhibitors, interestingly, employed click chemistry to make analogues of the natural substrate²⁴. A library of 1,4-disubstituted-1,2,3-triazolyluridine (figure 5.9) derivatives was generated using Cu(I)-

catalysed Huisgen cycloaddition (presented in more detail in section 1.), starting with uridine azide.

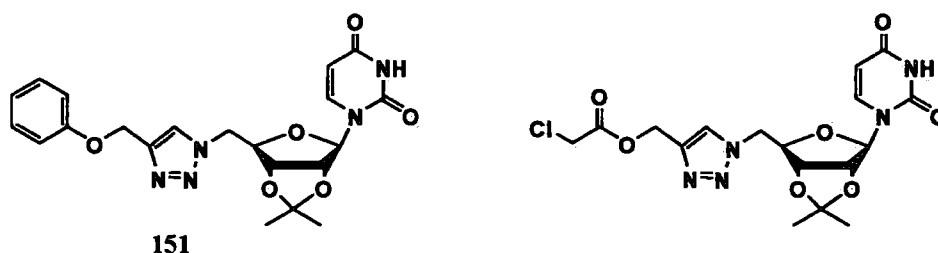


Figure 5. 9 Novel chitin synthase inhibitors made via the Huisgen click reaction between 5'-azidouridine and propargyl ethers (left) or esters (right)

Most of the compounds showed significant chitin synthase inhibition activity in assays performed against *Candida albicans* and *Candida neoformans*, with the lowest MIC being 18 μ M for compound 151. Even though the 1,3 dipolar cycloaddition of alkynes to azides, is considered to be very productive, the yields of the reactions ranged from 50-83%, and, coupled with the use of a protected uridine. These systems still needed laborious purification.

Extensive efforts have been invested into the synthesis of analogues of natural peptidyl nucleosides, as their similarity to the natural substrate potentially offers minimal side effects and maximal possibility of a positive outcome. While much has been accomplished, ideal antifungal agents have not yet been discovered. We focused our work on systems containing a nucleoside-bromoacetyl-thiophosphate features as a starting point for method development. In due course, we hoped to apply this methodology to the preparation of a library of potential drug-like agents. The goal is to produce structures that would mimic UDP-GlcNAc and, thus, inhibit chitin synthase, having the potential of antifungal activity.

5.3. The preparation of uridine 5'-O-monothiophosphate (UMPS)

The methods for the synthesis of phosphate esters of nucleosides were developed in the 1960s. Since then, there has been a huge expansion of investigations in this field, overlapping with our particular interest in the selective 5'-thiophosphorylation of nucleosides. All current procedures are broadly based on a few examples described below. A method that employed protected

ribonucleosides or unprotected 2'-deoxyribonucleosides was introduced by Eckstein^{57, 129}. Nucleosides were treated with triimidazolyl-1-phosphinesulfide and after a deprotection step and chromatographic purification, the 5'-monophosphorylated products were isolated in yields less than 35%. At about the same time Yoshikawa¹³⁰ presented a simple one-step procedure for making nucleoside-5'-phosphates in good yields. The idea of directly using phosphoryl chloride on an unprotected nucleoside was shown to be very attractive and showed near-perfect selectivity for the primary 5'-alcohol over the only slightly less nucleophilic 2'- and 3'-hydroxyl groups. The method involved the usage of trialkyl phosphates as solvents, which facilitate selective phosphorylation, by what is believed to be a decrease in the phosphoryl chloride reactivity through formation of an ionic structure:

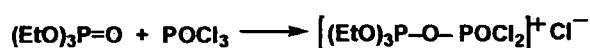
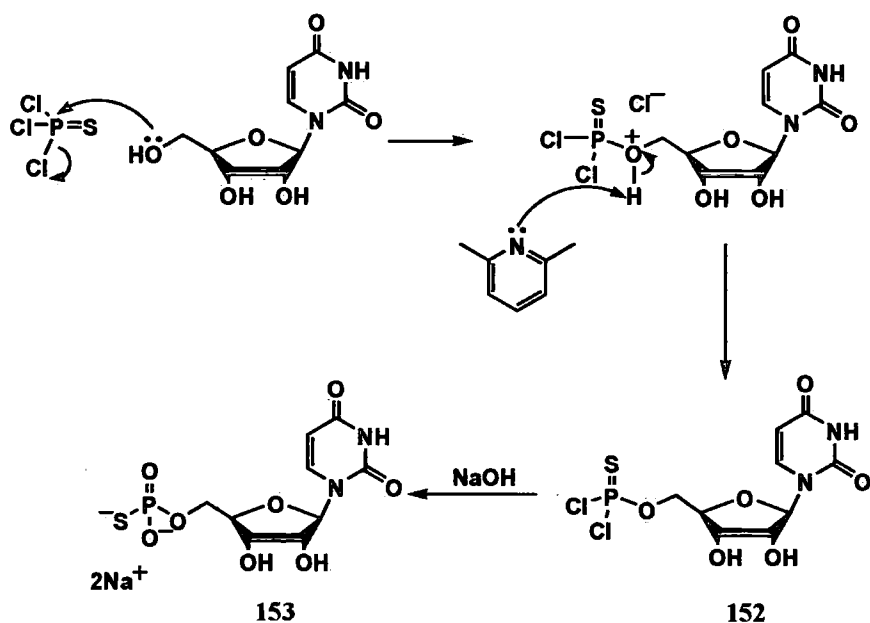


Figure 4. 10 Yoshikawa's proposed mechanism of controlling the reactivity of POCl_3

A later mechanistic proposal suggested that the reaction proceeds through a nucleoside-triethyl phosphate complex¹³¹, formed while preheating the nucleoside with trialkyl phosphate prior to the addition of phosphoryl chloride into the nucleoside solution. None of the mechanisms proposed, so far, have been proven, so the role of trialkyl phosphate in the phosphorylation process still remains a puzzle. Murray and Atkinson¹³² adopted the Yoshikawa procedure for the preparation of adenosine 5'-*O*-monophosphothioate (AMPS). After the formation of AMPS, thiophosphoryl chloride was hydrolysed *via* addition of barium acetate. The resulting barium phosphate can be, however, difficult to remove from the reaction mixture.

In conclusion, after reviewing previously published methods, we opted to follow the modified Yoshikawa procedure of Moran and Whitesides¹³³. In addition, no protection of ribose was required and with the use of 2,6-dimethyl pyridine (found to work better than pyridine) and triethyl phosphate we hoped for better thiophosphorylation of uridine. The reaction probably proceeds through mechanism shown below (scheme 5.5).



Scheme 5. 5 The proposed pathway of thiophosphorylation of unprotected uridine

In order to minimise the possibility of moisture affecting the reaction, all reagents were prepared immediately prior to the reaction (section 7.1) and the reaction was then performed under dry conditions. In contrast to guanosine (examined in our laboratory in different projects), uridine shows very good solubility in trialkyl phosphate solvents, with less heating and less solvent being needed to achieve fast dissolution. This, we hoped, would enable more efficient thiophosphorylation as it has been suggested in all previously explored methods that a homogenous nucleoside solution was an essential starting point for obtaining the highest possible yields. After the uridine solution in triethyl phosphate had been cooled in an ice bath, distilled thiophosphoryl chloride and dry 2,6-lutidine were added and the mixture was stirred at 4°C to control the exothermic thiophosphorylation reaction. Owing to its high boiling point (215 °C), triethyl phosphate was removed from the mixture *via* petroleum addition, which precipitated the uridine 5'-thiophosphorodichloridate **152** whilst the excess of thiophosphoryl chloride remained in the solution. The precipitate of uridine 5'-thiophosphorodichloridate was dissolved in water and hydrolysis was performed by, addition of sodium hydroxide pellets to achieve pH 8.

^{31}P NMR spectroscopy was performed directly on crude aqueous mixture and showed the expected peak at 44.0 ppm^{134} for the successful thiophosphorylation of uridine, but also the presence of triethyl phosphate ($\delta = 1\text{ ppm}$) and inorganic thiophosphate at $\delta = 32\text{ ppm}$. Since ^1H NMR spectra also indicated a mixture of products and starting materials, purification of the crude product was needed. As most of the impurities were soluble in water anion exchange chromatography appeared to be a good strategy for the purification of UMPS.

Anion exchange chromatography, using DEAE Sephadex A25 fast flow resin, was performed using a linear gradient of 50 to 400 mM of triethylammonium bicarbonate buffer, pH 7.5, detecting the product elution *via* UV absorbance measured at 280 nm (chromatogram shown below).

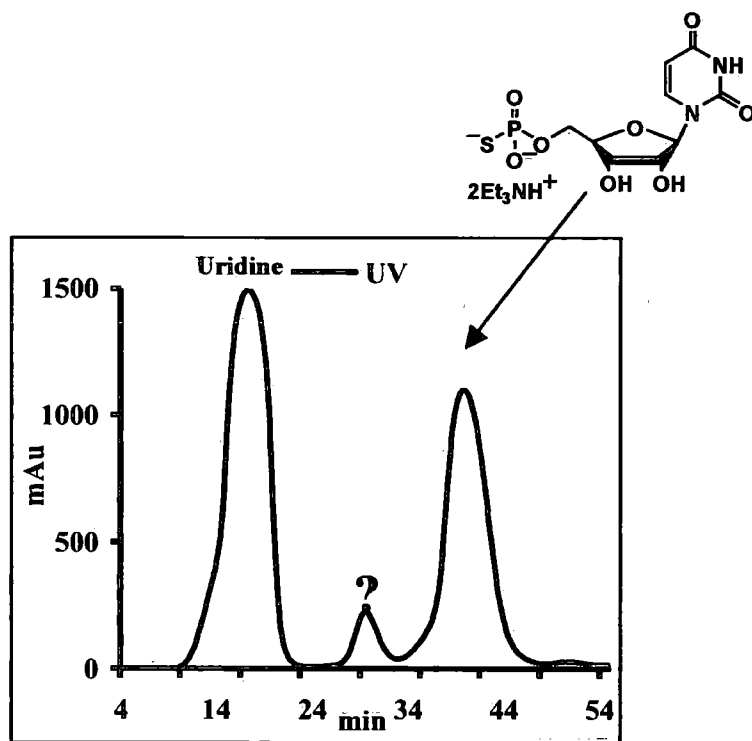


Figure 5. 10 Chromatogram of the purification of UMPS *via* anion exchange

Unreacted uridine, as a non-ionic molecule eluted from the column immediately, along with the cationic lutidinium salt. The product that eluted at higher buffer concentration (between 280 and 350 mM) was expected to be uridine 5'-O-monothiophosphate, due to its longer retention

time on the anion exchange material. ^{31}P NMR spectroscopy of this fraction showed only one signal at 43 ppm. It has been estimated via chromatogram integration that the conversion to 5'-O-monophosphothioate was 40%. The structure of the by-product forming the smaller peak in the middle of the run was not fully determined, but given that it did not give rise to any signal in the ^{31}P NMR spectra we concluded that the product was not of interest to us.

Since the desired product was gained in the form of a bis-triethylammonium salt, to facilitate handling, characterisation and further application, the triethylammonium ions were exchanged for sodium ions. This was achieved by using a simple sodium iodide-acetone system. An excess of sodium iodide, dissolved in acetone was added to the product that was dissolved in a minimal amount of water. Precipitation, supported with the addition of small amounts of methanol and diethyl ether, occurred. The solid was believed to be di-sodium salt of UMPS, which in contrast to the excess of sodium iodide and formed triethylammonium iodide, was not soluble in acetone and gave rise to a sticky precipitate. Following a simple centrifuge process, the final product was isolated as a solid by re-dissolving the pellet in water followed by lyophilisation and resulted in a fine white powder of spectroscopically pure di-sodium of UMPS. The product showed great stability (no degradation over two years) when stored dry at 4 °C.

Unfortunately, the synthesis of UMPS was not as efficient as we had hoped, giving only moderate yields (37%). The purification using anion exchange chromatography, with Sephadex A25 fast flow resin, displayed good resolution of the products, but, on the other side it was a very time consuming procedure and limited the amount of product that could be purified owing to the size of the chromatography column. However, we generated enough UMPS using this synthetic method to enable us to develop our bromoacetyl Tripartite chemistry.

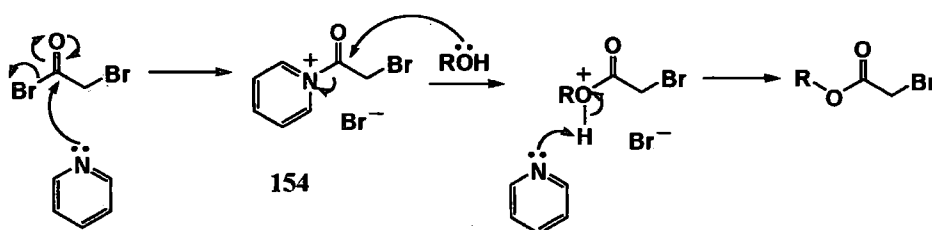
5.4. The synthesis of activated bromoacetyl esters

N-hydroxysuccinimide (NHS) and *N*-hydroxybenzotriazole (HOBt) are molecules that are widely used in the activation of carboxylic acids in peptide synthesis.¹³⁵ Active esters react readily with amino groups, in preference to water, to form amides. We wanted to use this

advantage and apply it towards the formation of amide bonds between amines and the bromoacetyl group.

We started with good leaving groups, such as HOBt or NHS, to form activated bromoacetyl esters, which on one end react readily with amino groups to form amides, allowing us to use a number of different amines. On the other end the nucleophilic sulfhydryl moieties of thiophosphoryl groups should be readily alkylated by the bromomethylene centre. HOBt has almost one unit lower pK_a than NHS (5.2 and 6.3 respectively) and, therefore, has the potential advantage of higher reactivity, which on the other side could reduce the selectivity and introduce the possibility of generating side products (especially hydrolysis products). In later studies we used *p*-nitrophenol, *m*-nitrophenol and phenol. These were expected to have much lower reactivity owing to their higher pK_a -s. This, on the other hand might give rise to higher degree of selectivity. In, addition both nitrophenol systems provide convenient chromophores that offer the possibility using simple UV-Vis kinetic experiments (section 5.9.2-5.10)

The general method for making these bromoacetyl esters (scheme 5.) involves dropwise addition of a pyridine solution in dichloromethane into a solution of bromoacetyl bromide also in dichloromethane. This caused the formation of a white precipitate which was likely the pyridinium bromoacetate salt **154**. To minimize the possible hydrolysis of bromoacetyl derivatives, a standard work up was performed very rapidly. Since there was a possibility that product could hydrolyse under basic conditions, the work up was performed with water instead of bicarbonate.



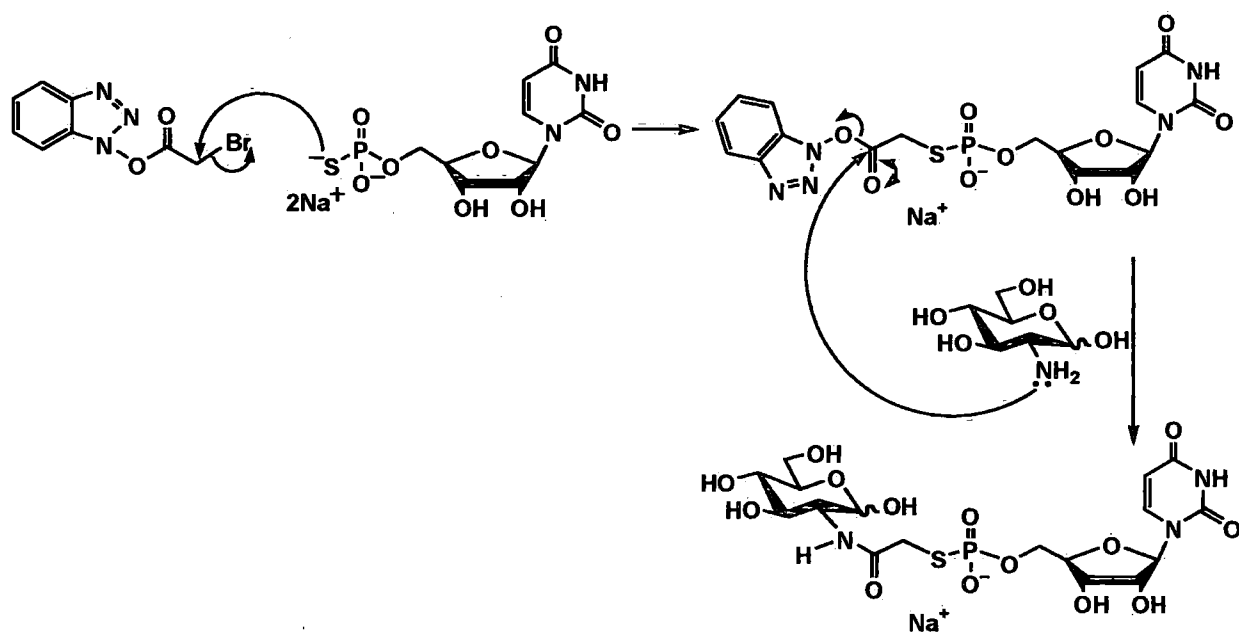
Scheme 5. 6 General mechanism for making bromoacetyl alkylating agent. R=leaving groups

The ^1H NMR spectra of the crude product bromoacetyl-OBt indicated incomplete conversion of the HOBt, unlike in the case of NHS, which generated clean product, with an isolated yield of 74%. Attempts to purify HOBt derivative failed because decomposition occurred during thin layer chromatography. As a result, this product was used as a crude material, with purity of 70%, estimated *via* ^1H NMR spectroscopy.

After being stored dry in the freezer for three months, the bromoacetyl-OBt showed some signs of degradation to HOBt and bromoacetic acid, according to ^1H and ^{13}C NMR spectroscopy. In contrast, bromoacetyl-NHS showed great stability over two years when stored dry in the freezer. So we can confirm that HOBt is much more reactive species than NHS, what we will try to use as the advantage in our Tripartite 'Click' approach presented in sections to follow. With pure UMPS and bromoacetyl derivatives in hands, we set off preliminary experiments in an attempt to establish and develop our bromoacetyl Tripartite approach.

5.5. The bromoacetyl Tripartite reaction: HOBt as the leaving group

Our first attempts used bromoacetyl-*N*-hydroxybenzotriazole as the alkylating agent and uridine 5'-monophosphorothioate. In order to imitate the *N*-acetyl glucosamine end of the substrate, D-glucosamine was used as the nucleophile to perform the substitution with the HOBt to form an amide. Reactions were performed with a very simple procedure of addition of the excess of bromoacetyl-OBt (1.2 Eq) in dry acetonitrile to an aqueous solution of disodium UMPS and D-glucosamine (1 Eq each). The choice of acetonitrile for the dissolution of alkylation agent was due its miscibility with water. Since the pH of the reaction mixture dropped as the alkylation of thiophosphate group was happening, the pH was adjusted to 9 *via* dropwise addition of aqueous sodium hydroxide. The mixture was left stirring for 12 hours at room temperature during which time reaction was believed to be proceed with the following mechanism.



155

Scheme 5.7 Tripartite 'Click' reaction: HOBt as leaving group

A ^{31}P NMR spectrum of the crude mixture suggested that a reaction occurred; owing to the shift of the phosphorus signal from $\delta=43$ ppm, assigned for the UMPS, two signals at $\delta=18$ ppm and $\delta=20$ ppm. The presence of two signals indicated the possibility of side reaction having occurred. In order to identify products and revise reaction conditions, the crude sample was subjected to the anion exchange chromatography, with DEAE Sepharose A 25 fast flow resin and TEAB buffer, pH 7.5, as the mobile phase. The resulting chromatogram is shown below.

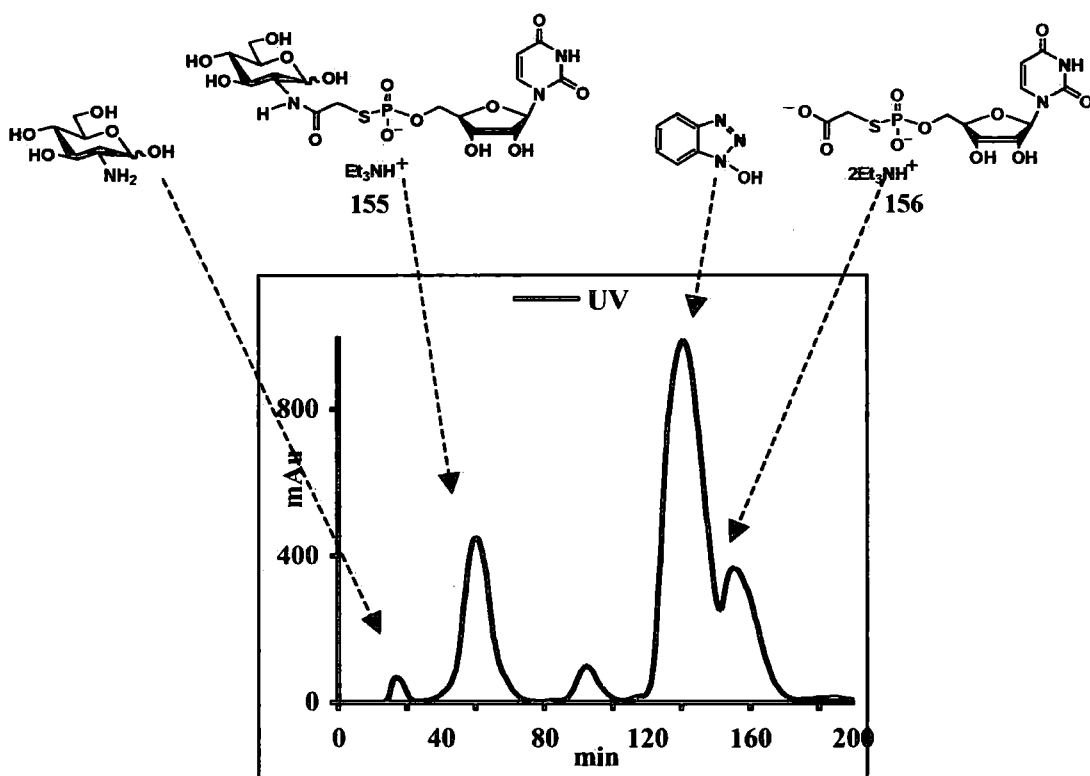
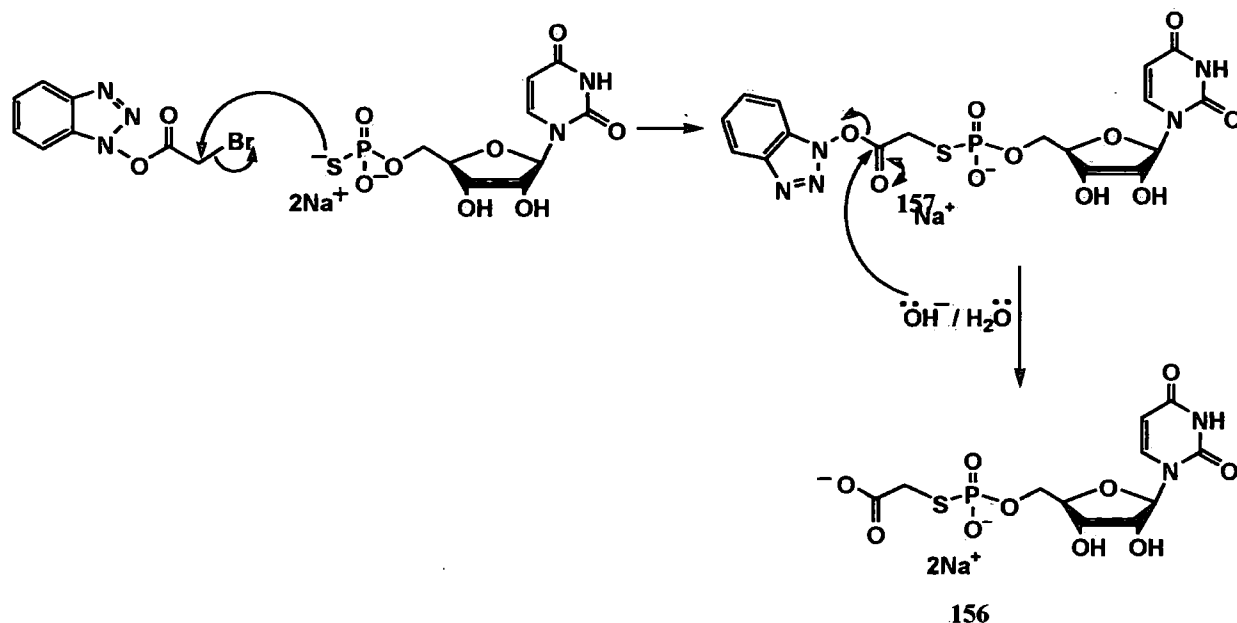


Figure 5.11 Anion exchange chromatography of the Tripartite reaction: HOBt as leaving group

The first peak in the chromatogram contained D-glucosamine, which as cation had short retention time on the anion exchange resin. D-glucosamine does not contain a chromophore absorbing at 280 nm, however, it likely co-eluted with material that was UV-active. The desired product **155**, GlcNHAcUMPS⁻, eluted between 70 mM and 90 mM of the TEAB buffer and showed a signal at 18 ppm in the ³¹P NMR spectrum. A small peak eluting just after the desired product contained a mixture of the desired product and HOBt. The side product **156**, AcUMPS²⁻, as di-ionic molecule, had a longer retention time on the anion exchange column, so it eluted at 170 mM TEAB buffer and was seen in the ³¹P NMR spectrum as a signal at $\delta=20$ ppm. The side product was overlapped with the big peak containing HOBt, which at the pH of the mobile phase was ionised owing to its pK_a of 5.3. With the help of ¹H NMR spectroscopy and ES⁻ mass spectroscopy we confirmed the structure of the by-product to be likely the result of the hydrolysis of intermediate **157**, formed through bromoacetyl-OBt

alkylation of UMPS (scheme 5.8). Since, AcUMPSNHGlc⁻ shows great stability over time, the possibility of hydrolysis product forming from desired product was excluded.



Scheme 5. 8 Tripartite reaction: competing hydrolysis reaction

Both GlcNHAcUMPS⁻ and AcUMPS²⁻ products were lyophilised after anion exchange chromatography to give rise to triethylammonium salt. For further characterisation these products were subjected to cation exchange chromatography.

By integration of the anion exchange chromatogram, we estimated the ratio of the desired product (AcUMPSNHGlc⁻) to the hydrolysis product (AcUMPS²⁻) to be close to 1:1, and this led to the conclusion that the reaction was only 50% successful, in terms of conversion. Therefore, we decided to investigate the possibility of optimization of this Tripartite reaction.

5.6. Tripartite reaction over a range of pH: HOBt as the leaving group

In order to analyze the effect of base concentration in the reaction mixture, a few experiments, involving different analytical approaches (TLC, anion exchange chromatography) were performed under a range of reaction conditions where pH was varied. The reaction mixtures

were prepared as in section 5.5, by mixing aqueous solutions of UMPS and GlcNH₂ with acetonitrile solutions of bromoacetyl-HOBt. In preliminary experiments, pH was adjusted by simply adding different amounts of aqueous sodium hydroxide solution to the mixture, after the alkylation agent had been added. The pH were estimated using pH paper and were found to remain constant within one unit, throughout the reaction time of 12 hours.

In the TLC experiments, slight differences in the size of the spots of desired product (lower R_f) and by-product (higher R_f) were noticed. The TLC method, which seemed appropriate for quick analyses, had the disadvantage of insensitivity and reliability in terms of repeatability. Therefore, priority was given to the use of anion exchange chromatography and more sensitive and quantitative UV detection system.

For the anion exchange chromatography experiments, a range of seven H₂O/MeCN solutions plus reactants was made with the addition of different volumes of aqueous sodium hydroxide to give a spectrum of reaction mixtures with pH (table 5.1).

Table 5. 1 The final pH of the mixtures in the bromoacetyl-HOBt system

Reaction vessel	I	II	III	IV	V	VI	VII
pH (H ₂ O/MeCN)	4.82	6.08	7.8	9.18	10.83	12.72	13.76

After 12 hours, all reaction mixtures were concentrated on the rotatory evaporator to remove acetonitrile and lyophilised. The solid was dissolved in 50 mM TEAB buffer and subjected to chromatography. Since the collection of a single anion exchange chromatogram (previous experiment, section 5.5) took about 5 hours (including equilibrating and washing the column), with the goal of speeding up the screen of the pH range reaction outcomes, analyses were carried out on analytical column (1 mL), with the same fast flow DEAE Sephadex A25 material. Anion exchange chromatography was performed using a linear gradient from 50 to 120 mM of triethylammonium bicarbonate buffer pH 7.5. The resulting chromatograms were plotted in parallel to outline the differences in outcomes of each experiment (figure 5.12).

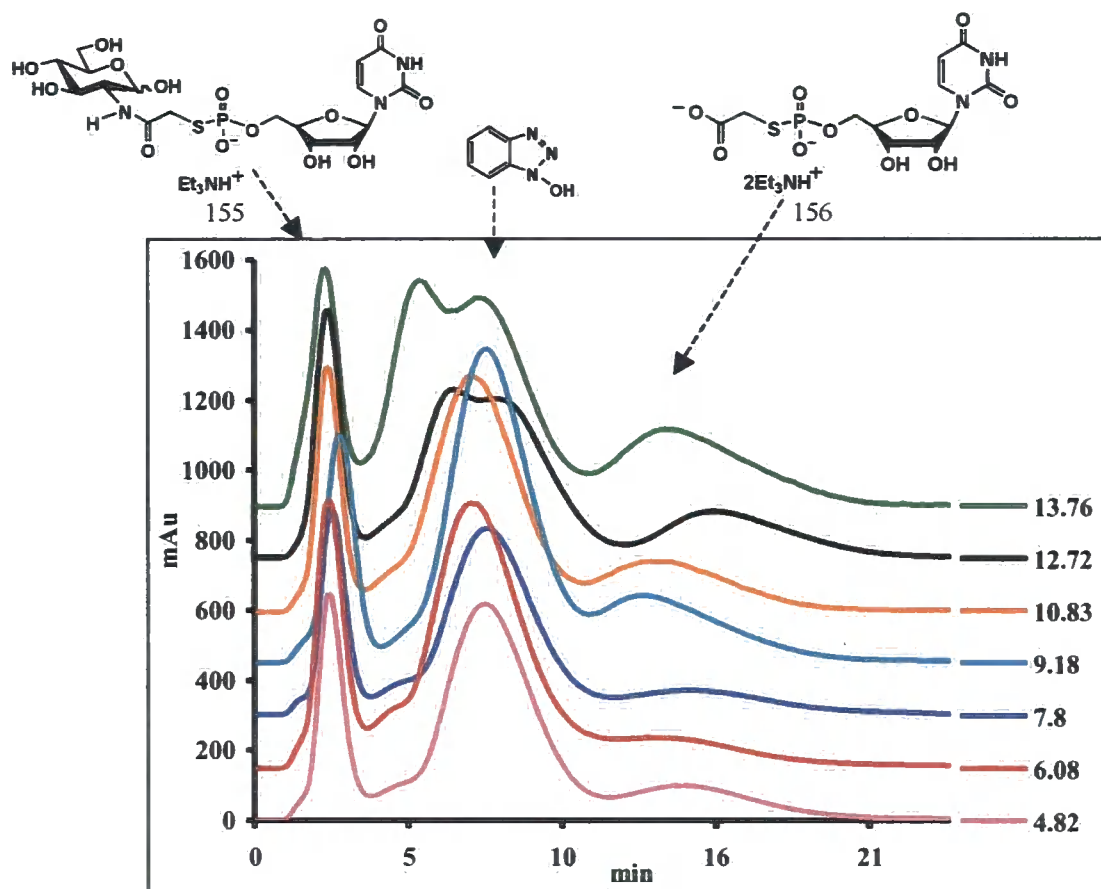


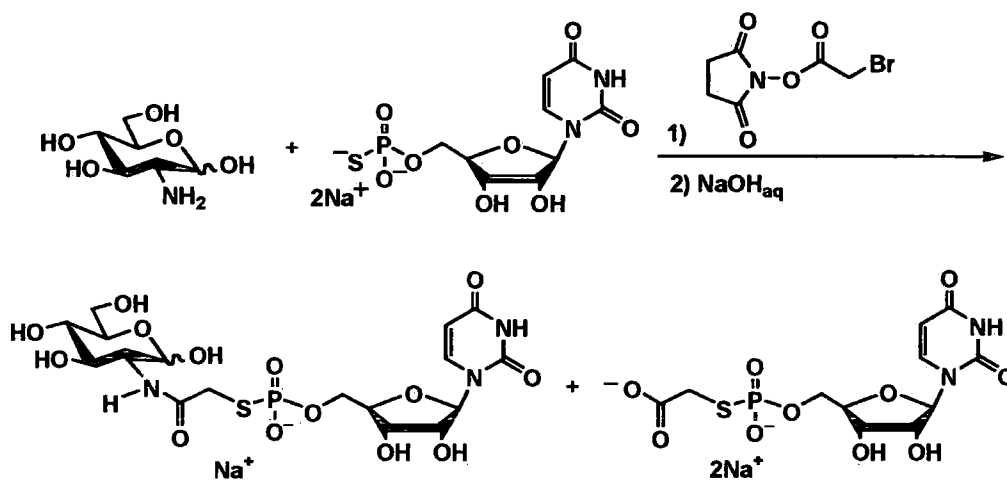
Figure 5.12 Tripartite reaction pH range: HOBt as leaving group. UV/time plot

The first eluting peak corresponds to the desired product, GlcNHAcUMPS^- , followed by the HOBt peak and the hydrolysis product, AcUMPS^{2-} , eluting at the end. All the components of the peaks were confirmed using purified standards to determine retention time. The ratio between the desired and the side products, estimated through integration of the chromatogram, suggested that the best results were achieved when the pH of the media was adjusted to 6.08 and 7.8 (around 65% GlcNHAcUMPS^- and 30% AcUMPS^- were produced in each experiment). This result for the highest outcome at the pH interval 6.08-7.8 was expected, due to the higher possibility of protonation and, therefore, nucleophilic deactivation of the reacting D-glucosamine, (pK_a 7.75) at lower pH and greater influence of competing hydrolysis reaction at higher hydroxide concentrations. HOBt is a good leaving group and its esters are amongst the

most reactive, and, according to our experiments, it might be too reactive for our system. The hydroxide ion and, more likely water at lower pH, have attacked the carbonyl group so that complete substitution of the intermediate ester with amine was not possible. *N*-Hydroxysuccinimide (NHS) could potentially offer more selectivity towards aminolysis in the presence of competing hydrolysis processes.

5.7. Tripartite reaction: NHS as the leaving group

This approach bromoacetyl-*N*-succinimide, as the alkylation agent with its less reactive ester leaving group owing to the pK_a of NHS being 6.3.



Scheme 5. 9 Tripartite reaction: NHS as leaving group

Single reaction was carried out and its outcome analysed with anion exchange chromatography in way as for the bromoacetyl-OBt experiments (section 5.9). As with bromoacetyl-OBt system, higher pH have, probably, stimulated hydrolysis, this example was performed at the pH 8 to compare the possible differences in these two carbonyl-activating groups (HOBt and NHS). The resulting chromatogram is shown below.

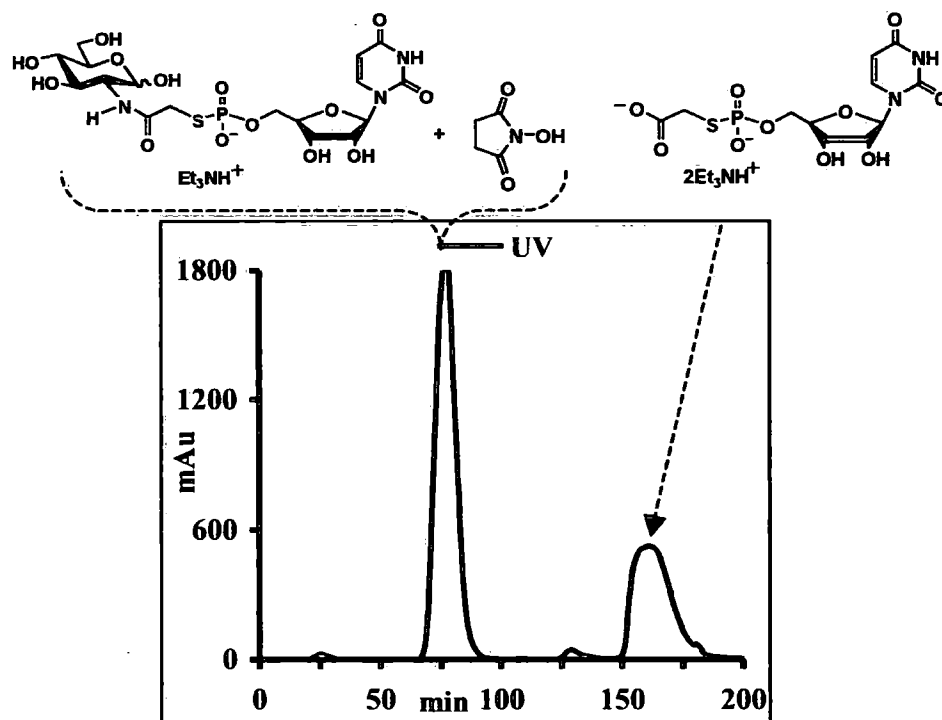


Figure 5.13 Chromatogram of the Tripartite reaction: NHS as leaving group

The eluate that peaked at around 80 mM TEAB, contained a mixture of *N*-hydroxysuccinamide and the desired product uridine 5'-O-monophosphorothioate-S-acetylglucosamide (GlcNHAcUMPS⁻). ³¹P NMR spectroscopy of this fraction showed that the shift from $\delta=44$ ppm for UMPS to 18 ppm for GlcNHAcUMPS⁻ occurred, which was a good indicator that the Tripartite reaction has occurred. Although the exact ratio of the products in the fraction could not be determined, owing to the overlap in the chromatogram, the intensities of the signals in ¹H NMR spectra led to the conclusion that the conversion of the reaction in the direction of desired product was very poor. The second peak in the chromatogram, at the buffer concentration of 400 mM, was the product of the side hydrolysis reaction, owing to the 20 ppm signal in the ³¹P NMR spectra.

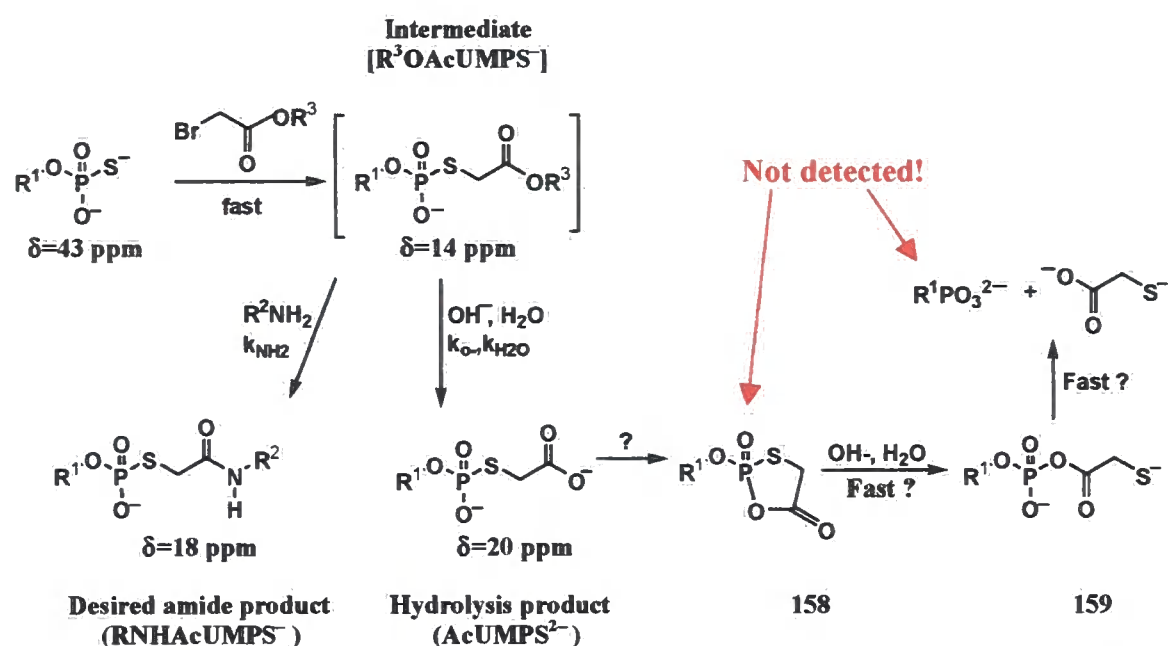
In conclusion, NHS might have offered better possibilities for the higher yielding synthesis of 5'-thiophosphoronyl nucleoside derivatives, as a less reactive species, but due to the shared

retention time during anion exchange chromatography with the desired product, possible further studies were disabled. Instead, a new approach of using NMR spectroscopy and UV-Vis spectrometry as tools for studying the processes occurring in the bromoacetyl Tripartite ‘Click’ reactions, was explored and presented in the following sections.

5.8. Ester hydrolysis and aminolysis

5.9. Studies of the pH-rate dependence of amine formation: Dipartite ‘Click’ chemistry

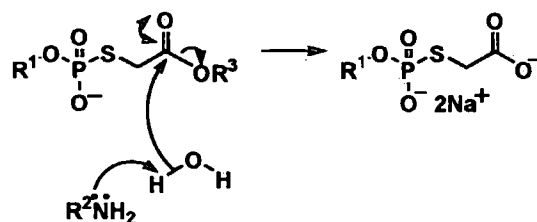
Preliminary studies on the Tripartite system, involving both bromoacetyl-OBt (section 5.) and bromoacetyl-NHS (section 5.), suggested that, beside formation of the desired amide from the intermediate ester and an amine, there was a competitive hydrolysis reaction occurring. Obviously, the pH of the reaction mixture had a big influence on the ratio between desired and side products. A general scheme of what we believe has happened is shown below.



Scheme 5. 10 Proposed pathways of bromoacetyl Tripartite reaction. **R¹**=uridine, **R²**= D-glucosamine, **OR³**=good leaving group. Shifts collected *via* ³¹P NMR spectroscopy

Pentacyclic thiophosphate **158** and phosphate product **159** (figure 5.10), which might have formed after P–S ring opening to release a free thiol group, were not detected either via NMR

or mass spectroscopy, owing to their possible short life times or even, simply, that the reaction did not proceed along this path (further details in a similar vein are discussed with the respect to thiophosphoramidate-acetyl molecules (section 5.10). The side hydrolysis reaction of intermediate ester $R^3OAcUMPS^-$ that led to $AcUMPS^{2-}$ into the product mixture has probably occurred with the help of catalysis from hydroxide. There is also the possibility of general base catalysis caused by the added amine via the mechanism shown below.



Scheme 5. 11 Proposed mechanism for the amine general base catalysis. R^1 =uridine, R^2 =any aliphatic, aromatic moiety, OR^3 =good leaving group

The alkylation of thiophosphate group with bromoacetyl moiety is relatively fast (we did not determine the alkylation rates but the reaction was completed within a minute) and it occurred with complete conversion (^{31}P NMR spectroscopy showed the presence of a single signal at 14 ppm for the intermediate $R^3OAcUMPS^-$ and no signal for $UMPS$ at 43 ppm was detected). However, we are interested in the rates of:

amide formation ($k_{NH_2} [RNH_2] [R^3OAcUMPS^-]$), and

the competing intermediate hydrolysis ($(k_w [H_2O] + k_{OH} [OH^-]) [R^3OAcUMPS^-]$)

general base hydrolysis $k_{GB} [RNH_2] [R^3OAcUMPS^-]$)

that would potentially allow us to predict the behaviour of different compounds used, leaving groups and amines. In order to understand the hydrolysis and aminolysis process during the Tripartite reaction we set up experiments so these could be studied separately. Then our conclusions could be used to establish the best conditions to perform the synthesis of an array of substituted thiophosphoronucleosides with respect to amide formation.

Our investigation tactics involved studies on the rates of the ester transformation using intermediate $R^3OAcUMPS^-$ as starting material. This we call the Dipartite approach, where

UMPS dissolved in water would be alkylated with bromoacetylating agent containing one of the leaving groups presented in section 5.1 in acetonitrile solution and, after lyophilisation, the material would be isolated as a dry, kinetically stable material. Then, the intermediate $R^3OAcUMPS^-$ would be exposed to a range of buffers, for hydrolysis studies or buffer and amine, for the aminolysis studies. The conversion would be followed *via* a chosen analytical technique that, in first instance, was be NMR spectroscopy, but later we used more simple and suitable UV-Vis spectroscopy approach. These experiments will form the majority of contents of the following sections.

5.9.1. ^{31}P NMR kinetic studies

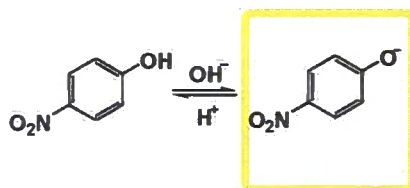
As previously introduced, the starting material, UMPS, the intermediate, $NHSAcUMPS^-$, and the products formed in the bromoacetyl Tripartite reaction, namely the amide $RNHAcUMPS^-$ and the acid $AcUMPS^{2-}$ (scheme 5.10) all give distinct signals in ^{31}P NMR spectra ($\delta=43, 14, 18$ and 20 ppm, respectively). A Dipartite method was used to prepare intermediate, which was then dissolved in a range of buffers with or without amine ($GlcNH_2$) and subjected to ^{31}P NMR spectra collection. The processes occurring at different pH would be then analysed by monitoring the decreases/increases in the signal intensities of the intermediate/products, respectively, in the ^{31}P NMR spectra. Therefore, NMR spectrometry seemed like a quick and easy strategy towards desired rates of hydrolysis and aminolysis reactions.

Firstly, hydrolysis experiments on the intermediate $NHSAcUMPS^-$. In these experiments, an excess of alkylating agent was used to ensure complete consumption of UMPS, avoiding any confusion in the ^{31}P NMR spectrum. The collection and manipulation of the hydrolysis NMR kinetic data was performed as described for the thiophosphoramidate hydrolysis, section 2.5.3 However, the experimental data on the hydrolysis of intermediate $NHSAcUMPS^-$ in a range of buffers were very scattered and the fit to the $\log k_o$ -pH curve was very poor. Possible reasons for this lay in the NMR experiment performance where the concentrations of the sample were very high to ensure good quality data, along with a large excess of buffer used to maintain constant pH (10-fold). Therefore, the quality of the NMR performance and pD measurement

could have been influenced by high ionic strength. Application of the ^{31}P NMR spectroscopy, as the method for kinetic analysis of pathways in bromoacetyl Tripartite reaction, was based on the idea that it would be simple and quick (compared to e.g. chromatography methods), however, this was not the case here. Therefore, the application of UV-Vis spectroscopy, as another analytical technique for the kinetic studies was explored.

5.9.2. UV kinetic studies

Owing to the higher $\text{p}K_{\text{a}}$ s of phenols, the phenolate-based bromoacetyl systems were expected to react slower than HOBt and NHS homologues. The *p*-nitrophenolate ester of bromoacetic acid would potentially present higher selectivity than HOBt and NHS and would, possibly, decrease the effect of side reactions occurring. The *m*-nitrophenolate ester, where *m*-nitrophenol has even higher $\text{p}K_{\text{a}}$ value and thus the ester would, potentially, be even more selective in its substitution reactions with amines over hydrolysis. In addition, an advantage why *p*- and *m*-nitrophenols are very suitable for the kinetic experiments is the bright yellow colour of the nitrophenolates that are formed in the basic media due to their $\text{p}K_{\text{a}}$ s (7.1 and 8.3, respectively) and can be easily detected in the visible spectrum.



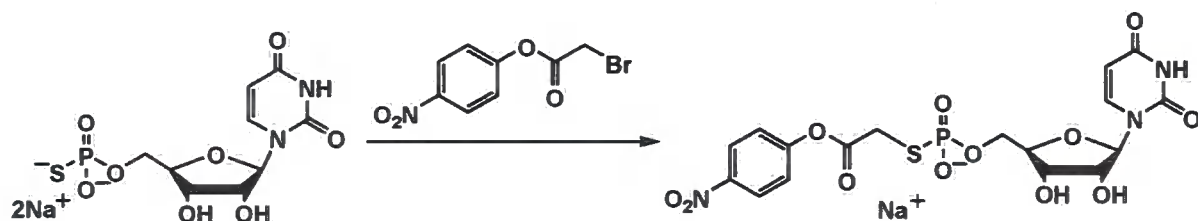
Scheme 5. 12 Change in colour of nitrophenols with the change of pH

This sensitivity of UV-Vis spectroscopy is much greater than that of the NMR spectroscopy. Therefore, the requirements for the quantity of sample used per experiment can be decreased by several orders of magnitude (from 30mg down to 1.3 μg). Along with the sample amount decrease goes the buffer used to control pH, so the possible issues with high ionic strength of the analysed solution, as seen in the NMR kinetic study, can be excluded. As well, owing to the spectrometer being equipped with the cell-changer, there was a possibility of multiple runs (17) being performed in parallel, which enabled faster and easier creation of the pH profiles.

In order to avoid repetition, because the same method for both *p*-nitrophenol and *m*-nitrophenol UV-Vis kinetic studies was performed, in the following sections we will present the experiments that used *p*-nitrophenylate ester followed by briefly outlining *m*-nitrophenylate ester kinetic results.

5.9.3. Preparation of samples for the UV-Vis kinetic studies

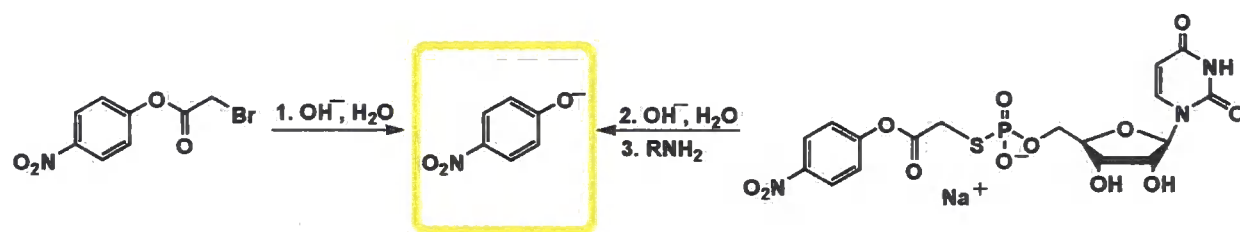
Preparation of the intermediate $p\text{NPAcUMP}^-$ that was used for UV-Vis kinetic studies, was performed by dissolving UMPS in water and mixing with acetonitrile solution of bromoacetyl-*p*NP, prior to solvent removal and lyophilisation (figure 5.13). A stock solution (6 M) was made by dissolution of the intermediate, $p\text{NPAcUMPS}^-$, in water and this was divided in to aliquots that were stored in freezer until they were needed.



Scheme 5.13 Formation of the intermediate, $p\text{NPAcUMPS}^-$, used for kinetic studies

What differs from the NMR approach is that in this case an excess of the bromoacetyl agent would cause confusion in the interpretation of the kinetics. In these experiments, if an excess of nitrophenyl-bromoacetyl was used, *p*-nitrophenolate could derive from three processes (figure 5.14):

1. hydrolysis of the bromoacetyl-*p*NP
2. hydrolysis of the $p\text{NPAcUMPS}^-$
3. aminolysis of the $p\text{NPAcUMPS}^-$



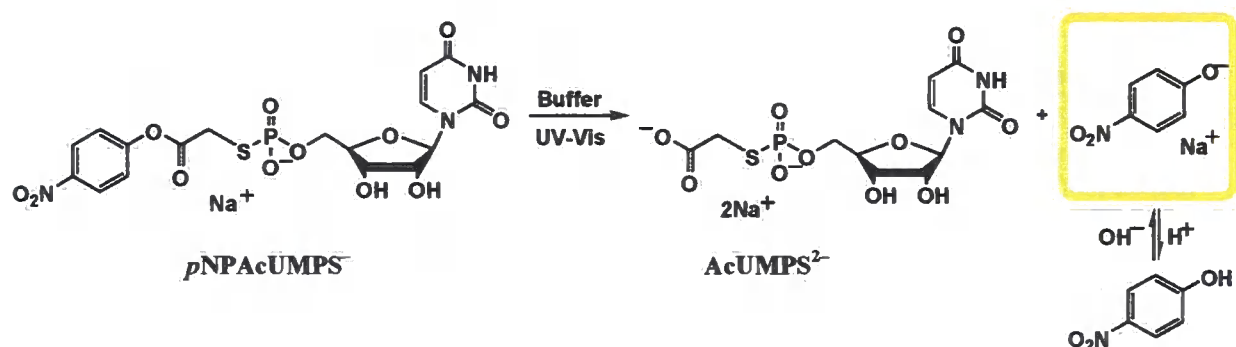
Scheme 5.14 Possible origin of the realised *p*-nitrophenol

Therefore, if an excess (20%) of UMPS over alkylation agent is applied, with the assumption, that all of the bromoacetyl-*p*-NP would be used up in the formation of the intermediate *p*NPAcUMPS⁻ and detected all *p*-nitrophenolate would derive from the hydrolysis or/and aminolysis reaction of *p*NPAcUMPS alone.

The maximum absorbance wavelength of *p*-nitrophenolate was determined *via* scanning the absorbance of an AcUMPS-*p*NP solution through the range from 200 nm to 800 nm over time. We found that $\lambda=402$ nm was the most convenient wavelength at which to monitor formation of *p*-nitrophenolate release.

5.9.4. UV-Vis hydrolysis studies: *p*-nitrophenol as the leaving group

As, we discussed in the previous section, examination of the rates of hydrolysis of the *p*NPAcUMPS intermediate can be followed by monitoring the rate of release of yellow *p*-nitrophenolate. UV-Vis experiments were performed by addition of *p*NPAcUMPS⁻ stock solution (6 M) into an appropriate buffer, generating a final concentration of the intermediate in the cuvette of 0.1 mM. Depending on the chosen buffer, time intervals between reading of absorbance varied (every 15s -fast kinetics or 1 min-slow kinetics) and, therefore, different periods of observations were applied (from 3 min to 15 hours). The concentration of hydrolysis product was reflected in the measured absorbance of the released *p*-nitrophenolate at 402 nm.



Scheme 5. 15 Intermediate hydrolysis in a range of buffers releasing side product and detectible *p*-nitrophenolate

The processes were considered to be first order (section 4.), owing to the large excesses of hydroxyl ions and water over the studied molecule. These absorbance readings were plotted as a function of time to give observed rate constant, k_o at various pH. The data showed the increasing absorbance of *p*NP and they were least square fitted into exponential function (eq.1):

$$A_t = A_0 + A_\infty \times (1 - e^{-k_o \times t}) \quad \text{eq.1}$$

where, A_t is the absorbance at the examined time, t

A_0 is the value of the starting absorbance ($t=0$),

A_∞ is the maximal absorbance change ($t=\infty$).

All plots of absorbance vs time had $R=0.99-0.9999$ (an example graph is shown below).

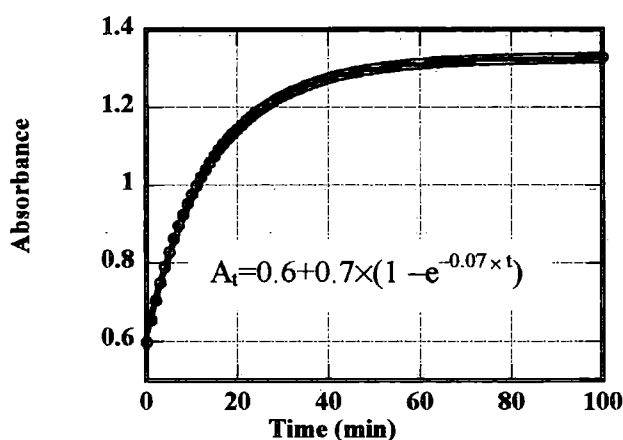


Figure 5. 14 A representative absorbance–time plot for the hydrolysis *p*NPAcUMPS⁻ followed by UV-Vis spectrometry

Checking for possible general base (B) catalysis was done by performing kinetics experiments over ranges of buffer concentrations (50, 100, 200, 300 and 500 mM). Observed rate constants, k_o plotted as functions of buffer concentrations were fitted into linear equation 8 showed

$$k_o = k_w + k_{OH} [OH^-] + k_{GB} [B] \quad \text{eq.8}^{136}$$

The intercept with the y-axis represents the sum of the water and hydroxide rate constant, k_w and k_{OH} respectively, where the gradient, if there is any, determines the general base rate constant, k_{GB} . In some of our experiments no gradient occurred (MES, Actetate), confirming the absence of general catalysis. In the case of HEPES and EPPS buffers, general base catalysis was detected ($k_{GB}=0.03-0.07 \text{ M}^{-1}\text{min}^{-1}$). As for CAPS buffer negative slope had occurred, what

was unexpected result and was left unexplained. However, we opted to perform the kinetic experiments to get the feeling about the rates of hydrolysis and aminolysis at different pH and use understood for the improvement of synthetic strategies. Therefore, kinetic study was simplified and the possible general base catalysis derived from the buffers was not considered.

5.9.5. pH hydrolysis rate profile: *p*-nitrophenol as the leaving group

The data extracted from the previously presented experiments, performed on the hydrolysis of *p*NPAcUMPS in a range of buffers with different pH (4.5-10.5) are presented in decreasing pH order in table 5.2

Table 5. 2 k_o and corresponding $\log k_o$ and $t_{1/2}$ for the *p*NP-intermediate hydrolysis in the range of pH

pH	k_o (min^{-1})	$\log k_o$	$t_{1/2}$ (min)	Buffer
10.5	4.59	0.66	0.15	CAPS
10.2	2.79	0.44	0.23	CAPS
9.8	0.68	-0.16	1	CHES
9.4	0.36	-0.44	2	CHES
9	0.18	-0.75	4	CHES
8.4	0.21	-0.68	3	EPPS
8	0.03	-1.52	23	EPPS
7.6	0.013	-1.90	55	HEPES
7.2	0.006	-2.17	102	HEPES
6.6	0.002	-2.64	302	MES
6.2	0.0017	-2.75	393	MES
5.8	0.001	-2.98	665	MES
5.2	0.0018	-2.73	372	ACET
4.8	0.0021	-2.68	331	ACET
4.6	0.0018	-2.74	384	ACET

Through manipulation of the acquired data from the above table and with the help of equation for the observed hydrolysis rate:

$$k_o = k_w + k_{OH} [OH^-] \quad \text{eq.2}^{136}$$

we could plot and perform a least square fit k_o -pH that was then used for the design of the log k_o -pH plot that is most commonly used as the pH profile presentation (figure 5.14). The data that make up the plateau were fitted separately, with the goal to increase the accuracy. k_o , as a constant that defines the rate of the water catalysed process, was assigned to be the average value of the rate constants observed for pH range from 4.6 to 6.6. The residual data was, then, fitted and combined to build the pH hydrolysis profile shown below.

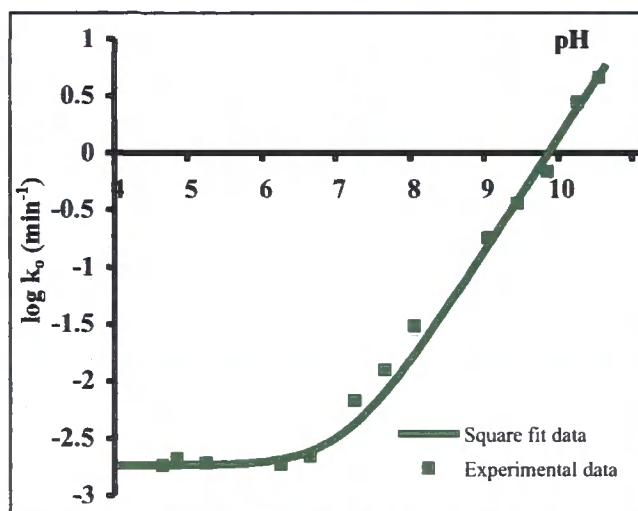


Figure 5. 15 $p\text{NPAcUMPS}^-$ hydrolysis pH profile for the $k_o = 0.0018 + 15058 [OH^-]$

The plateau region was found to range from pH 4.5 to 6.6, with the pH-independent half-life being around 6 h. As k_o has a value 0.0018 min^{-1} , the water reaction is quite slow. EPPS and HEPES buffers, with pH ranging from 7.1 to 8 showed some signs of general base catalysis thus these points lie a small way above the fitted curve. As the concentration of hydroxyl ions increases rapidly, the effect on rate of hydrolysis increases rapidly decreasing the half-life of the intermediate to about 9 seconds at pH 10.5. The essential section of the curve, for the successful desired aminolysis reaction, is the one that encourages an amine to perform nucleophilic attack on the intermediate $p\text{NPAcUMPS}$ with priority over hydrolysis. This requires that the amine is not protonated, but the pH is not too high. In order to meet this

window of opportunity, we need to perform studies that involve the aminolysis process as well, and analyse it separately from the hydrolysis that occurs in parallel.

5.9.6. UV-Vis aminolysis studies: *p*-nitrophenol as the leaving group

To assess the ability of amine nucleophilic attack on the carbonyl group of the *p*NPAcUMPS intermediate in comparison to the hydrolysis processes, investigations involving D-glucosamine as the amine were performed. As an example of a *N*-nucleophile, D-glucosamine was chosen owing to its price, availability in the laboratory and solubility in water, fitting nicely into the experimental conditions that were established. The pK_a of D-glucosamine is 7.75. In this study, only 500 mM buffers were used to speed up and simplify the study. A 500-fold excess of D-glucosamine over examined intermediate was used in the experiments. Several other concentrations were previously tested (20, 50 and 100 fold of D-glucosamine towards the *p*-nitrophenol intermediate molecule) and the 500-fold excess was shown, unsurprisingly, to give the fastest rates of *p*-nitrophenolate formation.

The assays were managed in the same way as for the studies of the hydrolysis process, with the addition of amine into the buffered intermediate solution. After the addition of *p*NPAcUMPS stock solution into the amine dissolved in buffer and mixing, absorbance ($\lambda=402$ nm) was measured over time. The same principle of manipulating data applies for the aminolysis experiments as described for hydrolysis and the resulting parameters and pH profile are shown in the table and figure below, respectively.

Table 5. 3 Total reaction data (k_T), hydrolysis plus aminolysis: pNPAcUMPS⁻

pH	k_T (min⁻¹)	log k_T	$t_{1/2}$ (min)	Buffer
10.2	0.65	-0.18	1.06	CAPS
9.8	1.50	0.17	0.46	CHES
9.4	0.53	-0.27	1.31	CHES
9	0.31	-0.50	2.22	CHES
8.4	0.16	-0.79	4.34	EPPS
8	0.17	-0.77	4.13	EPPS
7.6	0.12	-0.91	5.68	HEPES
7.2	0.07	-1.15	9.87	HEPES
6.6	0.02	-1.71	35.73	MES
6.2	0.006	-2.19	109.03	MES
5.8	0.002	-2.58	265.20	MES
5.2	0.0005	-3.31	1434.19	ACET

The overall process happening in this assay includes both effects of the hydroxyl ion and amine attacking the intermediate. Therefore, the rate of the detected *p*-nitrophenol release depends on both rates of hydrolysis and aminolysis (scheme 5.16). An equation for the observed total reaction rate constant and the corresponding least square fit curve is:

$$k_T = k_o + k_N = k_W + k_{OH} [OH^-] + k_{NH_2} \times [RNH_2] K_a / ([H^+] + K_a) \quad \text{eq.3}$$

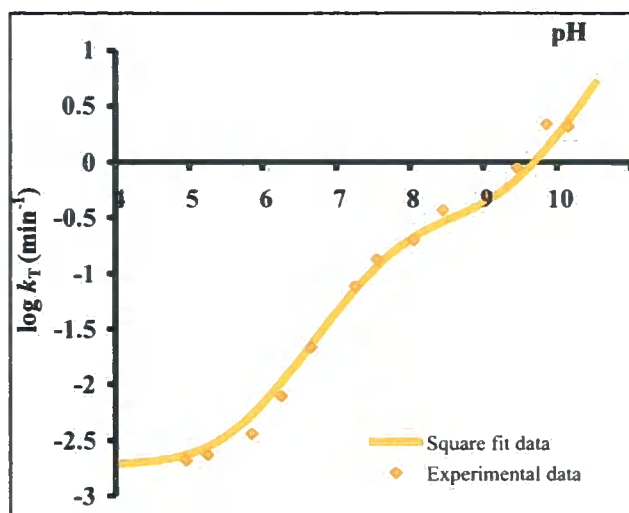
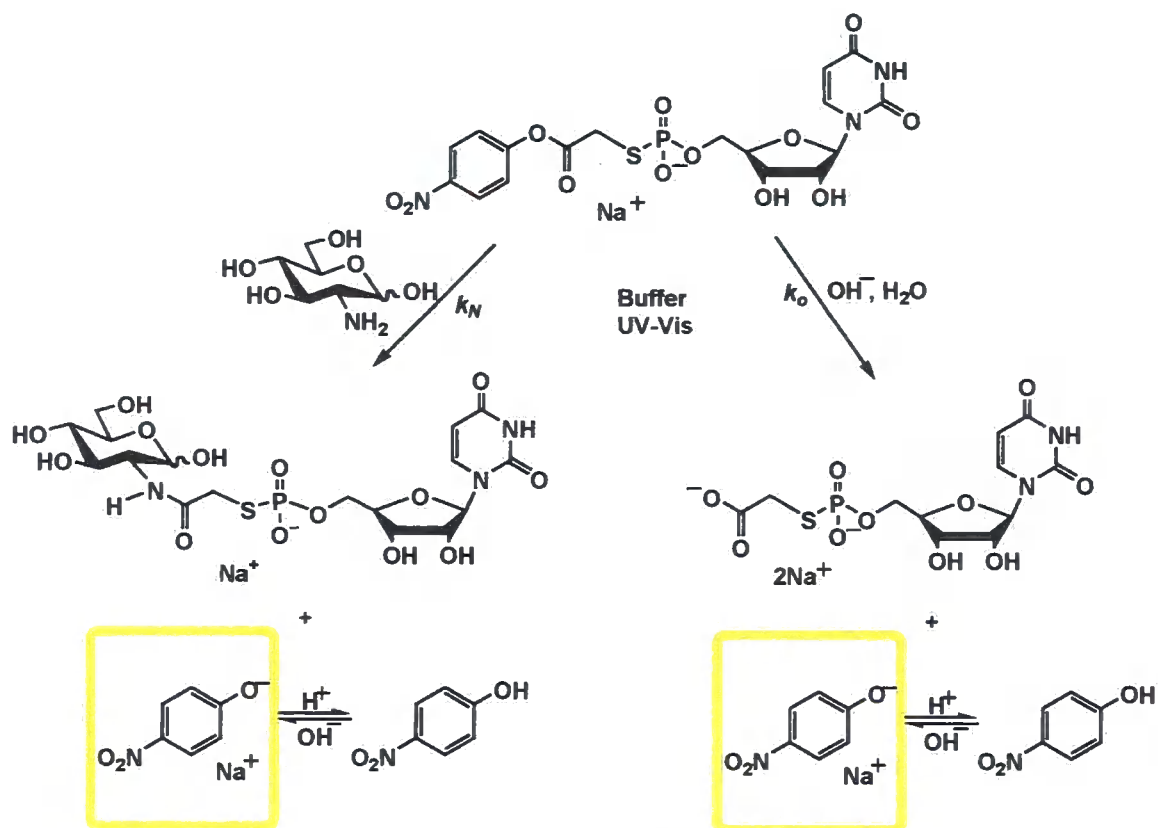


Figure 5. 16 pH rate profile for overall *p*-NPacUMPS⁻ aminolysis in the presence of hydrolysis



Scheme 5. 16 The total process occurring during aminolysis of intermediate in the event of hydrolysis competing process

In order to enable evaluation of the aminolysis rate constants only, observed hydrolysis rate constants (table 5.3) were subtracted from the observed total reaction rate constants (table 5.2) for the corresponding pH. The resulting values, assigned to be the observed aminolysis rate constants only, are presented in the table below.

Table 5. 4 Calculated experimental details for the UV/Vis studies on pNPAcUMPS⁻: aminolysis only

pH	k_{NH_2} (min⁻¹)	log k_{NH_2}	$t_{1/2}$ (min)	Buffer
10.2	0.65	-0.18	1.06	CAPS
9.8	1.50	0.17	0.46	CHES
9.4	0.53	-0.27	1.31	CHES
9	0.31	-0.50	2.22	CHES
8.4	0.16	-0.79	4.34	EPPS
8	0.17	-0.77	4.13	EPPS
7.6	0.12	-0.91	5.68	HEPES
7.2	0.07	-1.15	9.87	HEPES
6.6	0.02	-1.71	35.73	MES
6.2	0.006	-2.19	109.03	MES
5.8	0.002	-2.58	265.20	MES
5.2	0.0005	-3.31	1434.19	ACET

The calculated observed rate constants were then fitted using equation

$$k_N = k_{\text{NH}_2} \times [\text{RNH}_2]_t K_a / ([\text{H}^+] + K_a) \quad \text{eq.4}$$

and the corresponding log k_{NH_2} -pH plot is shown below.

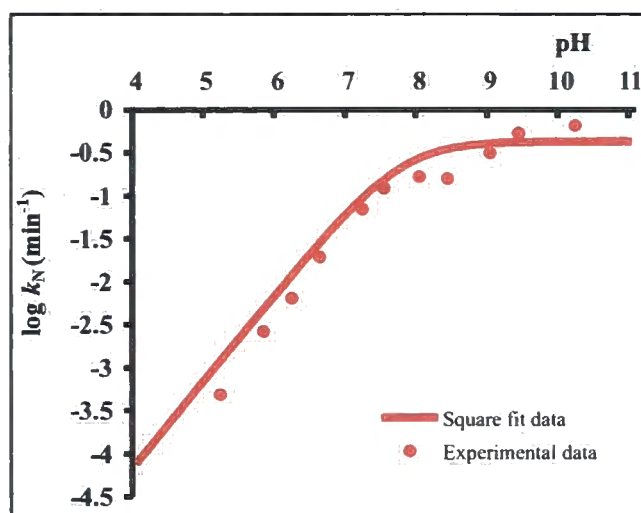


Figure 5. 17 pH profile of *p*-NPAcUMPS⁻ aminolysis where resulting equation is $k_N = 8.55 \times 0.5 K_a / ([H^+] + K_a)$, with pK_a of GlcNH_2 is 7.75

Owing to the pK_a of the applied nucleophile (7.75), the rate of the aminolysis process was increasing rapidly as the pH of the media rose, up to the pH point close to amine's pK_a value. Soon after the maximal rate of aminolysis was achieved, where all amine was in the base form and the reaction became pH independent.

5.9.7. Selectivity: *p*-nitrophenol as the leaving group

When competing reactions occur in the system that is studied, a good way to express the ratio between the desired and the side reactions is through selectivity, often referred as the 'window of opportunity' (introduced in the section 1.4). In our case, it refers to the fraction of the intermediate, *p*-NPAcUMPS that has been converted from ester to the desired amide product: Selectivity = desired reaction/overall process

The equation that defines this term is shown below:

$$f = \frac{k_N}{k_T} = \frac{k_{\text{NH}_2} [\text{RNH}_2] K_a / ([H^+] + K_a)}{k_w + k_{\text{OH}^-} [\text{OH}^-] + k_{\text{NH}_2} [\text{Nuc}_T] K_a / ([H^+] + K_a)} \quad \text{eq.5}$$

and it was used to present the selectivity in a graphical form (figure 5.18). Along with the selectivity, the graph shows how hydrolysis and aminolysis of the intermediate are changing upon change of pH.

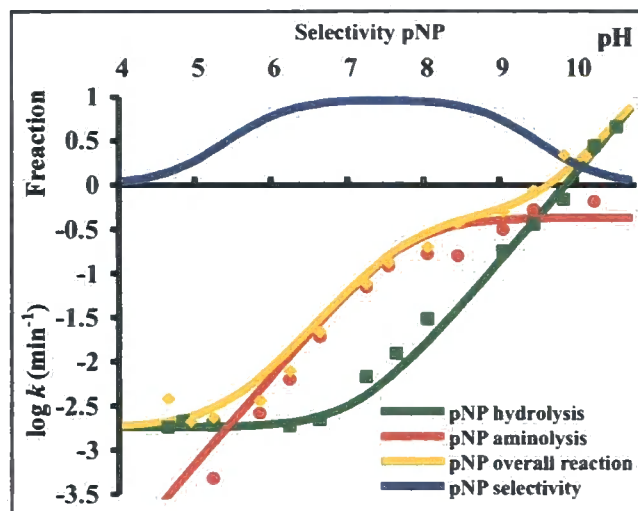


Figure 5. 18 The overall plot of hydrolysis vs aminolysis process, with the selectivity curve for the aminolysis over hydrolysis process of *p*-NPAcUMPS⁻. GlcNH₂ in the 500-fold excess

The efficacy of the amine as nucleophile, over hydrolysis, was found to be the greatest when pH of the reaction media was between 7.5 and 8.5. This was due to the balance between protonation of amine at lower pH and fast hydrolysis of the *p*-nitrophenol intermediate in very basic conditions. The inherent limitation of this selectivity is the narrow plateau. Therefore, the number of amines that can be used under these reaction conditions is restricted by the pK_a their conjugate acid being in the range that selectivity allows.

With the goal to extend the selectivity window in the process of aminolysis of the intermediate ester, a new set of experiments using *m*-nitrophenol, with pK_a more than one unit higher (8.3) than *p*-nitrophenol, will be investigated. Hopefully, with the reduction in hydrolysis of the intermediate, the amine should overtake the hydrolysis as the dominant nucleophilic substitution at the carbonyl group.

5.9.8. UV-Vis hydrolysis studies: *m*-nitrophenol as the leaving group

In the following sections, we will outline the differences that application of *m*-nitrophenol brought in comparison to *p*-nitrophenol.

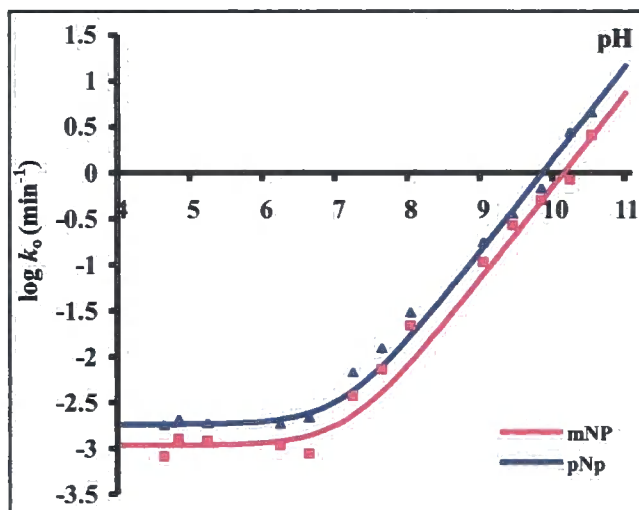


Figure 5. 19 pH hydrolysis rate profile: *m*-NPAcUMPS⁻

$$p\text{-nitrophenol (}pK_a=7.1\text{): } k_o = 0.0018 + 15058 [\text{OH}^-]$$

$$m\text{-nitrophenol (}pK_a=8.3\text{): } k_o = 0.0011 + 7623 [\text{OH}^-]$$

Hydrolysis of the intermediate, *m*NPAcUMPS, follows the same pattern as in the case of the *p*-nitrophenol intermediate, with the difference being slightly slower rates of the release of *m*-nitrophenolate than *p*-nitrophenolate. We also performed us to perform aminolysis studies, using again D-glucosamine in order to make the study comparable with previously explored *p*-nitrophenol.

5.9.9. UV-Vis aminolysis studies: *m*-nitrophenol as the leaving group

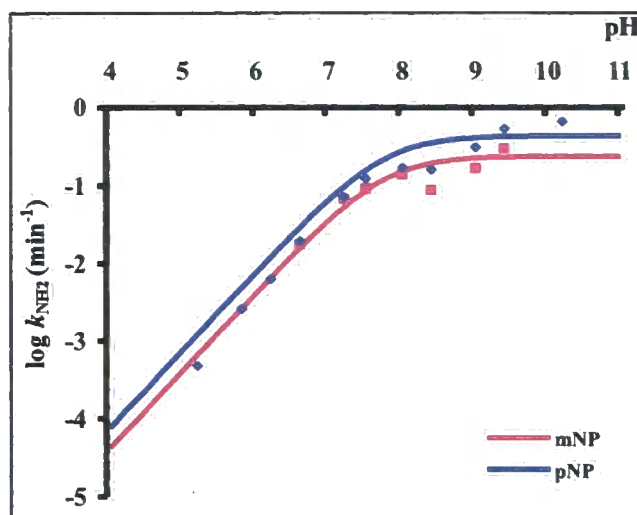


Figure 5. 20 pH aminolysis rate profile: *m*-NPacUMPS⁻

p-nitrophenol ($\text{p}K_{\text{a}}=7.1$): $k_{\text{NH}_2}= 8.55 \times 0.5 K_{\text{a}} / ([\text{H}^+] + K_{\text{a}})$, where $\text{p}K_{\text{a}}$ of GlcNH_2 is 7.75

m-nitrophenol ($\text{p}K_{\text{a}}=8.3$): $k_{\text{NH}_2}= 4.7 \times 0.5 K_{\text{a}} / ([\text{H}^+] + K_{\text{a}})$

The above aminolysis $\log k_{\text{NH}_2}$ -pH plot suggest that the rate of amine substitution decreased when *m*-nitrophenol was used as the leaving group of the intermediate, *m*NPacUMPS. With one $\text{p}K_{\text{a}}$ unit higher for *m*-nitrophenol, we hoped for an improvement in the selectivity in amide formation.

5.9.10. Selectivity: *p*-nitrophenol vs *m*-nitrophenol as the leaving groups

We have used observed rate constants for hydrolysis and aminolysis of both both intermediates containing *p*-nitrophenol vs *m*-nitrophenol to estimate the reaction outcome under synthetic conditions and the resulting selectivity plot is shown below.

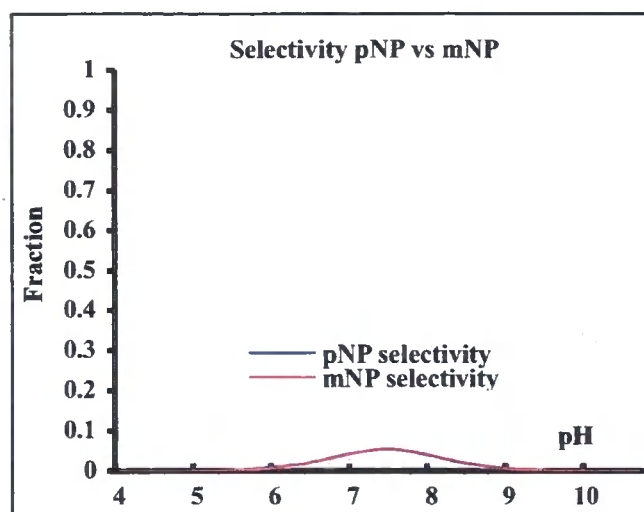


Figure 5. 21 Calculated selectivity curves using aminolysis and hydrolysis rate constants, for *p*-NPAcUMPS⁻ and *m*-NPAcUMPS⁻, in the synthetic conditions where amine was used in the 1.2-fold excess

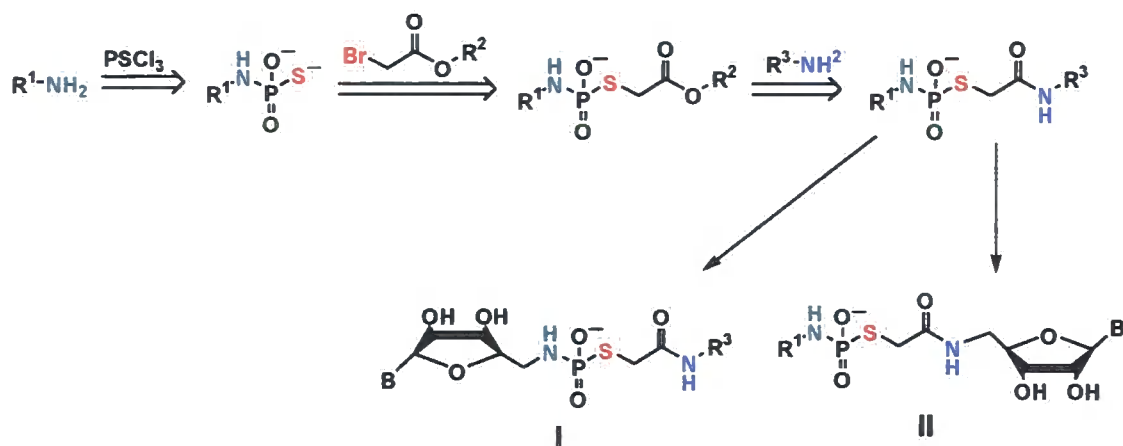
These investigations did not give us satisfactory results, owing to unsuccessful improvement of the Dipartite reaction conditions *via* the use of the *m*-NP leaving group. As can be seen from the above graph, our system does not offer good selectivity for amine attack towards activated ester. Ester aminolyses have been extensively studied on different systems such as substituted aryl acetates and aryl carbonates.^{137, 138} However, our system contains a thiophosphoryl function in the α -position near to the carbonyl centre that potentially interacts with the zwitterionic tetrahedral intermediate of the ester aminolysis reaction thus a direct comparison with these literature systems is not possible. In addition the difference in the selectivity plateau between, *p*- and *m*-nitrophenol leaving groups is minimal, indeed was minimal, almost non-existent, suggesting that amine attack the rate determining step. However, more mechanistic investigations are needed on these bromoacetyl systems in order to get a clearer picture of the effect that the thiophosphoryl group brings to these systems.

As we have recognised the possibility for combining our studies on the thiophosphoramidate system and the bromoacetyl strategy, the next few sections will describe the preliminary experiments that uses this approach with the goal to expand the possibilities for the synthesis of

new NDP-sugar analogues and help avoiding time-consuming procedures of thiophosphorylation of alcohols (i.e. synthesis of UMPS).

5.10. Exploring the strategy of combining bromoacetyl and thiophosphoramidates system

The success of our aqueous method for the introduction of a thiophosphoryl group onto an amine moiety (Chapter 2.), offered us an array of possibilities in terms of applications. Amines, lipophilic or water-soluble, were easily thiophosphorylated with high conversions that could be further *S*-alkylated effectively. The synthesis of UMPS was a much more demanding procedure, requiring anion exchange purification and it generated poor yields. On the other side, preparation of the 5'-amino-5'-deoxyguanosine, involved few steps and but no chromatographic purifications (section 3.2.4). Bromoacetyl system opened up a new way of introducing different amines into the thiophosphoryl 'Click' chemistry again using available amines and we propose a new strategy that combines both the thiophosphoramidate and bromoacetyl approaches.

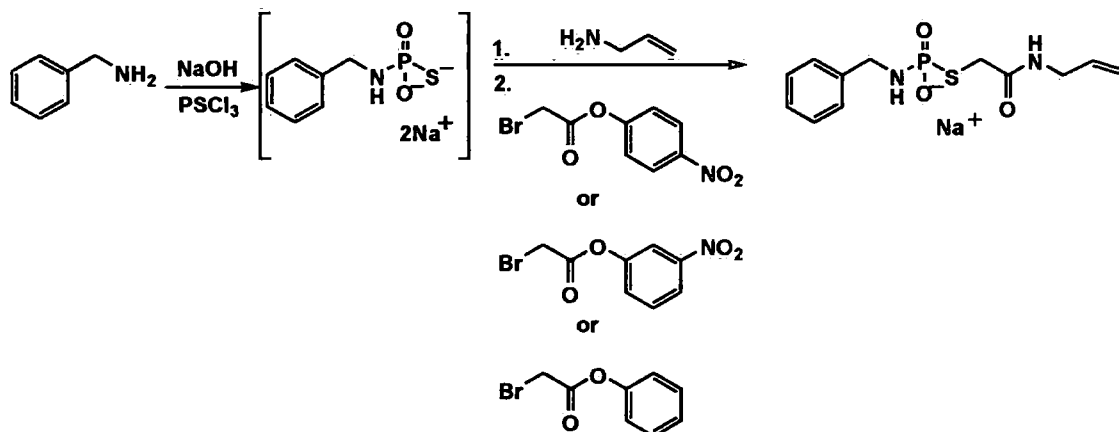


Scheme 5. 17 The strategy of the bromoacetyl-thiophosphoramidate systems, where **B**=adenozyl, uracyl, gunanosyl, and **R^{1,3}**=any aliphatic group, **OR²**-good leaving group

Nucleoside amines could be situated on either end of the thiophosphoramidate-acetyl feature, allowing for the introduction of the commercially available amines on the opposite end. Considering the time frame, we opted to perform preliminary experiments on just one version of the structures **II**, where a nucleoside was involved in formation of the amide bond. In order

to establish the reaction conditions and to set up the method, allylamine and benzylamine, were used on both ends in the first instance.

5.10.1. Bromoacetyl-thiophosphoramidate system: allylamine



Scheme 5. 18 Bromoacetyl agent in the thiophosphoramidate chemistry: allylamine

The reaction was performed was very similar to the already established aqueous thiophosphorylation method (Chapter 2.). Benzylamine (1 Eq) was thiophosphorylated using the aqueous method (section 2.14), followed by addition of allylamine. Allylamine was used in the slight excess in order to ensure complete reaction and could be easily removed *via* extraction. A phenylate ester of bromoacetic acid was, then, added (table 5.5) and the mixture was vigorously stirred for 15 minutes. Both *m*- and *p*-nitrophenol esters were tested with the introduction of phenol intermediate. The reaction probably proceeds through intermediates shown below as *S*-alkylations were probably rapid.

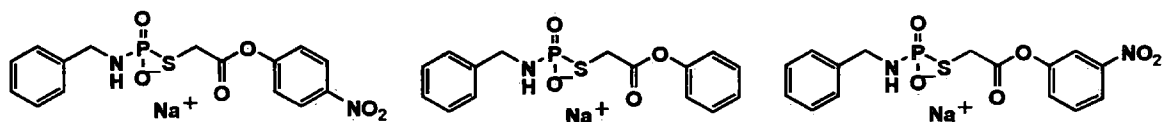
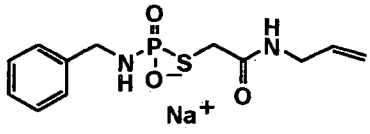
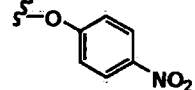
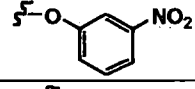
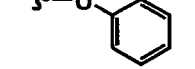


Figure 5. 22 Intermediates in bromoacetyl-thiophosphoramidate system

Since the phenolates released in the aminolysis reaction, are soluble in water, extraction of the released leaving group can be performed after protonation of the phenoxide group. Therefore, the pH of the mixture was adjusted using diluted hydrochloric acid according to table 5.5,

depending on the pK_a of the leaving group, followed by ethyl acetate extraction. Then, pH was adjusted back to pH 9 and the extraction was repeated using chloroform to remove unreacted amines, followed by lyophilisation of the aqueous solution of product.

Table 5. 5 The experimental details of the bromoacetyl-thiophosphoroamidate system

Crude product	Bromoacetyl-P	pK_a	pH	Purity (%)
		7.1	7	91 ^a , 69 ^b
		8.3	8	92 ^a , 72 ^b
		9.9	10	80 ^a , 69 ^b

The reaction has given satisfactory conversions. With the highest pK_a , we were hoping that intermediate with phenol as the leaving group would be the most selective and, therefore, the reaction would proceed with the maximal relative amount of amide product. Impurities in the sample were alkylated inorganic thiophosphates (ester **161** and acid **162** form) and some of the product that contained benzylamine on both ends **163**.

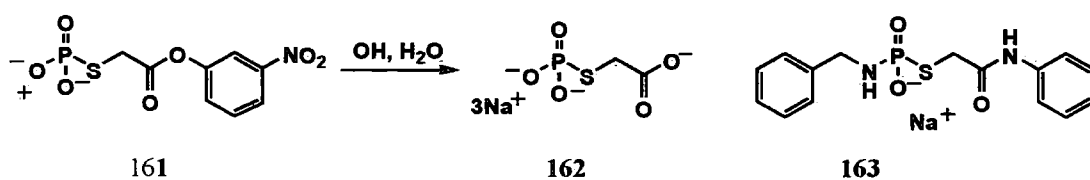
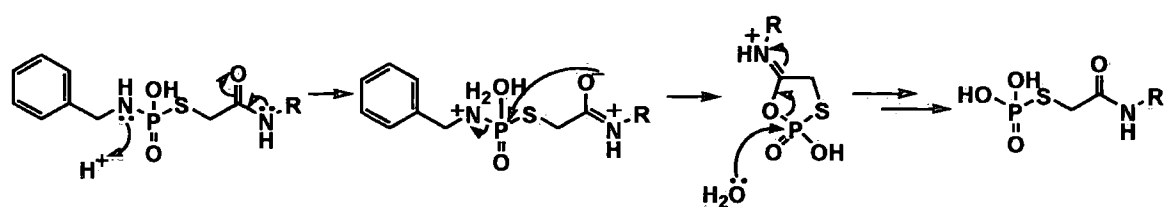


Figure 5. 23 Impurities in the bromoacetyl-thiophosphoroamidate system

These products showed signs of instability if kept in solution at neutral pH of mildly basic media. Protonation of thiophosphoroamidate nitrogen, probably during extraction of the phenolates induced the hydrolysis of the P-N bond and the release of the free benzylamine. In addition, there is potential for an intramolecular process with the acetyl moiety, which may have increased the instability. The degradation, we believe, goes through the pathways shown in the scheme below.

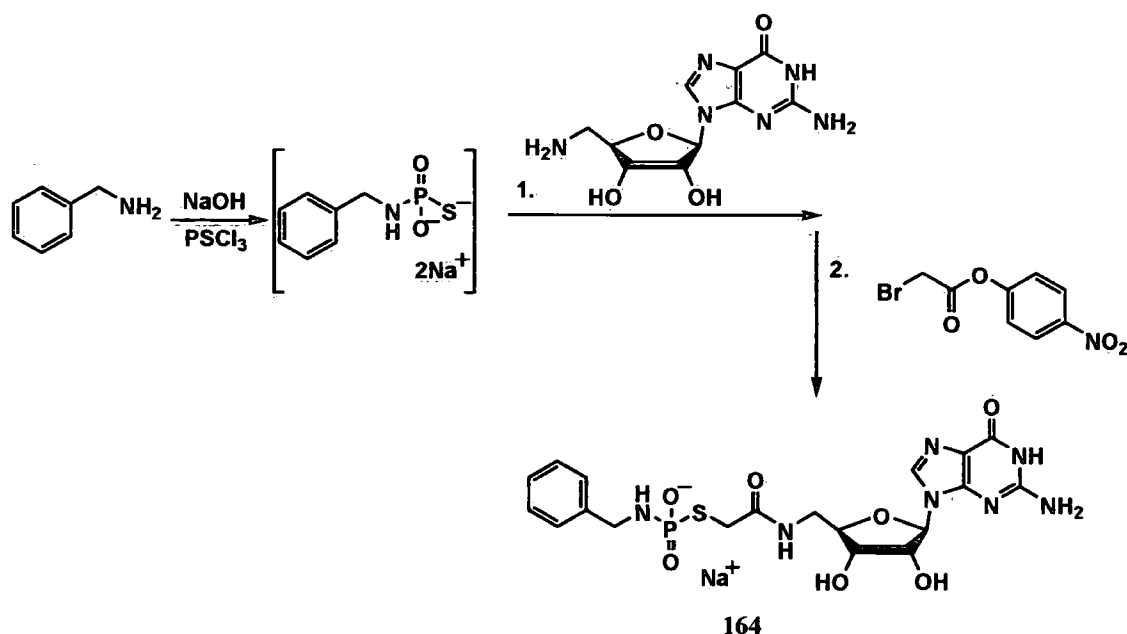


Scheme 5. 19 The proposed mechanism for the product 4 degradation. R=allyl, guanosyl substituent

The success with commercially available amines encouraged us to test more challenging 5'-amine-5'-deoxyguanosine applying *p*-nitrophenol intermediate. The results are presented in the following section.

5.10.2. Bromoacetyl-thiophosphoramidate system: 5'-amino-5'-guanosine

5'-Amino-5'-guanosine was introduced onto the bromoacetyl-thiophosphoramidate moiety (figure 5.19) as described for allylamine (section 5.4.3).



Scheme 5. 20 Bromoacetyl agent in the thiophosphoramidate chemistry: guanosine amine

The reaction proceeds through the formation of the *p*NP-intermediate (figure 5.) prior to amine substitution and *p*-nitrophenolate release. *Via* ^{31}P NMR spectrometry a moderate conversion to product 164 (around 67%) was seen, with the appearance of several impurities (figure 5.). In

The remaining 9% of the impurities were spread across the chromatogram and were not examined. The benzyl amide product, **164a**, formed probably owing to the presence of free benzylamine in the reaction mixture deriving from incomplete thiophosphorylation or P-N hydrolysis of the thiophosphoroamidate products.

Guanosine derivative **164** showed instability characteristics as allylamide, which relates to an intramolecular reaction with the introduced carbonyl moiety, since the stability of previously studied thiophosphoroamides (excluding quinoline system) was very high (section 2.5.3). The mechanism follows a similar path to that presented in the scheme 5.18.

For complete characterisation, guanosine product, **164** was cation exchanged and analysis of the sodium salt suggested the presence of benzyl amide product, **164a**, and inorganic phosphate, which had the same retention time on both anion and cation chromatography. In addition, thiophosphoroamidate hydrolysis continued during the cation exchange. A final estimation of the purity is presented in the table below.

Table 5. 7 Content of the guanosine derivative 164 after anion and cation exchange chromatography (%)

164	164a	164b	Guanosine	Pi
80 ^a , 68 ^b	9 ^a , 15 ^b	7 ^a , 9 ^b	8 ^b	4 ^a

^aDetermined by ³¹P NMR spectroscopy. ^bDetermined by ¹H NMR spectroscopy.

5.11. Conclusion and future work involving bromoacetyl strategy

In the Bromoacetyl system that consists of linking three components, namely, uridine 5'-O-monophosphothioate to the D-glucosamine with the help of an activated bromoacetyl ester-bridge, we applied Tripartite and Dipartite approaches. In the Tripartite HOBt and HNS esters were employed and it was noticed that a considerable portion of hydrolysis product occurred, decreasing the formation of the desired amide product. Both HOBt and NHS are good leaving groups and it was not surprising that their high reactivity induced low selectivity of their acetate esters in the choice between hydroxide ion and amine. Then, we moved to phenol structures

that are still good leaving groups, however, we hoped for better selectivity. Additionally *m*- and *p*-nitrophenols are yellow coloured in basic media, which allowed for a simple UV-Vis spectrophotometric kinetic assay for monitoring hydrolysis and aminolysis. When NHS was used as the leaving group in the ^{31}P NMR spectroscopic hydrolysis study of intermediate, NHSAcUMPS⁻, a number of issues were encountered and the studies were abandoned.

In the kinetic studies, where we compared the effect of using *p*-nitrophenol and *m*-nitrophenol as leaving groups in the aminolysis of the intermediate, NHSAcUMPS⁻ through the pH range, and almost no difference in reactivity was noticed. This suggested that in this system the slow step was nucleophilic attack of amine to the carbonyl group in the activated ester and the expulsion of the aryloxy group was faster. A study involving a leaving group with even higher $\text{p}K_{\text{a}}$, such as phenol with $\text{p}K_{\text{a}}$ 9.95, should be pursued along with further kinetic studies. Unfortunately, due to non-existing Vis chromophore new detection approach is required. Some preliminary studies were performed involving phenol and along with proposal for the new approach involving phenol intermediate built with thiophosphoramidate feature were presented in the future work section. This survey offers, as well, the possibility of creating a plot where we can outline the effect of leaving groups used in our optimisation studies of Dipartate 'Click' reaction.

Potentially, the amine that we were using as nucleophile was not suitable for our system. Because it was cheap, commercially available and water-soluble, D-glucosamine seemed like a reasonable choice. The $\text{p}K_{\text{a}}$ of this amine fitted well considering the pH hydrolysis rate profile, since amines with much higher $\text{p}K_{\text{a}}$ would probably be inactivated by protonation. However, due to the presence of the neighbouring OH groups in this molecule, there is the possibility of intramolecular side reactions could be interfering with the desired amidation of esters. Therefore, it was concluded that D-glucosamine may have been too challenging a structure for methodology establishment and, therefore, will be substituted with simpler systems in future investigations.

We have also demonstrated that a combination of the thiophosphoramidate and bromoacetyl systems gives satisfactory conversions. With easily prepared thiophosphoramidates, the thiophosphoryl moiety was readily available for the alkylation by a bromoacetyl ester. Then, with the exposure of formed intermediate to an amine, conversions as high as 92% were seen by ^{31}P NMR spectroscopy. As introduced in the section 5.10, another strategy in thiophosphoramidate-bromoacetyl system that involves thiophosphorylation of nucleoside amines followed by the bromoalkylation may offer better performance as lipophilic amines used in excess could improve the kinetics of the aminolysis process and be easily removed via extraction (I, scheme 5.). The occurred instability of the generated thiophosphoramidate-acetamide product could be avoided with the application of the higher pH during a more controlled extraction where phenol-leaving groups are removed.

6.0 Conclusions and future work after thesis

We hope that this thesis was a good guide through the path of the establishment of a novel, thiophosphoryl 'Click' chemistry that branched into two directions, Thiophosphoramidate and Bromoacetyl system, and finally crossed each other's achievements in the combined Thiophosphoramidate-Bromoacetyl strategy. Owing to the conclusions and proposed future investigations being presented following each chapter, here, we will briefly outline what possibilities these systems provide.

Aqueous thiophosphorylation offers quick, simple and widely applicable introduction of thiophosphoryl moiety to amines. The resulting thiophosphoramidates were quite stable through basic pH region, which were the most optimal conditions for the performed alkylation. A number of different amines and alkylation agents were employed in the founding of the one-pot Tripartite method that enables production of alkylated thiophosphoramidates in the 'one pot' manner. This is a practical tactic that would ideally be used for the direct synthesis in the microtitre plates, where generated products could be subjected to the activity tests against target enzymes, e.g. glycosyltransferases. With this in mind, we opted to investigate on the formation of nucleoside diphosphate analogues that are biologically important features using the principles of the thiophosphoramidate system that we have already successfully applied in the production of the monothiophosphorylated 5'-amino-5'-deoxyguanosine and 5'-amino-5'-deoxyadenosine. In addition, 5'-iodo-5'-deoxyguanosine was introduced as an alkylating agent expanding the possibilities of involvement of nucleoside derivatives in the thiophosphoramidate system. Initial investigations on the application of this system onto synthesis of potential antileishmanial agents that are quinoline-based suggested the promising but inconsistent results. Therefore, this is the area that as well deserves the attention in the future research.

Second thiophosphoryl system uses bromoacetyl esters that were activated by ranging leaving groups, from very fast reacting HOBt and NHS to phenols that presented slower rates of both hydrolysis and aminolysis of studied esters. This was investigated with the goal to efficiently amidate esters that were made by alkylation of the uridine 5'-O-monothiophosphoramidates

using bromoacetyl esters. Hydrolysis and aminolysis studies potentially suggested the rate determining step to be nucleophilic attack of amine towards carbonyl ester electrophile, as with the introduction of the slower leaving group *m*-nitrophenol made almost no difference in the total process aminolysis over hydrolyses in comparison to more acidic *p*-nitrophenol. The investigations on the application of different nucleophile amines rather than D-glucosamine that seemed as an inadequate model for the optimisation studies with a number of disadvantages potentially deriving from surrounding groups that possibly lower the nucleophilicity. As in the kinetic studies of hydrolyses and aminolysis of bromoacetyl system, we have investigated on two leaving groups, *m*-nitrophenol and *p*-nitrophenol, and a need for another few points corresponding to leaving groups that would maybe offer better selectivity by slower reactions, such as phenols, will be involved in the future work.

Finally, preliminary experiments on the combining practicality of the thiophosphorylation of amines, avoiding time-consuming and less effective preparations of thiophosphates, and the variation that effective alkylation agents, bromoacetyl esters offer with interaction with amines, presented satisfactory results. Allylamine and 5'-amino-5'-guanosine were employed for the amide bond formation, while all phenols presented in this chapter were involved as the leaving groups of the bromoacetyl alkylated benzylamine thiophosphoramidate.

We believe that all of these three systems have just been touched on the surface and further investigations would hopefully be very fruitful, both in the synthetic field and consequentially in the biological systems.

7.0 Experimental section

7.1. General Methods

Reagents

Chemical reagents were purchased from Aldrich, Acros, Fisher, Apollo Scientific Ltd, Goss Scientific Instruments and Amersham Biosciences, and were usually used as supplied. Otherwise, starting materials were purified prior to use as described below then used immediately.

Uridine was ground using a mortar and pestle, then heated for 1 h at 60 °C under vacuum, using a Büchi B-585 glass oven with phosphorus pentoxide as drying agent.

Molecular sieves were dried at 60 °C in the Büchi B-585 glass oven under vacuum with phosphorus pentoxide as drying agent.

Triethylphosphate was stirred over calcium hydride then distilled by heating slowly to 140 °C under vacuum.

Thiophosphorylchloride was distilled under an atmosphere of nitrogen.

2,6-Dimethyl pyridine was dried over potassium hydroxide pellets under nitrogen stored overnight in the refrigerator.

Triethylamine, used for chromatography, was distilled under a nitrogen atmosphere.

Pyridine was refluxed over calcium hydride in a still for at least 3 h before being extracted for use.

Dry dichloromethane and tetrahydrofuran were purchased from the solvent service, Chemistry Department, Durham University (Pure Solv MD Solvent Purification System 400, Inovative technology).

Equipment

Solvents were removed under reduced pressure using a Büchi Rotavapor R 110.

Centrifugation was performed on a Beckman Coulter Allegra[™] X22R centrifuge, 4500 rpm.

pH measurements were made on a calibrated (4.00 ± 0.1 , 7.02 ± 0.1 , 10.04 ± 0.1) HANNA 210 Microprocessor pH meter at 22 °C using one of two electrodes: for larger (Hanna combination electrode) and smaller (Orion micro PerpHecT ROSS combination electrode) volumes.

Lyophilisation was carried out on a Jouan high vacuum system.

UV-VIS spectrometry

All measurements were performed on a Varian 50 Cary Bio spectrometer, thermostated at 25 °C.

Chromatography

Anion exchange chromatography was performed on DEAE Sepharose® fast flow columns of the following dimensions using the flow rates described below:

500 mL, 30 × 5 cm, 1 g load, 30mL/min

50 mL, 10 × 3 cm, 200 mg load, 3 mL/min.

The mobile phase for anion exchange chromatography was prepared by vigorously stirring freshly distilled triethylamine (140.5 mL, 0.98 mol) made up to 1 L with water whilst bubbling through CO₂. This produced a 1 M triethylammonium bicarbonate (TEAB) solution pH 7.6. Prior to every purification run, the column was equilibrated by flushing with two column volumes of 50 mM TEAB buffer.

Cation exchange chromatography was carried out on a column packed with Dowex® 50W×2, 200-400 (50 mL, 30 × 2 cm, 200 mg load, 3 mL/min). The column was prepared for the run *via* regeneration with two column volumes of aqueous sodium hydroxide (0.1 M) and then washed with water. Water was used as the mobile phase for the actual exchange process.

All aqueous chromatography was run with the help of an Äkta Prime Plus FPLC instrument, from Amersham Biosciences supported with automated sampler, pump, UV detector (set at 280 nm for all runs described in the experimental section below) and a PC running Primeview 5.0 and Evaluation software.

Infrared spectroscopy

Infra-red absorption spectra were recorded on a Perkin-Elmer 1600 Series FT-IR spectrometer, using KBr discs.

NMR spectroscopy

^1H , ^{13}C , ^{31}P NMR spectra were recorded on the following spectrometers, operating at the quoted frequencies:

Varian Mercury 200 MHz (^1H 199.991 MHz; ^{31}P 80.957 MHz)

Varian Mercury 400 MHz (^1H 399.958 MHz; ^{31}P 161.906 MHz)

Varian Mercury 500 MHz (^1H 499.768 MHz; ^{13}C 125.666 MHz)

Varian Mercury 700 MHz (^1H 699.737 MHz; ^{31}P 283.257 MHz; ^{13}C 175.948 MHz)

Bruker 400 MHz (^1H 400.130 MHz; ^{31}P 161.943 MHz; ^{13}C 100.612 MHz)

^1H chemical shifts (δ) are reported as parts per million (ppm) upfield relative to tetramethylsilane ($\delta = 0.00$ ppm) and are referenced to the residual protic solvent (HOD, $\delta = 4.79$ ppm, CHD_2Cl_3 , $\delta = 7.26$ ppm and $(\text{CHD}_2)\text{SOCD}_3$, $\delta = 2.50$ ppm).

^{31}P NMR spectra were recorded both in proton decoupled and coupled modes where the multiplicities of the signals are presented along with the coupling constant J (Hz). In optimisation experiments, most of the ^{31}P spectra were collected in a mixed $\text{H}_2\text{O}/\text{THF}$ solvent system without locking or shimming.

^{19}F NMR spectra were proton coupled and the multiplicity of each is presented along with the coupling constant $^nJ_{\text{H-F}}$, expressed in Hz.

^{13}C NMR spectra were proton decoupled and unless stated otherwise, the multiplicity was singlet.

Signal assignments are presented in the form of RSC (Royal Society of Chemistry) reports: chemical shift (ppm) (number of nuclei, multiplicity of signal, coupling constant J (Hz), assignment).

For the library synthesis and synthetic methodology validation experiments, sample purity was assessed with the help of ^1H NMR spectroscopy and ^{31}P NMR spectroscopy. If the structure of the impurity present in the sample was known, its share was presented as the appropriate molar percentage in the total mixture of products. The estimation of the unidentified impurities in the sample, present in both ^1H and ^{31}P NMR spectra, was expressed as the integration percentage of the total integral across the spectra. In addition, the signals were rated if they were present at more than 2%.

Mass spectrometry

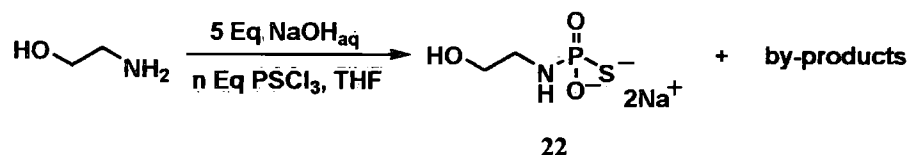
Mass spectra were acquired on Thermo Electron LTQ and a time-of-flight Micromass LCT spectrometers.

Fitting of kinetic data

All data fittings, presented in the experimental section, for both NMR and UV-Vis kinetic studies were performed by applying KaleidaGraph's least squares fitting method $\sum_{(all\ n)}(y_n - \bar{y}_n)^2$. This approach minimizes the square of the error between the original data (y_n) and the values predicted by the equation (\bar{y}_n). All plots of normalised peak area (NMR) or absorbance (UV/Vis) against time, had linear correlation coefficient (R) of 0.99-0.9999. In order to decrease fitting error, the fitting of the experimental data was performed on k_o vs pH data plots. However, pH rate profiles are presented as plots of $\log k_o$ against pH.

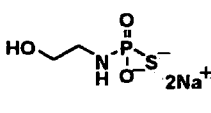
7.2. The optimization of the ethanolamine thiophosphorylation

In order to optimize thiophosphorylation of ethanolamine, several experiments were performed where the number of equivalents of thiophosphoryl chloride was varied.



Ethanolamine (1 Eq, 0.27 mL, 4.6 mmol) was vigorously stirred with an aqueous solution of sodium hydroxide (5 Eq, 1 M, 22.8 mL, 22.8 mmol) and water (2.96 mL) in a 100 mL round bottomed flask with indents, placed in an ice bath. Thiophosphoryl chloride (see table 7.1.) was dissolved in dry tetrahydrofuran (14 mL) and added dropwise to the stirred aqueous mixture over the course of 10 minutes. The mixture was vigorously stirred for 1 h followed by removal of THF on the rotatory evaporator. The residual aqueous solution was then lyophilised, to afford a white powder of crude ethanolamine thiophosphoroamidate **22**, **22a**, **22b** and **22c**. Four repeat attempts were made and conversion estimations by ^1H and ^{31}P NMR spectroscopy are shown in table 7.1.

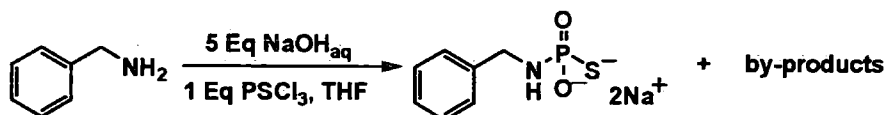
Table 7. 1 Optimisation of thiophosphorylation of ethanolamine: the excess of thiophosphoryl chloride

	1 M NaOH (Eq)	PSCl ₃			SPi (%)	Unreacted ethanolamine (%)	Purity (%)
		Eq	μL	mmol			
22	5	1	464	4.6	1.1 ^a	3.2 ^a	96 ^a , 95 ^b
22a	5.1	1.1	510	5.1	5.2 ^a	5.1 ^a	93 ^a , 94 ^b
22b	5.2	1.2	557	5.5	5.3 ^a	2.1 ^a	93 ^a , 96 ^b
22c	5.3	1.3	603	5.9	8.3 ^a	1.6 ^a	91 ^a , 93 ^b

^aDetermined by ³¹P NMR spectroscopy. ^bDetermined by ¹H NMR spectroscopy.

The other impurities present in the samples were Pi and unidentified structures, containing phosphate moiety. Crude compound **22**: δ_{H} (400 MHz; D₂O) 3.76 (2 H, t, *J* 5.7, OHCH₂), 3.04 (2 H, dt, *J* 9.4 and 5.7, CH₂NH); $\delta_{\text{P}}[^1\text{H}]$ (162 MHz; D₂O) 44.7 (t, *J* 9.1, NHPS); δ_{C} (101 MHz; D₂O) 62.6 (d, ³*J*_{C-P} 8.1, OHCH₂), 44.6 (CH₂NH); *m/z* (ES⁻) 155.9888 (M - H. C₂H₇NO₃PS requires 155.9889).

7.3. Thiophosphorylation of benzylamine



23

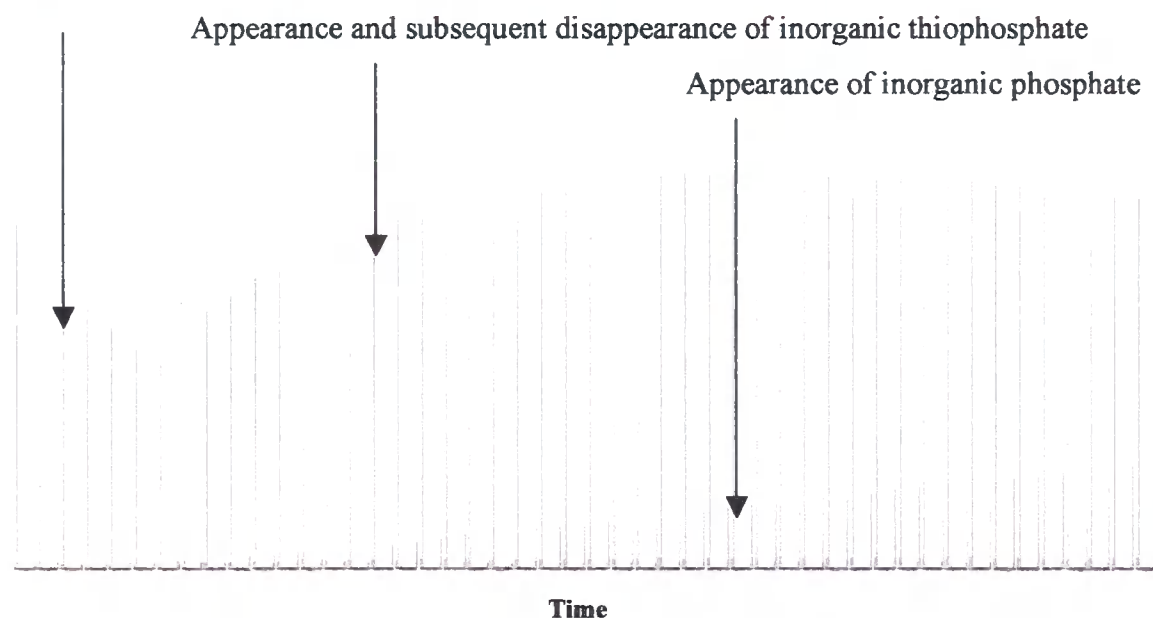
Benzylamine (1 Eq, 0.5 mL, 4.6 mmol) was vigorously stirred with an aqueous solution of sodium hydroxide (5 Eq, 1 M, 22.8 mL, 22.8 mmol) and water (2.96 mL) in a 100 mL round bottomed flask with indents, placed in an ice bath. Thiophosphoryl chloride (1 Eq, 0.464 mL, 4.6 mmol) was dissolved in dry tetrahydrofuran (14 mL) and added dropwise to the stirred aqueous mixture over the course of 10 minutes. The mixture was vigorously stirred for 15 minutes followed by removal of THF on the rotatory evaporator. The residual aqueous solution was then lyophilised affording a white powder of crude benzyl thiophosphoroamidate **23** (99% pure by ¹H and ³¹P NMR spectroscopy). δ_{H} (400 MHz; D₂O) 7.39–7.25 (5 H, m, C₆H₅), 3.92 (2 H, d, *J* 6.8, CH₂NH); $\delta_{\text{P}}[^1\text{H}]$ (162 MHz; D₂O) 44 (t, *J* 6.9, NHPS); δ_{C} (101 MHz; D₂O) 141.3 (d,

$^3J_{C-P}$ 12.4, *i*-C₆H₅), 128.8 (*o*-C₆H₅), 128.2 (*m*-C₆H₅), 127.1 (*p*-C₆H₅), 47.1 (CH₂NH); *m/z* (ES⁻) 202.0099 (M – H. C₇H₉NO₂PS requires 202.0097)

7.4. NMR kinetic studies of thiophosphoroamidate stability

The crude ethanolamine thiophosphoroamidate (**22**, 30 mg) was dissolved in the appropriate buffer (0.5 M, 4 mL or 0.5 mL, see table 7.) and lyophilised. Buffer solutions were prepared via dissolution of appropriate buffer components in water and pH adjustment by the addition of base or acid, as required. The lyophilised residual solid was then dissolved in D₂O (0.5 mL), the pD was recorded and the sample was submitted for ³¹P NMR spectroscopy. As the rigorous deuterium exchange was not performed, pD value potentially varied ± 10%. The spectra were collected at 50 °C every 30 (CAPS, CHES, EPPS, HEPES), 15 (MES), 10 (acetate buffer) or 8 (citric buffer) minutes. An example of the resulting NMR data is shown below.

Disappearance of the thiophosphoroamidate



The intensities of the peaks corresponding to the thiophosphoroamidate, normalised with the highest intensity peak in the spectra, set to have the value 1, were plotted as a pseudo first order function of time and least square fitting was performed against an exponential decay curve (example graph shown below):

$$I_t = I_0 \times e^{-k_s \times t}$$

where, I_t is the peak intensity at the examined time, t

I_0 is starting value of the normalised peak area,

k_0 is the pseudo first order rate constant for the studied thiophosphoramidate degradation for certain pH conditions.

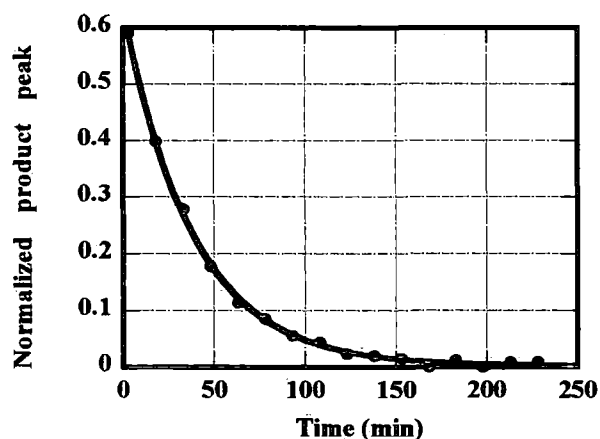


Figure 7. 2 An example of thiophosphoramidate degradation followed by ^{31}P NMR

The recorded pD of the analysed solution was then expressed as $\text{pH} \pm 10\%$ ($\text{pH} = \text{pD} - 0.4$) and plotted against k_{obs} for the corresponding buffer. Since some of the pH values were not constant throughout the experiment, in the case of 0.5 M buffer, pH was represented as the interval from the start to the end of experiment (table 7.2).

Table 7. 2 Experimental details of the NMR kinetic studies: thiophosphoramidate

Gained pH	4 M buffer data			0.5 M buffer data			Buffer
	k_o (min^{-1})	$\log k_{\text{obs}}$	$t_{1/2}$ (min)	k_o (min^{-1})	$\log k_{\text{obs}}$	$t_{1/2}$ (min)	
10.2	0.00021	-3.68	3300	0.00008	-4.11	8884	CAPS
9.5-9.3	/	/	/	0.0013	-2.88	533	CHES
9.2	0.0012	-2.93	597	/	/	/	CHES
8.5-9.2	/	/	/	0.0025	-2.59	272	EPPS
8.7	0.0023	-2.64	301	/	/	/	EPPS
7.9	0.0046	-2.33	150	/	/	/	TRIS
7.4-7.7	/	/	/	0.016	-1.77	43	TRIS
7.5	n.d.	n.d.	n.d.	0.019	-1.72	36	HEPES
7.4	0.0075	-1.12	91	n.d.	n.d.	n.d.	TRIS
7.1	0.014	-1.86	50	n.d.	n.d.	n.d.	HEPES
6.9-7.1	/	/	/	0.033	-1.48	21	MEŠ
6.8	0.027	-1.57	26	/	/	/	MES
5.7-6.2	/	/	/	0.035	-1.45	20	Acetate
5.8	0.03	-1.52	23	n.d.	n.d.	n.d.	MES
5.3	0.027	-1.57	26	/	/	/	Acetate
5	0.023	-1.64	30	n.d.	n.d.	n.d.	Acetate
3.6	0.028	-1.55	25	n.d.	n.d.	n.d.	Citric
2.9	0.015	-1.83	47	n.d.	n.d.	n.d.	Citric
2.2	0.023	-1.64	30	n.d.	n.d.	n.d.	Citric

Equations used for least square fitting:

4 M buffer: $k_{\text{obs}} = 0.026 / (1 + K_a / [\text{H}^+])$, $\text{p}K_a = 7.26$

0.5 M buffer: $k_{\text{obs}} = 0.038 / (1 + K_a / [\text{H}^+])$, $\text{p}K_a = 7.61$

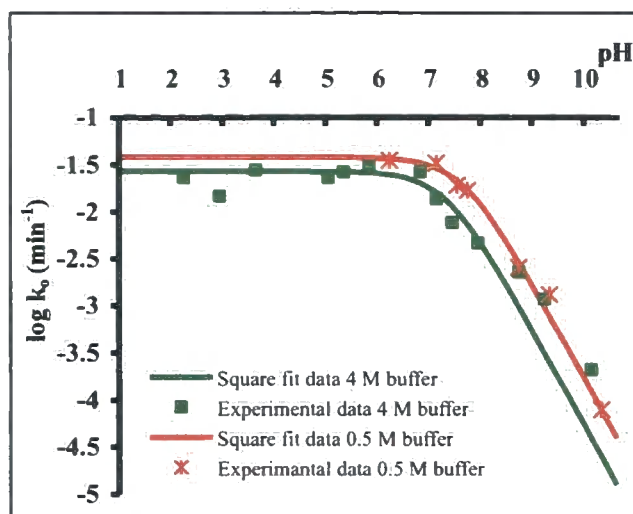
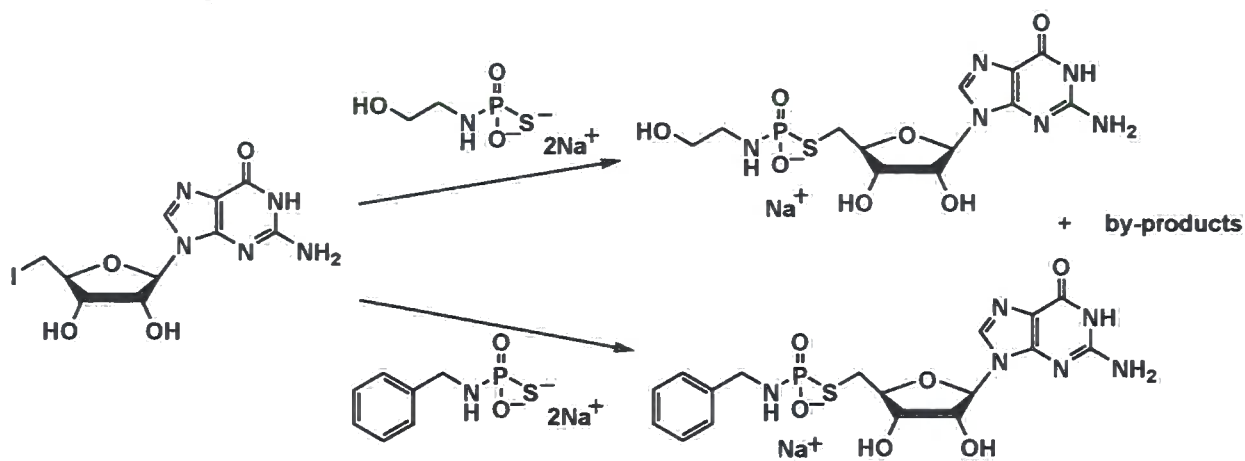
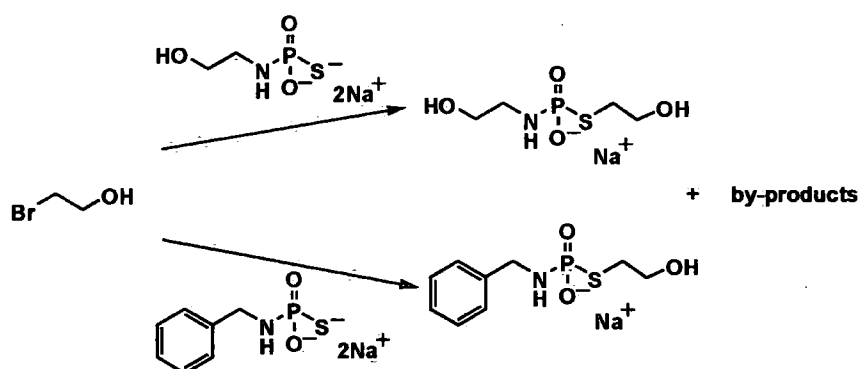


Figure 7.3 pH rate profile for ethanolamine thiophosphoroamidate hydrolysis: 4 M vs 0.5 M buffer

7.5. Stepwise alkylation of thiophosphoroamidates

7.5.1. Use of an excess of the thiophosphoroamidate with the respect to alkylation agent





5'-iodo-5'-deoxyguanosine (19 mg, 0.05 mmol) or 2-bromoethanol (3.5 μL , 0.05 mmol) was measured directly into an NMR tube. Crude benzylamine thiophosphoramidate **23** (101.5 mg) or ethanolamine thiophosphoramidate **22** (78.5 mg) was dissolved in D_2O (0.5 mL) and added to the alkylation agent. The mixture was then subjected to ^{31}P NMR spectroscopy at 50 $^\circ\text{C}$ over 12 h with spectra being collected every 30 minutes. All the signals appearing in the spectra were integrated. The increase in the amount of desired product formed, was presented as an increase of the normalised peak area that was assigned to be a fraction of the total peak area. The normalised peak area for the signal at 25 ppm (quintet in the coupled spectra, $J=10.7$ Hz), corresponding to the alkylated product, was then plotted against time using the least squares fitting method for the exponential equation (graphs shown below):

$$I_t = I \times (1 - e^{-k_A \times t})$$

where, I_t is the normalised peak area at the time point, t

I is the maximal value for the normalised peak area

k_A is the observed rate constant for the alkylation process.

70 °C: 2-Bromoethanol (35 μL , 0.05 mmol) was added to a solution of crude benzyl thiophosphoroamidate (101.5 mg) in 0.4 mL of D_2O in a NMR tube. ^{31}P NMR spectra were collected every 30 minutes at 70 °C. The increase in the intensity of the peak at 41 ppm (multiplet, conversion 65% estimated *via* ^{31}P NMR), corresponding to the both *S*- and *N*-alkylated product **39** was then plotted against time using the least square fitting method for the exponential equation as described in section 7.6.1. The resulting graphs are shown below.

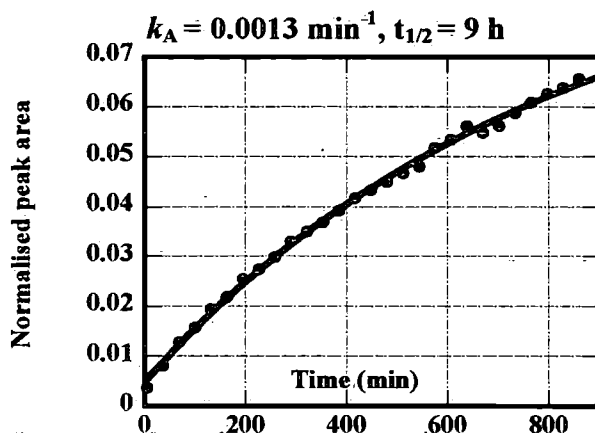
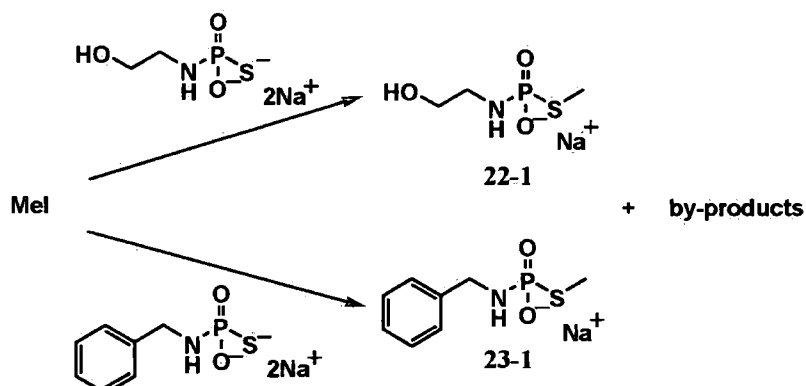


Figure 7. 6 Rate of the formation of the N- alkylation of S-alkylated benzyl thiophosphoroamidate. Bimolecular rate constant is $0.003 \text{ M}^{-1}\text{min}^{-1}$

90 °C: The same method was applied as for the 70° C, but the reaction was completed after 70 minutes yielding the dialkylated product **39** (75% pure by ^{31}P NMR spectroscopy). $\delta_{\text{P}}[^1\text{H}](162 \text{ MHz; H}_2\text{O})$ 40.4 (m, $(\text{CH}_2)_2\text{NPSCH}_2$); m/z (ES^-) 290.0624 (M – H. $\text{C}_{11}\text{H}_{17}\text{NO}_4\text{PS}$ requires 290.0621). The impurities present: $\delta_{\text{P}}[^1\text{H}](162 \text{ MHz; H}_2\text{O})$ 25.6 (m, benzylamine thiophosphoroamidate **23**), 1.6 (s, Pi).

7.5.3. Use of thiophosphoroamidate and alkylation agent in a 1:1 molar ratio

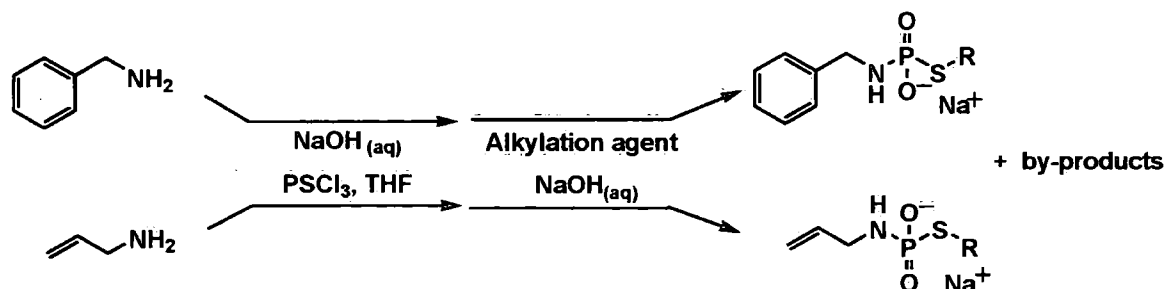


The crude benzyl thiophosphoroamidate **23** (101.5 mg) or ethanolamine thiophosphoroamidate **22** (78.5 mg) was dissolved in D₂O (0.5 mL) and transferred into an NMR tube. Methyl iodide (61 μ L, 0.1 mmol) was added to the solution and the alkylation process was followed *via* ³¹P NMR spectroscopy. Upon completion, ammonium hydroxide solution (30% w/v, 1.5 mL) was added to the reaction mixture and the mixture was concentrated under reduced pressure. The resulting aqueous solution was freeze-dried and the product was analysed. Crude compound 22-1 (purity: 97% by ³¹P and 93% by ¹H NMR spectroscopy): δ_{H} (400 MHz; D₂O) 3.57 (2 H, t, *J* 5.9, OHCH₂), 2.88 (2 H, dt, *J* 5.6, CH₂NH), 2.03 (3 H, d, *J* 13.2, NHPSCH₃); $\delta_{\text{P}}[^1\text{H}]$ (162 MHz; D₂O) 27.8 (sx, *J* 12.9, NHPS); δ_{C} (101 MHz; D₂O), 62.3 (d, OHCH₂), 43.5 (CH₂NH), 12.1 (NHPSCH₃); *m/z* (ES⁻) 170.0048 (M – H. C₃H₉NO₃PS requires 170.0046).

Crude compound 23-1 (purity: 95% by ³¹P and 82% by ¹H NMR spectroscopy): δ_{H} (400 MHz; D₂O) 7.39–7.25 (5 H, m, C₆H₅), 3.97 (2 H, d, *J* 10.8, CH₂NH), 2.03 (3 H, d, *J* 13.2, NHPSCH₃); $\delta_{\text{P}}[^1\text{H}]$ (162 MHz; D₂O) 27.3 (sx, *J* 12.9, NHPS); δ_{C} (101 MHz; D₂O) 140.9 (d, *i*-C₆H₅), 129.4 (*o*-C₆H₅), 127.9 (*m*-C₆H₅), 127.4 (*p*-C₆H₅), 45.6 (CH₂NH), 12.1 (NHPSCH₃); *m/z* (ES⁻) 216.0255 (M – H. C₈H₁₁NO₂PS requires 216.0253).

7.6. Continuous method for the preparation of alkylated thiophosphoramidates

7.6.1. Lipophilic amines: benzylamine and allylamine

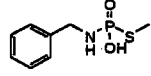
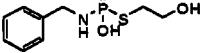
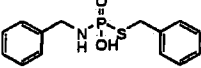
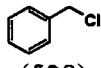
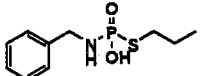
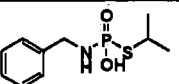


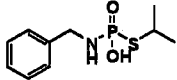
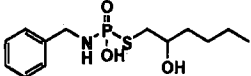
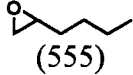
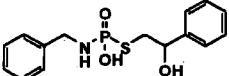
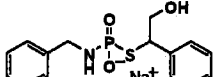
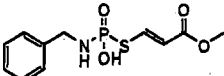
Benzylamine (1.2 Eq, 0.3 mL, 2.76 mmol) or allylamine (1.2 Eq, 0.206 mL, 2.76 mmol) was mixed with sodium hydroxide (5 Eq, 1 M aqueous solution, 11.5 mL, 11.5 mmol) and water (1.48 mL) in a 50 mL round-bottomed flask with indents. Thiophosphoryl chloride (1 Eq, 0.232 mL, 2.3 mmol) dissolved in THF (7 mL) was added dropwise to the aqueous mixture over the course of 10 minutes. After vigorous mixing for 15 minutes, an alkylating agent was added (2 Eq, 4.6 mmol, table 7.3) along with additional sodium hydroxide solution and vigorous mixing was continued for a prescribed period. Then, ether extraction (3 × 30 mL) was performed and the aqueous layer was lyophilised.

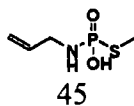
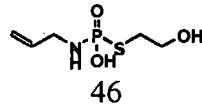
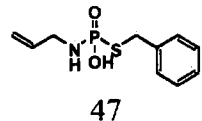
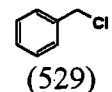
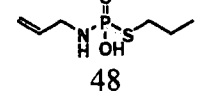
The exceptions from this general method were:

- in the case of alkylation with 2-propyl iodide, two experiments were performed:
 1. after the addition of the alkylating agent (10 Eq, 23 mmol) the reaction mixture was stirred at 50 °C (44a)
 2. the alkylating agent was used in a slightly higher excess (11 Eq, 25.3 mmol) and applied in three separate additions of 5+5+1 Eq. Following addition of the alkylation agent, aqueous sodium hydroxide (1 M, 5+5 Eq) was added in batches as well. The experiment was performed stirring at 80 °C (44b)
- when 1,2-epoxyhexane was used as the alkylating agent (product 418), prior to freeze-drying, the pH of the aqueous solution of the crude mixture was adjusted to 8 using hydrochloric acid (0.05 M, 1 Eq, 46 mL, 2.3 mmol).

Table 7. 3 one-pot method: benzylamine and allylamine

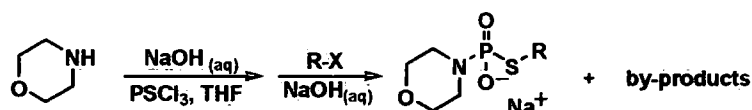
Crude product	Alkylation agent (μL)	1 M NaOH (Eq)	Time (hour)	Purity (%)	Characterisation of the desired compound
 40	MeI (286)	0	0.25	98 ^a 96 ^b	δ_{H} (400 MHz; D ₂ O) 7.41–7.15 (5 H, m, C ₆ H ₅), 3.88 (2 H, d, <i>J</i> 10.4, CH ₂ NH), 1.93 (3 H, d, <i>J</i> 12.8, SCH ₃); $\delta_{\text{P}}[^1\text{H}]$ (283 MHz; D ₂ O) 27.1 (m, NHPS); δ_{C} (176 MHz; D ₂ O) 141.1 (d, ³ J _{C-P} 8.7, <i>i</i> -C ₆ H ₅), 129.0 (<i>m</i> -C ₆ H ₅), 128.1 (<i>o</i> -C ₆ H ₅), 127.5 (<i>p</i> -C ₆ H ₅), 45.7 (CH ₂ NH), 12.2 (SCH ₃); <i>m/z</i> (ES ⁻) 216.0252 (M – H. C ₈ H ₁₁ NO ₂ PS requires 216.0253).
 41	Br-CH ₂ -CH ₂ -OH (326)	0	17 ^c	100 ^a 99 ^b	δ_{H} (400 MHz; D ₂ O) 7.37–7.19 (5 H, m, C ₆ H ₅), 3.9 (2 H, d, <i>J</i> 10.8, CH ₂ NH), 3.57 (2 H, t, <i>J</i> 6.4, CH ₂ OH), 2.65 (2 H, dt, <i>J</i> 11.9 and 6.4, SCH ₂); $\delta_{\text{P}}[^1\text{H}]$ (162 MHz; D ₂ O) 25.6 (qn, <i>J</i> 11.5, NHPS); δ_{C} (101 MHz; D ₂ O) 140.7 (d, ³ J _{C-P} 8.1, <i>i</i> -C ₆ H ₅), 129.1 (<i>m</i> -C ₆ H ₅), 128.1 (<i>o</i> -C ₆ H ₅), 127.5 (<i>p</i> -C ₆ H ₅), 61.7 (d, ³ J _{C-P} 5.1, CH ₂ OH) 45.4 (CH ₂ NH), 32.1 (SCH ₂); <i>m/z</i> (ES ⁻) 246.0356 (M – H. C ₉ H ₁₃ NO ₃ PS requires 246.0359).
 42	 (529)	0	22	100 ^a 98 ^b	δ_{H} (400 MHz; D ₂ O) 7.31–7.18 (10 H, m, 2 × C ₆ H ₅), 3.75 (4 H, 2 × d, <i>J</i> 10.4, 2 × CH ₂ NH); $\delta_{\text{P}}[^1\text{H}]$ (162 MHz; D ₂ O) 24.5 (qn, <i>J</i> 10.3, NHPS); δ_{C} (101 MHz; D ₂ O) 140.5 (d, ³ J _{C-P} 8.1, <i>i</i> -C ₆ H ₅ CH ₂ NH), 139.2 (d, ³ J _{C-P} 5.1, <i>i</i> -C ₆ H ₅ CH ₂ S), 128.8 (<i>m</i> -C ₆ H ₅ CH ₂ NH), 128.7 (<i>m</i> -C ₆ H ₅ SCH ₂), 128.6 (<i>o</i> -C ₆ H ₅ CH ₂ NH), 127.7 (<i>o</i> -C ₆ H ₅ SCH ₂), 127.3 (<i>p</i> -C ₆ H ₅ CH ₂ NH), 127.2 (<i>p</i> -C ₆ H ₅ SCH ₂), 45.4 (CH ₂ NH), 34.5 (SCH ₂); <i>m/z</i> (ES ⁻) 292.0564 (M – H. C ₁₄ H ₁₅ NO ₂ PS requires 292.0566).
 43	 (448)	0	25	100 ^a 100 ^b	δ_{H} (400 MHz; D ₂ O) 7.28–7.18 (5 H, m, C ₆ H ₅), 3.90 (2 H, d, <i>J</i> 10.4, CH ₂ NH), 2.47 (2 H, dt, <i>J</i> 10.8 and 7.4, SCH ₂), 1.43 (2 H, sx, <i>J</i> 7.4, CH ₂ CH ₂ CH ₃), 0.78 (3 H, t, <i>J</i> 7.4, CH ₂ CH ₃); $\delta_{\text{P}}[^1\text{H}]$ (162 MHz; D ₂ O) 25.6 (qn, <i>J</i> 10.5, NHPS); δ_{C} (101 MHz; D ₂ O) 140.7 (d, ³ J _{C-P} 7.1, <i>i</i> -C ₆ H ₅), 129 (<i>m</i> -C ₆ H ₅), 128.1 (<i>o</i> -C ₆ H ₅), 127.5 (<i>p</i> -C ₆ H ₅), 45.4 (CH ₂ NH), 32.2 (SCH ₂), 23.7 (d, ³ J _{C-P} 5.8, CH ₂ CH ₂ CH ₃), 12.8 (CH ₂ CH ₃); <i>m/z</i> (ES ⁻) 244.0564 (M – H. C ₁₀ H ₁₅ NO ₂ PS requires 244.0566).
 44	 (2295)	5	96	94 ^a 92 ^b	δ_{H} (400 MHz; D ₂ O) 7.28–7.20 (5 H, m, C ₆ H ₅), 3.92 (2 H, d, <i>J</i> 10.4, CH ₂ NH), 3.03 (1 H, m, CH(CH ₃) ₂), 1.43 (3 H, d, <i>J</i> 7.6, CH(CH ₃) ₂);

44-I					δ_P [1H](162 MHz; D ₂ O) 24.8 (q, <i>J</i> 10.3, NHPS); δ_C (101 MHz; D ₂ O) 140.8 (d, $^3J_{C-P}$ 8.1, <i>i</i> -C ₆ H ₅), 128.7 (<i>m</i> -C ₆ H ₅), 128.1 (<i>o</i> -C ₆ H ₅), 127.5 (<i>p</i> -C ₆ H ₅), 45.6 (CH ₂ NH), 36.2 (CH(CH ₃) ₂), 25.2 (d, $^3J_{C-P}$ 5.1, CH(CH ₃) ₂); <i>m/z</i> (ES ⁻) 244.0567 (M - H. C ₁₀ H ₁₅ NO ₂ PS requires 244.0566).
 44-II	 (2524)	5+5	24	90 ^a 89 ^b	The same signals as for the compound 44-I.
 104	 (555)	0	5	96 ^a 95 ^b	δ_H (400 MHz; D ₂ O) 7.38–6.90 (5 H, m, C ₆ H ₅), 3.87 (2 H, d, <i>J</i> 10.8, CH ₂ NH), 3.46 (1 H, qn, <i>J</i> 6.4 and 5.6, CH ₂ CHOH), 2.55–2.31 (2 H, m, SCH ₂ CH), 1.24 (2 H, q, <i>J</i> 13.4 and 7.0, OHCHCH ₂), 1.15–0.91 (4 H, m, OHCH(CH ₂) ₂), 0.70 (3 H, t, <i>J</i> 7.0, CH ₂ CH ₃); δ_P [1H](162 MHz; D ₂ O) 24.8 (qn, <i>J</i> 10.7, NHPS); δ_C (101 MHz; D ₂ O) 140.7 (d, $^3J_{C-P}$ 7.3, <i>i</i> -C ₆ H ₅), 128.5 (<i>m</i> -C ₆ H ₅), 127.8 (<i>o</i> -C ₆ H ₅), 126.9 (<i>p</i> -C ₆ H ₅), 71.3 (d, $^3J_{C-P}$ 5.8, CH ₂ CHOH), 45.6 (CH ₂ NH), 36.8 (SCH ₂ CH), 35.3 (OHCHCH ₂), 27.4 (CHCH ₂ CH ₂), 22.3 (CH ₂ CH ₂ CH ₂), 13.8 (CH ₂ CH ₃); <i>m/z</i> (ES ⁻) 302.0984 (M - H. C ₁₃ H ₂₁ NO ₃ PS requires 302.0984).
 102A  103B	 (526)	0	19	A63 ^a A ^b n.d. B26 ^a B ^b n.d.	δ_H (400 MHz; D ₂ O) 7.33–6.67 (20 H, m, 2 × C ₆ H ₅), 4.53 (1 H _A , m, OHCH ₂ CH), 3.68 (2 H _A +2 H _B , d, <i>J</i> 10.8, CH ₂ NH), 2.88–2.69 (2 H _A , m, OHCH ₂ CH), the other signals were not resolved; δ_P [1H](162 MHz; D ₂ O) 25.6 (A: qn, <i>J</i> 10.7, NHPS), 23.8 (B: q, <i>J</i> 9.2, NHPS); δ_C (101 MHz; D ₂ O) 142.5 (<i>i</i> _A -C ₆ H ₅), 141.1 (<i>i</i> _B -C ₆ H ₅), 140.6 (d, $^3J_{C-P}$ 7.2, <i>i</i> _A -C ₆ H ₅ CH ₂ NH), 140.1 (d, $^3J_{C-P}$ 9.6, <i>i</i> _B -C ₆ H ₅ CH ₂ NH), 128.7–126.3 (4 × C ₆ H ₅), 73.4 (d, $^3J_{C-P}$ 5.8, C _A H ₂ CH), 66.2 (d, $^3J_{C-P}$ 6.7, C _B H ₂ CH), 50.8 (OHC _B HCH ₂), 45.6 (C _B H ₂ NH), 45.4 (C _A H ₂ NH), 38.0 (OHC _A H ₂ CH); <i>m/z</i> (ES ⁻) 322.0674 (M - H. C ₁₅ H ₁₇ NO ₃ PS requires 322.0672).
 109	 (411)	0	5	92 ^a 94 ^b	δ_H (400 MHz; D ₂ O) 7.28–7.05 (5 H, m, C ₆ H ₅), 5.82 (1 H, d, <i>J</i> 10.4, SCH=CH), 3.90 (2 H, d, <i>J</i> 12.0, CH ₂ NH), 3.55 (3 H, s, OCH ₃); δ_P [1H](162 MHz; D ₂ O) 21.5 (qn, <i>J</i> 11.8, NHPS); δ_C (101 MHz; D ₂ O) 168.7 (C=O), 145.2 (SCH=CH), 140.2 (d, $^3J_{C-P}$ 6.3, <i>i</i> -C ₆ H ₅ CH ₂ NH), 128.7 (<i>m</i> -C ₆ H ₅), 127.8 (<i>o</i> -C ₆ H ₅), 127.2 (<i>p</i> -C ₆ H ₅), 115.7 (d, $^3J_{C-P}$ 7.7,

					SCH=CH), 45.7 (CH ₂ NH), 51.8 (OCH ₃); <i>m/z</i> (ES ⁻) 286.0308 (M - H. C ₁₁ H ₁₃ NO ₄ PS requires 286.0308).
	MeI (286)	0	0.3	98 ^a 91 ^b	δ_{H} (400 MHz; D ₂ O) 5.91 (1 H, ddt, <i>J</i> 17.2, 10.2 and 6.0 CH ₂ =CH), 5.26 (2 H, dq, <i>J</i> 17.2, 10.2 and 1.8, CH ₂ =CH), 3.47 (2 H, ddt, <i>J</i> 10.8, 6.0 and 1.6, CH ₂ NH), 2.13 (3 H, d, <i>J</i> 13.0, SCH ₃); $\delta_{\text{P}}[^1\text{H}]$ (162 MHz; D ₂ O) 27.6 (m, NHPS); δ_{C} (101 MHz; D ₂ O) 137.4 (d, ³ <i>J</i> _{C-P} 7.3, CH ₂ =CH), 115.6 (CH ₂ =CH), 44.4 (CH ₂ NH), 12.3 (SCH ₃); <i>m/z</i> (ES ⁻) 166.0097 (M - H. C ₄ H ₉ NO ₂ PS requires 166.0097).
	Br-CH ₂ -CH ₂ -OH (326)	0.9	1.5	100 ^a 95 ^b	δ_{H} (400 MHz; D ₂ O) 5.85 (1 H, ddt, <i>J</i> 17.2, 10.0 and 6.0 CH ₂ =CH), 5.26 (2 H, dq, <i>J</i> 17.2, 10.0 and 1.6, CH ₂ =CH), 3.67 (2 H, t, <i>J</i> 6.0, CH ₂ OH), 3.37 (2 H, ddt, <i>J</i> 10.4 and 5.2, CH ₂ NH), 2.74 (2 H, dt, <i>J</i> 6.0 and 6.4, SCH ₂); $\delta_{\text{P}}[^1\text{H}]$ (162 MHz; D ₂ O) 27.6 (m, NHPS); δ_{C} (101 MHz; D ₂ O) 137.2 (d, ³ <i>J</i> _{C-P} 8.1, CH ₂ =CH), 115.3 (CH ₂ =CH), 61.9 (d, ³ <i>J</i> _{C-P} 7.3, CH ₂ OH), 44.3 (CH ₂ NH), 32.2 (SCH ₂); <i>m/z</i> (ES ⁻) 196.0201 (M - H. C ₅ H ₁₁ NO ₃ PS requires 196.0203).
	 (529)	0.4	23	99 ^a 99 ^b	δ_{H} (400 MHz; D ₂ O) 7.29–7.13 (5 H, m, C ₆ H ₅), 5.69 ((1 H, ddt, <i>J</i> 17.2, 10.0 and 6.0 CH ₂ =CH), 4.95 (2 H, dq, <i>J</i> 17.2 and 10.0, CH ₂ =CH), 3.75 (2 H, d, <i>J</i> 10.8, SCH ₂), 3.37 (2 H, ddt, <i>J</i> 10.4 and 6.0, CH ₂ NH); $\delta_{\text{P}}[^1\text{H}]$ (162 MHz; D ₂ O) 25.0 (m, NHPS); δ_{C} (101 MHz; D ₂ O) 139.2 (d, ³ <i>J</i> _{C-P} 6.1, <i>i</i> -C ₆ H ₅ CH ₂ S), 136.8 (d, ³ <i>J</i> _{C-P} 8.1, CH ₂ =CH), 128.9 (<i>m</i> -C ₆ H ₅), 128.8 (<i>o</i> -C ₆ H ₅), 127.4 (<i>p</i> -C ₆ H ₅), 115.3 (CH ₂ =CH), 44.2 (CH ₂ NH), 34.2 (d, ³ <i>J</i> _{C-P} 2.9, SCH ₂); <i>m/z</i> (ES ⁻) 242.0411 (M - H. C ₁₀ H ₁₃ NO ₂ PS requires 242.0410).
	 (448)	0	120 ^c	97 ^a 99 ^b	δ_{H} (400 MHz; D ₂ O) 5.98 (1 H, ddt, <i>J</i> 17.2, 10.8 and 5.8 CH ₂ =CH), 5.20 (2 H, dq, <i>J</i> 17.2, 10.8 and 1.2, CH ₂ =CH), 3.46 (2 H, ddt, <i>J</i> 10.8 and 5.8, CH ₂ NH), 2.67 (2 H, dt, <i>J</i> 10.8 and 7.4, SCH ₂), 1.64 (2 H, sx, <i>J</i> 7.4, CH ₂ CH ₃), 0.97 (3 H, t, <i>J</i> 7.4 CH ₂ CH ₃); $\delta_{\text{P}}[^1\text{H}]$ (162 MHz; D ₂ O) 26.9 (qnJ 10.7, NHPS); δ_{C} (101 MHz; D ₂ O) 137.4 (d, ³ <i>J</i> _{C-P} 8.1, CH ₂ =CH), 115.3 (CH ₂ =CH), 44.5 (CH ₂ NH), 32.5 (SCH ₂), 24.1 (d, ³ <i>J</i> _{C-P} 5.8, CH ₂ CH ₃), 13.1 (CH ₂ CH ₃); <i>m/z</i> (ES ⁻) 194.0410 (M - H. C ₆ H ₁₃ NO ₂ PS requires 194.0410).

^aDetermined by ³¹P NMR spectroscopy. ^bDetermined by ¹H NMR spectroscopy. ^cExperiment was left stirring overnight

7.6.2. Hydrophilic amines: morpholine

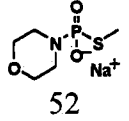
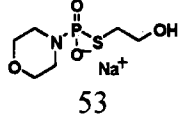
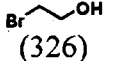
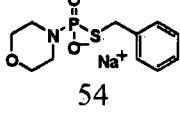
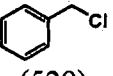
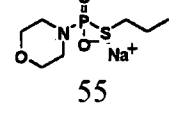
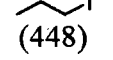
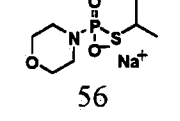
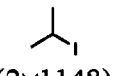


Alkylated morpholine thiophosphoramidates were prepared by repeating the procedure as described for the production of benzylamine derivatives (section 7.4) using morpholine (1.2 Eq, 241 μ L, 2.76 mmol). The exceptions from the existing method were:

- during the thiophosphorylation step, the reaction mixture was allowed to stir for 1 h,
- in the case of alkylation with benzyl chloride, 1-propyl iodide and 2-propyl iodide, heating (80 °C) was applied,
- 2-propyl iodide was used in excess (10 Eq, 23 mmol) and was added in two batches of 5 Eq. With the addition of the first batch of 2-propyl iodide, aqueous sodium hydroxide (2 Eq, 1 M) was added and the mixture was stirred for 1 h at 80 °C. Then, the second batch was added with another 2 Eq of sodium hydroxide and the mixture was stirred overnight at 80 °C.
- chloroform was used as the extraction solvent.

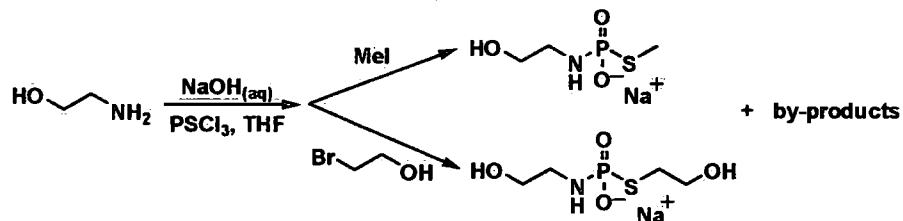
Alkylation agents and conversion levels to products are shown in the table 7.3.

Table 7. 4 one-pot method: morpholine

Crude product	RX (μL)	1 M NaOH (Eq)	Time (h)	Purity (%)	Characterisation of the desired compound
 52	MeI (286)	0	1.5	98 ^a 92 ^b	δ_{H} (400 MHz; D ₂ O) 3.78–3.74 (4 H, m, O(CH ₂) ₂), 3.17–3.12 (4 H, m, (CH ₂) ₂ N), 2.23 (3 H, d, <i>J</i> 12.8, SCH ₃); δ_{P} [¹ H](162 MHz; D ₂ O) 25.3 (m, NPS); δ_{C} (101 MHz; D ₂ O) 67.4 (d, ³ <i>J</i> _{C-P} 7.3, O(CH ₂) ₂), 45.3 ((CH ₂) ₂ N), 12.0 (d, ³ <i>J</i> _{C-P} 2.9, SCH ₃); <i>m/z</i> (ES ⁻) 196.0202 (M – H. C ₅ H ₁₁ NO ₃ PS requires 196.0203).
 53	 (326)	0.8	1	91 ^a 88 ^b	δ_{H} (400 MHz; D ₂ O) 3.72 (2 H, t, <i>J</i> 6.3, CH ₂ OH), 3.65–3.63 (4 H, m, O(CH ₂) ₂), 3.06–3.02 (4 H, m, (CH ₂) ₂ N), 2.83 (2 H, dt, <i>J</i> 11.9 and 6.3, SCH ₂); δ_{P} [¹ H](162 MHz; D ₂ O) 25.3 (m, NPS); δ_{C} (101 MHz; D ₂ O) 67.3 (d, ³ <i>J</i> _{C-P} 11.3, O(CH ₂) ₂), 62.1 (d, ³ <i>J</i> _{C-P} 11.3, CH ₂ OH), 45.1 ((CH ₂) ₂ N), 31.8 (d, ³ <i>J</i> _{C-P} 2.9, SCH ₂); <i>m/z</i> (ES ⁻) 226.0308 (M – H. C ₆ H ₁₃ NO ₄ PS requires 226.0308).
 54	 (529)	1.7	4	92 ^a 89 ^b	δ_{H} (400 MHz; D ₂ O) 7.18 (2 H, d, <i>J</i> 7.8, <i>o</i> -C ₆ H ₅ CH ₂ S), 7.07 (2 H, t, <i>J</i> 7.4, <i>m</i> -C ₆ H ₅ CH ₂ S), 6.98 (1 H, t, <i>J</i> 7.4, <i>p</i> -C ₆ H ₅ CH ₂ S), 3.75 (2 H, d, <i>J</i> 9.9, SCH ₂), 3.52–3.40 (4 H, m, O(CH ₂) ₂), 2.92–2.79 (4 H, m, (CH ₂) ₂ N); δ_{P} [¹ H](162 MHz; D ₂ O) 23.7 (m, NPS); δ_{C} (101 MHz; D ₂ O) 139.2 (d, ³ <i>J</i> _{C-P} 6.1, <i>p</i> -C ₆ H ₅ CH ₂ S), 128.9 (<i>m</i> -C ₆ H ₅), 128.8 (<i>o</i> -C ₆ H ₅), 127.2 (<i>p</i> -C ₆ H ₅), 67.2 (d, ³ <i>J</i> _{C-P} 7.7, O(CH ₂) ₂), 45.4 ((CH ₂) ₂ N), 34.4 (SCH ₂); <i>m/z</i> (ES ⁻) 272.0514 (M – H. C ₁₁ H ₁₅ NO ₃ PS requires 272.0516).
 55	 (448)	0.4	7	95 ^a 92 ^b	δ_{H} (400 MHz; D ₂ O) 3.75–3.72 (4 H, m, O(CH ₂) ₂), 3.13–3.09 (4 H, m, (CH ₂) ₂ N), 2.74 (2 H, dt, <i>J</i> 11.6 and 7.4, SCH ₂), 1.66 (2 H, sx, <i>J</i> 7.4, CH ₂ CH ₂ CH ₃), 0.99 (3 H, t, <i>J</i> 7.4, CH ₂ CH ₃); δ_{P} [¹ H](162 MHz; D ₂ O) 24.6 (m, NPS); δ_{C} (101 MHz; D ₂ O) 67.3 (d, ³ <i>J</i> _{C-P} 7.3, O(CH ₂) ₂), 45.2 ((CH ₂) ₂ N), 32.0 (d, ³ <i>J</i> _{C-P} 2.9, SCH ₂), 24.4 (d, ³ <i>J</i> _{C-P} 5.8, CH ₂ CH ₂), 13.1 (CH ₂ CH ₃); <i>m/z</i> (ES ⁻) 224.0516 (M – H. C ₇ H ₁₅ NO ₃ PS requires 224.0515).
 56	 (2×1148)	2+2	1+ 16 ^c	95 ^a 95 ^b	δ_{H} (400 MHz; D ₂ O) 3.77–3.75 (4 H, m, O(CH ₂) ₂), 3.36–3.26 (1 H, m, SCH), 3.15–3.11 (4 H, m, (CH ₂) ₂ N), 1.40 (6 H, d, <i>J</i> 6.8, CH(CH ₃) ₂); δ_{P} [¹ H](162 MHz; D ₂ O) 23.6 (m, NPS); δ_{C} (101 MHz; D ₂ O) 67.3 (d, ³ <i>J</i> _{C-P} 7.3, O(CH ₂) ₂), 45.2 ((CH ₂) ₂ N), 36.1 (CHCH ₃), 25.9 (d, ³ <i>J</i> _{C-P} 5.1, CHCH ₃); <i>m/z</i> (ES ⁻) 224.0516 (M – H. C ₇ H ₁₅ NO ₃ PS requires 224.0515).

^a Determined by ³¹P NMR spectroscopy. ^b Determined by ¹H NMR spectroscopy. ^c Experiment was left stirring overnight

7.6.3. Hydrophilic amines: the use of equal numbers of equivalents of ethanolamine and thiophosphoryl chloride



Alkylated ethanolamine thiophosphoramidate was prepared using the same procedure as for the production of benzylamine derivatives (section 7.4.) with the following exceptions:

- 1 Eq of ethanolamine was used (138 μ L, 2.3 mol)
- the thiophosphorylation step was performed for 1 hour
- chloroform was used as the extraction solvent.

The alkylation agents used and conversions levels are shown in table 7.5.

Table 7. 5 one-pot method: ethanolamine and thiophosphoryl chloride in 1:1 molar ratio

Crude compound	Alkylation agent (μ L)	Time (hour)	Purity (%)
57	MeI (286)	4	92 ^a , 89 ^b
58	Br-CH ₂ -CH ₂ -OH (326)	20	84 ^a , 85 ^b

^a Determined by ³¹P NMR spectroscopy. ^b Determined by ¹H NMR spectroscopy.

Compound 57: δ_{H} (400 MHz; D₂O) 3.57 (2 H, t, *J* 5.6, OHCH₂), 2.88 (2 H, dt, *J* 10.8 and 5.6, CH₂NH), 2.05 (3 H, d, *J* 12.4, SCH₃); $\delta_{\text{P}}[^1\text{H}]$ (162 MHz; D₂O) 28.0 (m, NHPS); δ_{C} (101 MHz; D₂O) 62.3 (d, ³*J*_{C-P} 8.1, OHCH₂), 43.5 (CH₂NH), 12.1.2 (SCH₃); *m/z* (ES⁻) 170.0046 (M – H. C₃H₉NO₃PS requires 170.0046).

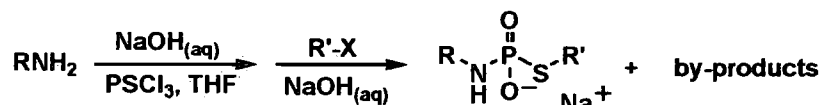
Compound 58: δ_{H} (400 MHz; D₂O) 3.67 (2 H, t, *J* 6.4, CH₂OH), 3.54 (2 H, t, *J* 5.6, OHCH₂), 2.88 (2 H, dt, *J* 10.7 and 5.6, CH₂NH), 2.74 (2 H, dt, *J* 12.4 and 6.4, SCH₂); $\delta_{\text{P}}[^1\text{H}]$ (162 MHz; D₂O) 25.6 (qn, *J* 11.5, NHPS); δ_{C} (101 MHz; D₂O) 62.3 (d, ³*J*_{C-P} 8.1, OHCH₂), 61.8 (d, ³*J*_{C-P} 5.0, CH₂OH), 43.5 (CH₂NH), 32.2 (SCH₂); *m/z* (ES⁻) 200.0151 (M – H. C₄H₁₁NO₄PS requires 200.0151).

A range of quantities of sodium hydroxide were tested in the case of 2-bromoethanol alkylation and the conversion levels were recorded. (table 7.4.)

Table 7. 6 The effect of additional sodium hydroxide on the reaction outcome: 2-bromoethanol

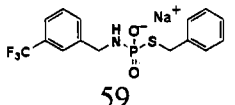
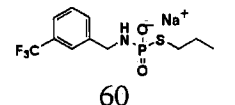
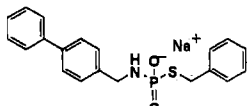
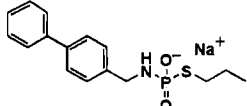
1M NaOH (Eq)	0	0.5	0.9	1.5	1.7
³¹ P NMR (in H ₂ O/THF)	98%	87%	90%	80%	66%

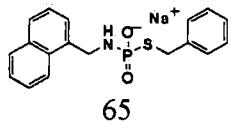
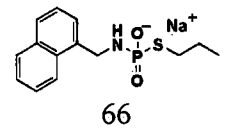
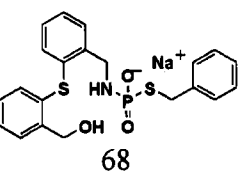
7.6.4. A library of amines

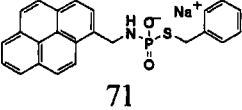
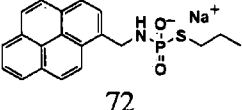
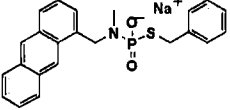


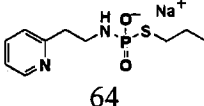
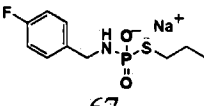
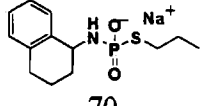
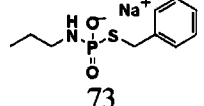
Amine (1.2 Eq 0.582 mmol, table 5.3., RNH₂) was mixed/dissolved in a mixture of sodium hydroxide (5 Eq, 1M aqueous solution, 2.425 mL, 2.425 mmol) and water (0.312 mL) in a 50 mL round-bottomed flask with indents. Thiophosphoryl chloride (1 Eq, 0.049 mL, 0.485 mmol), dissolved in THF (1.476 mL) was added *via* a dropping funnel to the amine solution/suspension over the course of 10 minutes. After mixing for one hour, alkylation agent (R'X), benzyl chloride (2 Eq, 0.97 mmol, 111 μL) or propyl iodide (0.97 mmol, 94 μL), along with additional aqueous sodium hydroxide (table 7.11) was added and vigorous mixing was continued overnight. Then, ether extraction (3 × 20 mL) was performed and the aqueous sample was lyophilized. In cases where a white precipitate appeared during the extraction (71, 72 74, 75) the sample was centrifuged and the precipitate was dried overnight in a vacuum desiccator before being analysed. Estimations of the level of purity of the products are presented in the form of ¹H and ³¹P NMR spectroscopy data.

Table 7. 7 Estimation of the purity of the library amine derivates along with experimental data from performance of experiments

Crude product	Amine	1 M NaOH (Eq)	Purity (%)	Characterisation of the desired product
 <p>59</p>	83 μL	0	97 ^a 97 ^b 92 ^c	δ_{H} (700 MHz; CD ₃ OD) 7.61 (1 H, s, 2-CH), 7.52 (1 H, d, <i>J</i> 7.5, 5-CH), 7.46 (1 H, d, <i>J</i> 7.7, 4-CH), 7.43 (1 H, t, <i>J</i> 7.6, 6-CH), 7.32 (2 H, d, <i>J</i> 7.6, <i>o</i> -C ₆ H ₅ CH ₂ S), 7.23 (2 H, t, <i>J</i> 7.5, <i>m</i> -C ₆ H ₅ CH ₂ S), 7.15 (1 H, t, <i>J</i> 7.3, <i>p</i> -C ₆ H ₅ CH ₂ S), 3.91 (2 H, d, <i>J</i> 9.2, SCH ₂), 3.86 (2 H, d, <i>J</i> 10.1, CH ₂ NH); δ_{P} [¹ H](283 MHz; CD ₃ OD) 22.3 (qn, <i>J</i> 9.4, NHPS); δ_{F} (376 MHz; CD ₃ OD) -63.9 (s, CF ₃); δ_{C} (176 MHz; CD ₃ OD) 142.9 (d, ³ <i>J</i> _{C-P} 8.8, CCH ₂ NH), 140.1 (d, ³ <i>J</i> _{C-P} 5.1, <i>i</i> -C ₆ H ₅ CH ₂ S), 131.0 (4-CH), 130.0 (q, ² <i>J</i> _{C-F} 31.2, CCF ₃), 128.4 (<i>m</i> -C ₆ H ₅ CH ₂ S), 128.4 (5-CH), 127.9 (<i>o</i> -C ₆ H ₅ CH ₂ S), 126.2 (<i>p</i> -C ₆ H ₅ CH ₂ S), 124.4 (q, <i>J</i> _{C-F} 271.4, CF ₃), 123.9 (q, ³ <i>J</i> _{C-F} 3.9, 2-CH), 122.9 (q, ³ <i>J</i> _{C-F} 3.8, 6-CH), 45.4 (CH ₂ NH), 34.6 (SCH ₂), <i>m/z</i> (ES ⁻) 360.0442 (M - H. C ₁₅ H ₁₄ NO ₂ F ₃ PS requires 360.0440).
 <p>60</p>	83 μL	0	98 ^a 100 ^b 100 ^c	δ_{H} (700 MHz; CD ₃ OD) 7.83 (1 H, s, 2-CH), 7.65 (1 H, d, <i>J</i> 7.5, 5-CH), 7.48 (1 H, d, <i>J</i> 7.7, 4-CH), 7.46 (1 H, t, <i>J</i> 7.6, 6-CH), 4.12 (2 H, d, <i>J</i> 9.8, SCH ₂), 2.61 (2 H, dt, <i>J</i> 10.5 and 7.4, SCH ₂), 1.60 (2 H, sx, <i>J</i> 7.4, CH ₂ CH ₂ CH ₃), 0.99 (3 H, t, <i>J</i> 7.4, CH ₂ CH ₃); δ_{P} [¹ H](283 MHz; CD ₃ OD) 23.7 (m, NHPS); δ_{F} (376 MHz; CD ₃ OD) -63.9 (s, CF ₃); δ_{C} (176 MHz; CD ₃ OD) 142.9 (d, ³ <i>J</i> _{C-P} 7.4, CCH ₂ NH), 131.0 (4-CH), 130.0 (q, ² <i>J</i> _{C-F} 31.5, CCF ₃), 128.4 (5-CH), 124.3 (q, <i>J</i> _{C-F} 271.2, CF ₃), 123.9 (q, ³ <i>J</i> _{C-F} 3.2, 2-CH), 122.8 (q, ³ <i>J</i> _{C-F} 3.6, 6-CH), 45.4 (CH ₂ NH), 32.3 (SCH ₂), 24.2 (d, ³ <i>J</i> _{C-P} 6.8, CH ₂ CH ₂), 12.7 (CH ₂ CH ₃); <i>m/z</i> (ES ⁻) 312.0439 (M - H. C ₁₁ H ₁₄ NO ₂ F ₃ PS requires 312.0440).
 <p>62</p>	105 mg	0	98 ^a 96 ^b	δ_{H} (700 MHz; CD ₃ OD) 7.57 (2 H, dd, <i>J</i> 8.3 and 1.2, <i>o</i> -C ₆ H ₅ C ₆ H ₄ CH ₂ NH), 7.50 (2 H, d, <i>J</i> 8.4, <i>o</i> -C ₆ H ₅ C ₆ H ₄ CH ₂ NH), 7.40 (2 H, t, <i>J</i> 7.5, <i>m</i> -C ₆ H ₅ C ₆ H ₄ CH ₂ NH), 7.35 (2 H, d, <i>J</i> 8.4, <i>m</i> -C ₆ H ₅ C ₆ H ₄ CH ₂ NH), 7.29 (3 H, <i>p</i> -C ₆ H ₅ C ₆ H ₄ CH ₂ NH and <i>o</i> -C ₆ H ₅ CH ₂ S), 7.21 (2 H, d, <i>J</i> 7.6, <i>m</i> -C ₆ H ₅ CH ₂ S), 7.14 (1 H, t, <i>J</i> 7.5, <i>p</i> -C ₆ H ₅ CH ₂ S), 3.91 (2 H, d, <i>J</i> 9.1, SCH ₂), 3.85 (2 H, d, <i>J</i> 9.8, CH ₂ NH); δ_{P} [¹ H](283 MHz; CD ₃ OD) 22.5 (m, NHPS); δ_{C} (176 MHz; CD ₃ OD) 140.92 (CC), 140.50 (d, ³ <i>J</i> _{C-P} 8.5, CCH ₂ NH), 139.8 (d, ³ <i>J</i> _{C-P} 5.1, <i>i</i> -C ₆ H ₅ CH ₂ S), 139.5 (CC), 128.5 (<i>o</i> -C ₆ H ₄ CH ₂ S), 128.4 (<i>o</i> -C ₆ H ₅ C ₆ H ₄ CH ₂ NH), 127.9 (<i>m</i> -C ₆ H ₅ CH ₂ S), 127.8 (<i>m</i> -C ₆ H ₅ C ₆ H ₄ CH ₂ NH), 126.7 (<i>p</i> -C ₆ H ₅ C ₆ H ₄ CH ₂ NH), 126.4 (<i>o</i> -C ₆ H ₅ C ₆ H ₄ CH ₂ NH), 126.4 (<i>m</i> -C ₆ H ₅ C ₆ H ₄ CH ₂ NH), 126.2 (<i>p</i> -C ₆ H ₅ CH ₂ S), 45.6 (CH ₂ NH), 34.6 (SCH ₂); <i>m/z</i> (ES ⁻) 368.0879 (M - H. C ₂₀ H ₁₉ NO ₂ PS requires 368.0879).
	105 mg	0	98 ^a 95 ^b	δ_{H} (700 MHz; CD ₃ OD) 7.56 (2 H, d, <i>J</i> 7.8, <i>o</i> -C ₆ H ₅ C ₆ H ₄), 7.52 (2 H, d, <i>J</i> 8.3, <i>o</i> -C ₆ H ₅ C ₆ H ₄), 7.46 (2 H, d, <i>J</i> 8.4, <i>m</i> -C ₆ H ₅ C ₆ H ₄), 7.39 (1 H, t, <i>J</i> 7.7, <i>m</i> -C ₆ H ₅ C ₆ H ₄), 7.29 (1 H, d, <i>J</i> 7.7, <i>p</i> -C ₆ H ₅ C ₆ H ₄), 4.08 (2 H, d, <i>J</i> 9.8, CH ₂ NH), 2.63 (2 H, dt, <i>J</i> 10.5 and 7.4,

463				SCH_2), 1.61 (2 H, <i>sx</i> , J 7.4, $\text{CH}_2\text{CH}_2\text{CH}_3$), 0.95 (3 H, <i>t</i> , J 7.4, CH_2CH_3); $\delta_{\text{P}}[^1\text{H}]$ (283 MHz; CD_3OD) 22.5 (<i>m</i> , NHPS); δ_{C} (176 MHz; CD_3OD) 140.9 (<i>CC</i>), 140.5 (<i>d</i> , $^3J_{\text{C-P}}$ 8.5, CCH_2NH), 139.5 (<i>CC</i>), 128.4 (<i>o</i> - $\text{C}_6\text{H}_5\text{C}_6\text{H}_4$), 127.8 (<i>m</i> - $\text{C}_6\text{H}_5\text{C}_6\text{H}_4$), 126.7 (<i>p</i> - $\text{C}_6\text{H}_5\text{C}_6\text{H}_4$), 126.4 (<i>o</i> - $\text{C}_6\text{H}_5\text{C}_6\text{H}_4$), 126.4 (<i>m</i> - $\text{C}_6\text{H}_5\text{C}_6\text{H}_4$), 45.6 (CH_2NH), 32.4 (SCH_2), 24.2 (<i>d</i> , $^3J_{\text{C-P}}$ 6.7, CH_2CH_2), 12.8 (CH_2CH_3); m/z (ES^-) 320.0879 (<i>M</i> - <i>H</i> . $\text{C}_{16}\text{H}_{19}\text{NO}_2\text{PS}$ requires 320.0879).
 65	83 μL	0	95 ^a 97 ^b	δ_{H} (700 MHz; CD_3OD) 8.15 (1 H, <i>d</i> , J 8.5, 8- <i>CH</i>), 7.82 (1 H, <i>d</i> , J 8.0, 4- <i>CH</i>), 7.72 (1 H, <i>d</i> , J 8.1, 5- <i>CH</i>), 7.57 (1 H, <i>d</i> , J 6.8, 2- <i>CH</i>), 7.47 (1 H, <i>ddd</i> , J 8.4, 6.8 and 1.5, 7- <i>CH</i>), 7.43 (1 H, <i>ddd</i> , J 8.4, 7.0 and 1.4, 6- <i>CH</i>), 7.39 (1 H, <i>d</i> , J 6.8, 2- <i>CH</i>), 7.36 (1 H, <i>m</i> , 3- <i>CH</i>), 7.33 (2 H, <i>d</i> , J 7.6, <i>o</i> - $\text{C}_6\text{H}_5\text{CH}_2\text{S}$), 7.23 (2 H, <i>d</i> , J 7.6, <i>m</i> - $\text{C}_6\text{H}_5\text{CH}_2\text{S}$), 7.15 (1 H, <i>t</i> , J 7.4, <i>p</i> - $\text{C}_6\text{H}_5\text{CH}_2\text{S}$), 4.30 (2 H, <i>d</i> , J 7.4, CH_2NH), 4.30 (2 H, <i>d</i> , J 10.2, SCH_2); $\delta_{\text{P}}[^1\text{H}]$ (283 MHz; CD_3OD) 22.3 (<i>m</i> , NHPS); δ_{C} (176 MHz; CD_3OD) 140.2 (<i>d</i> , $^3J_{\text{C-P}}$ 4.0, <i>i</i> - $\text{C}_6\text{H}_5\text{CH}_2\text{S}$), 136.3 (<i>d</i> , $^3J_{\text{C-P}}$ 9.0, <i>i</i> - $\text{C}_6\text{H}_4\text{CH}_2\text{NH}$), 133.9 (10- <i>C</i>), 131.5 (9- <i>C</i>), 128.1 (5- <i>CH</i>), 128.0 (<i>o</i> - $\text{C}_6\text{H}_5\text{CH}_2\text{S}$), 127.2 (4- <i>CH</i>), 127.1 (<i>m</i> - $\text{C}_6\text{H}_5\text{CH}_2\text{S}$), 126.3 (<i>p</i> - $\text{C}_6\text{H}_5\text{CH}_2\text{S}$), 125.5 (7- <i>CH</i>), 125.23 (6- <i>CH</i>), 125.15 (3- <i>CH</i>), 125.00 (2- <i>CH</i>), 123.5 (8- <i>CH</i>), 43.6 (CH_2NH), 34.6 (SCH_2); m/z (ES^-) 342.0723 (<i>M</i> - <i>H</i> . $\text{C}_{18}\text{H}_{17}\text{NO}_2\text{PS}$ requires 342.0723).
 66	83 μL	0	98 ^a 98 ^b	δ_{H} (700 MHz; CD_3OD) 8.24 (1 H, <i>d</i> , J 8.3, 8- <i>CH</i>), 7.84 (1 H, <i>d</i> , J 8.1, 4- <i>CH</i>), 7.75 (1 H, <i>d</i> , J 8.2, 5- <i>CH</i>), 7.57 (1 H, <i>d</i> , J 6.8, 2- <i>CH</i>), 7.50 (1 H, <i>ddd</i> , J 8.3, 6.8 and 1.3, 7- <i>CH</i>), 7.43 (1 H, <i>ddd</i> , J 8.4, 6.9 and 1.4, 6- <i>CH</i>), 7.40 (1 H, <i>dd</i> , J 8.1, 7.1), 4.51 (2 H, <i>d</i> , J 7.7, CH_2NH), 2.64 (2 H, <i>dt</i> , J 10.5 and 7.4, SCH_2), 1.63 (2 H, <i>sx</i> , J 7.4, $\text{CH}_2\text{CH}_2\text{CH}_3$), 0.95 (3 H, <i>t</i> , J 7.4, CH_2CH_3); $\delta_{\text{P}}[^1\text{H}]$ (283 MHz; CD_3OD) 23.7 (<i>m</i> , NHPS); δ_{C} (176 MHz; CD_3OD) 136.3 (<i>d</i> , $^3J_{\text{C-P}}$ 9.0, <i>i</i> - $\text{C}_6\text{H}_4\text{CH}_2\text{NH}$), 133.9 (10- <i>C</i>), 131.5 (9- <i>C</i>), 128.1 (5- <i>CH</i>), 127.2 (4- <i>CH</i>), 125.5 (7- <i>CH</i>), 125.2 (6- <i>CH</i>), 125.2 (3- <i>CH</i>), 125.0 (2- <i>CH</i>), 123.5 (8- <i>CH</i>), 43.6 (CH_2NH), 32.2 (SCH_2), 24.0 (<i>d</i> , $^3J_{\text{C-P}}$ 6.5, CH_2CH_2), 12.5 (CH_2CH_3); m/z (ES^-) 294.0723 (<i>M</i> - <i>H</i> . $\text{C}_{14}\text{H}_{17}\text{NO}_2\text{PS}$ requires 294.0723).
 68	142 mg	0.2	92 ^a 94 ^b	δ_{H} (700 MHz; CD_3OD) 7.56 (1 H, <i>d</i> , J 7.7, 2- $\text{C}_6\text{H}_4\text{CH}_2\text{OH}$), 7.54 (1 H, <i>d</i> , J 7.7, 2- $\text{C}_6\text{H}_4\text{CH}_2\text{NH}$), 7.28–7.10 (9 H, <i>m</i> , $\text{C}_{12}\text{H}_8\text{S}$ and C_6H_5), 7.04 (2 H, <i>d</i> , J 7.0, 9- <i>CH</i>), 7.04 (2 H, $2 \times \text{d}$, J 7.7, 5- $\text{C}_6\text{H}_4\text{CH}_2\text{OH}$ and 5- $\text{C}_6\text{H}_4\text{CH}_2\text{NH}$), 4.71 (2 H, <i>s</i> , CH_2OH), 4.06 (2 H, <i>d</i> , J 9.4, CH_2NH), 3.81 (2 H, <i>d</i> , J 9.2, SCH_2); $\delta_{\text{P}}[^1\text{H}]$ (283 MHz; CD_3OD) 22.6 (<i>qn</i> , J 9.6, NHPS); δ_{C} (176 MHz; CD_3OD) 141.9 (CCH_2OH), 139.9 (<i>i</i> - $\text{C}_6\text{H}_5\text{CH}_2\text{S}$), 133.0 (1- $\text{C}_6\text{H}_4\text{CH}_2\text{OH}$), 132.8 (1- $\text{C}_6\text{H}_4\text{CH}_2\text{NH}_2$), 131.3 (<i>d</i> , $^3J_{\text{C-P}}$ 8.1, CCH_2NH), 128.8–126.4 ($12 \times \text{s}$, $\text{C}_{12}\text{H}_8\text{S}$ and $\text{C}_6\text{H}_4\text{CH}_2\text{S}$), 126.5 (<i>p</i> - $\text{C}_6\text{H}_4\text{CH}_2\text{S}$), 61.3 (CH_2OH), 46.1 (CH_2NH), 35.4 (SCH_2); m/z (ES^-) 430.0710 (<i>M</i> - <i>H</i> . $\text{C}_{21}\text{H}_{21}\text{NO}_3\text{PS}_2$ requires 430.0705).

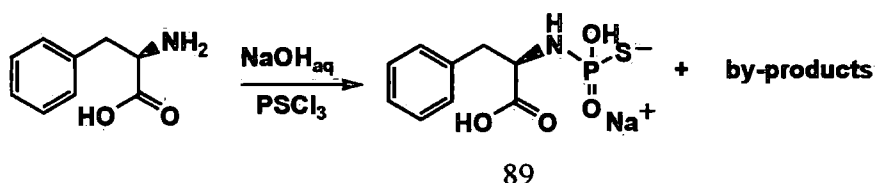
 <p>69</p>	142 mg	0.2	93 ^a 94 ^b	<p>δ_{H}(700 MHz; CD₃OD) 7.64 (1 H, d, <i>J</i> 7.7, 2-C₆H₄CH₂OH), 7.54 (1 H, d, <i>J</i> 7.7, 2-C₆H₄CH₂NH), 7.28 (1 H, t, <i>J</i> 7.5, 3-C₆H₄CH₂OH), 7.25 (1 H, t, <i>J</i> 7.5, 3-C₆H₄CH₂NH), 7.17 (1 H, t, <i>J</i> 7.6, 4-C₆H₄CH₂OH), 7.14 (1 H, t, <i>J</i> 7.6, 4-C₆H₄CH₂NH), 7.06 (1 H, d, <i>J</i> 7.7, 5-C₆H₄CH₂OH), 7.06 (1 H, d, <i>J</i> 7.7, 5-C₆H₄CH₂NH), 4.72 (2 H, s, CH₂OH), 4.17 (2 H, d, <i>J</i> 9.4, CH₂NH), 2.56 (2 H, dt, <i>J</i> 10.5 and 7.4, SCH₂), 1.60 (2 H, sx, <i>J</i> 7.4, CH₂CH₂CH₃), 0.90 (3 H, t, <i>J</i> 7.4, CH₂CH₃); $\delta_{\text{P}}[^1\text{H}]$(283 MHz; CD₃OD) 23.9 (qn, <i>J</i> 9.6, NHPS); δ_{C}(176 MHz; CD₃OD) 141.9 (CCH₂OH), 133.0 (1-C₆H₄CH₂OH), 132.8 (1-C₆H₄CH₂NH₂), 131.3 (d, ³<i>J</i>_{C-P} 11.2, CCH₂NH), 129.1 (C₁₂H₈S), 127.9 (C₁₂H₈S), 127.5 (C₁₂H₈S), 127.4 (C₁₂H₈S), 127.3 (C₁₂H₈S), 62.3 (CH₂OH), 46.1 (CH₂NH), 35.4 (SCH₂), 27.2 (d, ³<i>J</i>_{C-P} 6.2, CH₂CH₂), 16.8 (CH₂CH₃); <i>m/z</i> (ES⁻) 382.0709 (M - H. C₁₇H₂₁NO₃PS₂ requires 382.0706).</p>
 <p>71</p>	156 mg	0.2	94 ^a 97 ^b	<p>δ_{H}(700 MHz; CD₃OD) 8.39 (1 H, d, <i>J</i> 9.2, 3-CH), 8.14 (2 H, 2 × d, <i>J</i> 7.4, 6- and 8-CH), 8.07 (1 H, d, <i>J</i> 7.0, 2-CH), 8.06 (1 H, d, <i>J</i> 7.7, 10-CH), 8.00 (2 H, m, 4- and 5-CH), 7.95 (1 H, t, <i>J</i> 7.6, 7-CH), 7.94 (1 H, d, <i>J</i> 7.6, 9-CH), 7.30 (2 H, d, <i>J</i> 7.3, <i>o</i>-C₆H₅CH₂S), 7.18 (2 H, t, <i>J</i> 7.6, <i>m</i>-C₆H₅CH₂S), 7.12 (1 H, t, <i>J</i> 7.4, <i>p</i>-C₆H₅CH₂S), 4.56 (2 H, d, <i>J</i> 7.7, CH₂NH), 3.89 (2 H, d, <i>J</i> 10.2, SCH₂); $\delta_{\text{P}}[^1\text{H}]$(283 MHz; CD₃OD) 22.2 (m, NHPS); δ_{C}(176 MHz; CD₃OD) 140.1 (CCH₂NH), 134.2 (<i>i</i>-C₆H₅CH₂S), 131.3 (4° pyrene), 130.8 (4° pyrene), 130.5 (4° pyrene), 128.5 (4° pyrene), 128.4 (<i>o</i>-C₆H₄CH₂S), 127.9 (<i>m</i>-C₆H₄CH₂S), 127.0 (pyrene), 126.9 (pyrene), 126.5 (pyrene), 126.4 (pyrene), 126.2 (<i>p</i>-C₆H₄CH₂S), 125.5 (pyrene), 124.5 (pyrene), 124.4 (pyrene), 123.1 (3-CH), 43.7 (CH₂NH), 34.5 (SCH₂); <i>m/z</i> (ES⁻) 416.0881 (M - H. C₂₄H₁₉NO₂PS requires 416.0879)</p>
 <p>72</p>	156 mg	0.2	97 ^a 98 ^b	<p>δ_{H}(700 MHz; CD₃OD) 8.39 (1 H, d, <i>J</i> 9.2, 3-CH), 8.14 (2 H, 2 × d, <i>J</i> 8.3, 8- and 6-CH), 8.11 (2 H, m, 9- and 10-CH), 8.07 (1 H, d, <i>J</i> 9.2, 2-CH), 8.06 (2 H, m, 4- and 5-CH), 7.96 (1 H, t, <i>J</i> 7.6, 7-CH), 4.46 (2 H, d, <i>J</i> 7.7, CH₂NH), 2.63 (2 H, dt, <i>J</i> 9.8 and 7.4, SCH₂), 1.60 (2 H, sx, <i>J</i> 7.4, CH₂CH₂CH₃), 0.94 (3 H, t, <i>J</i> 7.4, CH₂CH₃); $\delta_{\text{P}}[^1\text{H}]$(283 MHz; CD₃OD) 22.2 (m, NHPS); δ_{C}(176 MHz; CD₃OD) 134.4 (d, ³<i>J</i>_{C-P} 11.7, CCH₂NH), 131.3 (4° pyrene), 130.8 (4° pyrene), 130.5 (4° pyrene), 128.5 (4° pyrene), 127.0 (pyrene), 126.9 (pyrene), 126.5 (pyrene), 126.4 (pyrene), 125.5 (pyrene), 124.5 (pyrene), 124.4 (pyrene), 124.3 (3-CH), 44.1 (CH₂NH), 32.5 (SCH₂), 24.2 (d, ³<i>J</i>_{C-P} 6.7, CH₂CH₂), 12.7 (CH₂CH₃); <i>m/z</i> (ES⁻) 368.0883 (M - H. C₂₀H₁₉NO₂PS requires 368.0879).</p>
 <p>74</p>	178 mg	0	99 ^a 100 ^b	<p>δ_{H}(700 MHz; CD₃OD) 8.58 (2 H, d, <i>J</i> 8.9, 1- and 8-CH), 8.38 (1 H, s, 10-CH), 7.95 (2 H, d, <i>J</i> 8.3, 4- and 5-CH), 7.50 (2 H, d, <i>J</i> 7.3, <i>o</i>-C₆H₅CH₂S), 7.48–7.43 (2 H, 2 × t, <i>J</i> 7.4, 2- and 7-CH), 7.43–7.38 (2 H, 2 × t, <i>J</i> 7.4, 3- and 6-CH), 7.33 (2 H, t, <i>J</i> 7.6, <i>m</i>-C₆H₅CH₂S), 7.23 (1 H, t, <i>J</i> 7.3, <i>p</i>-C₆H₅CH₂S), 4.99 (2 H, d, <i>J</i> 3.8, CH₂NH), 4.15 (2 H, d, <i>J</i> 10.5, SCH₂), 2.19 (3 H, d, <i>J</i> 12.6, NCH₃); $\delta_{\text{P}}[^1\text{H}]$(283 MHz; CD₃OD) 23.5 (m, NHPS); δ_{C}(176</p>

				7.6, CH ₂ CH ₂), 24.3 (d, ³ J _{C-P} 6.0, CH ₂ CH ₃), 12.8 (CH ₂ CH ₃); <i>m/z</i> (ES ⁻) 281.10967 (M - H. C ₁₀ H ₂₂ N ₂ O ₃ PS requires 281.10943).
	70 μL	0.75	95 ^a 82 ^b	δ_{H} (700 MHz; CD ₃ OD) 8.42 (1 H, ddd, <i>J</i> 5.0, 1.7 and 0.9, 6-CH), 7.74 (1 H, td, <i>J</i> 7.7 and 1.8, 4-CH), 7.37 (1 H, d, <i>J</i> 7.8, 3-CH), 7.24 (1 H, ddd, <i>J</i> 7.5, 5.0 and 0.9, 5-CH), 3.22 (2 H, dt, <i>J</i> 9.8 and 7.2, CH ₂ CH ₂ NH), 2.98 (2 H, t, <i>J</i> 7.2, CH ₂ CH ₂ NH), 2.55 (2 H, dt, <i>J</i> 9.8 and 7.2, SCH ₂), 1.58 (2 H, sx, <i>J</i> 7.4, CH ₂ CH ₃), 0.93 (3 H, t, <i>J</i> 7.4, CH ₂ CH ₃); $\delta_{\text{P}}[^1\text{H}]$ (283 MHz; CD ₃ OD) 24.0 (m, NHPS); δ_{C} (176 MHz; CD ₃ OD) 160.1 (2-CH), 148.5 (6-CH), 137.3 (4-CH), 124.0 (3-CH), 121.7 (5-CH), 41.8 (CH ₂ CH ₂ NH), 39.4 (d, ³ J _{C-P} 8.3, CH ₂ CH ₂ NH), 32.3 (SCH ₂), 24.2 (d, ³ J _{C-P} 6.2, CH ₂ CH ₃), 12.8 (CH ₂ CH ₃); <i>m/z</i> (ES ⁻) 259.06778 (M - H. C ₁₀ H ₁₆ N ₂ O ₂ PS requires 259.06756)
	67 μL	0.75	96 ^a 96 ^b 100 ^c	δ_{H} (700 MHz; CD ₃ OD) 7.40 (2 H, m, CH=CCH ₂), 6.98 (2 H, m, FC=CH), 4.01 (2 H, d, <i>J</i> 9.1, CH ₂ NH), 2.61 (2 H, dt, <i>J</i> 10.5 and 7.4, SCH ₂), 1.61 (2 H, sx, <i>J</i> 7.4, CH ₂ CH ₃), 0.95 (3 H, t, <i>J</i> 7.4, CH ₂ CH ₃); $\delta_{\text{P}}[^1\text{H}]$ (283 MHz; CD ₃ OD) 23.7 (m, NHPS); δ_{F} (376 MHz; CD ₃ OD) -119.0 (s, F); δ_{C} (176 MHz; CD ₃ OD) 162.0 (d, <i>J</i> 243.2, FC), 137.7 (d, ³ J _{C-P} 8.3, <i>i</i> -C ₆ H ₅ CH ₂ NH), 129.3 (d, ³ J _{C-P} 8.1, FC=CH=CH), 114.5 (d, ² J _{C-P} 21.8, FC=CH=CH), 45.2 (CH ₂ NH), 32.4 (SCH ₂), 24.2 (d, ³ J _{C-P} 6.9, CH ₂ CH ₃), 12.7 (CH ₂ CH ₃); <i>m/z</i> (ES ⁻) 262.04744 (M - H. C ₁₀ H ₁₄ NO ₂ FPS requires 262.04724)
	83 μL	0.75	79 ^a 87 ^b	δ_{H} (700 MHz; CD ₃ OD) 7.63 (1 H, d, <i>J</i> 7.4, 5-CH), 7.06 (2 H, m, 6- and 7-CH), 6.99 (1 H, d, <i>J</i> 7.4, 8-CH), 4.34-4.29 (1 H, m, CHNH), 2.72 (2 H, m, 3-CH ₂), 2.70 (2 H, m, SCH ₂), 2.11-2.05 (1 H, m, 4-CH ₂), 1.95-1.90 (1 H, m, 4-CH ₂), 1.89-1.83 (1 H, m, 2-CH ₂), 1.78-1.72 (2 H, m, 2-CH ₂), 1.67 (2 H, sx, <i>J</i> 7.4, CH ₂ CH ₃), 0.99 (3 H, t, <i>J</i> 7.4, CH ₂ CH ₃); $\delta_{\text{P}}[^1\text{H}]$ (283 MHz; CD ₃ OD) 22.1 (m, NHPS); δ_{C} (176 MHz; CD ₃ OD) 140.3 (d, ³ J _{C-P} 5.7, CCHNH), 136.9 (10-C), 129.1 (5-CH), 128.3 (8-CH), 126.3 (6-CH), 125.4 (7-CH), 49.9 (CHNH), 32.7 (2-CH), 32.5 (SCH ₂), 29.2, (4-CH), 24.2 (d, ³ J _{C-P} 6.8, CH ₂ CH ₃), 20.0 (3-CH), 12.8 (CH ₂ CH ₃); <i>m/z</i> (ES ⁻) 284.0882 (M - H. C ₁₃ H ₁₉ NO ₂ PS requires 284.08796)
	48 μL	0	95 ^a 92 ^b	δ_{H} (700 MHz; CD ₃ OD) 7.38 (2 H, d, <i>J</i> 7.3, <i>o</i> -C ₆ H ₅ CH ₂ S), 7.28 (2 H, t, <i>J</i> 7.6, <i>m</i> -C ₆ H ₅ CH ₂ S), 7.21 (1 H, t, <i>J</i> 7.3, <i>p</i> -C ₆ H ₅ CH ₂ S), 3.89 (2 H, d, <i>J</i> 10.0, SCH ₂), 2.68 (2 H, dt, <i>J</i> 8.5 and 7.5, CH ₂ NH), 1.39 (2 H, sx, <i>J</i> 7.4, CH ₃ CH ₂), 0.87 (3 H, t, <i>J</i> 7.5, CH ₃ CH ₂); $\delta_{\text{P}}[^1\text{H}]$ (283 MHz; CD ₃ OD) 23.1 (m, NHPS); δ_{C} (176 MHz; CD ₃ OD) 140.2 (d, ³ J _{C-P} 6.5, <i>i</i> -C ₆ H ₅ CH ₂ S), 128.7 (<i>m</i> -C ₆ H ₅), 128.2 (<i>o</i> -C ₆ H ₅), 126.5 (<i>p</i> -C ₆ H ₅), 43.7 (CH ₂ NH), 34.6 (d, ² J _{C-P} 2.9, SCH ₂), 24.5 (d, ³ J _{C-P} 8.7, CH ₂ CH ₃), 10.7 (CH ₂ CH ₃); <i>m/z</i> (ES ⁻) 244.0562 (M - H. C ₁₀ H ₁₅ NO ₂ PS requires 244.0566)

^a Determined by ³¹P NMR spectroscopy. ^b Determined by ¹H NMR spectroscopy. ^c Determined by ¹⁹F NMR spectroscopy.

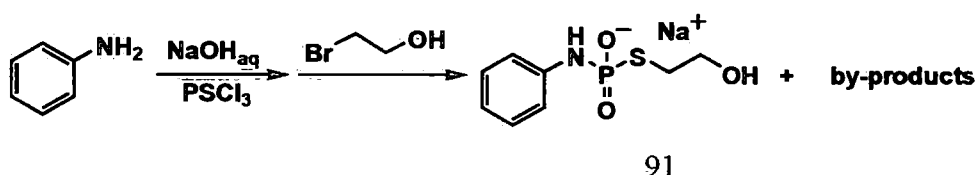
7.6.5. 'Challenging' amines: phenylalanine, aniline, D-glucosamine

Phenylalanine: The aqueous thiophosphorylation was performed as it was described for the ethanolamine (section 7.) using an excess of thiophosphoryl chloride (1.2 Eq). The conversions we estimated using ^{31}P NMR spectroscopy (70%) and ^1H NMR spectroscopy (95%). No alkylation product was gained. Other impurities were phosphoramidate of phenylalanine (3% by ^{31}P NMR spectroscopy and 6% by ^1H NMR spectroscopy), inorganic thiophosphate (19% by ^{31}P NMR spectroscopy) and a number of unidentified impurities. Carbon NMR not assigned owing to the low intensity of the spectrum.



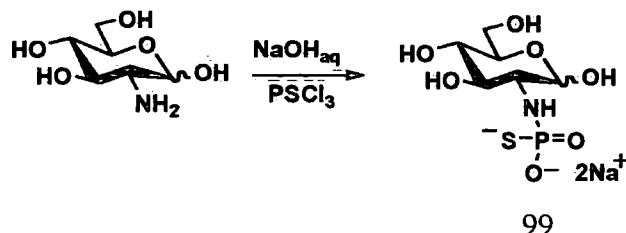
δ_{H} (400 MHz; D_2O) 7.26–7.17 (6 H, m, C_6H_5), 3.82–3.75 (1 H, ddd, J 12.4, 7.9, 4.5, CH_x), 3.07 (1 H, ABX system, J_{AB} 13.0 and J_{BX} 4.5, CH_AH_B), 2.83 (1 H, ABX system, J_{AB} 13.0 and J_{AX} 7.9, $5' -\text{CH}_A\text{H}_B$); δ_{P} (162 MHz; D_2O) 42.4 (d, $^3J_{\text{H-P}}$ 12.4, NPS); m/z (ES^+) 262.03 ($\text{M} + \text{H}^+$); m/z (ES^-) 244.0383 (phosphoramidate, ($\text{M} - \text{H}$). $\text{C}_9\text{H}_{11}\text{NO}_5\text{P}$ requires 244.0380).

Aniline: The one-pot method was applied (section 2.) using bromoethanol (4.6 mmol, 326 μL) as alkylation agent. The conversions we estimated using ^{31}P NMR spectroscopy (47%) and ^1H NMR spectroscopy (41%). The other impurities present were aniline 19% and alkylated inorganic thiophosphosphate 31% by both ^{31}P NMR and ^1H NMR spectroscopy.



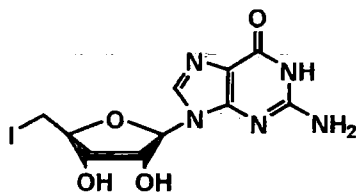
δ_{H} (400 MHz; D_2O) 7.26 (2 H, t, J 7.9, $m\text{-C}_6\text{H}_5$), 7.09 (2 H, d, J 8.0, $o\text{-C}_6\text{H}_5$), 6.94 (1 H, m, $p\text{-C}_6\text{H}_5$), 3.57 (2 H, t, J 6.4, CH_2OH), 2.78 (2 H, dt, J 11.9 and 6.4, SCH_2); δ_{P} (162 MHz; D_2O) 18.7 (t, $^3J_{\text{H-P}}$ 13.4, NPS); δ_{C} (101 MHz; D_2O) 141.7 ($i\text{-C}_6\text{H}_5$), 129.4 ($m\text{-C}_6\text{H}_5$), 121.3 ($p\text{-C}_6\text{H}_5$), 118.2 (d, $^3J_{\text{C-P}}$ 6.5, $o\text{-C}_6\text{H}_5$), 61.6 (d, $^3J_{\text{C-P}}$ 5.1, CH_2OH), 32.1 (SCH_2); m/z (ES^-) 232.0203 ($\text{M} - \text{H}$. $\text{C}_8\text{H}_{11}\text{NO}_3\text{PS}$ requires 232.0203).

D-glucosamine: The aqueous thiophosphorylation was performed as it was described for the ethanolamine (section 7.). The conversions we estimated using ^{31}P NMR spectroscopy (65%, 32+33% for α and β) and ^1H NMR spectroscopy (63%). The other impurities present were D-glucosamine and broad peak at ~ 38 ppm. Carbon NMR not assigned owing to the low intensity of the spectrum.



δ_{H} (400 MHz; D_2O) 5.21 (1 H, m, α -CH), 4.47 (1 H, m, β -CH), 3.80–3.22 (12 H, m, GlcNH);
 δ_{P} (162 MHz; D_2O) 44.7 (d, $^3J_{\text{H-P}}$ 11, α -NPS), 42.7 (d, $^3J_{\text{H-P}}$ 11.3, β -NPS).

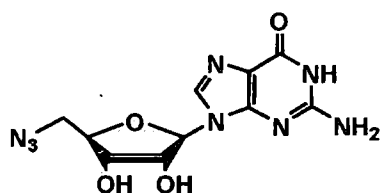
7.7. Preparation of 5'-deoxy-5'-iodoguanosine⁹⁹



Iodine (13.34 g, 52 mmol) was added over 5 minutes to a stirred suspension of guanosine (5 g, 17.66 mmol), triphenylphosphine (14.6 g, 55.7 mmol), imidazole (7.5 g, 110 mmol) and *N*-methyl pyrrolidinone (68 mL, dried over activated molecular sieves) in a 500 mL round-bottomed flask. In order to minimize the entry of light and moisture the flask was covered with aluminium foil and fitted with a calcium chloride drying tube. Due the course of 3 h of stirring at room temperature the solid dissolved and the solution became bright yellow. DCM (670 mL) and water (200 mL) were then added to the reaction mixture, which caused the precipitation of a white solid. The reaction mixture transferred was into a 1 L glass bottle and placed in the cold room for 48 h to maximise precipitation. The white solid was collected on a Büchner funnel and the crude material was then refluxed for 1 h in DCM (200 mL) and then in water (200 mL). The solid was collected on a Büchner funnel and dried overnight in an oven at 95 °C to afford in white powder of 5'-deoxy-5'-iodoguanosine (3.82 g, 55 %). mp= 200 °C (dec); δ_{H} (400 MHz; $\text{DMSO}-d_6$) 10.68 (1 H, s, NH), 7.94 (1 H, s, 8-H), 6.50 (2 H, s, NH_2), 5.72 (1 H, d, J 6.4, 1'-H),

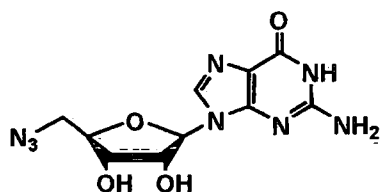
5.56 (1 H, d, J 6.0, 2'-OH), 5.40 (1 H, d, J 4.8, 3'-OH), 4.64 (1 H, q, J 4.8, 2'-H), 4.18–3.99 (1 H, m, 3'-H), 3.99–3.82 (1 H, m, 4'-CH_x), 3.57 (1 H, ABX system, J_{AB} 10.4 and J_{BX} 6.0, 5'-CH_AH_B), 3.42 (1 H, ABX system, J_{AB} 10.4 and J_{AX} 6.7, 5'-CH_AH_B); δ_C (101 MHz; DMSO-*d*₆) 156.7 (6-C), 153.5 (2-C), 151.4 (4-C), 135.8 (8-C), 116.7 (5-C), 86.5 (1'-C), 83.7 (4'-C), 73.1 (2'-C), 72.7 (3'-C), 7.9 (5'-CH₂I); m/z (ES⁺) 415.9828 (M + Na⁺. C₁₀H₁₂N₅O₄INa requires 415.9826).

7.8. Preparation of 5'-azido-5'-deoxyguanosine⁵⁵



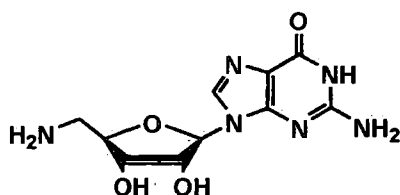
5'-deoxy-5'-iodoguanosine (2.265 g, 5.76mmol) was suspended in *N,N*-dimethylformamide (24 mL, dried over molecular sieves). Sodium azide (0.865 g, 13.31 mol) was then added to the mixture in a flask fitted with an air condenser kept under a nitrogen atmosphere and stirred for 20 h at 80 °C. [CAUTION: used blast shield]. After cooling to room temperature, the solvent was removed under reduced pressure to give a white solid. Water (100 mL) was added to the solid and the mixture was stirred for 30 minutes to remove any remaining sodium azide. The crude white solid was collected on a Hirsch funnel and washed with cold water (2 × 40 mL) to remove residual inorganic azide. To remove water the solid was washed with cold ethanol (28 mL) and then with diethyl ether (20 mL) to remove ethanol. The white powder was dried in a vacuum desiccator to give 5'-azido-5'-deoxyguanosine (0.842 g, 47%). mp=205° C (dec); δ_H (400 MHz; DMSO-*d*₆) 7.89 (1 H, s, 8-H), 6.52 (2 H, s, NH₂), 5.70 (1 H, d, J 5.6, 1'-H), 5.54 (1 H, br s, 2'-OH), 5.40 (1 H, br s, 3'-OH), 4.56 (1 H, t, J 5.2, 2'-H), 4.07–3.99 (1 H, m, 3'-H), 3.99–3.82 (1 H, m, 4'-CH_x), 3.64 (1 H, ABX system, J_{AB} 13.2 and J_{BX} 7.2, 5'-CH_AH_B), 3.48 (1 H, ABX system, J_{AB} 13.2 and J_{AX} 3.2, 5'-CH_AH_B); δ_C (101 MHz; DMSO-*d*₆) 156.9 (6-C), 153.7 (2-C), 151.3 (4-C), 135.8 (8-C), 116.8 (5-C), 86.8 (1'-C), 82.8 (4'-C), 72.6 (2'-C), 70.9 (3'-C), 51.8 (5'-CH₂N₃); m/z (ES⁺) 331.0876 (M + Na⁺. C₁₀H₁₂N₈O₄Na requires 331.0873).

7.9. Aqueous method for preparation of 5'-azido-5'-deoxyguanosine



Sodium azide (650 mg, 3.08 mmol) was added to a stirred suspension of 5'-deoxy-5'-iodoguanosine (200 mg, 0.5 mmol) in water (5 mL) and the mixture was heated at 110 °C in an oil bath for 20 h. [CAUTION: used blast shield]. The solution was then transferred into a centrifuge tube and chilled for 3 days, upon which a white precipitate was formed. The suspension was centrifuged, the supernatant was decanted, and the precipitate was allowed to stand repeatedly in cold water (3 × 2 mL) and re-centrifuged. The precipitate was then dried overnight in a vacuum desiccator to give rise to a white powder of 5'-azido-5'-deoxyguanosine (64.5 mg, 42%). mp= 200 °C (dec); δ_{H} (400 MHz; DMSO- d_6) 7.91 (1 H, s, 8-*H*), 6.56 (2 H, s, NH₂), 5.72 (1 H, d, *J* 6.0, 1'-*H*), 5.54 (1 H, br s, 2'-OH), 5.40 (1 H, br s, 3'-OH), 4.58 (1 H, t, *J* 5.6, 2'-*H*), 4.07–3.99 (1 H, m, 3'-*H*), 3.99–3.82 (1 H, m, 4'-CH_x), 3.66 (1 H, ABX system, *J*_{AB} 13.2 and *J*_{BX} 6.8, 5'-CH_AH_B), 3.53 (1 H, ABX system, *J*_{AB} 13.2 and *J*_{AX} 4.0, 5'-CH_AH_B); δ_{C} (101 MHz; DMSO- d_6) 156.9 (6-*C*), 153.7 (2-*C*), 151.3 (4-*C*), 135.8 (8-*C*), 116.8 (5-*C*), 86.8 (1'-*C*), 82.8 (4'-*C*), 72.6 (2'-*C*), 70.9 (3'-*C*), 51.8 (5'-CH₂N₃); *m/z* (ES⁺) 331.0875 (M + Na⁺. C₁₀H₁₂N₈O₄Na requires 331.0873).

7.10. Aqueous method for preparation of 5'-amino-5'-deoxyguanosine

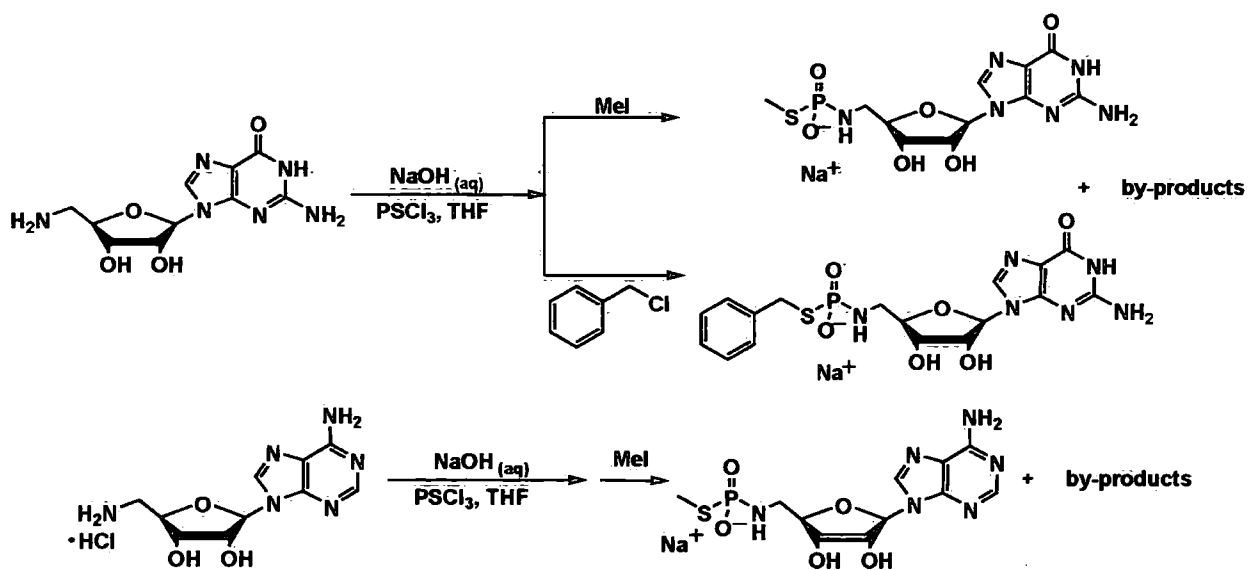


Sodium thiophosphate (518 mg, 2.88 mmol) was added to a stirred suspension of 5'-azido-5'-deoxyguanosine (740 mg, 2.4 mmol) in water (27.75 mL). The mixture was heated at 110 °C in an oil bath for 1 h to give a pale orange solution. The solution was then transferred into a centrifuge tube and chilled overnight. The beige precipitate was collected by centrifugation and washed with cold water (~5 × 10 mL) until the washings were colourless. The product was dried in a vacuum desiccator overnight yielding in light beige powder of 5'-amino-5'-

deoxyguanosine (470 mg, 70%). mp= 210 °C (dec.); (lit.,⁵⁵ 219-220 °C (from water) and lit.,¹³⁹ 221 °C); δ_H (400 MHz; DMSO-*d*₆) 7.93 (1 H, s, 8-*H*), 6.56 (2 H, s, NH₂), 5.67 (1 H, d, *J* 6.0, 1'-*H*), 4.46 (1 H, t, *J* 5.6, 2'-*H*), 4.09 (1 H, t, *J* 4.8, 3'-*H*), 3.77–3.83 (1 H, m, 4'-CH_x), 2.77 (1 H, *ABX* system, *J*_{AB} 13.2 and *J*_{BX} 4.4, 5'-CH_AH_B), 2.75 (1 H, *ABX* system, *J*_{AB} 13.2 and *J*_{AX} 5.2, 5'-CH_AH_B); δ_C (101 MHz; DMSO-*d*₆) 157.2 (6-*C*), 153.9 (2-*C*), 151.4 (4-*C*), 135.8 (8-*C*), 116.8 (5-*C*), 86.4 (1'-*C*), 85.5 (4'-*C*), 73.2 (2'-*C*), 70.7 (3'-*C*), 43.5 (5'-CH₂NH₂); *m/z* (ES⁺) 283.1151 (M + H⁺. C₁₀H₁₅N₆O₄ requires 283.1149).

7.11. Nucleosides in the one-pot method for the preparation of alkylated thiophosphoramidates:

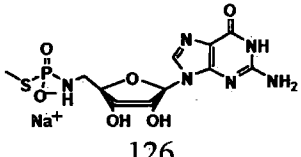
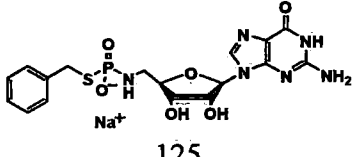
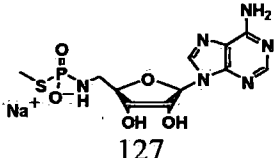
7.11.1. Nucleoside amines: guanosine and adenosine



5'-Amino-5'-deoxynucleoside (1 Eq, 0.23 mmol, table 7.10) was dissolved in a mixture of aqueous sodium hydroxide and water (table 7.10) in a 50 mL round bottomed flask with indents in an ice bath. Thiophosphoryl chloride (1 Eq, 23.2 μ L, 0.23 mmol) in THF (0.7 mL) was added dropwise to the aqueous solution over the course of 10 minutes and the mixture was then stirred for a further one hour. Methyl iodide (2 Eq, 28.6 μ L, 0.46 mmol) or benzyl chloride (2 Eq, 52.9 μ L, 0.46 mL), with additional aqueous sodium hydroxide solution (1 Eq) were added to the flask and stirring was continued for 1 h. The excess of alkylation agent was removed by ether extraction (3 \times 10 mL). The residual aqueous solution was then lyophilised

and analysed. Experimental details concerning amounts of the components used along with the conversions achieved are presented in the table 7.7

Table 7. 8 Nucleoside amines reaction details

Crude product	5'-Amino-5'-deoxy nucleoside (mg)	1M NaOH (Eq)	H ₂ O (μL)	Purity (%)
 126	G-NH ₂ 61	5	148	74 ^a 69 ^b
 125	G-NH ₂ 61	5	148	78 ^a 76 ^b
 127	A-NH ₂ •2HCl ^d 75	7	/	71 ^a 74 ^b

^a Determined by ³¹P NMR spectroscopy. ^b Determined by ¹H NMR spectroscopy. ^d 5'-Amino-5'-deoxy adenosine dihydrochloride, used in the experiment, was made by the project student, Gemma R. Freeman.

In contrast to compound 125 that was characterised as crude material, crude compounds 126 and 127 were analysed following purification *via* ion exchange chromatography and will be presented in further text.

Crude compound 125: δ_{H} (400 MHz; D₂O) 7.62 (1 H, s, 8-*H*), 7.21–6.79 (5 H, m, C₆H₅), 5.37 (1 H, d, *J* 7.2, 1'-*H*), 4.49 (1 H, t, *J* 6.8 2'-*H*), 3.96 (1 H, d, *J* 5.2, 3'-*H*), 3.93–3.89 (1 H, m, 4'-*H*), 3.75–3.63 (2 H, m, CH₂S), 2.80–2.52 (2 H, m, 5'-*H*); $\delta_{\text{P}}[^1\text{H}]$ (162 MHz; D₂O) 25.4 (m, NHPS); δ_{C} (101 MHz; D₂O) 162.4 (6-*C*), 156.4 (2-*C*), 151.4 (4-*C*), 139.0 (8-*C*), 138.7 (CCH₂S), 128.4 (*o*- and *m*-C₆H₅CH₂S), 126.8 (*p*-C₆H₅CH₂S), 117.2 (5-*C*), 88.7 (1'-*C*), 85.5 (d, ³*J*_{C-P} 10.8, 4'-*C*), 71.6 (2'-*C*), 71.4 (3'-*C*), 43.5 (5'-CH₂), 34.1 (CH₂S); *m/z* (ES⁻) 467.0911 (M - H. C₁₇H₂₀N₆O₆PS requires 467.0908).

Anion exchange chromatography of the crude compound 126:

A sample (50 mg) was dissolved in 50 mM TEAB buffer, pH 7.5 (5 mL) and purified on DEAE Sepharose[®] FF column (50 mL, 10 × 3 mm, 3 mL/min), using a TEAB buffer gradient 50-250 mM (chromatogram shown below).

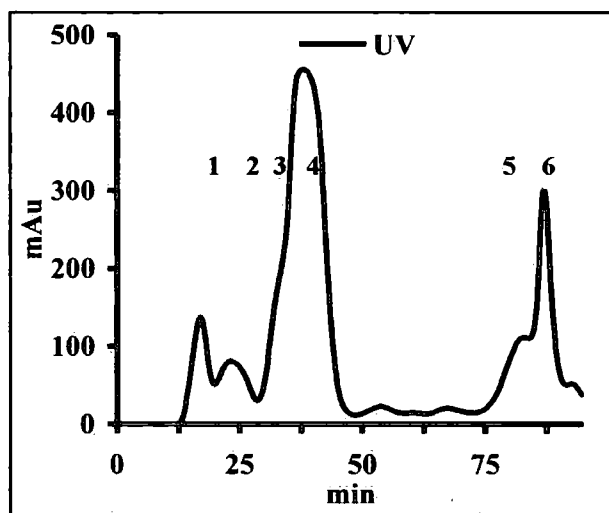


Figure 7. 7 Anion exchange chromatography of crude product 126. UV trace at 280 nm

The fractions corresponding to the peaks 1-6 were collected and lyophilised (table 7.8).

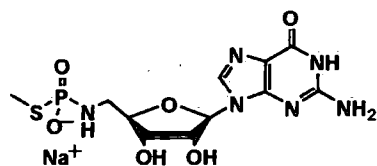
Table 7. 9 Collected fractions of the anion exchange chromatography of the crude mixture 465

1	2	3	4	5	6
7 ^c	3 ^c	6 ^c	61 ^c	8 ^c	15 ^c
0 ^a	0 ^a	Weak 26 and 23 ppm ^a	90 ^a 26 ppm (m, 126) and 10 ^a (Pi)	Weak 26, 20.4 and 20.1 (dd) ppm ^a	Weak 27, 26, 20.1 (dd), Pi and 0.4 (d) ppm ^a
Weak peaks for guanosine-like structures			126 as the triethylammonium salt	Weak peaks for guanosine-like structures ^b	

% ^a Determined by ³¹P NMR spectroscopy. ^b Determined by ¹H NMR spectroscopy. ^c Determined by anionexchange chromatography.

Cation exchange chromatography

The triethylammonium salt of product from peak 4 (figure 7., table 7.) was dissolved in water (5 mL) and run with water on a Dowex[®] 50W×2, 200-400 (50 mL, 30 × 2 mm, 3 mL/min) column, with water as the mobile phase. The fractions containing product, detected *via* UV trace (280 nm), were collected and lyophilised.



126

The purity of the compound 126 after cation exchange chromatography, was estimated using ^{31}P NMR (95% and 5% Pi) and ^1H NMR (100%) spectrometry. δ_{H} (700 MHz; D_2O) 7.72 (1 H, s, 8-*H*), 5.66 (1 H, d, *J* 7.6, 1'-*H*), 4.98 (1 H, t, *J* 6.6 2'-*H*), 4.64 (1 H, d, *J* 4.9, 3'-*H*), 4.22–4.19 (1 H, m, 4'-*H*), 3.00–3.04 (2 H, m, 5'-*H*), 1.96 (3 H, d, *J* 12.6, CH_3S); $\delta_{\text{P}}[^1\text{H}]$ (283 MHz; D_2O) 23.3 (m, NHPS); δ_{C} (176 MHz; D_2O) could not be assigned due to very low intensity of the collected spectrum; *m/z* (ES^-) 391.0594 (*M* – H. $\text{C}_{11}\text{H}_{16}\text{N}_6\text{O}_6\text{PS}$ requires 391.0595).

Anion exchange chromatography of the crude compound 127:

A sample (50 mg) was dissolved in a 50 mM TEAB buffer, pH 7.5 (5 mL) and purified on DEAE Sepharose[®] FF column (50 mL, 10 × 3 mm, 3 mL/min), running TEAB buffer with a gradient 50-300 mM (chromatogram shown below):

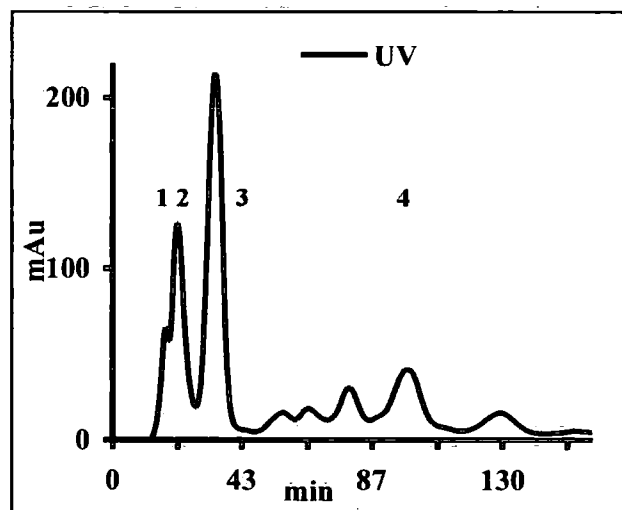


Figure 7. 8 Cation exchange chromatography of the compound 127. UV trace at 280 nm

The fractions corresponding to the peaks 1, 2, 3 and 4 were collected and lyophilised (table 7.9). The other peaks in the chromatogram were not collected and no attempt to identify them was made.

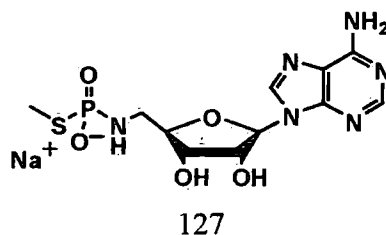
Table 7. 10 Collected fractions in the anion exchange chromatography of the crude compound 378

1	2	3	4
5 ^c	20 ^c	40 ^c	15 ^c
0 ^a	0 ^a	100 ^a 26 ppm (m, 127)	Traces of 26 ppm and Pi ^a
Weak peaks for adenosine-like structures ^b		127 as the triethylammonium salt	Weak peaks for adenosine-like structures ^b

% ^a Determined by ³¹P NMR spectroscopy. ^b Determined by ¹H NMR spectroscopy. ^c Determined by anion exchange chromatography.

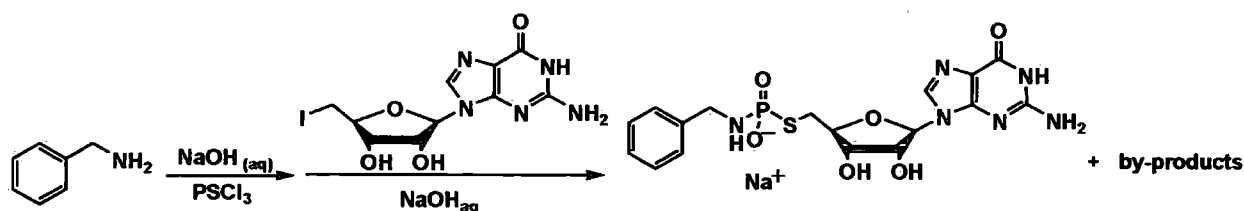
Cation exchange chromatography

The triethylammonium salt of the product from peak 3 (figure 7., table 7.) was dissolved in water (5 mL) and run with water on a Dowex[®] 50W×2, 200-400 (50 mL, 30 × 2 mm, 3 mL/min) column. The fractions containing product, detected *via* UV trace (280 nm), were collected and lyophilised.



The purity of the sample 127 after cation exchange chromatography, was estimated using ³¹P NMR (100%) and ¹H NMR (100%) spectrometry. δ_H (700 MHz; D₂O) 8.19 (1 H, s, 2-*H*), 8.08 (1 H, s, 8-*H*), 5.87 (1 H, d, *J* 6.3, 1'-*H*), 2'-*H*), 4.64 (1 H, t, *J* 5.7, 2'-*H*), 4.33–4.30 (1 H, m, 3'-*H*), 4.16–4.13 (1 H, m, 4'-*H*), 3.15–3.03 (2 H, m, 5'-*H*), 1.95 (3 H, d, *J* 13.3, CH₃S); δ_P [¹H](283 MHz; D₂O) 24.5 (m, NHPS); δ_C (176 MHz; D₂O) 155.8 (6-*C*), 153.1 (2-*C*), 149.1 (br s, 2-*C*), 140.8 (4-*C*), 140.3 (8-*C*), 119.3 (5-*C*), 87.9 (1'-*C*), 85.4 (d, ³*J*_{C-P} 8.1, 4'-*C*), 73.3 (2'-*C*), 71.3 (3'-*C*), 43.5 (5'-NH₂CH₂), 11.8 (d, ³*J*_{C-P} 8.1, CH₃S); *m/z* (ES⁻) 375.0643 (M - H. C₁₁H₁₆N₆O₅PS requires 375.0646).

7.12. Iodo-guanosine as the alkylation agent



Benzylamine (1 Eq, 38 μ L, 0.34 mol) was mixed with sodium hydroxide (5 Eq, 1 M aqueous solution, 1.7 mL, 1.7 mmol) and water (218 μ L) in a 50 mL round-bottomed flask with indents. Thiophosphoryl chloride (1 Eq, 34 μ L, 0.34 mmol), dissolved in THF (1 mL) was added dropwise to the aqueous mixture over the course of 10 minutes. 5'-deoxy-5'-iodoguanosine and additional sodium hydroxide solution were added in portions according to the table 7.10 and vigorous mixing was continued at 50 °C for a certain time (table 7.10). Then, ether extraction (3×10 mL) was performed and the resulting aqueous solution was lyophilised. Conversions gained are presented in table 7.10 along with some of the experimental details.

Table 7. 11 The batches of iodoguanosine and sodium hydroxide added and conversions gained

G-I			1M NaOH (Eq)	Time (h)	³¹ P NMR	¹ H NMR
Eq	mg	mmol				
1	135	0.34	3	48	32%	n.d.
1	135	0.34	0	32	73%	Product 501 and excess of G-I

Anion exchange chromatography of the crude compound 128:

A sample (60 mg) was dissolved in 50 mM TEAB buffer, pH 7.5 (5 mL) and purified on a DEAE Sepharose® FF (50 mL, 10 \times 3 mm, 3 mL/min), TEAB buffer gradient 50-300 mM.

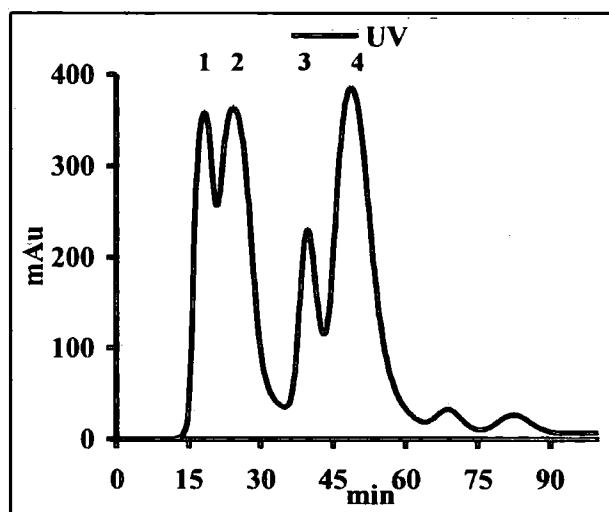


Figure 7. 9 Anion exchange chromatography of the crude product 128. UV trace at 280 nm

Four fractions collected as shown above were collected and lyophilised (table 7.11).

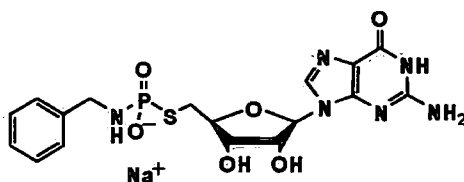
Table 7. 12 Collected fractions of the anion exchange chromatography of the crude mixture 501

1	2	3	4
17 ^c	30 ^c	11 ^c	38 ^c
0 ^a	Pi ^a	Pi ^a	97 ^a 26 ppm (m, 128) and 3 ^a (Pi)
Guanosine-like structures ^b		0 ^b	128 as the triethylammonium salt

% ^a Determined by ³¹P NMR spectroscopy. ^b Determined by ¹H NMR spectroscopy. ^c Determined by anion exchange chromatography

Cation exchange chromatography

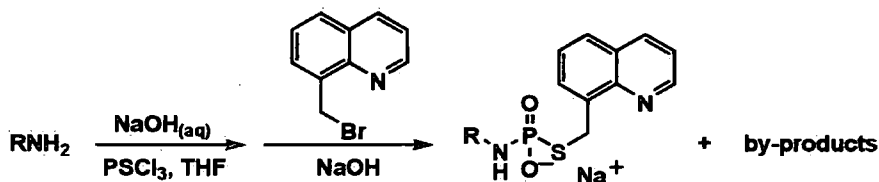
The triethylammonium salt of the product from peak 4 (figure 7., table 7.) was dissolved in water (5 mL) and run with water on a Dowex[®] 50W×2, 200-400 (50 mL, 30 × 2 mm, 3 mL/min) column. The fractions containing product, detected *via* UV trace (280 nm), were collected and lyophilised.



128

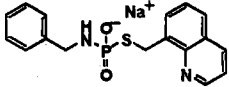
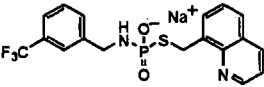
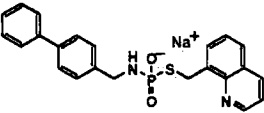
The purity of the sample 128 cation exchange chromatography, was estimated using ³¹P NMR (95% and 5% Pi) and ¹H NMR (100%) spectrometry. δ_H (700 MHz; D₂O) 7.78 (1 H, s, 8-*H*), 7.14–6.99 (5 H, m, C₆H₅), 5.67 (1 H, d, *J* 5.6, 1'-*H*), 2'-*H*), 4.64 (1 H, 2'-*H*, covered with the HOD signal), 4.17 (1 H, d, *J* 4.2, 3'-*H*), 4.13–4.09 (1 H, m, 4'-*H*), 3.75–3.69 (2 H, m, CH₂S), 2.95–2.83 (2 H, m, 5'-*H*); δ_P [¹H](283 MHz; D₂O) 24.5 (m, NHPS); δ_C (176 MHz; D₂O) 161.0 (6-*C*), 154.8 (br s, 2-*C*), 151.7 (4-*C*), 140.3 (8-*C*), 137.8 (CH₂S), 128.6 (*o*-C₆H₅CH₂S), 127.4 (*m*-C₆H₅CH₂S), 127.2 (*p*-C₆H₅CH₂S), 117.0 (5-*C*), 87.5 (1'-*C*), 84.1 (d, ³*J*_{C-P} 4.9, 4'-*C*), 73.1 (2'-*C*), 72.6 (3'-*C*), 45.6 (5'-NH₂CH₂), 32.7 (CH₂S); *m/z* (ES⁻) 467.0916 (M - H. C₁₇H₂₀N₆O₆PS requires 467.0908).

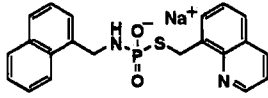
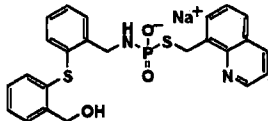
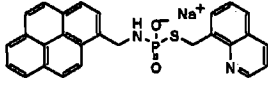
7.13. Synthesis of the quinoline derivative library

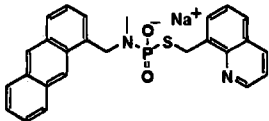
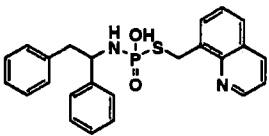


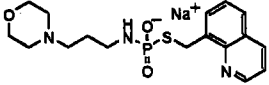
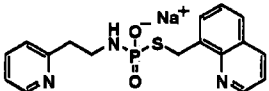
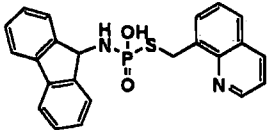
Thiophosphyryl chloride (1 Eq, 0.18 mmol, 0.018 mL) was dissolved in THF (0.548 mL) and added *via a* dropping funnel over the course of 10 minutes to the suspension/solution of amine (1.2 Eq, 0.216 mmol, table 5.1. RNH_2) in aqueous sodium hydroxide (5 Eq, 1 M, 0.9 mL, 0.9 mmol) and water (0.116 mL). After stirring for 1 h in the round-bottomed flask with indents, 8-(bromomethyl) quinoline (2 Eq, 0.36 mmol, 80 mg), along with additional aqueous sodium hydroxide (table 7.12) was added and vigorous mixing was continued for 1 h. Then, an ether extraction was performed (3×5 mL) and the aqueous solution was lyophilised. In cases where a white precipitate appeared extraction was performed the water layer was centrifuged and the precipitate was collected and dried overnight in a vacuum desiccator. The purities of the products were estimated by ^1H and ^{31}P NMR spectroscopy.

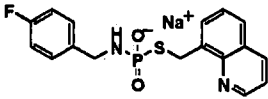
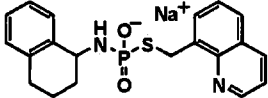
Table 7. 13 Approximation of the quinoline derivatives library purity

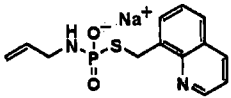
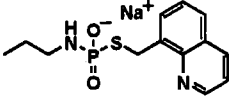
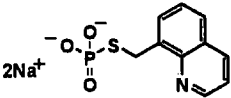
Crude product	Amine	1M NaOH (Eq)	Purity (%)	Characterisation of the desired product
 <p>132</p>	23 μ L	0	91 ^a 95 ^b	δ_{H} (700 MHz; CD ₃ OD) 8.80 (1 H, dd, <i>J</i> 4.2 and 1.7, Qu2-CH), 8.25 (1 H, dd, <i>J</i> 8.2 and 1.7, Qu4-CH), 7.82 (1 H, d, <i>J</i> 7.1, Qu5-CH), 7.76 (1 H, d, <i>J</i> 8.1, Qu7-CH), 7.47 (1 H, t, <i>J</i> 7.7, Qu6-CH), 7.44 (1 H, dd, <i>J</i> 8.2 and 4.2, Qu3-CH), 7.22 – 7.10 (5 H, m, C ₆ H ₅), 4.56 (2 H, d, <i>J</i> 11.2, SCH ₂), 3.74 (2 H, d, <i>J</i> 7.7, CH ₂ NH); δ_{P} [¹ H](283 MHz; CD ₃ OD) 23.6 (m, NHPS); δ_{C} (176 MHz; CD ₃ OD) 149.2 (Qu2-CH), 145.8 (Qu9-CH), 140.2 (d, ³ <i>J</i> _{C-P} not resolved, CCH ₂ NH), 138.1 (d, ³ <i>J</i> _{C-P} not resolved, SCH ₂ C), 136.5 (Qu4-CH), 129.7 (Qu7-CH), 128.5 (Qu10-CH), 127.7 (<i>o</i> -C ₆ H ₅), 127.2 (<i>m</i> -C ₆ H ₅), 126.8 (Qu5-CH), 126.1 (Qu6-CH), 126.0 (<i>p</i> -C ₆ H ₅), 120.9 (Qu3-CH), 46.0 (CH ₂ NH), 30.0 (SCH ₂); <i>m/z</i> (ES ⁻) 343.0678 (M – H. C ₁₇ H ₁₆ N ₂ O ₂ PS requires 343.0678)
 <p>133</p>	31 μ L	0	81 ^a 60 ^b 54 ^c	δ_{H} (700 MHz; CD ₃ OD) 8.77 (1 H, dd, <i>J</i> 10.0 and 4.1, Qu2-CH), 8.25 (1 H, d, <i>J</i> 8.3, Qu4-CH), 7.82 (1 H, d, <i>J</i> 7.0, Qu5-CH), 7.76 (1 H, d, <i>J</i> 8.1, Qu7-CH), 7.50 (1 H, s, CF ₃ CCHC), 7.48–7.32 (9, H, m, CF ₃ C ₆ H ₄ and C ₉ H ₆ N) 4.56 (2 H, d, <i>J</i> 11.2, SCH ₂), 3.80 (2 H, d, <i>J</i> 8.4, CH ₂ NH); δ_{P} [¹ H](283 MHz; CD ₃ OD) 23.5 (qn, <i>J</i> 9.4, NHPS); δ_{F} (376 MHz; CD ₃ OD) –63.8 (s, CF ₃); δ_{C} (176 MHz; CD ₃ OD) 149.2 (2-CH), 145.7 (Qu9-CH), 142.2 (d, ³ <i>J</i> _{C-P} 10.8, CCH ₂ NH), 138.0 (d, ³ <i>J</i> _{C-P} not resolved, SCH ₂ C), 136.5 (4-CH), 130.9 (CF ₃ 6-CH), 129.7 (Qu7-CH), 128.7 (CF ₃ 5-CH), 128.4 (Qu10-CH), 127.7 (<i>o</i> -C ₆ H ₅), 127.2 (<i>m</i> -C ₆ H ₅), 126.9 (Qu5-CH), 126.1 (Qu6-CH), 126.0 (<i>p</i> -C ₆ H ₅), 123.7 (q, ² <i>J</i> _{C-F} 10.9, CF ₃ 2-CH), 122.8 (q, ³ <i>J</i> _{C-F} 3.0, CF ₃ 4-CH), 120.9 (Qu3-CH), 45.6 (CH ₂ NH), 30.0 (SCH ₂), the other peaks have not been resolved; <i>m/z</i> (ES ⁻) 411.0547 (M – H. C ₁₈ H ₁₅ N ₂ O ₂ F ₃ PS requires 411.0549)
 <p>134</p>	39 mg	0.5	79 ^a 80 ^b	δ_{H} (500 MHz; CD ₃ OD) 8.80 (1 H, dd, <i>J</i> 4.2 and 1.7, Qu2-CH), 8.21 (1 H, dd, <i>J</i> 8.3 and 1.7, Qu4-CH), 7.74 (1 H, d, <i>J</i> 7.0, Qu5-CH), 7.74 (1 H, dd, <i>J</i> 8.1 and 1.1, Qu7-CH), 7.59–7.24 (8 H, m, C ₆ H ₅ C ₆ H ₄), 7.21 (2 H, d, <i>J</i> 8.2, Qu6- and 3-CH), 4.56 (2 H, d, <i>J</i> 11.1, SCH ₂), 3.80 (2 H, d, <i>J</i> 8.2, CH ₂ NH); δ_{P} [¹ H](283 MHz; CD ₃ OD) 23.7 (m, NHPS); δ_{C} (125 MHz; CD ₃ OD) 149.2 (Qu2-CH), 145.8 (Qu9-CH), 140.8 (CC), 140.1 (d, ³ <i>J</i> _{C-P} 10.5,

				CCH ₂ NH), 139.3 (CC), 138.0 (d, ³ J _{C-P} 4.4, SCH ₂ C), 136.6 (Qu4-CH), 129.7 (Qu7-CH), 128.6 (Qu10-CH), 128.4 (<i>o</i> -C ₆ H ₅), 127.8 (<i>m</i> -C ₆ H ₅), 126.8 (Qu5-CH), 126.4 (<i>p</i> -C ₆ H ₅), 126.3 (<i>o</i> -C ₆ H ₄ CH ₂ NH), 126.2 (<i>m</i> -C ₆ H ₄ CH ₂ NH), 126.0 (Qu6-CH), 120.8 (Qu3-CH), 43.9 (CH ₂ NH), 30.1 (SCH ₂); <i>m/z</i> (ES ⁻) 419.0993 (M - H. C ₂₃ H ₂₀ N ₂ O ₂ PS requires 419.0988).
 <p>135</p>	31 μL	0.5	75 ^a 68 ^b	δ_{H} (700 MHz; CD ₃ OD) 8.72 (1 H, dd, <i>J</i> 4.1 and 1.7, Qu2-CH), 8.12 (1 H, dd, <i>J</i> 8.2 and 1.6, Qu4-CH), 8.02 (1 H, d, <i>J</i> 8.3, 8-C ₁₀ H ₇), 7.79 (1 H, d, <i>J</i> 7.0, Qu5-CH), 7.78 (1 H, d, <i>J</i> 7.9, Qu7-CH), 7.68–7.60 (3 H, m, C ₁₀ H ₇), 7.37–7.31 (5 H, m, C ₁₀ H ₇ and Qu), 7.24 (1 H, dd, <i>J</i> 8.0 and 7.1, Qu6-CH), 7.18 (1 H, d, <i>J</i> 6.9, 2-C ₁₀ H ₇), 4.57 (2 H, d, <i>J</i> 11.2, SCH ₂), 4.18 (2 H, d, <i>J</i> 7.0, CH ₂ NH); δ_{P} [¹ H](283 MHz; CD ₃ OD) 23.5 (m, NHPS); δ_{C} (176 MHz; CD ₃ OD) 149.4 (Qu2-CH), 146.0 (Qu9-CH), 138.3 (d, ³ J _{C-P} 3.3, SCH ₂ C), 136.9 (Qu4-CH), 136.1 (d, ³ J _{C-P} 11, CCH ₂ NH), 133.7 (10-C ₁₀ H ₇), 131.4 (9-C ₁₀ H ₇), 129.6 (Qu7-CH), 128.5 (Qu10-CH), 127.9 (5-C ₁₀ H ₇), 127.1 (4-C ₁₀ H ₇), 126.9 (Qu5-CH), 126.0 (Qu6-CH), 125.4 (7-C ₁₀ H ₇), 125.1 (6-C ₁₀ H ₇), 125.0 (3-C ₁₀ H ₇), 124.9 (2-C ₁₀ H ₇), 123.5 (8-C ₁₀ H ₇), 43.6 (CH ₂ NH), 32.2 (SCH ₂); <i>m/z</i> (ES ⁻) 393.0834 (M - H. C ₂₁ H ₁₈ N ₂ O ₂ PS requires 393.0832).
 <p>136</p>	53 mg	1.1	90 ^a 90 ^b	δ_{H} (500 MHz; CD ₃ OD) 8.76 (1 H, dd, <i>J</i> 3.5 and 1.4, Qu2-CH), 8.17 (1 H, d, <i>J</i> 8.2, Qu4-CH), 7.76 (1 H, d, <i>J</i> 7.1, Qu5-CH), 7.68 (1 H, d, <i>J</i> 8.1, Qu7-CH), 7.50 (2 H, t, <i>J</i> 6.9, 3-Qu and 2-C ₆ H ₄ CH ₂ OH), 7.42 – 7.36 (2 H, m, Qu6- and 2-C ₆ H ₄ CH ₂ NH), 7.24 (1 H, t, <i>J</i> 7.5, 3-C ₆ H ₄ CH ₂ OH), 7.14 (1 H, t, <i>J</i> 7.5, 3-C ₆ H ₄ CH ₂ NH), 7.11 (1 H, t, <i>J</i> 7.6, 4-C ₆ H ₄ CH ₂ OH), 7.08 (1 H, t, <i>J</i> 7.6, 4-C ₆ H ₄ CH ₂ NH), 7.06 (2 H, m, 5-C ₆ H ₄ CH ₂ OH and 5-C ₆ H ₄ CH ₂ NH), 4.61 (2 H, s, CH ₂ OH), 4.52 (2 H, d, <i>J</i> 11.0, SCH ₂), 3.92 (2 H, d, <i>J</i> 8.9, CH ₂ NH); δ_{P} [¹ H](283 MHz; CD ₃ OD) 23.8 (m, NHPS); δ_{C} (125 MHz; CD ₃ OD) 149.2 (2-Qu CH), 145.7 (Qu9-CH), 141.9 (CCH ₂ OH), 136.6 (Qu4-CH), 133.0 (1-C ₆ H ₄ CH ₂ OH), 132.8 (1-C ₆ H ₄ CH ₂ NH ₂), 141.3 (d, ³ J _{C-P} 11.2, CCH ₂ NH), 129.7 (Qu7-CH), 129.1 (C ₁₂ H ₈ S), 128.4 (Qu10-CH), 127.9 (C ₁₂ H ₈ S), 127.5 (Qu5-CH), 127.5 (C ₁₂ H ₈ S), 127.4 (C ₁₂ H ₈ S), 127.3 (C ₁₂ H ₈ S), 127.1 (Qu6-CH), 120.9 (Qu3-CH), 61.7 (CH ₂ OH), 44.0 (CH ₂ NH), 30.1 (SCH ₂); <i>m/z</i> (ES ⁻) 481.0822 (M - H. C ₂₄ H ₂₂ N ₂ O ₂ PS requires 481.0815).
 <p>137</p>	58 mg	0	93 ^a 90 ^b	δ_{H} (500 MHz; CD ₃ OD) 8.66 (1 H, dd, <i>J</i> 4.1 and 1.7, Qu2-CH), 8.24 (1 H, d, <i>J</i> 9.2, 3-CH), 8.11 (1 H, d, <i>J</i> 7.5, 8-CH), 8.10 (1 H, d, <i>J</i> 7.6, 6-CH), 7.99 (1 H, dd, <i>J</i> 8.1 and 1.7, Qu4-CH), 7.97–7.89 (5 H, m, pyrene), 7.76 (1 H, d, <i>J</i> 7.0, Qu5-CH), 7.73 (1 H, d, <i>J</i> 7.7, Qu7-CH), 7.53 (1 H, d, <i>J</i> 7.7, 9-CH), 7.30 (1 H, dd, <i>J</i> 7.7 and 7.0, Qu6-CH), 7.21 (1 H, dd, <i>J</i> 8.2 and 4.1, Qu3-CH), 4.58 (2 H, d, <i>J</i> 11.7, SCH ₂), 4.44 (2 H, d, <i>J</i> 7.4, CH ₂ NH);

				δ_P [1H](283 MHz; CD ₃ OD) 23.3 (m, NHPS); δ_C (125 MHz; CD ₃ OD) 149.3 (Qu2-CH), 145.9 (Qu9-CH), 137.8 (d, $^3J_{C-P}$ not resolved, SCH ₂ C), 134.0 (d, $^3J_{C-P}$ 11.2, CCH ₂ NH), 136.6 (Qu4-CH), 131.3 (4°pyrene), 130.8 (4°pyrene), 130.5 (4°pyrene), 128.5 (4°pyrene), 129.5 (Qu7-CH), 128.4 (Qu10-CH), 127.0 (pyrene), 126.7 (pyrene), 126.3 (Qu5-CH), 126.1 (pyrene), 125.4 (Qu6-CH), 125.8 (pyrene), 124.4 (pyrene), 124.4 (pyrene), 124.2 (pyrene), 123.2 (3-CH), 120.7 (Qu3-CH), 44.0 (CH ₂ NH), 30.1 (SCH ₂); m/z (ES ⁻) 467.0996 (M - H. C ₂₇ H ₂₀ N ₂ O ₂ PS requires 467.0988).
 <p>138</p>	66 mg	1.1	61 ^a 80 ^b	δ_H (700 MHz; CD ₃ OD) 8.87 (1 H, d, J 4.0, Qu2-CH), 8.59 (2 H, d, J 8.9, 1- and 8-CH), 8.30 (1 H, s, 10-CH), 8.19 (1 H, d, J 8.1, Qu4-CH), 8.01 (1 H, d, J 7.0, Qu5-CH), 7.89 (2 H, d, J 8.4, 4- and 5-CH), 7.73 (1 H, d, J 8.1, Qu7-CH), 7.49 (1 H, t, J 7.6, 2-CH), 7.41 (1 H, t, J 9.1, 9-CH), 7.40 (2 H, d, J 8.4, 3- and 6-CH), 7.35 (1 H, dd, J 7.7 and 7.0, Qu6-CH), 7.20 (1 H, dd, J 8.2 and 4.1, Qu3-CH), 5.10 (2 H, d, J 3.6, CH ₂ N), 4.84 (2 H, d, J 9.6, SCH ₂), 2.25 (3 H, d, J 12.2, NCH ₃); δ_P [1H](283 MHz; CD ₃ OD) 24.0 (m, NHPS); δ_C (176 MHz; CD ₃ OD) 149.4 (Qu2-CH), 145.9 (Qu9-CH), 138.4 (d, $^3J_{C-P}$ 4.0, SCH ₂ C), 136.8 (Qu4-CH), 131.4 (4° anthracene), 131.3 (4° anthracene), 129.9 (Qu7-CH), 129.5 (d, $^3J_{C-P}$ 11.7, CCH ₂ NH), 128.5 (Qu10-CH), 128.4 (4- and 5-CH), 126.9 (Qu5-CH), 126.8 (10-CH), 126.2 (Qu6-CH), 125.1 (3- and 6-CH), 124.9 (2- and 7-CH), 124.4 (1- and 8-CH), 121.1 (Qu3-CH), 44.8 (CH ₂ NH), 32.7 (d, $^3J_{C-P}$ 1.9, NCH ₃), 29.8 (SCH ₂); m/z (ES ⁻) 457.1153 (M - H. C ₂₆ H ₂₂ N ₂ O ₂ PS requires 457.1145)
 <p>170</p>	42 μ L	0	65 ^a 65 ^b	δ_H (700 MHz; CD ₃ OD) 8.79 (1 H, dd, J 4.2 and 1.8, Qu2-CH), 8.21 (1 H, dd, J 8.2 and 1.8, Qu4-CH), 7.71 (1 H, dd, J 8.2 and 1.3, Qu7-CH), 7.61 (1 H, d, J 6.9, Qu5-CH), 7.43 (1 H, dd, J 8.2 and 4.2, Qu3-CH), 7.39 (1 H, dd, J 8.1 and 7.2, Qu6-CH), 7.10–6.96 (8 H, m, 2 \times C ₆ H ₅), 6.95 (2 H, 2 \times d, J 8.0, C ₆ H ₅ CH _X), 4.51 (1 H, AB system, J_{AB} 12.7 and $^3J_{B-P}$ 9.6, SCH ₂), 4.38 (1 H, ddd, J 11.1, 9.6 and 4.1, CH ₂ CH _X), 4.31 (1 H, AB system, J_{AB} 12.7 and $^3J_{A-P}$ 10.3, SCH ₂), 3.19 (1 H, ABX system, J_{AB} 13.1 and J_{BX} 4.6, CH ₂ CH _X), 2.74 (1 H, ABX system, J_{AB} 13.1 and J_{AX} 9.5, CH ₂ CH _X); δ_P [1H](283 MHz; CD ₃ OD) 21.6 (m, NHPS); δ_C (176 MHz; CD ₃ OD) 149.1 (Qu2-CH), 145.9 (Qu9-CH), 144.0 (CCHNH), 138.4 (CCH ₂ CH), 137.7 (m, SCH ₂ C), 136.5 (Qu4-CH), 129.7–125.9 (11 \times s, 2 \times C ₆ H ₅ and Qu), 120.6 (Qu3-CH), 57.6 (CH ₂ CH _X), 45.0 (CH ₂ CH _X), 30.0 (SCH ₂); m/z (ES ⁻) 433.1143 (M - H. C ₂₄ H ₂₂ N ₂ O ₂ PS requires 433.1145)

 <p>139</p>	31 μ L	0	81 ^a 67 ^b	δ_{H} (700 MHz; CD ₃ OD) 8.86 (1 H, dd, <i>J</i> 4.2 and 1.7, Qu2-CH), 8.26 (1 H, dd, <i>J</i> 8.2 and 1.7, Qu4-CH), 7.87 (1 H, d, <i>J</i> 7.0, Qu5-CH), 7.78 (1 H, d, <i>J</i> 8.1, Qu7-CH), 7.50 (1 H, dd, <i>J</i> 7.7 and 7.0, Qu3-CH), 7.47 (1 H, dd, <i>J</i> 8.2 and 4.2, Qu6-CH), 4.54 (2 H, d, <i>J</i> 10.8, SCH ₂), 3.60 (4 H, t, <i>J</i> 4.6, O(CH ₂) ₂), 2.67 (2 H, dt, <i>J</i> 9.1 and 7.4, CH ₂ NH), 2.30 (4 H, br s, (CH ₂) ₂ N), 2.42 (2 H, t, <i>J</i> 7.4, NCH ₂), 1.46 (2 H, qn, <i>J</i> 7.4, CH ₂ CH ₂ CH ₂); $\delta_{\text{P}}[^1\text{H}](283 \text{ MHz; CD}_3\text{OD})$ 23.7 (m, NHPS); $\delta_{\text{C}}(176 \text{ MHz; CD}_3\text{OD})$ 149.3 (2-CH), 145.8 (9-CH), 138.1 (d, ³ <i>J</i> _{C-P} 3.3, SCH ₂ C), 136.6 (4-CH), 129.6 (7-CH), 128.5 (10-CH), 126.8 (5-CH), 126.1 (6-CH), 121.0 (3-CH), 66.3 (O(CH ₂) ₂), 56.7 (NCH ₂), 53.4 ((CH ₂) ₂ N), 40.2 (CH ₂ NH), 29.8 (SCH ₂), 27.3 (d, ³ <i>J</i> _{C-P} 7.5, CH ₂ CH ₂); <i>m/z</i> (ES ⁻) 380.1202 (M - H. C ₁₇ H ₂₃ N ₃ O ₃ PS requires 380.1203)
 <p>140</p>	26 μ L	0	87 ^a 75 ^b	δ_{H} (700 MHz; CD ₃ OD) 8.81 (1 H, dd, <i>J</i> 4.2 and 1.6, Qu2-CH), 8.37 (1 H, d, <i>J</i> 4.9, 6-CH), 8.23 (1 H, dd, <i>J</i> 8.2 and 1.6, Qu4-CH), 7.82 (1 H, d, <i>J</i> 7.0, Qu5-CH), 7.74 (1 H, d, <i>J</i> 8.1, Qu7-CH), 7.65 (1 H, td, <i>J</i> 7.7 and 1.7, 4-CH), 7.47–7.42 (2 H, m, Qu3- and 6-CH), 7.20 (1 H, d, <i>J</i> 7.8, 3-CH), 7.17 (1 H, dd, <i>J</i> 6.9 and 5.5, 5-CH), 4.50 (2 H, d, <i>J</i> 10.4, SCH ₂), 3.01 (2 H, dt, <i>J</i> 16.1 and 7.5, CH ₂ CH ₂ NH), 2.81 (2 H, t, <i>J</i> 7.5, CH ₂ CH ₂ NH); $\delta_{\text{P}}[^1\text{H}](283 \text{ MHz; CD}_3\text{OD})$ 23.5 (m, NHPS); $\delta_{\text{C}}(176 \text{ MHz; CD}_3\text{OD})$ 160.1 (2-CH), 149.4 (Qu2-CH), 148.4 (6-CH), 146.0 (Qu9-CH), 138.1 (d, ³ <i>J</i> _{C-P} not resolved, SCH ₂ C), 137.3 (4-CH), 136.8 (Qu4-CH), 129.9 (Qu7-CH), 128.7 (Qu10-CH), 127.1 (Qu5-CH), 126.3 (Qu6-CH), 123.8 (3-CH), 121.7 (5-CH), 121.2 (Qu3-CH), 41.8 (CH ₂ NH), 39.3 (d, ³ <i>J</i> _{C-P} 7.6, CH ₂ CH ₂ NH), 30.2 (SCH ₂); <i>m/z</i> (ES ⁻) 358.0786 (M - H. C ₁₇ H ₁₇ N ₃ O ₂ PS requires 358.0784).
 <p>171</p>	47 mg	1.1	54 ^a 68 ^b	δ_{H} (700 MHz; CD ₃ OD) 8.84 (1 H, dd, <i>J</i> 4.0 and 1.7, Qu2-CH), 8.26 (1 H, dd, <i>J</i> 8.3 and 1.7, Qu4-CH), 7.92 (1 H, d, <i>J</i> 7.0, Qu5-CH), 7.75 (1 H, d, <i>J</i> 8.2, Qu7-CH), 7.74 (2 H, d, <i>J</i> 7.5, 4- and 5-CH), 7.61 (2 H, d, <i>J</i> 7.5, 1- and 8-CH), 7.49–7.43 (2 H, m, Qu3- and 6-CH), 7.25 (2 H, t, <i>J</i> 7.4, 2 and 7-CH), 7.17 (1 H, 2 × t, <i>J</i> 7.7, 3- and 6-CH), 5.30 (1 H, d, <i>J</i> 12.5, CHNH), 4.76 (2 H, d, <i>J</i> 10.1, SCH ₂); $\delta_{\text{P}}[^1\text{H}](283 \text{ MHz; CD}_3\text{OD})$ 22.3 (m, NHPS); $\delta_{\text{C}}(176 \text{ MHz; CD}_3\text{OD})$ 149.1 (Qu2-CH), 147.3 (9-CH), 146.0 (Qu9-CH), 139.6 (1a- and 8a-C), 138.0 (d, ³ <i>J</i> _{C-P} not resolved, SCH ₂ C), 137.0 (4a and 5a-C), 136.5 (Qu4-CH), 129.8 (Qu7-CH), 128.6 (Qu10-CH), 126.7 (3- and 6-CH), 126.7 (Qu5-CH), 125.4 (Qu6-CH), 121.2 (Qu3-CH), 57.8 (CHNH), 30.7 (SCH ₂); <i>m/z</i> (ES ⁻) 417.0830 (M - H. C ₂₃ H ₁₈ N ₂ O ₂ PS requires 417.0832).

 <p style="text-align: center;">141</p>	25 μ L	0	90 ^a 92 ^b 84 ^c	δ_{H} (700 MHz; CD ₃ OD) 8.79 (1 H, dd, <i>J</i> 4.2 and 1.7, 2-CH), 8.23 (1 H, dd, <i>J</i> 8.2 and 1.6, 4-CH), 7.81 (1 H, d, <i>J</i> 7.0, 5-CH), 7.74 (1 H, d, <i>J</i> 8.1, 7-CH), 7.46 (1 H, dd, <i>J</i> 9.8 and 5.4, 6-CH), 7.51 (1 H, dd, <i>J</i> 8.5 and 4.5, 3-CH), 7.42 (2 H, m, CH=CCH ₂), 6.98 (2 H, m, FC=CH), 4.54 (2 H, d, <i>J</i> 11.1, SCH ₂), 3.73 (2 H, d, <i>J</i> 8.3, CH ₂ NH); $\delta_{\text{P}}[^1\text{H}](283 \text{ MHz}; \text{CD}_3\text{OD})$ 23.5 (m, NHPS); δ_{F} (376 MHz; CD ₃ OD) -118.8 (s, F); δ_{C} (176 MHz; CD ₃ OD) 162.0 (d, <i>J</i> 242.7, FC), 149.2 (2-CH), 145.7 (9-CH), 138.3 (d, ³ <i>J</i> _{C-P} not resolved, SCH ₂ C), 137.7 (d, ³ <i>J</i> _{C-P} 10.6, CCH ₂ NH), 136.6 (4-CH), 129.9 (7-CH), 129.3 (d, ³ <i>J</i> _{C-P} , 7.9, FC=CH=CH), 128.5 (10-CH), 126.9 (5-CH), 126.1 (6-CH), 120.9 (3-CH), 114.2 (d, ² <i>J</i> _{C-P} , 21.5, FC=CH=CH), 45.3 (CH ₂ NH), 30.0 (SCH ₂); <i>m/z</i> (ES ⁻) 361.0583 (M - H. C ₁₇ H ₁₅ N ₂ O ₂ FPS requires 361.0581).
 <p style="text-align: center;">142</p>	31 μ L	1.1	75 ^a 78 ^b	δ_{H} (700 MHz; CD ₃ OD) 8.83 (1 H, d, <i>J</i> 2.8, Qu2-CH), 8.25 (1 H, d, <i>J</i> 8.2, Qu4-CH), 7.88 (1 H, d, <i>J</i> 7.0, Qu5-CH), 7.76 (1 H, d, <i>J</i> 8.0, Qu7-CH), 7.57 (1 H, d, <i>J</i> 7.6, 5-CH), 7.51-7.43 (3 H, m, Qu3- and 6-CH), 7.00 (1 H, t, <i>J</i> 7.3, 7-CH), 6.93 (2 H, m, 6- and 8-CH), 4.67 - 4.59 (2 H, m, SCH ₂), 4.32-4.24 (1 H, m, CHNH), 2.72 (2 H, m, 3-CH ₂), 2.70-2.56 (2 H, m, SCH ₂), 1.96-1.82 (1 H, m, 4-CH ₂), 1.82-1.71 (1 H, m, 4-CH ₂), 1.71-1.63 (1 H, m, 2-CH ₂), 1.63-1.58 (1 H, m, 2-CH ₂); $\delta_{\text{P}}[^1\text{H}](283 \text{ MHz}; \text{CD}_3\text{OD})$ 21.3 (m, NHPS); δ_{C} (176 MHz; CD ₃ OD) 149.1 (Qu2-CH), 145.9 (Qu9-CH), 139.9 (d, ³ <i>J</i> _{C-P} 5.7, CCHNH), 137.9 (d, ³ <i>J</i> _{C-P} 4.8 SCH ₂ C), 136.9 (10-C), 136.6 (Qu4-CH), 129.7 (Qu7-CH), 129.1 (5-CH), 128.6 (Qu10-CH), 128.3 (8-CH), 126.8 (6-CH), 126.3 (Qu5-CH), 125.4 (Qu6-CH), 125.2 (7-CH), 121.1 (Qu3-CH), 49.9 (CHNH), 32.1, (4-CH), 30.5 (d, ³ <i>J</i> _{C-P} 2.6, 2-CH), 29.18 (SCH ₂), 20.0 (3-CH), 12.8 (CH ₂ CH ₃); <i>m/z</i> (ES ⁻) 383.0987 (M - H. C ₂₀ H ₂₀ N ₂ O ₂ PS requires 383.0988).

 <p>143</p>	16 μ L	0.5	94 ^a 96 ^b	δ_{H} (500 MHz; CD ₃ OD) 8.89 (1 H, dd, <i>J</i> 4.2 and 1.8, 2-CH), 8.30 (1 H, dd, <i>J</i> 8.3 and 1.7, 4-CH), 7.88 (1 H, dd, <i>J</i> 7.1 and 1.3, 5-CH), 7.82 (1 H, dd, <i>J</i> 8.2 and 1.3, 7-CH), 7.55–7.49 (2 H, m, 3- and 6-CH), 5.77 (1 H, ddt, <i>J</i> 16.0, 9.5 and 5.7 CH ₂ =CH), 4.99 (2 H, dq, <i>J</i> 17.1 and 1.7, CH ₂ =CH), 4.57 (2 H, d, <i>J</i> 11.1, SCH ₂), 3.23 (2 H, ddt, <i>J</i> 9.5, 5.7 and 1.7, CH ₂ NH); $\delta_{\text{P}}[^1\text{H}]$ (283 MHz; CD ₃ OD) 27.6 (m, NHPS); δ_{C} (125 MHz; CD ₃ OD) 149.5 (2-CH), 146.0 (9-CH), 138.3 (d, ³ <i>J</i> _{C-P} 4.9, SCH ₂ C), 137.4 (d, ³ <i>J</i> _{C-P} 10.1, CHCH ₂), 136.9 (4-CH), 129.9 (7-CH), 128.9 (10-CH), 127.2 (5-CH), 126.4 (6-CH), 121.2 (3-CH), 113.6 (CH ₂ =CH), 44.7 (CH ₂ NH), 30.0 (SCH ₂); <i>m/z</i> (ES ⁻) 293.0522 (M–H. C ₁₃ H ₁₄ N ₂ O ₂ PS requires 293.0519).
 <p>144</p>	18 μ L	0	93 ^a 96 ^b	δ_{H} (500 MHz; CD ₃ OD) 8.89 (1 H, dd, <i>J</i> 4.2 and 1.8, 2-CH), 8.30 (1 H, dd, <i>J</i> 8.3 and 1.7, 4-CH), 7.88 (1 H, dd, <i>J</i> 7.1 and 1.0, 5-CH), 7.82 (1 H, dd, <i>J</i> 8.2 and 1.2, 7-CH), 7.53 (1 H, dd, <i>J</i> 8.0 and 7.0, 6-CH), 7.51 (1 H, dd, <i>J</i> 8.5 and 4.5, 3-CH), 4.56 (2 H, d, <i>J</i> 11.2, SCH ₂), 2.57 (2 H, dt, <i>J</i> 8.7 and 7.4, CH ₂ NH), 1.31 (2 H, sx, <i>J</i> 7.4, CH ₃ CH ₂), 0.77 (3 H, t, <i>J</i> 7.4, CH ₃ CH ₂); $\delta_{\text{P}}[^1\text{H}]$ (283 MHz; CD ₃ OD) 24.1 (m, NHPS); δ_{C} (125 MHz; CD ₃ OD) 149.4 (2-CH), 146.1 (9-CH), 138.3 (d, ³ <i>J</i> _{C-P} 4.6, SCH ₂ C), 136.9 (4-CH), 129.9 (7-CH), 128.8 (10-CH), 127.2 (5-CH), 126.4 (6-CH), 121.2 (3-CH), 43.8 (CH ₂ NH), 30.1 (d, ³ <i>J</i> _{C-P} 2.7, SCH ₂), 24.4 (d, ³ <i>J</i> _{C-P} 9.1, CH ₂ CH ₂), 10.7 (CH ₃ CH ₂); <i>m/z</i> (ES ⁻) 295.0677 (M–H. C ₁₃ H ₁₆ N ₂ O ₂ PS requires 295.0675)
 <p>155</p>				δ_{H} (500 MHz; CD ₃ OD) 8.86 (1 H, m, 2-CH), 8.27 (1 H, m, 4-CH), 7.97 (1 H, m, 5-CH), 7.75 (1 H, m, 7-CH), 7.50 (1 H, n, 6-CH), 7.47 (1 H, m, 3-CH), 4.63 (2 H, m, SCH ₂); $\delta_{\text{P}}[^1\text{H}]$ (283 MHz; CD ₃ OD) 18.1 (t, ³ <i>J</i> _{H-P} 6.7, NHPS); δ_{C} (125 MHz; CD ₃ OD) 149.4 (2-CH), 146.1 (9-CH), 138.3 (d, ³ <i>J</i> _{C-P} 4.2, SCH ₂ C), 136.9 (4-CH), 129.9 (7-CH), 128.8 (10-CH), 127.2 (5-CH), 126.4 (6-CH), 121.2 (3-CH), 43.8 (CH ₂ NH); <i>m/z</i> (ES ⁻) 254.0047 (M–H. C ₁₀ H ₉ NO ₂ PS requires 254.0046).

^aDetermined by ³¹P NMR spectroscopy. ^bDetermined by ¹H NMR spectroscopy. ^cDetermined by ¹⁹F NMR spectroscopy.

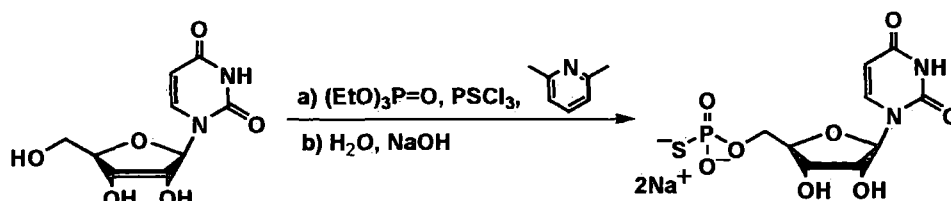
7.14. Initial screening

Leishmania mexicana parasites were used for the assay in the exponential growth phase. Parasites were suspended in the Schneider's Gibco® media (10 µL) and applied to the Neubauer hemacytometer and the number of cells was recorded. A dilution of the suspension in Schneider's Gibco® media was performed to afford a concentration of 2×10^6 parasites/mL. A solution of test compound in DMSO (10 mM, 5 µL) was added to the wells containing parasite suspension (0.5 mL) in duplicate to give a final compound concentration of 100 µM (1/100 dilution). Negative and positive controls were DMSO and miltefosine, respectively (final concentration of miltefosine was 15 µM using 1.5 mM stock). 24-well plates were then incubated for 72 h at 31 °C. Then, the mixtures with either compound or positive or negative control (10 µL) were applied onto Neubauer hemacytometer and the number of live parasites (bright and round) was recorded.

7.15. The estimation of the IC₅₀ of the studied compounds

IC₅₀ values were determined using a range of compound dilutions (0.8 µM, 4 µM, 25 µM and 100 µM) using the *Leishmania mexicana* parasites and determining the effect on the cell growth. The starting concentration of the parasites was made by adjusting the stock solution to 2×10^6 parasites/ mL. Miltefosine in a range of final concentrations of 0.24 µM, 1.2 µM, 6 µM and 30 µM and DMSO were used as positive and negative controls, respectively. The assays for the IC₅₀ estimations were performed the same way as for the initial screening with the addition of a series of a dilution of miltefosine or test compound or DMSO in triplicate. Plots of the number of bright and round (live) parasites against concentration of the compounds or miltefosine solution was used to estimate the IC₅₀ (section 4.4.2, figure 4.1.). IC₅₀ values are presented as mean ± SEM.

7.16. UMPS preparation¹³³



Dry uridine (1 g, 4.1 mmol) was dissolved in freshly distilled triethylphosphate (10 mL) by heated at 50 °C under a nitrogen atmosphere. The flask was then transferred onto an ice bath. Cooled 2,6-dimethyl pyridine (1.4 mL, 12.3 mmol) and cooled thiophosphoryl chloride (0.75 ml, 7.4 mmol) were added sequentially to the solution and the mixture was stirred for 2 h at 4 °C under a nitrogen atmosphere. Then, the mixture was allowed to warm to room temperature and the resulting suspension was poured into petroleum ether (b.p. 40-60, 300 mL). The white precipitate was allowed to settle, the solvents were decanted and the residual white solid was washed with petroleum ether (2×100 mL). Iced water (50 mL) was then added and the mixture was stirred at 4 °C for 2 h. The solution was adjusted to pH 8 by addition of potassium hydroxide while warming up to room temperature. Then, washing with diethyl ether (2×100 mL) and petroleum ether (b.p. 40- 60, 2×100 mL) was performed leaving the products in the aqueous layer, which was lyophilised for the storage before anion exchange chromatography was performed.

Purification via anion exchange chromatography

The crude UMPS was dissolved in equilibrating buffer (50 mM TEAB, 0.02 g/mL) and loaded, using a 50 mL superloop onto a DEAE Sepharose FF column (500 ml, 30×5 cm). Anion exchange chromatography was performed using a linear gradient of TEAB (50-600 mM) pH 7.6, over 2 h with a flow rate of 30 mL/minute. Fractions containing the desired product, eluted between 200 and 300 mM of triethylammonium bicarbonate were combined and lyophilized to give solid product as bis (triethylammonium) salt.

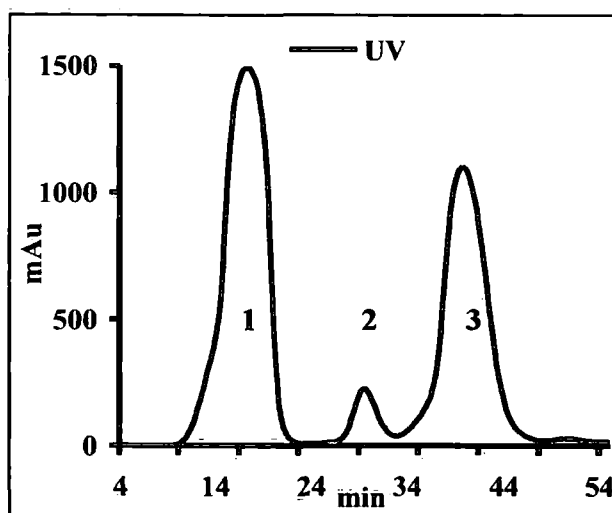
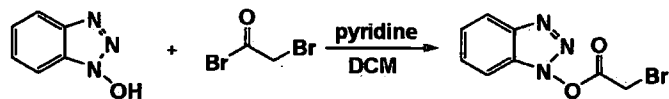


Figure 7. 10 UMPS anion exchange chromatography: 1. Uridine (54%) 2. Unidentified product (5%) 3. UMPS²⁻ (Et₃NH⁺)₂ (49%). UV trace at 280 nm

7.17. Cation exchange using NaI/acetone system

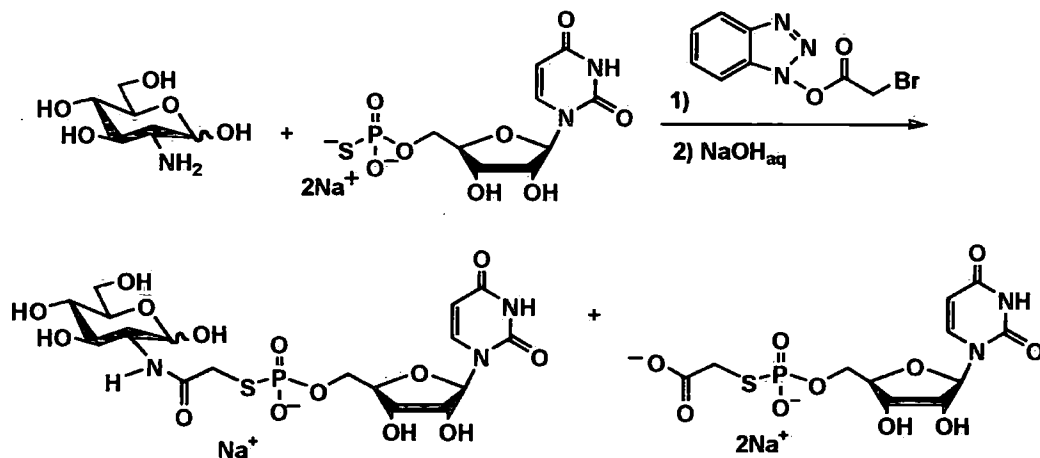
The exchange of triethylammonium ions for sodium ions was performed by mixing solution of the bis (triethylammonium) UMPS salt (0.6 g in 2.5 mL) in water and a solution of sodium iodide (0.6 g, 4 mmol) in acetone (12.5 mL). Methanol (2.5 mL) and diethyl ether (2.5 mL) were added to support the precipitation. The mixture was centrifuged at 4500 rpm for 10 minutes and the supernatant was decanted. After washing with acetone (2 × 25 mL), pellet was re-dissolved in water and lyophilised to afford a white powder of the disodium salt of uridine 5'-O-monophosphorothioate (0.3 g, 37%). (Found C, 24.98; H, 3.76; N, 6.38. C₉H₁₁O₈N₂PSNa₂ requires C, 24.67; H, 3.91; N, 6.39%); ν_{\max} (KBr disk)/cm⁻¹ 3220 (OH), 1690 (CO imide), 1270 (PO), 620m (PS); δ_{H} (500 MHz; D₂O) 7.99 (1H, d, *J* 8.0, 6-CH), 5.82 (1H, d, *J* 5.4, 1'-CH), 5.79 (1H, d, *J* 8.1, 5-CH), 4.24 (1H, t, *J* 5.1, 2'-CH), 4.20 (1H, t, *J* 4.5, 3'-CH), 4.08–4.12 (1 H, m, 4'-CH), 3.82-3.93 (2 H, m, 5'-CH); δ_{P} (400 MHz, D₂O) 44.2; δ_{C} (500 MHz; D₂O) 167.3 (4-C=O), 152.7 (2-C=O), 142.3 (6-CH), 102.8 (5-CH), 88.3 (1'-CH), 84.2 (4'-CHP), 74.1 (2'-CH), 70.3 (3'-CH), 63.6 (5'-CH₂); *m/z* (ES⁻) 339.0059 (M - H. C₉H₁₂N₂O₈PS requires 339.0057).

7.18. Bromoacetyl-N-hydroxybenzotriazole



A solution of pyridine (0.71 mL, 8.7 mmol) in dry DCM (10 mL) was added dropwise to a stirred solution of bromoacetyl bromide (0.76 mL, 8.7 mmol) in dry DCM (10 mL) placed in an ice bath. Following the careful addition of HOBT (0.6 g, 8.7 mmol), the reaction mixture was stirred for 1 h. The work-up consisted of quick washes of the organic phase with water (2×10 mL), hydrochloric acid (0.1 M, 3×10 mL) and saturated sodium chloride solution (10 mL). The organic extracts were then dried over anhydrous magnesium sulphate and the solvent was removed under reduced pressure to give the crude product as dark a yellow solid (0.83 g, 75%). The purity was estimated by ^1H NMR spectroscopy (70%). δ_{H} (500 MHz; CDCl_3) 8.34 (1 H, d, J 8.5, 7-CH), 7.96 (1 H, d, J 8.4, 4-CH), 7.77 (1 H, t, J 7.8, 6-CH), 7.55 (1 H, t, J 7.7, 5-CH), 4.53 (2 H, s, CH_2Br); δ_{C} (126 MHz; D_2O) 162.6 (C=O), 138.7.6 (4°C) 133.5 (6-CH), 131.4 (4°C), 127.5 (5-CH), 116.1 (7-CH), 115.7 (4-CH), 25.6 (CH_2Br).

7.19. Tripartite reaction: *N*-hydroxybenzotriazole as the leaving group



A solution of crude bromoacetyl-*N*-hydroxybenzotriazole (23.1 mg) in dry acetonitrile (3 mL) was mixed with an aqueous solution (2 mL) of Na_2UMPS (30 mg, 0.075 mmol) and D-glucosamine (19.5 mg, 0.086 mmol). Aqueous sodium hydroxide (1 M) was added dropwise until the pH reached ~ 9 (pH paper). The mixture was then stirred for 12 h followed by removal of the acetonitrile under reduced pressure leaving the product mixture in a basic aqueous solution.

Purification of resulting crude mixture via anion exchange chromatography

The aqueous solution of crude sample was loaded to a pre-equilibrated anion exchange DEAE Sephadex FF column (50 ml, 10 × 3 cm) and run using TEAB buffer, pH 7.6 linear gradient (50–400 mM). Fractions eluted between 70 and 100 mM (peak 2) of TEAB buffer and between 200 and 230 mM of TEAB (peak 5) were then were pooled and lyophilised.

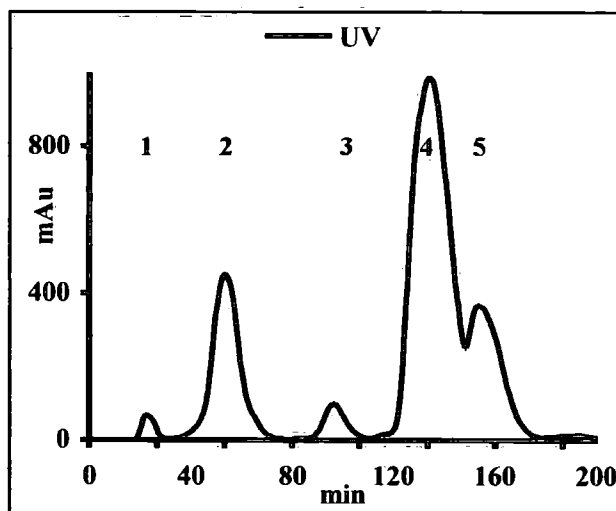
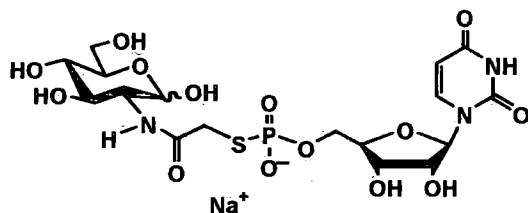


Figure 7. 11 Anion exchange chromatography: Tripartite reaction with HOBT as the leaving group. 1. GlcNH₂, 2. Product 156 as triethylammonium salt (41%), 3. the mixture of amide product and HOBT, 4. HOBT, 5. Product 155 as the triethylammonium salt (30%) UV trace at 280 nm

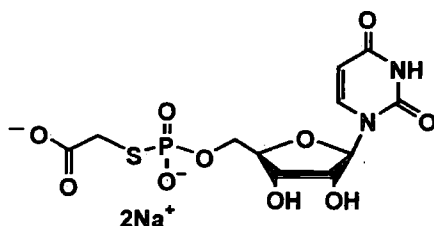
The triethylammonium salts of peaks 2 and 5 were subjected to cation exchange and then fully characterised.

Cation exchange chromatography

The triethylammonium salt of the product from peak 2 and 5 (figure 7..) were dissolved in water (5 mL) and run with water on a Dowex[®] 50W×2, 200–400 (50 mL, 30 × 2 mm, 3 mL/min) column. The fractions containing product, detected *via* UV trace (280 nm), were collected and lyophilised.



The purity of the compound was estimated *via* ^{31}P and ^1H NMR spectroscopy (both 100%) and the share of each anomeric form in the (α 55 % and β 45%). ν_{max} (KBr disc)/ cm^{-1} 3330 (OH), 2940 (NH imide), 1690 (CO imide), 1230 (PO), 570 (PSR); δ_{H} (500 MHz; D_2O) 7.74 (1 H ($\alpha+\beta$), d, J 8.1, 5-CH), 5.80 (1 H ($\alpha+\beta$), d, J 5.1, 1'-CH), 5.78 (1 H ($\alpha+\beta$), d, J 8.1, 6-CH), 5.03 (1H, d, J 3.5, α -CH), 4.5 (1H, d, J 8.3, β -CH), 4.21–4.10 (3 H ($\alpha+\beta$), m, 2'-, 3'- and 4'-CH), 3.76–3.28 (8 H ($\alpha+\beta$), m, CH_2S and GlcNH), 4.09–3.94 (2 H ($\alpha+\beta$), m, CHCH_2OP); δ_{P} (400 MHz, D_2O) 18.3; δ_{C} (500MHz; D_2O) 174.3 ($2 \times$ d, $^3J_{\text{C-P}}$ 2.2 and 4.1, α and β -C=O CH_2S), 166.3 (($\alpha+\beta$) 4-C=O), 151.8 (($\alpha+\beta$) 2-C=O), 141.7 (($\alpha+\beta$) 6-CH), 102.7 (($\alpha+\beta$) 5-CH), 94.8 (β -CH), 90.9 (α -CH), 88.9 ($2 \times$ s, ($\alpha+\beta$) 1'-CH), 82.9 (m, ($\alpha+\beta$) 4'-CH), 76.1 (β - CH_2CHO), 73.8 (α - CH_2CHO), 73.8 ($2 \times$ s, ($\alpha+\beta$) 2'-CH), 71.7–69.8 ($4 \times$ s, ($\alpha+\beta$)-GlcNH), 69.7 ($2 \times$ s, ($\alpha+\beta$) 3'-CH), 65.0 (m, ($\alpha+\beta$) 5'- CH_2), 60.8 ($2 \times$ s, ($\alpha+\beta$) CH_2OH), 57.5 (β -CHNH), 54.6 (α -CHNH), 33.4 ($2 \times$ s, ($\alpha+\beta$) CH_2S); m/z (ES^-) 550.0795 (M-H. $\text{C}_{17}\text{H}_{25}\text{N}_3\text{O}_{14}\text{PS}$ requires 558.0800).



ν_{max} (KBr disc)/ cm^{-1} 3250 (OH), 2940 (NH imide), 1690 (CO amide), 1260 (PO), 1210 (PO), 570 (PSR); δ_{H} (400 MHz; D_2O) 7.74 (1 H, d, J 8.1, 5-CH), 5.80 (1 H, d, J 5.0, 1'-CH), 5.78 (1 H, d, J 8.1, 6-CH), 4.17 (1 H, t, J 5.1, 2'-CH), 4.14 (1 H, t, J 5.0, 3'-CH), 4.10–4.08 (1 H, 4'-CH), 4.05–3.91 (2 H, m, 5'- CH_2), 3.38 (2 H, d, J 14.5, CH_2S); δ_{P} (400 MHz, D_2O) 19.8; δ_{C} (500 MHz; D_2O) 174.0 (d, $^3J_{\text{C-P}}$ 3.9, C=O CH_2S), 166.3 (4-C=O), 151.9 (2-C=O), 141.7 (6-CH), 102.7 (5-CH), 88.7 (1'-CH), 83.0 (d, $^3J_{\text{C-P}}$ 9.0, 4'-CH), 73.8 (2'-CH), 69.7 (3'-CH), 65.0 (d, $^3J_{\text{C-P}}$ 6.3, 5'- CH_2), 32.1 (CH_2S); m/z (ES^-) 397.0111 (M-H. $\text{C}_{11}\text{H}_{14}\text{N}_2\text{O}_{10}\text{PS}$ requires 397.0112).

7.20. pH range Tripartite reaction: *N*-hydroxybenzotriazole as the leaving group

Reactions were performed by preparation of a range of reaction mixtures with different pH values. Solutions of 5'-O-monophosphorothioate (20 mg, 0.05 mmol) in water (0.1 mL) and D-glucosamine hydrochloride (13.6 mg, 0.06 mmol) in water (0.2 mL) were mixed in each tube.

Crude bromoacetyl-*N*-hydroxybenzotriazole (13.5 mg) was dissolved in acetonitrile (0.4 mL), previously dried over molecular sieves, and added to each of the aqueous solutions. Then, sodium hydroxide (1 M aqueous solution) was added according to the to table 7.9, to adjust the specific pH, measured using a pH meter, and each mixture was then left stirring for 12 h. The acetonitrile was evaporated under reduced pressure and the samples were lyophilised prior to being subjected to anion exchange chromatography.

Table 7. 14 Quantity of sodium hydroxide added to adjust the pH of the reaction mixtures (I-VII)

Reaction	I	II	III	IV	V	VI	VII
Eq of 1M NaOH	0.5	0.75	1	1.25	1.5	1.75	2.25
pH (H ₂ O, MeCN)	4.8	6.1	7.8	9.2	10.8	12.7	13.7

Purification of resulting crude mixtures via analytical anion exchange chromatography

The samples were prepared by dissolving of lyophilised solid (1 mg) in TEAB solution (50 M, 0.5 mL) and running the sample to a pre-equilibrated analytical (1 mL) anion exchange column (DEAE Sepharose FF). Linear gradient 50–120 mM of TEAB buffer, pH 7.6, with the flow rate of 1 mL/min was performed during 30 minutes. All chromatograms of reaction mixtures were then compared showing different reaction outcome, depending on the pH of the reaction system.

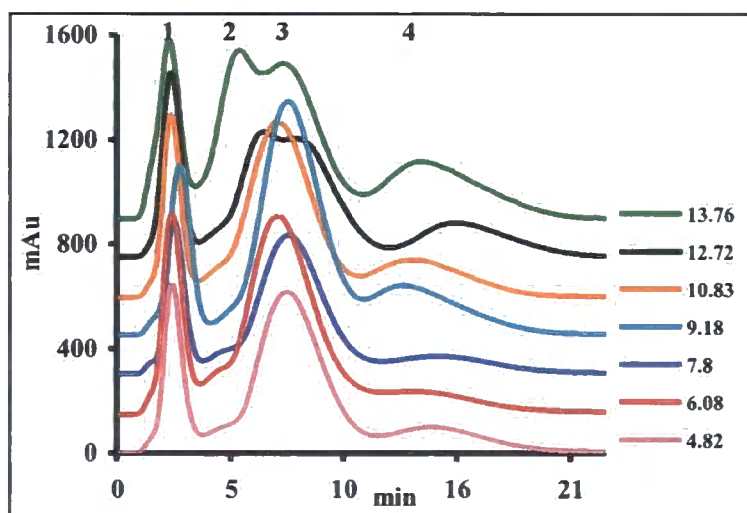
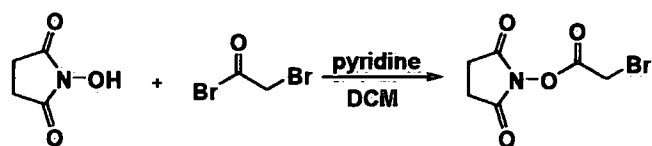


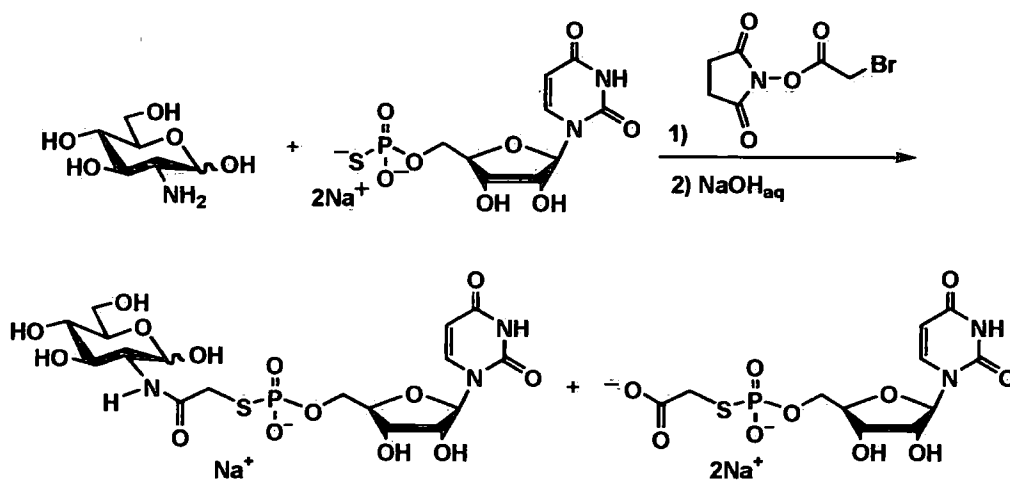
Figure 7. 12 Tripartite reaction pH range: HOBT 1. 156 as triethylammonium salt, 2. the mixture of amide product and HOBT, 3. HOBT, 4. 155 as the triethylammonium salt. UV trace at 280 nm

7.21. Bromoacetyl-*N*-hydroxysuccinimide



The same procedure as for the synthesis of bromoacetyl-*N*-hydroxybenzyltriazole (section 7.18) was applied with the use of *N*-hydroxysuccinimide (1 g, 8.7 mmol) in place of HOBt and the use of saturated sodium bicarbonate as the first step of the reaction work up (1.52 g, 74 %). The purity was estimated by ¹H NMR spectroscopy (100%). mp= 97-102 °C (dec); ν_{\max} (KBr disk)/cm⁻¹ 2937-3056 (CH₂), 1750-1811 (CO); δ_{H} (400 MHz; CDCl₃) 4.09 (2 H, s, CH₂Br), 2.79 (4 H, s, CH₂CH₂); δ_{C} (400 MHz; CDCl₃) 168.5 (OC=O), 163.1 (NC=O), 25.6 (CH₂Br) 21.2 (CH₂CH₂); *m/z* (EI) 234.9 and 236.9 .

7.22. Tripartate reaction: *N*-hydroxysuccinimide as the leaving group



Solutions of 5'-O-monophosphorothioate (30 mg, 0.075 mmol) in water (0.5 mL) and D-glucosamine hydrochloride (30 mg, 0.14 mmol) in water (0.5 mL) were mixed, followed by the addition of sodium hydroxide (1 M aqueous solution) to maintain the pH ~ 8 (pH paper). Bromoacetyl-*N*-hydroxysuccinimide (19.6 mg) was dissolved in acetonitrile (1 mL), and added to the aqueous mixture. After 12 h of stirring the organic solvent was evaporated under reduced pressure and the residual aqueous solution purified *via* anion exchange chromatography.

Purification of crude mixture *via* anion exchange chromatography

The aqueous solution of crude sample was loaded to a pre-equilibrated anion exchange DEAE Sephadex FF column (50 ml, 10 × 3 cm) and run using TEAB buffer, pH 7.6 linear gradient (50-350 mM). Fractions eluted between 70 and 90 mM (peak 1) of TEAB buffer and between 200 and 240 mM of TEAB (peak 2) were then were pooled and lyophilised.

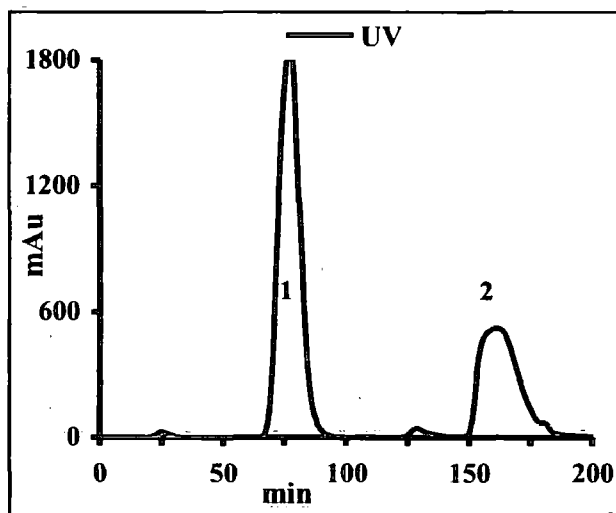
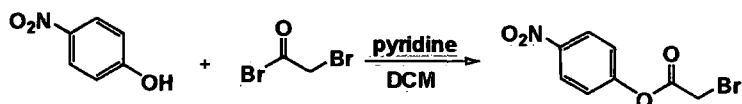


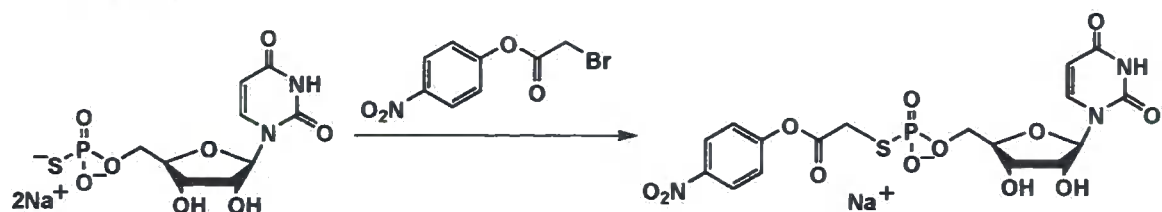
Figure 7. 13 Anion exchange chromatography: Tripartite reaction with NHS as leaving group. 1.NHS and product 156 as triethylammonium salt 2. product 155 as triethylammonium salt. UV trace at 280 nm

7.23. Bromoacetyl *p*-nitrophenol



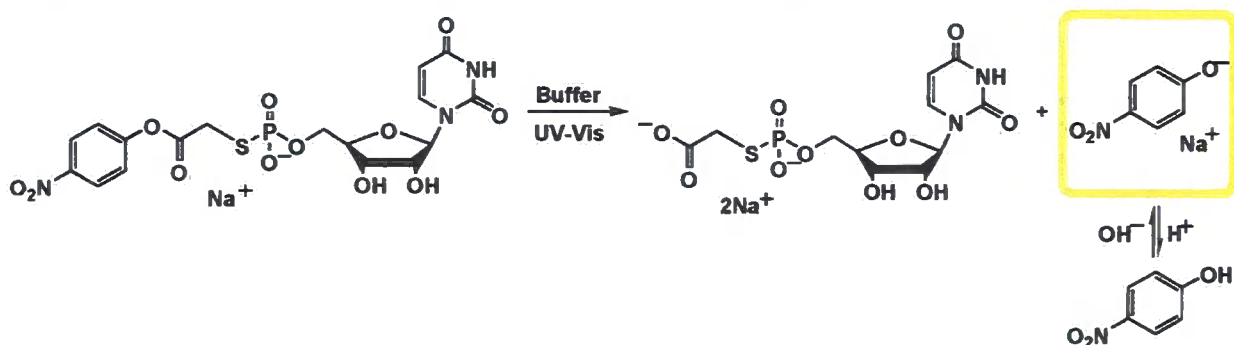
The procedure for preparation of bromoacetyl-*p*-nitrophenol was performed as for the synthesis of bromoacetyl-*N*-hydroxybenzotriazole (section 7.18), using *p*-nitrophenol (0.6 g, 4.3 mmol) in place of HOBt and the use of saturated sodium bicarbonate, as the first work up step, yielding in 0.752 g, 67 %. The purity was estimated by ¹H NMR spectroscopy (99%). mp= 72–75 °C (dec); (Found C, 36.94; H, 2.31; N, 5.17. C₇H₆BrNO₄ requires C, 36.92; H, 2.31; N, 5.38%); ν_{\max} (KBr disc)/cm⁻¹ 3110-2963 (CH), 2847 (CH₂), 1770 (ester CO), 1488 -1616 (C=C); δ_{H} (500 MHz; CDCl₃) 8.31 (2 H, d, *J* 9.0, CHCNO₂), 7.34 (2 H, d, *J* 9.3, CHCO), 4.08 (2 H, s, COCH₂Br); δ_{C} (125 MHz; CDCl₃) 165.2 (C=O), 155.1 (CO), 145.9 (CNO₂), 125.6 (NO₂CCH), 122.4 (CHCO), 25.3 (CH₂Br); *m/z* (EI) 258.9 and 260.9.

7.24. UV-Vis kinetic studies of Dipartate 'Click' chemistry: *p*-nitrophenol as leaving group



Sample preparation both for hydrolysis and aminolysis UV-Vis kinetic studies was performed by dissolving UMPS (1 Eq, 20 mg, 58.8 mmol) in deionised water (0.5 mL) and stirring with a solution of BrAc-pNP (0.8 Eq, 12 mg, 47 mmol) in acetonitrile (0.5 mL) for one minute. The mixture was then rapidly frozen in liquid nitrogen followed by lyophilisation to give a light yellow solid of intermediate, UMPSAc-pNP (81% pure by ^1H NMR spectroscopy). A stock of UV-Vis sample (6 M) was prepared by dissolving UMPSAc-pNP (10 mg) in deionised water (3 mL), which was further divided in to portions and that was frozen quickly in liquid nitrogen. Owing to the instability of UMPSAc-pNP in aqueous solution limited analyses were performed. δ_{H} (500 MHz; D_2O) 8.11 (2 H, d, J 9.2, CHCNO_2), 7.55 (1 H, d, J 8.2, 5-CH), 7.24 (2H, d, J 9.2, CHCO), 5.72 (1H, d, J 3.9, 1'-CH), 5.55 (1H, d, J 8.2, 6-CH), 4.32–3.91 (5 H, m, 2'-5'-CH), 3.7 (2 H, d, J 15.4, SCH_2); δ_{P} (80 MHz; D_2O) 19.2; m/z (ES $^-$) 518.0 (M-H for UMPSAc-pNP), 379.1 (M-H for the cyclic hydrolysis product, UMPSAc)

7.25. Hydrolysis assays: *p*-nitrophenol as the leaving group



The maximum absorbance of *p*-nitrophenol (401.9 nm) was determined prior to the kinetic studies, *via* scanning the absorbance of a UMPSAc-pNP solution through a range from 200 nm to 800 nm. Kinetic measurements of hydrolysis performed by mixing sample stock UMPSAc-pNP (6 M, 25 μL) with buffer (1.5 mL) to give 0.1 mM final concentration of UMPSAc-pNP in

the cuvette. The absorbance of the yellow-coloured *p*-nitrophenate released in the process of UMPSAc-*p*NP hydrolysis, was measured at $\lambda=401.9$ nm and 25 °C during time depending on the chosen buffer. Increasing absorbance of *p*NP, projected as the function of time (*t*), gave the rate constant of the UMPSAc-*p*NP hydrolysis, k_0 for the studied pH. The hydrolysis kinetics were examined as a pseudo first order process and the data were fitted into an exponential function:

$$A_t = A_0 + A_\infty \times (1 - e^{-k_0 \times t})$$

where, A_t is the absorbance at the examined time, *t*

A_0 is the value of the starting absorbance ($t=0$),

A_∞ is the the maximal absorbance of the compound ($t=\infty$) and

k_0 - pseudo first order constant for studied pH conditions.

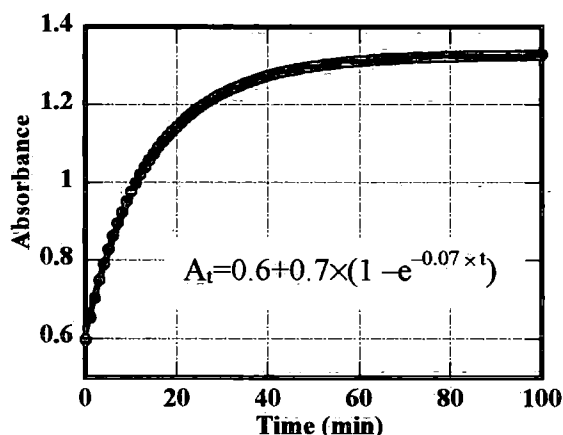


Figure 7. 14 A representative absorbance–time plot for the hydrolysis *p*NPAcUMPS⁻ followed by UV-Vis spectrometry

The data extracted from the hydrolysis experiments of UMPSAc-*p*NP are presented in table 7.15.

Table 7. 15 Experimental details of the UV/Vis kinetic studies, *p*-nitrophenol: hydrolysis

pH	k_o (min ⁻¹)	log k_o	$t_{1/2}$ (min)	Buffer
10.5	4.59	0.66	9 s	CAPS
10.2	2.79	0.44	14 s	CAPS
9.8	0.68	-0.16	1	CHES
9.4	0.36	-0.44	2	CHES
9	0.18	-0.75	4	CHES
8.4	0.21	-0.68	3	EPPS
8	0.03	-1.52	23	EPPS
7.6	0.013	-1.90	55	HEPES
7.2	0.006	-2.17	102	HEPES
6.6	0.002	-2.64	302	MES
6.2	0.0017	-2.75	393	MES
5.8	0.001	-2.98	665	MES
5.2	0.0018	-2.73	372	ACET
4.8	0.0021	-2.68	331	ACET
4.6	0.0018	-2.74	384	ACET

A plot of k_o values against corresponding pH was fitted using the least squares method to the function:

$$k_o = k_w + k_{OH} \times 10^{-14} / 10^{-pH}$$

where, k_o is the observed rate constant for examined system

k_w is water catalysis rate constant and

k_{OH} is hydroxyl ion catalysed reaction rate constant.

Rate constants were then extracted and used to create hydrolysis pH profile presented in the form of log k_o as a function of pH of the reaction media. The projected plateau of the resulting curve did not match the experimentally collected data. Therefore, k_o was determined as the average value of the observed rate constants for the pH range 4.6-6.6 giving the final

UMPSAc-pNP hydrolysis rate function (square fit $\log k_o$ vs pH graph shown below). The ‘mismatching’ problem occurred due to the insensitivity of least squares fitting to smaller values.

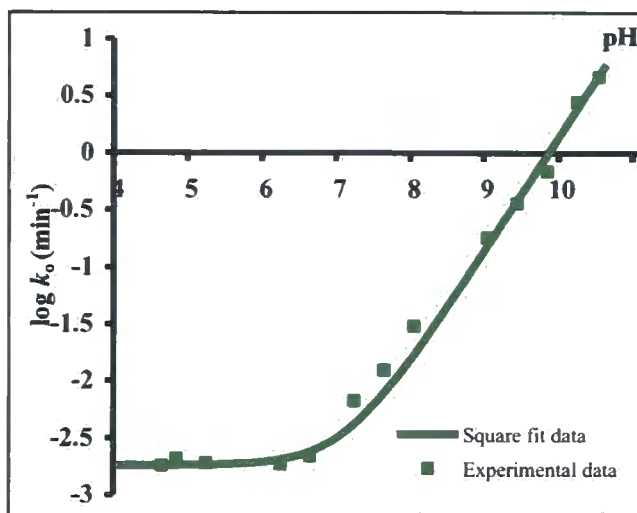
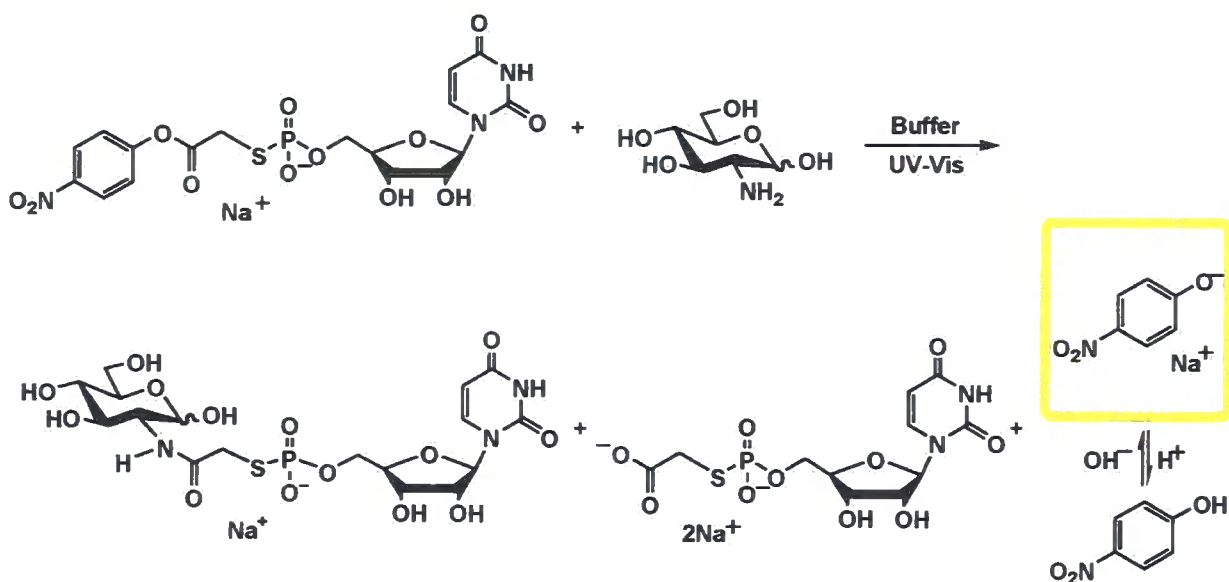


Figure 7.15 pH rate profile for *p*-nitrophenol intermediate hydrolysis $k_o = 0.0018 + 15058 [\text{OH}^-]$

7.26. Aminolysis: *p*-nitrophenol as the leaving group



The aminolysis studies on the intermediate UMPSAc-pNP were performed by mixing the solution of D-glucosamine in water (1.24 M, 60 μL) with appropriate buffer (0.5 M, 1.44 mL) to generate 50 mM final concentration of D-glucosamine in the UV-VIS cuvette. Then, stock solution of intermediate UMPSAc-pNP was added to the mixture (6 M, 25 μL). This resulted in a 500-fold ratio of D-glucosamine to intermediate UMPSAc-pNP. Released *p*-nitrophenolate, which arose as the product of both aminolysis and hydrolysis processes was measured *via* UV-

Vis absorbance at $\lambda=401.9$ nm and 25 °C and plotted against time. This data was fitted to obtain k_T over a range pH. Fitting was performed as described for the hydrolysis experiment. The resulting k_T values, presented in table 7.14, are the observed rate constant for total process, the sum of hydrolysis (k_o) and aminolysis (k_{NH_2}) rate constants.

Table 7. 16 Experimental details of the UV/Vis kinetic studies, *p*-nitrophenol: overall process

pH	k_T (min ⁻¹)	log k_T	$t_{1/2}$ (min)	Buffer
10.2	0.65	-0.18	1.06	CAPS
9.8	1.50	0.17	0.46	CHES
9.4	0.53	-0.27	1.31	CHES
9	0.31	-0.50	2.22	CHES
8.4	0.16	-0.79	4.34	EPPS
8	0.17	-0.77	4.13	EPPS
7.6	0.12	-0.91	5.68	HEPES
7.2	0.07	-1.15	9.87	HEPES
6.6	0.02	-1.71	35.73	MES
6.2	0.006	-2.19	109.03	MES
5.8	0.002	-2.58	265.20	MES
5.2	0.0005	-3.31	1434.19	ACET

The square fit data was done using following equation and is presented in the graph below:

$$k_T = k_o + k_N = k_W + k_{OH} \times 10^{-14} / 10^{-pH} + k_{NH_2} \times [\text{amine}] / (1 + 10^{-pH + pK_a})$$

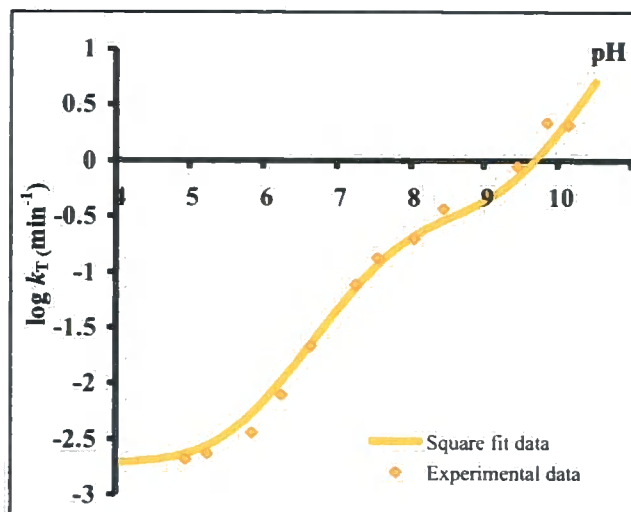


Figure 7. 16 pH rate profile for overall *p*-nitrophenol intermediate aminolysis in the presence of hydrolysis (500 fold amine nucleophile)

To analyze the aminolysis process in isolation, observed hydrolysis rate constant k_O was subtracted from the combined, aminolysis and hydrolysis observed rate constants k_T and the resulting k_N values are shown in the table 7.15.

Table 7. 17 Experimental details of the UV/Vis kinetic studies, *p*-nitrophenol: aminolysis only

pH	k_N (min ⁻¹)	log k_N	$t_{1/2}$ (min)	Buffer
10.2	0.65	-0.18	1.06	CAPS
9.8	1.50	0.17	0.46	CHES
9.4	0.53	-0.27	1.31	CHES
9	0.31	-0.50	2.22	CHES
8.4	0.16	-0.79	4.34	EPPS
8	0.17	-0.77	4.13	EPPS
7.6	0.12	-0.91	5.68	HEPES
7.2	0.07	-1.15	9.87	HEPES
6.6	0.02	-1.71	35.73	MES
6.2	0.006	-2.19	109.03	MES
5.8	0.002	-2.58	265.20	MES
5.2	0.0005	-3.31	1434.19	ACET

The aminolysis pH profile was plotted using resulting k_N values and fitted to the curve (graph shown below) using least square fitting.

$$k_N = k_{\text{NH}_2} \times [\text{amine}] / (1 + 10^{-\text{pH} + \text{p}K_a})$$

where, k_N is the aminolysis observed rate constant for studied pH

k_{NH_2} is amine catalysed 2nd order reaction rate constant,

[amine] is the starting concentration of amine (50 mM), which remains constant

$\text{p}K_a$ of the amine nucleophile (in this case D-glucosamine 7.75).

Corresponding $\log k_N$ - pH plot is shown in the graph below.

$$k_N = 8.55 \times 0.05 / (1 + [\text{H}^+]/K_a), \text{p}K_a = 7.75$$

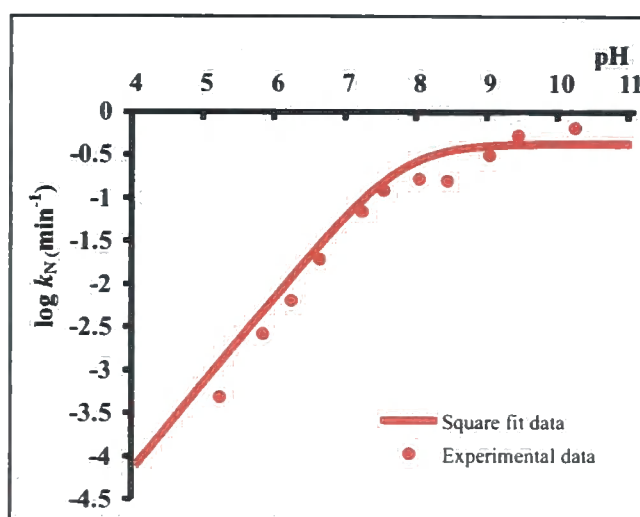
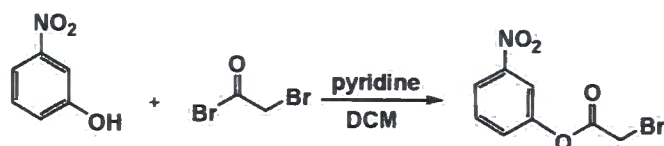


Figure 7. 17 pH profile of the *p*-nitrophenol intermediate aminolysis (500 fold excess amine nucleophile)

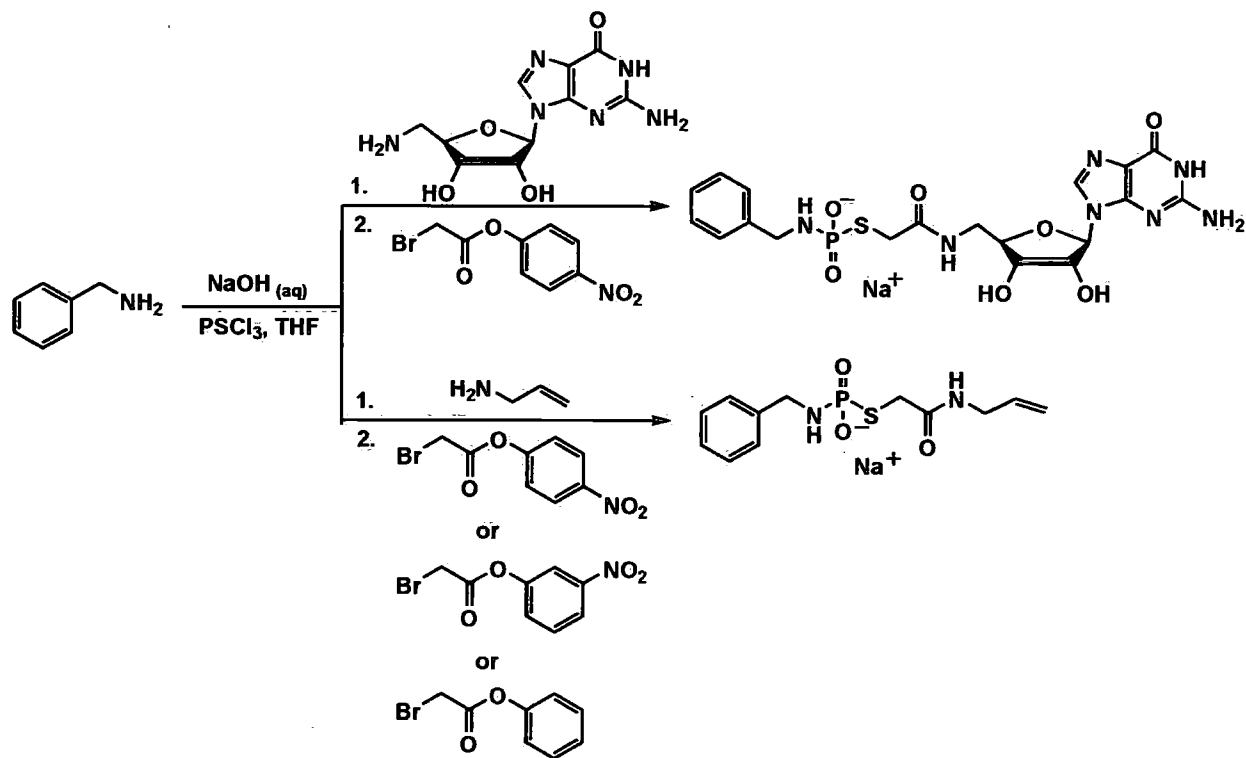
7.27. Bromoacetyl *m*-nitrophenol



Procedure for preparation of bromoacetyl *p*-nitrophenol was performed as for the synthesis of bromoacetyl-*N*-hydroxybenzotriazole (section 7.18) using *m*-nitrophenol (0.6 g, 4.3 mmol) yielding white powder (0.6965 g, 62 %). The purity was estimated by ¹H NMR spectroscopy (98%). mp= 50–53 °C (dec); (Found C, 36.96; H, 2.31; N, 5.39. C₇H₆BrNO₄ requires C, 36.92; H, 2.31; N, 5.38%); ν_{max} (KBr disc)/cm⁻¹ 3116-3011 (CH), 2864 (CH₂), 1777 (ester CO), 1473-1528 (C=C); δ_{H} (500 MHz; CDCl₃) 8.16 (1 H, d, *J* 8.8, 4-CH), 8.05 (1 H, s, 4-CH), 7.63 (1 H, t,

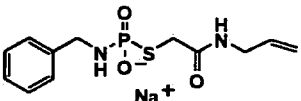
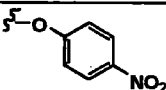
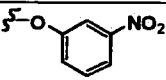
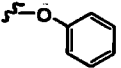
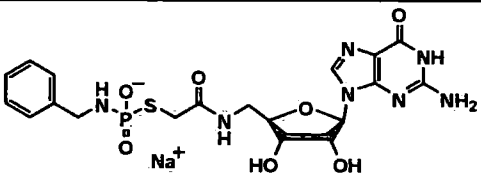
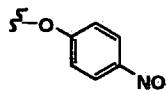
J 8.1, 5-CH), 7.53 (1 H, t, J 8.2, 6-CH), 4.10 (2 H, s, CH_2Br); δ_{C} (125 MHz; CDCl_3) 165.5 (C=O), 150.7 (CO), 149.0 (CNO₂), 130.6 (5-CH), 127.8 (6-CH), 121.6 (4-CH), 117.3 (2-CH), 25.2 (CH_2Br); m/z (EI) 258.9 and 260.9.

7.28. Bromoacetyl system and thiophosphoramidates: allylamine and guanosine amine



Benzylamine (1 Eq, 25 μL , 0.23 mmol) was thiophosphorylated as described in section 7.2. Allylamine (2 Eq, 32 μL , 0.46 mmol) or 5'-amino-5'-deoxyguanosine (1 Eq, 65 mg, 0.23 mmol) was added to aqueous/THF solution of the thiophosphorylated benzylamine and mixed for several minutes, before bromoacetyl-*P* (1 Eq, 0.23 mmol, table 7.21) was added. After 15 minutes of vigorous stirring, the pH of the mixture was adjusted using 50 mM hydrochloric acid (Table 7.21, pH paper) followed by ethyl acetate extraction (3×10 mL). Then, the pH was adjusted back to pH 9 and the extraction was performed using chloroform (3×10 mL). The aqueous sample was lyophilized and dry solid was analysed.

Table 7. 18 The experimental details of the bromoacetyl-thiophosphoramidate system

Crude compound		Bromoacetyl~P (mg)	pH	Purity (%)
160a		 (60)	7	91 ^a , 69 ^b
160b		 (60)	8	92 ^a , 72 ^b
160c		 (49)	9	80 ^a , 69 ^b
164		 (60)	7	65 ^a n.d. ^b

Product 160 is characterised as crude, while crude product 164 was subjected to the anion and cation exchange chromatography.

The crude product **160**: δ_{H} (400 MHz; D₂O) 7.45–7.22 (5 H, m, C₆H₅), 5.80 (1 H, ddt, *J* 17.3, 10.4 and 5.2 CH₂=CH), 4.95 (2 H, m, CH₂=CH), 4.00 (2 H, d, *J* 10.9, CH₂NH), 3.72 (2 H, dt, *J* 5.1 and 1.6, CHCH₂), 3.34 (2 H, d, *J* 12.9, SCH₂); $\delta_{\text{P}}[^1\text{H}]$ (162 MHz; D₂O) 21.9 (m, NHPS); δ_{C} (101 MHz; D₂O) 172.4 (d, ³*J*_{C-P} 3.6, C=O), 140.6 (d, ³*J*_{C-P} 7.2, CCH₂NH), 133.6 (CH=CH₂), 128.9 (*m*-C₆H₅), 128.8 (*o*-C₆H₅), 127.4 (*p*-C₆H₅), 116.4 (CH₂=CH), 45.6 (CH₂NH), 42.2 (CH₂CH), 33.7 (SCH₂); *m/z* (ES⁻) 299.0627 (M–H. C₁₂H₁₆N₂O₃PS requires 299.0624).

Anion exchange chromatography of the crude compound 498:

The crude sample (50 mg) was dissolved in a 50 mM TEAB buffer, pH 7.5 (5 mL) and purified on DEAE Sepharose® FF column (50 mL, 10 × 3 mm, 3 mL/min), running TEAB buffer gradient 50-200 mM (chromatogram shown below).

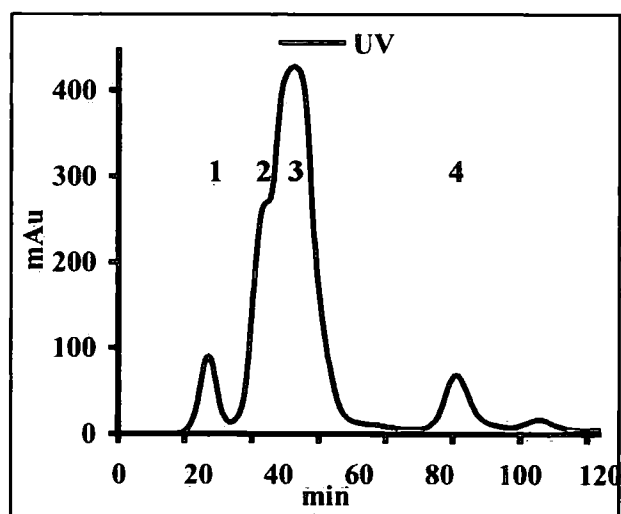


Figure 7. 18 Anion exchange chromatography of the crude product 164. UV trace at 280 nm

The fractions of the peaks containing the same product (figure 7., table 7.1.) were collected and lyophilised.

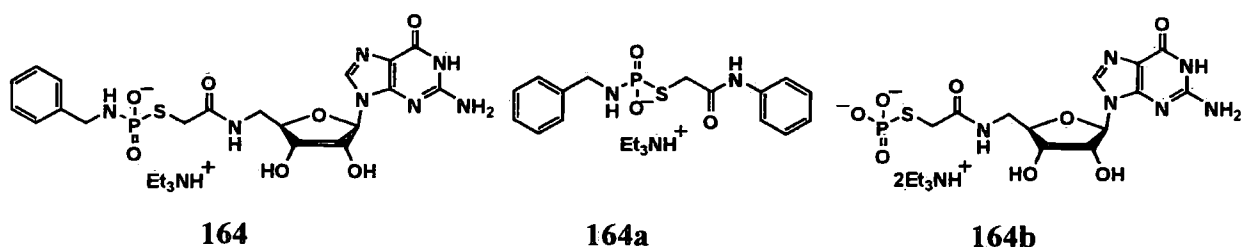


Figure 7. 19 Product and impurities in detected after anion exchange chromatography of crude product 498

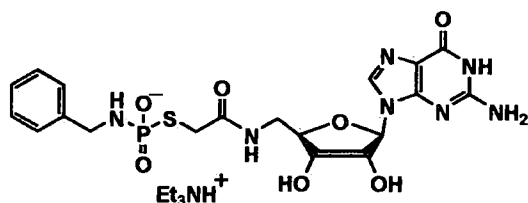
Table 7. 19 Collected fractions of the anion exchange chromatography of the crude mixture 498

1	2	3	4
6 ^c	84 ^c	8 ^c	2 ^c
0 ^a	Equal traces ^a of: 23.5 ppm (m, 164a) 23.1 ppm (m, 164) 14 ppm (t, 164b)	10 ^a 23.5 ppm (m, 164a) 87 ^a 23 ppm (m, 164) 3 ^a 3ppm (s, Pi)	16 ppm (t, <i>J</i> 11.8, 164b)
Weak ^b peaks for adenosine-like structures		78 ^b (164), 17 ^b (164a)	164b

^a Determined by ³¹P NMR spectroscopy. ^b Determined by ¹H NMR spectroscopy. ^c Determined by anion exchange chromatography.

Cation exchange chromatography

The triethylammonium salt of the compound from the peak 3 (table 7.17) was dissolved in water (5 mL) and run through a regenerated Dowex[®] 50W×2, 200-400 (50 mL, 30 × 2 mm, 3 mL/min) column, with water as the mobile phase. The fractions containing product, detected *via* UV trace (280 nm), were collected and lyophilised.



The hydrolysis of thiophosphoramidate group of compound 498 occurred during cation exchange chromatography, therefore, the purity after cation exchange chromatography was 80 % estimated by ³¹P NMR and 68% estimated by ¹H NMR spectroscopy). The resulting mixture contained, beside target molecule fully characterised (shown below), also the benzyl amide product and the product of the thiophosphoramidate hydrolysis (structures shown in the figure 7.18). δ_{H} (700 MHz; D₂O) 7.74 (1 H, s, 8-*H*), 7.11–7.00 (5 H, m, C₆H₅), 5.57 (1 H, d, *J* 4.9, 1'-*H*), 4.47 (1 H, t, *J* 5.0, 2'-*H*), 4.16 (1 H, t, *J* 5.3, 3'-*H*), 4.11–4.07 (1 H, m, 4'-*H*_X), 3.66 (2 H, m, CH₂NH), 3.57 (1 H, *ABX* system, *J*_{AB} 14.3 and *J*_{BX} 7.5, 5'-CH_AH_B), 3.42 (1 H, *ABX* system, *J*_{AB} 14.5 and *J*_{AX} 3.4, 5'-CH_AH_B), 3.28–3.18 (2 H, m, SCH₂); $\delta_{\text{P}}[^1\text{H}]$ (162 MHz; D₂O) 22.7 (m, NHPS); δ_{C} (101 MHz; D₂O) 173.1 (d, ³*J*_{C-P} 2.6, C=O), 160.0 (6-*C*), 153.9 (2-*C*), 151.3 (4-*C*), 140.4 (8-*C*), 137.6 (CCH₂S), 128.5 (*o*-C₆H₅CH₂S), 127.3 (*o*- and *m*-C₆H₅CH₂S), 126.9 (*p*-C₆H₅CH₂S), 116.7 (5-*C*), 87.9 (1'-*C*), 82.3 (4'-*C*), 73.7 (2'-*C*), 71.1 (3'-*C*), 45.2 (CH₂NH), 41.6 (5'-CH₂), 33.6 (SCH₂); *m/z* (ES⁻) 524.1127 (M – H. C₁₉H₂₃N₇O₇PS requires 524.1123).

8.0 References

1. H. C. Kolb, M. G. Finn and K. B. Sharpless, *Angew. Chem. Intl. Ed.*, 2001, **40**, 2004-2021.
2. H. C. Kolb and K. B. Sharpless, *Drug Discovery Today*, 2003, **8**, 1128-1137.
3. R. S. Bohacek, C. McMartin and W. C. Guida, *Med. Res. Rev.*, 1996, **16**, 3-50.
4. D. C. Rideout and R. Breslow, *J. Am. Chem. Soc.*, 1980, **102**, 7816-7817.
5. V. V. Rostovtsev, L. G. Green, V. V. Fokin and K. B. Sharpless, *Angew. Chem. Intl. Ed.*, 2002, **41**, 2596-2599.
6. L. V. Lee, M. L. Mitchell, S. J. Huang, V. V. Fokin, K. B. Sharpless and C. H. Wong, *J. Am. Chem. Soc.*, 2003, **125**, 9588-9589.
7. P. Appukkuttan, W. Dehaen, V. V. Fokin and E. Van der Eycken, *Org. Lett.*, 2004, **6**, 4223-4225.
8. L. Zhang, X. G. Chen, P. Xue, H. H. Y. Sun, I. D. Williams, K. B. Sharpless, V. V. Fokin and G. C. Jia, *J. Am. Chem. Soc.*, 2005, **127**, 15998-15999.
9. S. Narayan, J. Muldoon, M. G. Finn, V. V. Fokin, H. C. Kolb and K. B. Sharpless, *Angew. Chem. Intl. Ed.*, 2005, **44**, 3275-3279.
10. N. Rieber, J. Alberts, J. A. Lipsky and D. M. Lemal, *J. Am. Chem. Soc.*, 1969, **91**, 5668-5669.
11. S. Otto and J. B. F. N. Engberts, *Org. Biomol. Chem.*, 2003, **1**, 2809-2820.
12. G. K. vanderWel, J. W. Wijnen and J. Engberts, *J. Org. Chem.*, 1996, **61**, 9001-9005.
13. J. F. King, R. Rathore, J. Y. L. Lam, Z. R. Guo and D. F. Klassen, *J. Am. Chem. Soc.*, 1992, **114**, 3028-3033.
14. W. Blokzijl, M. J. Blandamer and J. B. F. N. Engberts, *J. Am. Chem. Soc.*, 1991, **113**, 4241-4246.
15. J. E. Moses and A. D. Moorhouse, *Chem Soc Rev*, 2007, **36**, 1249-1262.
16. S. Lober, P. Rodriguez-Loaiza and P. Gmeiner, *Org. Lett.*, 2003, **5**, 1753-1755.
17. S. L. Ng, P. Y. Yang, K. Y. T. Chen, R. Srinivasan and S. Q. Yao, *Org. Biomol. Chem.*, 2008, **6**, 844-847.
18. C. W. Tornøe, C. Christensen and M. Meldal, *J. Org. Chem.*, 2002, **67**, 3057-3064.
19. Q. Chen, F. Yang and Y. G. Du, *Carbohydr. Res.*, 2005, **340**, 2476-2482.
20. R. Manetsch, A. Krasinski, Z. Radic, J. Rauschel, P. Taylor, K. B. Sharpless and H. C. Kolb, *J. Am. Chem. Soc.*, 2004, **126**, 12809-12818.
21. W. G. Lewis, L. G. Green, F. Grynszpan, Z. Radic, P. R. Carlier, P. Taylor, M. G. Finn and K. B. Sharpless, *Angew. Chem. Intl. Ed.*, 2002, **41**, 1053-1057.
22. A. E. Speers, G. C. Adam and B. F. Cravatt, *J. Am. Chem. Soc.*, 2003, **125**, 4686-4687.
23. A. E. Speers and B. F. Cravatt, *Chemistry & Biology*, 2004, **11**, 535-546.
24. P. M. Chaudhary, S. R. Chavan, F. Shirazi, M. Razdan, P. Nimkar, S. P. Maybhate, A. P. Likhite, R. Gonnade, B. G. Hazara, M. V. Deshpande and S. R. Deshpande, *Bioorg. Med. Chem.*, 2009, **17**, 2433-2440.
25. W. L. Mock, T. A. Irra, J. P. Wepsiec and T. L. Manimaran, *J. Org. Chem.*, 1983, **48**, 3619-3620.
26. W. L. Mock, T. A. Irra, J. P. Wepsiec and M. Adhya, *J. Org. Chem.*, 1989, **54**, 5302-5308.
27. D. M. Quinn, *Chemical Reviews*, 1987, **87**, 955-979.
28. P. Taylor and Z. Radic, *Ann. Rev. Pharm. Toxic.*, 1994, **34**, 281-320.
29. A. E. Speers and B. F. Cravatt, *Chem. Biol.*, 2004, **11**, 535-546.
30. N. J. Agard, J. A. Prescher and C. R. Bertozzi, *J. Am. Chem. Soc.*, 2004, **126**, 15046-15047.
31. J. M. Baskin, J. A. Prescher, S. T. Laughlin, N. J. Agard, P. V. Chang, I. A. Miller, A. Lo, J. A. Codelli and C. R. Bertozzi, *Proc. Natl. Acad. Sci. USA*, 2007, **104**, 16793-16797.
32. S. Punna, E. Kaltgrad and M. G. Finn, *Bioconjugate Chem.*, 2005, **16**, 1536-1541.
33. Z. M. Guo, A. W. Lei, X. M. Liang and Q. Xu, *Chem. Commun.*, 2006, 4512-4514.
34. R. Vestberg, M. Malkoch, M. Kade, P. Wu, V. V. Fokin, K. B. Sharpless, E. Drockenmuller and C. J. Hawker, *J. Polymer. Chem. A*, 2007, **45**, 2835-2846.
35. S. Dedola, S. A. Nepogodiev and R. A. Field, *Org. Biomol. Chem.*, 2007, **5**, 1006-1017.
36. I. Lieberman, A. Kornberg and E. S. Simms, *J. Am. Chem. Soc.*, 1954, **76**, 3608-3609.
37. I. Lieberman, A. Kornberg and E. S. Simms, *J. Biol. Chem.*, 1955, **215**, 429-440.
38. J. G. Moffatt and H. G. Khorana, *J. Am. Chem. Soc.*, 1961, **83**, 649-658.
39. S. Roseman, J. J. Distler, J. G. Moffatt and H. G. Khorana, *J. Am. Chem. Soc.*, 1961, **83**, 659-663.
40. J. G. Moffatt and H. G. Khorana, *J. Am. Chem. Soc.*, 1958, **80**, 3756-3761.
41. J. G. Moffatt and H. G. Khorana, *J. Am. Chem. Soc.*, 1961, **83**, 649-658.
42. J. G. Moffatt and H. G. Khorana, *J. Am. Chem. Soc.*, 1961, **83**, 663-675.
43. V. J. Davisson, D. R. Davis, V. M. Dixit and C. D. Poulter, *J. Org. Chem.*, 1987, **52**, 1794-1801.

44. E. C. Dykhuizen and L. L. Kiessling, *Org. Lett.*, 2009, **11**, 193-196.
45. X. M. Zhu, F. Stolz and R. R. Schmidt, *J. Org. Chem.*, 2004, **69**, 7367-7370.
46. P. Brear, Freeman, G. R., Shankey, M. C., Trncic, M., Hodgson, D. R. W., *Chem. Commun.*, 2009, DOI:10.1039/B908727C.
47. J. F. King, Z. R. Guo and D. F. Klassen, *J. Org. Chem.*, 1994, **59**, 1095-1101.
48. J. F. Kirsch and W. P. Jencks, *J. Am. Chem. Soc.*, 1964, **86**, 837-846.
49. C. Castro and E. A. Castro, *J. Org. Chem.*, 1981, **46**, 2939-2943.
50. J. F. King, M. S. Gill and P. Ciubotaru, *Can. J. Chem.-Rev. Can. Chim.*, 2005, **83**, 1525-1535.
51. D. Williamson, M. J. Cann and D. R. W. Hodgson, *Chem. Commun.*, 2007, 5096-5098.
52. D. Williamson and D. R. W. Hodgson, *Org. Biomol. Chem.*, 2008, **6**, 1056-1062.
53. M. Ora, M. Murtola, S. Aho and M. Oivanen, *Org. Biomol. Chem.*, 2004, **2**, 593-600.
54. F. Eckstein and G. Gish, *Trends Biochem Sci*, 1989, **14**, 97-100.
55. D. K. Dean, *Synth. Commun.*, 2002, **32**, 1517-1521.
56. R. Duncan and D. G. Drueckhammer, *Tetrahedron Lett.*, 1993, **34**, 1733-1736.
57. F. Eckstein, *J. Am. Chem. Soc.*, 1970, **92**, 4718-4719.
58. I. Kers, A. Kers, J. Stawinski and A. Kraszewski, *Tetrahedron Lett.*, 1999, **40**, 3945-3948.
59. M. Lasker, C. D. Bui, P. G. Besant, K. Sugawara, P. Thai, G. Medzihradzsky and C. W. Turck, *Protein Science*, 1999, **8**, 2177-2185.
60. M. C. Pirrung, K. D. James and V. S. Rana, *J. Org. Chem.*, 2000, **65**, 8448-8453.
61. Z. J. Dominguez, M. T. Cortez and B. Gordillo, *Tetrahedron*, 2001, **57**, 9799-9812.
62. J. D. Chanley and E. Feageson, *J. Am. Chem. Soc.*, 1958, **80**, 2686-2691.
63. S. J. Benkovic and E. J. Sampson, *J. Am. Chem. Soc.*, 1971, **93**, 4009-4016.
64. C. McGuigan, M. Derudas, J. J. Bugert, G. Andrei, R. Snoeck and J. Balzarini, *Bioorganic & Medicinal Chemistry Letters*, 2008, **18**, 4364-4367.
65. C. McGuigan, F. Daverio, I. Najera, J. A. Martin, K. Klumpp and D. B. Smith, *Bioorg. Med. Chem. Lett.*, 2009, **19**, 3122-3124.
66. C. McGuigan, D. Cahard, H. M. Sheeka, E. DeClercq and J. Balzarini, *J. Med. Chem.*, 1996, **39**, 1748-1753.
67. M. Ora, K. Mattila, T. Lonnberg, M. Oivanen and H. Lonnberg, *J. Am. Chem. Soc.*, 2002, **124**, 14364-14372.
68. M. Ora, J. Ojanpera and H. Lonnberg, *Chem. Eur. J.*, 2007, **13**, 8591-8599.
69. T. K. Venkatachalam, G. Yu, P. Samuel, S. Qazi, S. Pendergrass and F. M. Uckun, *Eur. J. Med. Chem.*, 2004, **39**, 665-683.
70. P. K. Glasoe and F. A. Long, *J. Phys. Chem.*, 1960, **64**, 188-190.
71. R. Krishnamurthy, S. Guntha and A. Eschenmoser, *Angew. Chem. Intl. Ed.*, 2000, **39**, 2281-2285.
72. M. Chen, A. Maetzke, S. J. K. Jensen and K. V. Gothelf, *Eur. J. Org. Chem.*, 2007, 5826-5833.
73. M. Chen and K. V. Gothelf, *Org. Biomol. Chem.*, 2008, **6**, 908-911.
74. H. Mayr and A. R. Ofial, *J. Phys. Org. Chem.*, 2008, **21**, 584-595.
75. F. Brotzel, Y. C. Chu and H. Mayr, *J. Org. Chem.*, 2007, **72**, 3679-3688.
76. H. Mayr and A. R. Ofial, *J. Phys. Org. Chem.*, 2008, **21**, 584-595.
77. F. Brotzel and H. Mayr, *Org. Biomol. Chem.*, 2007, **5**, 3814-3820.
78. A. Hampton, L. W. Brox and M. Bayer, *Biochem.*, 1969, **8**, 2303-2311.
79. M. P. Kamps, S. S. Taylor and B. M. Sefton, *Nature*, 1984, **310**, 589-592.
80. J. Jayaram, S. Youn and E. W. Collisson, *Virology*, 2005, **339**, 127-135.
81. C. H. Wu, S. H. Yeh, Y. G. Tsay, Y. H. Shieh, C. L. Kao, Y. S. Chen, S. H. Wang, T. J. Kuo, D. S. Chen and P. J. Chen, *J. Biol. Chem.*, 2009, **284**, 5229-5239.
82. H. Inoue, Y. Baba, T. Furukawa, Y. Maeda and M. Tshako, *Chem. Pharm. Bull.*, 1993, **41**, 1895-1899.
83. S. Ayesa, C. Lindquist, T. Agback, K. Benkestock, B. Classon, I. Henderson, E. Hewitt, K. Jansson, A. Kallin, D. Sheppard and B. Samuelsson, *Bioorg. Med. Chem.*, 2009, **17**, 1307-1324.
84. D. H. Wasserman and A. E. Halseth, Copenhagen, Denmark, 1997.
85. D. Granot and N. Dal, *Cell Death and Differentiation*, 1997, **4**, 555-559.
86. H. Inoue, T. Yamada, H. Nakayama and M. Tshako, *Chem. Pharm. Bull.*, 2006, **54**, 1397-1402.
87. H. Inoue, M. Watanabe, H. Nakayama and M. Tshako, *Chem. Pharm. Bull.*, 2000, **48**, 802-807.
88. E. Staudacher, *Trends Glycosci. Glycotechnol.*, 1996, **8**, 391-408.
89. B. W. Murray, V. Wittmann, M. D. Burkart, S. C. Hung and C. H. Wong, *Biochem.*, 1997, **36**, 823-831.
90. T. Maeda and S. I. Nishimura, *Chem. Eur. J.*, 2008, **14**, 478-487.

91. M. D. Burkart, S. P. Vincent, A. Duffels, B. W. Murray, S. V. Ley and C. H. Wong, *Bioorg. Med. Chem.*, 2000, **8**, 1937-1946.
92. M. L. Mitchell, F. Tian, L. V. Lee and C. H. Wong, *Angew. Chem. Intl. Ed.*, 2002, **41**, 3041-3044.
93. A. J. Norris, J. P. Whitelegge, K. F. Faull and T. Toyokuni, *Anal. Chem.*, 2001, **73**, 6024-6029.
94. M. Izumi, S. Kaneko, H. Yuasa and H. Hashimoto, *Org. Biomol. Chem.*, 2006, **4**, 681-690.
95. M. Izumi, H. Yuasa and H. Hashimoto, *Curr. Top. Med. Chem.*, 2009, **9**, 87-105.
96. A. Khaled, O. Piotrowska, K. Dominiak and C. Auge, *Carbohydr. Res.*, 2008, **343**, 167-178.
97. G. Carchon, F. Chretien, P. Delannoy, A. Verbert and Y. Chapleur, *Tetrahedron Lett.*, 2001, **42**, 8821-8824.
98. G. Carchon, F. Chretien and Y. Chapleur, *Tetrahedron Lett.*, 2003, **44**, 5715-5718.
99. D. P. C. McGee and J. C. Martin, *Can. J. Chem.-Rev. Can. Chim.*, 1986, **64**, 1885-1889.
100. H. Staudinger and J. Meyer, *Helv Chim Acta*, 1919, 635.
101. R. V. Kolakowski, N. Shangquan, R. R. Sauers and L. J. Williams, *J. Am. Chem. Soc.*, 2006, **128**, 5695-5702.
102. L. E. da Silva, A. C. Joussef, L. K. Pacheco, D. G. da Silva, M. Steindel, R. A. Rebelo and B. Schmidt, *Bioorg. Med. Chem.*, 2008, **16**, 7079-7079.
103. M. C. Kimber, I. B. Mahadevan, S. F. Lincoln, A. D. Ward and E. R. T. Tiekink, *J. Org. Chem.*, 2000, **65**, 8204-8209.
104. S. L. Croft, S. Sundar and A. H. Fairlamb, *Clin. Microbiol. Rev.*, 2006, **19**, 111-169.
105. L. Kedzierski, Y. Zhu and E. Handman, *Expert Opinion on Drug Delivery*, 2008, **5**, 1057-1057.
106. P. Escobar, S. Matu, C. Marques and S. L. Croft, *Acta Tropica*, 2002, **81**, 151-157.
107. F. I. Carroll, B. D. Berrang and C. P. Linn, *J. Med. Chem.*, 1980, **23**, 581-584.
108. M. A. Fakhfakh, A. Fournet, E. Prina, J. F. Mouscadet, X. Franck, R. Hocquemiller and B. Figadere, *Bioorg. Med. Chem.*, 2003, **11**, 5013-5023.
109. S. Habtemariam, *BMC Pharmacology* 2003, DOI: 10.1186/1471-2210-3-6.
110. A. N. Dwyer, M. C. Grossel and P. N. Horton, *Supramolec. Chem.*, 2004, **16**, 405-410.
111. M. Ora, M. Oivanen and H. Lonnberg, *J. Chem. Soc. Perkin Trans. 2*, 1996, 771-774.
112. H. R. Watson, D. C. Apperley, D. P. Dixon, R. Edwards and D. R. W. Hodgson, *Biomacromol.*, 2009, **10**, 793-797.
113. D. A. Bulik, M. Olczak, H. A. Lucero, B. C. Osmond, P. W. Robbins and C. A. Specht, *Eukaryotic Cell*, 2003, **2**, 886-900.
114. T. Yabe, T. Yamada-Okabe, T. Nakajima, M. Sudoh, M. Arisawa and H. Yamada-Okabe, *Eur. J. Biochem.*, 1998, **258**, 941-947.
115. S. Nagahashi, M. Sudoh, N. Ono, R. Sawada, E. Yamaguchi, Y. Uchida, T. Mio, M. Takagi, M. Arisawa and H. Yamadaokabe, *J. Biol. Chem.*, 1995, **270**, 13961-13967.
116. Y. Uchida, O. Shimmi, M. Sudoh, M. Arisawa and H. YamadaOkabe, *J. Biol. Chem.*, 1996, **119**, 659-666.
117. H. Merzendorfer and L. Zimoch, *J. Exp. Biol.*, 2003, **206**, 4393-4412.
118. N. H. Georgopapadakou and S. A. Smith, *J. Bacter.*, 1985, **162**, 826-829.
119. T. Mio, T. Yabe, M. Sudoh, Y. Satoh, T. Nakajima, M. Arisawa and H. YamadaOkabe, *J. Bacter.*, 1996, **178**, 2416-2419.
120. J. A. Maertens and M. A. Boogaerts, *Curr. Pharm. Design*, 2000, **6**, 225-239.
121. A. Zumbuehl, D. Jeannerat, S. E. Martin, M. Sohrmann, P. Stano, T. Vigassy, D. D. Clark, S. L. Hussey, M. Peter, B. R. Peterson, E. Pretsch, P. Walde and E. M. Carreira, *Angew. Chem. Intl. Ed.*, 2004, **43**, 5181-5185.
122. A. Vermes, H. J. Guchelaar and J. Dankert, *J. Antimicrob. Chemother.*, 2000, **46**, 171-179.
123. K. Isono, J. Nagatsu, Kawashim. Y and S. Suzuki, *Agricul. Biol. Chem.*, 1965, **29**, 848-851.
124. J. P. Gaughran, M. H. Lai, D. R. Kirsch and S. J. Silverman, *J. Bacter.*, 1994, **176**, 5857-5860.
125. K. Obi, J. Uda, K. Iwase, O. Sugimoto, H. Ebisu and A. Matsuda, *Bioorg. Med. Chem. Letters*, 2000, **10**, 1451-1454.
126. J. B. Behr, T. Gurlain, A. Helimi and G. Guillerme, *Bioorg. Med. Chem. Letters*, 2003, **13**, 1713-1716.
127. A. Suda, A. Ohta, M. Sudoh, T. Tsukuda and N. Shimma, *Heterocycles*, 2001, **55**, 1023-1028.
128. A. Plant, P. Thompson and D. M. Williams, *J. Org. Chem.*, 2008, **73**, 3714-3724.
129. F. Eckstein, *J. Am. Chem. Soc.*, 1966, **88**, 4292-4294.
130. Yoshikaw.M, T. Kato and Takenish.T, *Tetrahedron Lett.*, 1967, 5065-5068.
131. T. Ikemoto, A. Haze, H. Hatano, Y. Kitamoto, M. Ishida and K. Nara, *Chem. Pharm. Bull.*, 1995, **43**, 210-215.
132. A. W. Murray and M. R. Atkinson, *Biochem.*, 1968, **7**, 4023-4029.

133. O. Abril, D. C. Crans and G. M. Whitesides, *J. Org. Chem.*, 1984, **49**, 1360-1364.
134. C. P. Da Costa, D. Krajewska, A. Okruszek, W. J. Stec and H. Sigel, *J. Biol. Inorg. Chem.*, 2002, **7**, 405-415.
135. G. W. Anderson, F. M. Callahan and J. E. Zimmerman, *J. Am. Chem. Soc.*, 1964, **86**, 1839-1842.
136. H. Maskill, *Structure and Reactivity in Organic Chemistry*, OUP, Oxford, 2000.
137. Satterth.Ac and W. P. Jencks, *J. Am. Chem. Soc.*, 1974, **96**, 7018-7031.
138. M. J. Gresser and W. P. Jencks, *J. Am. Chem. Soc.*, 1977, **99**, 6963-6970.
139. K. Schattka and B. Jastorff, *Chem. Ber.-Rec.*, 1972, **105**, 3824-3826.

